PHYTOCHEMISTRY AND BIOLOGICAL STUDIES OF CONSTITUENTS FROM *BREONADIA SALICINA* (VAHL) HEPPER & J.R.I. WOOD

BY

BAFEDILE DORCAS TLHAPI

(11617811)

A THESIS SUBMITTED IN FULFILLMENT OF THE REQUIREMENTS OF THE DOCTOR OF PHILOSOPHY DEGREE IN CHEMISTRY

TO THE DEPARTMENT OF CHEMISTRY

FACULTY OF SCIENCE, ENGINEERING AND AGRICULTURE

UNIVERSITY OF VENDA

THOHOYANDOU

SOUTH AFRICA

SUPERVISOR : PROF. IDI. RAMAITE (University of Venda)

CO-SUPERVISOR: PROF. T. VAN REE (University of Venda)

CO-SUPERVISOR: DR. CP. ANOKWURU (Babcock University)

DECLARATION

I, Bafedile Dorcas Tlhapi, hereby declare that this thesis for the doctoral degree (PhD) in chemistry, submitted at the University of Venda, is my original research and has not been submitted for any degree or examination at any other university. This thesis is my own work and does not contain any other persons' writing unless specifically acknowledged and referenced accordingly.

Tlhapi

…….……. 10 August 2023

(Signature of candidate) Date

PUBLICATIONS ARISING FROM THIS STUDY

- Tlhapi, D.B.; Ramaite, I.D.I.; Anokwuru, C.P. Metabolomic Profiling and Antioxidant Activities of *Breonadia salicina* Using ^{1}H-NMR and UPLC-QTOF-MS Analysis. *Molecules*, **2021**, 26, 6707.
- Tlhapi, D.B.; Ramaite, I.D.I.; Anokwuru, C.P.; van Ree, T.; Madala, N.E.; Hoppe, H,C. Effects of seasonal variation on phytochemicals contributing to the antimalarial and antitrypanosomal activities of *Breonadia salicina*, **2022** (Manuscript not yet published).
- Tlhapi, D.B.; Ramaite, I.D.I.; Anokwuru, C.P.; van Ree, T. Molecular networking-based metabolome, *in vitro* anti-diabetic, anti-inflammatory and cytotoxic effects of *Breonadia salicina* (Vahl) Hepper and J.R.I. Wood, **2022** (Manuscript not yet published).

CONFERENCE PROCEEDING ARISING FROM THIS STUDY

- Dorcas B Tlhapi, Isaiah D.I Ramaite, Teunis van Ree, Chinedu P Anokwuru, Heinrich C Hoppe. Phytochemistry and Biological Studies of *Breonadia salicina* (Vahl) Hepper and J.R.I. Wood (Poster). The 2nd African Traditional and Natural Products Medicine Conference. Protea Hotel Ranch Resort, Polokwane, South Africa, 19-21 October 2022.
- Dorcas B Tlhapi, Isaiah D.I Ramaite, Teunis van Ree, Chinedu P Anokwuru, Heinrich C Hoppe. Isolation, Chemical profile and Biological Studies of *Breonadia salicina* (Vahl) Hepper and J.R.I. Wood (Poster). H3D Symposium. Webersburg Estate, Stellenbosch, South Africa, 25-28 October 2022.

DEDICATIONS

I wish to dedicate this thesis to my mother (Maria Tlhapi), my father (Molefe Moses Tlhapi) and my younger sister (Moleboheng Thabia Tlhapi), who have always motivated, encouraged and supported me through difficult times. Thank you all for playing a role in my upbringing, my undergraduate and postgraduate studies. I also acknowledge my daughter Vhulenda; she has given me much happiness and joy. I trust this study will show that hard and purposeful work will yield good results.

ACKNOWLEDGEMENTS

First and foremost, I wish to thank God who gave me strength and protection throughout this study.

My heartfelt gratitude and thanks also to the following people and organizations:

My promoter, Prof. I.D.I. Ramaite, who gave me the chance to explore this fascinating field of natural product chemistry. His persistent guidance has contributed immensely towards the success of this project.

My co-promoter, Prof. T. van Ree for his assistance, valued vision, thorough feedback and continuous patience during the research project enabled me to finish this study.

My co-promoter, Dr C.P. Anokwuru for his advice, encouragement, guidance, support, passionate participation and input. It would have been impossible to conduct this project without his motivation. I am very grateful.

Prof. H. Hoppe of Rhodes University who supported the project with biological tests (antiplasmodial, antitrypanosomal and antiproliferation activities). The parasite screening was funded by the Grand Challenges Africa programme (GCA/DD/rnd3/032).

Prof. M. van der Venter of Nelson Mandela University for her assistance with biological tests (anti-diabetic, anti-inflammatory, cytotoxicity and genotoxicity activities).

Prof. P. Tshisikhawe and Dr K. Magwede of the University of Venda for their assistance with plant identification.

Dr N.R. Tshiluka and Mr G. Mafomo of the University of Venda for their assistance with plant collection.

Prof. N.E. Madala of the University of Venda for his assistance with UPLC-QTOF-MS analysis.

Prof. A.S. Traoré of the University of Venda for her assistance with biological tests (antioxidant activities).

Dr. S. Winks of the University of Cape Town for her assistance with biological tests (antimycobacterial activities).

Mr P. Pandelani of the University of Venda, who assisted with NMR spectroscopy.

Mr F.B. Mutshaeni of the University of Venda, who assisted with laboratory resources. Your help is appreciated.

Mr V.T. Bvuma of the University of Venda for proof-reading this research document.

Mr N. Ndou for his immeasurable personal support and encouragement.

University of Venda and the Department of Chemistry for their facilities, laboratory skills attained, invaluable advice and support.

The National Research Foundation, Sasol Inzalo foundation, and the University of Venda's Research and Publications Committee (RPC) for funding this study.

Abstract

Breonadia salicina (Vahl) Hepper and J.R.I. Wood is a tree used widely to treat numerous infectious diseases in South Africa and other African countries, and ethnopharmacological studies have shown a number of biological activities of the crude extracts. Furthermore, phytochemical studies have indicated that the stem bark is rich in tannins, and alkaloids have been isolated from the twigs and leaves. However, few studies have correlated the phytochemistry to the physiological activties. This study aimed to explore the phytochemistry of *B. salicina* using a metabolomic approach and correlating the phytochemistry to the biological activities for possible drug development.

Samples of *B. salicina* were collected at Fondwe, Limpopo Province, South Africa. Phytochemical studies followed a metabolomics approach, with repeated column chromatography and preparative thin-layer chromatography yielding a number of pure compounds. Antimalarial and antitrypanosomal activities of the crude extracts, pure compounds, fractions, and seasonal samples were evaluated using the parasite lactate dehydrogenase (pLDH) and *Trypanosoma brucei* assays, respectively. Furthermore, the antioxidant activities of the crude extracts, fractions and pure compounds were evaluated using DPPH (2,2-diphenyl-1-picrylhydrazyl) and reducing power assays. The antimycobacterial activities of the crude extracts and fractions were determined against *Mycobacterium tuberculosis* (H37RvMA strain), and anti-diabetic activities of the crude extracts were determined using α-amylase and α-glucosidase inhibition assays. The anti-inflammatory activities of the crude extracts were assessed using the Griess assay, while the *in vitro* toxicology of the crude extracts was evaluated using cell toxicity, NucRed nuclei dye, MTT (3-(4,5-dimethylthiazol-2-yl)-2,5-diphenyltetrazolium bromide) and Hoechst 33342/Propidium iodide (PI) dual staining assays.

Eight compounds (bodinioside Q, 5-*O*-caffeoylquinic acid, D-galactopyranose, hexadecane, kaempferol 3-*O*-(2''-*O*-galloyl)-glucuronide, lupeol, palmitic acid, and sucrose) were isolated for the first time from the root, stem bark, and leaf extracts of *B. salicina*, while 51 compounds were tentatively identified from the crude extracts, fractions and seasonal samples by UPLC-QTOF-MS and ^{1}H-NMR spectroscopy. The aligned UPLC-QTOF-MS data were analysed chemometrically to determine the chemical variability of the crude extracts of the roots, stem bark, and leaves collected during four different consecutive seasons. The principal component analysis (PCA) model, hierarchical cluster analysis (HCA) and partial least square discriminant

analysis (PLS-DA) were constructed. These indicated the presence of two main clusters related to the different parts of the plant (root, stem bark, and leaf). In the antiplasmodial activity, three fractions collected in the first year affected the viability of *Plasmodium falciparum*, with viabilities of 16.16 ± 8.63 %, 27.01 ± 4.47 % and 31.07 ± 6.71 %; and IC_{50} values of 2.19 ± 0.09 µg/mL, 1.91 ± 0.05 µg/mL and 3.02 ± 0.08 µg/mL, respectively, at a concentration of 10 µg/mL. However, all the tested crude extracts and fractions collected in the first year contained potent antiplasmodial activities at a concentration of 50 µg/mL. Furthermore, the dichloromethane leaf extract collected in the second year in autumn, winter, spring and summer displayed high activities, with viabilities of 18.57 ± 1.99 %, 32.07 ± 4.91 %, 38.11 ± 5.07 % and 20.21 ± 5.19 % at a concentration of of 50 µg/mL with IC_{50} values of 7.90 ± 0.06 µg/mL, 18.15 ± 0.07 µg/mL, 19.40 ± 0.06 µg/mL and 15.26 ± 0.05 µg/mL at a concentration of 300 µg/mL, respectively. The pure compounds, including kaempferol 3-*O*-(2''-*O*-galloyl)-glucuronide (**1**) and palmitic acid (**8**), caused a significant decrease in parasite viability at a concentration of 50 µg/mL, with viabilities of 29.37 ± 1.29 % and 24.97 ± 5.21 %; and IC_{50} values of 9.06 ± 0.036 µg/mL and 6.792 ± 0.046 µg/mL at a concentration of 200 µg/mL.

In the antitrypanosomal test, the crude methanol leaf extract, dichloromethane leaf extract, and two fractions attained in the first year strongly affected the viability of trypanosomes at the tested concentration of (50 µg/mL), with a viability of 6.74 ± 0.06 %, 6.38 ± 2.15 %, 7.78 ± 0.08 % and 5.05 ± 0.35 %; and IC_{50} values of 11.4 ± 0.42 µg/mL, 10.6 ± 0.07 µg/mL, 2.0 ± 0.09 µg/mL and 7.1 ± 0.14 µg/mL at a concentration of 300 µg/mL, respectively. Furthermore, the crude methanol leaf extract collected in the second year in autumn, spring and summer displayed higher activities, with viabilities of 5.84 ± 0.38 %, 26.66 ± 3.91 % and 9.05 ± 0.80 % at a concentration of 50 µg/mL; and IC_{50} values of 12.0 ± 0.36 µg/mL, 5.2 ± 0.74 µg/mL and 10.6 ± 0.07 µg/mL at a concentration of 300 µg/mL, respectively. However, the crude dichloromethane leaf extract collected in the second year in autumn, winter, spring and summer displayed higher activities, with viabilities of 3.50 ± 0.59 %, 4.13 ± 0.06 %, 29.47 ± 1.25 % and 3.85 ± 0.10 % at a concentration of 50 µg/mL; and IC_{50} values of 4.6 ± 1.82 µg/mL, 5.1 ± 0.30 µg/mL, 5.1 ± 0.72 µg/mL and 4.0 ± 0.08 µg/mL at a concentration of 300 µg/mL, respectively. The isolated compounds, including bodinioside Q (**4**), kaempferol 3-*O*-(2''-*O*-galloyl)-glucuronide (**1**), lupeol (**2**), and palmitic acid (**8**), exhibited antitrypanosomal activity with viabilities of 12.99 ± 0.53 %, 20.38 ± 2.35 %, 5.46 ± 0.04 %, and 5.83 ± 0.28 % at a concentration of 20 µg/mL; and IC_{50} values of 4.0 ± 0.09 µg/mL, 1.1 ± 0.22 µg/mL, 4.2 ± 0.27 µg/mL and 5.7 ± 0.09 µg/mL, respectively; On the other hand, the reference drug pentamidine

showed an IC_{50} of 10.2 ± 0.07 µg/mL. The anti-oxidant assays revealed that the crude stem bark extract had the highest DPPH free radical scavenging activity, with an IC_{50} of 41.7263 ± 7.6401 µg/mL. Furthermore, the crude root extract had the highest reducing power with an $IC_{0.5}$ of 0.1481 ± 0.1441 µg/mL.

In the antimycobacterial activity test, none of the tested plant samples produced significant antimycobacterial activity at a concentration of 90 µg/mL. All the samples produced a MIC value of >62.5 µg/mL against 7H9_ADC_GLU_TW, 7H9_ADC_GLU_N_TW and 7H9_ADC_GLY_TW media. Furthermore, the crude stem bark and root extracts showed very strong antidiabetic activity at the lowest tested concentration of 62.5 µg/mL, with an inhibition of 74.53 ± 0.737 % and 79.1 ± 1.494 % against α-amylase enzyme. However, for the α-glucosidase inhibition assay, the crude stem bark and root extracts showed complete inhibition at the lowest tested concentration of 31.3 µg/mL at 98.20 ± 0.15 % and 97.98 ± 0.22 %. The crude dichloromethane leaf extract showed a decrease in nitrite concentration at the highest concentration of 200 µg/mL, with a cell viability of 79.06 ± 1.88 %, indicating anti-inflammatory activity. The crude stem bark, root and methanol leaf extracts were not cytotoxic against Vero cells at the concentrations of 15.125 µg/mL, 31.25 µg/mL, 125 µg/mL and 250 µg/mL. Furthermore, none of the extracts were cytotoxic at the following concentrations: 50 µg/mL, 100 µg/mL and 200 µg/mL, against RAW 264.7 macrophages. However, the crude stem bark and root extracts showed cytotoxic effects against Vero cells at 250 µg/mL.

Keywords: *Breonadia salicina*, antimalarial activity, antitrypanosomal activity, antioxidant activity, antimycobacterial activity, anti-diabetic activity, anti-inflammatory activity, antiproliferation activity, genotoxicity, cytotoxicity, chemical profile, phytochemicals, metabolomics, chemometrics.

Table of Contents

List of Symbols and Abbreviations

δ	Chemical shift
°C	Degrees Celsius
IC_{50}	50 % inhibitory concentration
%	Percentage
% w/v	Percentage of weight of solute in the total volume of solution
ANOVA	One-way analysis of variance
cm	Centimetre
^{13}C-NMR	Carbon-13 nuclear magnetic resonance
COSY	Correlation spectroscopy
CH_2Cl_2	Dichloromethane (DCM)
DPPH	2,2-Diphenyl-1-picrylhydrazyl radical
ESI	Electrospray ionization
EtOAc	Ethyl acetate
FTIR	Fourier transform infrared spectroscopy
g	Gram
GC/MS	Gas chromatography-mass spectrometry
HeLa	Henrietta Lacks cervix adenocarcinoma cell line
HCA	Hierarchical cluster analysis
HMBC	Heteronuclear multiple bond coherence
^{1}H-NMR	Proton nuclear magnetic resonance
HPLC	High-pressure liquid chromatography
HSQC	Heteronuclear single quantum coherence
kg	Kilogram
L	Liter
LCMS	Liquid chromatography-mass spectrometry
MeOH	Methanol
µL	Microliter
mg	Milligram
mm	Millimeter
min	Minute

mL/min	Millilitre per minute
MS	Mass spectrometry
MTT	3-(4,5-Dimethylthiazol-2-yl)-2,5-diphenyltetrazolium bromide
m/z	Mass/charge ratio
$[M^+]$	Molecular ion
NBT	Nitroblue tetrazolium
NMR	Nuclear magnetic resonance spectroscopy
OPLS-DA	Orthogonal projection to latent structures-discriminant analysis
PCA	Principal component analysis
PDA	Photodiode array detector
PEG	Poly(ethylene glycol)
PES	Phenazine ethosulphate solution
pLDH	Parasite lactate dehydrogenase
ppm	Parts per million
PSL-DA	Partial least squares-discriminant analysis
Rt	Retention time
SD	Standard deviation
TLC	Thin-layer chromatogram
UPLC	Ultra-performance liquid chromatography
UV-Vis	Ultraviolet–visible
VIP	Variable importance of project scores

List of Figures and Schemes

List of Tables

CHAPTER 1 BACKGROUND TO THE STUDY

1.1. INTRODUCTION: Plants as sources of new drugs

A wide range of medicinal plants is used by about 80 % of people in developing countries, although in most cases no scientific research has been done to verify the efficacy and effectiveness of these medicinal plants (WHO, 2004). A great number of new inventive methods and techniques have been developed for determining new bioactive compounds from different plants during the last century. As a result, several drugs, such as morphine, codeine, atropine, tubocurarine, digitoxin, quinine, digoxin, vincristine, artemisinin and theophylline, have been isolated from plant species with recorded ancient use as traditional herbal medicines (Alamgir, 2017). Currently, various drugs established in the western world have been obtained from natural sources, with modes of action and receptors only acknowledged recently. The identification of drug receptors has provided better techniques or methods of screening for new bioactive constituents and to design and successfully synthesize or produce similar structures (Newman, 2017). Therefore, in the history of drug discovery, civilisation has moved from comprehensive screening on humans to performing experiments on animals towards creating a molecular-level testing methodology in which tests can be performed on a nanoscale, moving from a holistic empirical approach to a reductionist computational approach (Balunas and Kinghorn, 2005; Patwardhan *et al*., 2004). Furthermore, these tests have been further simplified by preparing extracts for pharmacological screening assays, to evaluate the mechanism of action by means of bioassay-guided fractionation, in order to isolate new lead compounds that can be used in the treatment of various diseases (Balunas and Kinghorn, 2005). The discovery of new drugs has become increasingly difficult because effective drugs that are used for major diseases are available. Hence, developing a good novel drug that is effective and inexpensive has become more difficult. However, novel approaches to discover new drugs will have to be applied in order to confirm the safety and effectiveness of these drugs. These include a holistic approach (which determines the effect of a traditional medicine in an *in-vivo* system), and a reductionist approach (which determines the paradigm single target, single compound) (Patwardhan and Vaidya, 2010).

1.2. Holistic approach

A holistic approach may be useful to find specific metabolites from medicinal plants with unstudied chemistry. Furthermore, a holistic approach might be important in finding a certain compound's mode of action; and may provide a general structure of compound(s) with specific actions (Verpoorte *et al*., 2005).

1.2.1. Introduction to medicinal plant metabolomics

Natural products extracted from medicinal plants are rich resources for development of new drugs (Veeresham, 2012). For many decades, several compounds derived from medicinal plants have had a significant lasting impact on human primary health care needs (Akinyemi *et al*., 2018). The structural variety and pharmacological potential of natural products suggest that still more therapeutically significant constituents may be found in plants (Lautie *et al*., 2020). Metabolomic studies of medicinally significant plant species could potentially provide a better appreciation of the metabolism of therapeutic plant species, and lead to the discovery of positions where novel structural types are synthesised and accumulated (Wurtele *et al*., 2012). Establishing a plant's metabolome comprises the description of compounds occurring in medicinal plants. This is because no analytical techniques can discover the full complement of chemical compounds in a plant (Okada *et al*., 2010). Studying a few phytochemicals provides an idea of the complexity of the important procedures, instead of studying a whole metabolic profile (Shafi and Zahoor, 2021).

1.2.2. Analytical techniques commonly used in metabolomics

1.2.2.1. Metabolomics

Metabolomics can be defined as the quantitative and qualitative investigation of constituents in an organism, cell system or biological fluid (Fiehn *et al*., 2000; Fiehn, 2002; Shyur and Yang, 2008; Roessner and Bowne, 2009). Furthermore, metabolomics include terms such as metabolic profiling, quantifies a selected class of metabolites in an organism, while metabolic fingerprinting quantifies a fingerprint of the metabolites without identifying the constituents in an organism (Koek *et al*., 2011). There are two different approaches to metabolomics, namely targeted (focusing on the analysis of a set of known metabolites) and non-targeted (involving identification of numerous unexpected metabolites).

In a targeted approach, one can use metabolite profiling, which focuses on the identification and quantification of known or unknown compounds of a dataset (Goodacre *et al*., 2004), whereas metabolomic fingerprinting focuses on categorising metabolites, by generating metabolic profiles of biological materials and comparing the differences between the samples, using an untargeted approach. Some of the techniques typically used to isolate, identify and quantify plant metabolites are column chromatography, electrophoresis, Fourier transform infrared (FTIR) spectroscopy, gas chromatography–mass spectrometry (GC-MS), high performance liquid chromatography (HPLC), mass spectrometry (MS), nuclear magnetic resonance spectroscopy (NMR), and thin-layer chromatography (TLC) (Griffiths *et al*., 2010; Patti *et al*., 2012; Li *et al*., 2019; Zhang *et al*., 2018; Martens *et al*., 2017).

1.2.2.2. Chemometrics

Chemometrics is the study of extracting information from chemical systems on a dataset, by applying mathematical and/or statistical methods. Statistical procedures known as "pattern-recognition methods" implement multivariate analysis to convert spectroscopic and chromatographic datasets of groups of materials into visual and quantitative expressions of classes, groups or categories within a dataset. A supervised or targeted approach uses linear discriminant analysis (LDA) or partial least square-discriminant analysis (PSL-DA) with orthogonal projection to convert data. On the other hand, untargeted or unsupervised methods use principal component analysis (PCA), self-organised mapping (SOM), and hierarchical cluster analysis (HCA) for data conversion (Yi *et al*., 2016; Sandasi *et al*., 2013).

1.3. Reductionist approach

The reductionist approach focuses on a search for a single or more compounds that is or are responsible for the biological activity detected in medicinal plants (Katiyar *et al*., 2012). For many years, the reductionist approach conquered the science world and has been applied in modern drug development and biology to expand and improve the computational and experimental techniques used for studying materials which are in lesser quantities in the biological system (Regenmortel, 2004). The reductionist approach aims to divide the biological system into different compounds, to get a clear picture of the biological response made by the

different compounds (Regenmortel, 2004). Therefore, the active compounds in the extracts of natural origin can be identified by bioassay-guided fractionation (Malviya and Malviya, 2017).

1.3.1. Bioassay-guided fractionation

Bioassay-guided fractionation is an example of a reductionist approach used to detect active compounds in extracts of natural products, by reducing and separating a mixture of compounds in a fraction, using various separation techniques to detect bioactive compounds (Dettweiler *et al*., 2020). Liquid chromatography (LC), thin layer chromatography (TLC), column chromatography, and gas chromatography (GC) are separation techniques which have been applied to separate different compounds from fractions (Sasidharan *et al*., 2011). After separation, the bioactivity of the fractions is determined, followed by isolation of the fractions which produced the best biological activity. Finally, the active isolated compounds are characterised and the structures are identified by comparing the spectroscopic data of the pure compounds with the data found in literature, to confirm the results. This is an approach used widely for the isolation and bioactivity determination of compounds in large quantities from a large amount of raw natural products (Weller, 2012).

1.4. Traditional medicine in South Africa

A wealth of South African indigenous knowledge has been transmitted from generation to generation (Mothibe and Sibanda, 2019). Many South Africans rely on plant-based traditional medicine for primary health-care. This is because plants are accessible, easy to prepare, and affordable (Street and Prinsloo, 2013). In South Africa, as in many other countries, the use of traditional medicine is an important cultural phenomenon, with some diseases or sicknesses recognised as specifically requiring traditional medicine (Van Wyk, 2011). The country has a rich diversified flora of over 30 000 species which are mostly endemic. More than 4000 of these medicinal plants are frequently used in traditional medicine (Van Vuuren, 2008). For centuries, traditional practitioners, healers, herbalists were the only people in South Africa who collected medicinal plants and used them to manage and control various diseases which affected their patients (Ngarivhume *et al*., 2015). Nowadays, many people can buy medicinal plants or drugs derived from natural products in both rural and urban markets (Ngarivhume *et*

al., 2015). Furthermore, many South African herbs and plants are being studied because of their potential marketing as medicinal products (Street and Prinsloo, 2013).

1.5. Importance of medicinal plants in drug discovery

A wide variety of different compound classes occurs in plants, and the methodology that has been developed to isolate single compounds with medicinal properties include extraction and isolation of compounds from medicinal plants, synthetic chemistry, combinatorial chemistry, and molecular modelling (Koparde *et al*., 2019). The discovery and development of new pharmaceuticals from natural plant products, and particularly medicinal plants, remains important: these compounds may themselves be clinically useful, or as starting materials for synthesis of known drugs, or as lead compounds for design and development of novel synthetic drugs (Pan *et al*., 2013). Medicinal plants have given western pharmacopoeia numerous essential therapeutic compounds, and currently some of these compounds derived from natural products are the best-selling drugs (Strohl, 2000). Natural plant products, especially those with novel structural features and several chiral centres, can also provide a starting point for novel synthetic compounds (Fitzgerald *et al*., 2020) and may be optimized by medicinal and synthetic chemistry (Fitzgerald *et al*., 2020).

1.6. Global market value of herbal drugs

The market value of medicinal plants as a source of foreign exchange for developed and developing countries depends on the use of plants as raw materials in the pharmaceutical industry (Chen *et al*., 2016; Bukar *et al*., 2016). They provide various opportunities for developing countries to improve rural well-being. The global trade in these plants is estimated to be more than $ 800 million per annum, and the market value was estimated to have increased to $1038.6 billion by 2021 at a compound annual growth rate (CAGR) of 6.9 % (Wakdikar, 2004). Furthermore, the market is expected to reach $1299.8 billion in 2025 at a CAGR of 6 % due to the fact that many companies improved their production after catering to the demand that developed exponentially during the COVID-19 pandemic in 2020. In 2020 the market value of Traditional Chinese Medicine (TCM) was valued at $9.53 billion, an increase of 31.2 % from the 2014 value (Mück *et al*., 2019). In Japan, the medicine market was estimated at $1.3 billion (Maegawa *et al*., 2014). In the Republic of Korea $177.48 million was spent on traditional medicine in 2000, rising to $677.6 million in 2019.

The South African traditional medicine market was estimated to be worth $75 to 150 million annually (Ndhlala *et al*., 2011). The Indian traditional herbal industry is especially vibrant at approximately $1 billion per annum (Sahoo and Manchikanti, 2013), while the United States' herbal market was worth an estimated $14.8 billion in 2008 (Soner *et al*., 2013).

1.7. Safety of herbal dugs

Traditional medicine is generally used in several developing countries for their primary health care needs. This is because they are easily obtained and inexpensive (Bussmann *et al*., 2011). Moreover, culture and tradition play an important part in Africa and elsewhere (Fennell *et al*., 2004). Traditional medicine is widely practiced in Africa, but the possible toxicity of many plants has not been investigated yet (Sowemimo *et al*., 2007). Because they have been in use for a long time, they are generally assumed to be safe, but many food plants or herbs used in traditional medicine have been shown to be potentially toxic, mutagenic or carcinogenic, resulting in the periodic removal of certain plant-derived products from the market due to human intolerance or toxicity (Edziri *et al*., 2011). The potential toxicity of herbal drugs can be assessed by considering their purity, herbal combinations, bio-absorption, bioavailability and reported adverse effects. Therefore, the efficacy and safety of medicinal plants should be studied to avoid severe side effects affecting organs such as the brain, heart, kidneys, liver, the nervous system, and the respiratory system (De Oliveira *et al*., 2011; Mulaudzi *et al*., 2013). Cytotoxicity bioassays often use organic dyes, such as INT (2-(4-iodophenyl)-3-(4-nitrophenyl)-5-phenyl-2*H*-tetrazolium), MTS (3-(4,5-dimethylthiazol-2-yl)-5-(3-carboxymethoxyphenyl)-2-(4-sulfophenyl)-2*H*-tetrazolium), MTT (3-(4,5-dimethylthiazol-2-yl)-2,5-diphenyltetrazolium bromide); and XTT (2,3-bis-(2-methoxy-4-nitro-5-sulfophenyl)-2*H*-tetrazolium-5-carboxanilide). These assays determine the metabolic function of the cellular adenosine triphosphate (ATP) levels or mitochondrial activity, by reducing the reagent to a coloured formazan product that can be used to measure the number of cells (Zhang *et al*., 2007).

1.8. Climatic factors and medicinal plants

Seasonal changes influence the availability of active components in medicinal plants, and therapeutic efficacy differs during different seasons (Soni *et al*., 2015). The active and non-active compounds differ quantitatively at different seasons and most of the different parts of plant are frequently collected when the plant materials are abundant and mature (Falasca *et al*., 2014). The nature of plants is also strongly affected by the local ecology, including climate, altitude, rainfall, light, temperature, water, humidity, air and wind (Gololo *et al*., 2016; Nchabeleng, *et al*., 2016). These environmental conditions may also influence the growth and development of plants affecting the quality of secondary metabolites present in certain species, even when it is produced in the same region or country (Sultan *et al*., 2018). Furthermore, these conditions may cause major variations in plant secondary metabolism (Geetha and Geetha, 2014). Many studies on medicinal plants have showed that the phytochemical composition of these plants differ with the developmental period or time of the plants. Therefore, seasonal variation of phytochemicals has been investigated extensively (Ncube *et al*., 2011; Kibungu *et al*., 2021; Soni *et al*., 2015; Sultan *et al*., 2018; Gololo *et al*., 2016; Bhardwaj *et al*., 2019; Demuner *et al*., 2011; Lubbe *et al*., 2013; Tomar *et al*., 2015; Scognamiglio *et al*. 2015; Kim *et al*., 2015; Gazim *et al*., 2010; Falasca *et al*., 2014).

1.9. Conclusion

Currently, the drug discovery paradigm has moved towards a reductionist approach. This is because the reductionist approach has dominated the pharmaceutical industry and various effective drugs have emerged from this approach (Duval, 2018). Although, many effective and valuable drugs are available on the market, various diseases are still not properly treated, regardless of the best efforts of drug scientists and inventers (Burke *et al*., 2007). Hence, there is a need to design pharmaceutical agents that act on multiple targets or disease pathways using holistic and reductionist drug discovery approaches. This is because these approaches are both autonomous and neither of the approaches has been confirmed to be greater than the other ones (Fang and Casadevall, 2011).

1.10. Rationale and motivation of the study

Medicinal plants are commonly used by more than 80 % of the people in developing countries around the world for their primary health care and well-being (WHO, 2004). The successive isolation, characterisation and identification of active compounds have been applied to determine the bioactivity of herbal medicinal plants using the reductionist approach (which determines the paradigm single target, single compound). However, this approach has been proven to be time-consuming in the process consisting of the isolation of known components and determining the structures of these compounds (Regenmortel, 2004; Malviya and Malviya, 2017). Therefore, a holistic approach is more suitable in the study of natural products because this approach focuses on active compounds or a mixture of chemical compounds acting synergistically (Fang and Casadevall, 2011). In this study, the phytochemicals contributing to the bioactivity of different *Breonadia salicina* parts were investigated using a reductionist approach and a holistic approach. The reductionist approach was carried out through bioactive-guided fractionation, while the holistic approach was carried out through metabolomics.

The medicinal plant *Breonadia salicina* is used in South Africa and other African countries to treat tachycardia, diarrhoea, vomiting, inflamed wounds, stomach pains, ulcers, fevers, headaches, gastrointestinal illness, malaria, cancer, diabetes, arthritis, pneumonia, as well as bacterial and fungal infections (Amusan *et al*., 2005; van Wyk *et al*., 2011; Venter and Venter, 2002). However, there is no evidence of documented data to correlate the chemistry of the biological activities of *Breonadia salicina*, despite its wide usage. Furthermore, many physiological or medicinal properties of this plant have been reported only for the crude extracts. Moreover, there is no available literature on the seasonal variations and distribution of compounds from various parts of *B. salicina*. Therefore, it is essential to evaluate any possible variation in chemical constituents contributing to the biological activities. This study therefore sought to explore the phytochemistry of *B. salicina* using a metabolomics approach and correlate the phytochemistry to the biological activities.

1.11. Aim of the study

This project set out to explore the phytochemistry and bioactivities of various parts of *B. salicina*.

1.12. Study objectives

The purpose of this study was to:

i. Extract and identify the secondary metabolites of *B. salicina* found in its stem bark, root and leaves.
ii. Determine the chemical profile of the various plant parts by NMR and UPLC-QTOF-MS analysis.
iii. Record the seasonal variation in the phytochemical components of different plant parts.
iv. Evaluate the effects of seasonal variation on the antimalarial and antitrypanosomal activities of different plant parts.
v. Determine the antioxidant, anti-TB, anti-diabetic and anti-inflammatory activities of *B. salicina* crude extracts.
vi. Evaluate the antiproliferation, genotoxicity and cytotoxicity activities against HeLa cells, Vero cells and RAW 264.7 macrophages.

1.13. References

Akinyemi, O.; Oyewole, S.O.; Jimoh, K.A. Medicinal plants and sustainable human health: a review. *Horticulture International Journal*, **2018**, 2, 194-195.

Alamgir, A.N.M. Therapeutic use of medicinal plants and their extracts: Volume 1. *Springer International Publishing AG*, **2017**.

Balunas, M. J.; Kinghorn, A. D. Drug discovery from medicinal plants. *Life Sciences,* **2005**, 78**,** 431-441.

Bhardwaj, S.; Rashmi.; Parcha, V. Effect of seasonal variation on chemical composition and physicochemical properties of *Hedychium spicatum* rhizomes essential oil. *Journal of Essential Oil Bearing Plants*, **2019**, 22, 1593-1600.

Bukar, B.B.; Dayom, D.W.; Uguru, M.O. The growing economic importance of medicinal plants and the need for developing countries to harness from it: A mini review. *Journal of Pharmacology*, **2016**, 6, 2250-3013.

Burke, S.P.; Stratton, K.; Baciu, A. The future of drug safety: promoting and protecting the health of the public. *National Academies Press*, **2007**.

Bussmann, R.W.; Malca, G.; Glenn, A.; Sharon, D.; Nilsen, B.; Parris, B.; Dubose, D.; Ruiz, D.; Saleda, J.; Martinez, M.; Carillo, L. Toxicity of medicinal plants used in traditional medicine in Northern Peru. *Journal of ethnopharmacology*, **2011**, 137, 121-140.

Chen, S.L.; Yu, H.; Luo, H.M.; Wu, Q.; Li, C.F.; Steinmetz, A. Conservation and sustainable use of medicinal plants: problems, progress, and prospects. *Chinese Medicine*, **2016**, 11, 1-10.

Demuner, A.J.; Almeida Barbosa, L.C.; Gonçalves Magalhaes, C.; Da Silva, C.J.; Alvares Maltha, C.R.; Lelis Pinheiro, A. Seasonal variation in the chemical composition and antimicrobial activity of volatile oils of three species of *Leptospermum* (Myrtaceae) grown in Brazil. *Molecules*, **2011**, 16, 1181-1191.

De Oliveira, R.B.; De Paula, D.A.C.; Rocha, B.A.; Franco, J.J.; Gobbo-Neto, L.; Uyemura, S.A.; Dos Santos, W.F.; Da Costa, F.B. Renal toxicity caused by oral use of medicinal plants: the yacon example. *Journal of Ethnopharmacology*, **2011**, 133, 434-441.

Dettweiler, M.; Marquez, L.; Bao, M.; Quave, C.L. Quantifying synergy in the bioassay-guided fractionation of natural product extracts. *Plos one*, **2020**, 15, 0235723.

Duval, M.X. The inadequacy of the reductionist approach in discovering new therapeutic agents against complex diseases. *Experimental Biology and Medicine*, **2018**, 243, 1004-1013.

Edziri, H.; Mastouri, M.; Mahjoub, A.; Anthonissen, R.; Mertens, B.; Cammaerts, S.; Gevaert, L.; Verschaeve, L. Toxic and mutagenic properties of extracts from Tunisian traditional medicinal plants investigated by the neutral red uptake, VITOTOX and alkaline comet assays. *South African Journal of Botany*, **2011**, 77, 703-710.

Falasca, A.; Melck, D.; Paris, D.; Saviano, G.; Motta, A.; Iorizzi, M. Seasonal changes in the metabolic fingerprint of *Juniperus communis* L. berry extracts by ^{1}H-NMR-based metabolomics. *Metabolomics*, **2014**, 10, 165-174.

Fang, F. C.; Casadevall, A. Reductionistic and holistic science. *Infection and Immunity*, **2011**, 79, 1401–1404.

Fennell, C.W.; Lindsey, K.L.; McGaw, L.J.; Sparg, S.G.; Stafford, G.I.; Elgorashi, E.E.; Grace, O.M.; Van Staden, J. Assessing African medicinal plants for efficacy and safety: pharmacological screening and toxicology. *Journal of Ethnopharmacology*, **2004**, 94, 205-217.

Fiehn, O. Metabolomics: the link between genotypes and phenotypes. *Plant Molecular Biology*, **2002**, 48, 155-171.

Fiehn, O.; Kopka, J.; Dörmann, P. Metabolite profiling for plant functional genomics. *Nature Biotechnology*, **2000**, 18, 1157-1161.

Fitzgerald, M.; Heinrich, M.; Booker, A. Medicinal plant analysis: A historical and regional discussion of emergent complex techniques. *Frontiers in Pharmacology*, **2020**, 10, 1480.

Gazim, Z.C.; Amorim, A.C.L.; Hovell, A.M.C.; Rezende, C.M.; Nascimento, I.A.; Ferreira, G.A.; Cortez, D.A.G., 2010. Seasonal variation, chemical composition, and analgesic and antimicrobial activities of the essential oil from leaves of *Tetradenia riparia* (Hochst.) Codd in Southern Brazil. *Molecules*, **2010**, 15, 5509-5524.

Geetha, T.S.; Geetha, N. Phytochemical screening, quantitative analysis of primary and secondary metabolites of *Cymbopogan citratus* (DC) Stapf. leaves from Kodaikanal hills, Tamilnadu. *International Journal of Pharmtech Research*, **2014**, 6, 521-529.

Gololo, S.S.; Shai, L.J.; Agyei, N.M.; Mogale, M.A. Effect of seasonal changes on the quantity of phytochemicals in the leaves of three medicinal plants from Limpopo province, South Africa. *Journal of Pharmacognosy and Phytotherapy*, **2016**, 8, 168-172.

Goodacre, R.; Vaidyanathan, S.; Dunn, W.B.; Harrigan, G.G.; Kell, D.B. Metabolomics by numbers: acquiring and understanding global metabolite data. *Trends in Biotechnology*, **2004**, 22, 245-252.

Griffiths, W. J., Koal, T., Wang, Y., Kohl, M., Enot, D. P.; Deigner, H. P. Targeted metabolomics for biomarker discovery. *Angewandte Chemie International Edition,* **2010**, 49, 5426-5445.

Katiyar, C.; Gupta, A.; Kanjilal, S.; Katiyar, S. Drug discovery from plant sources: An integrated approach. *Ayu*, **2012**, 33, 10–19.

Kibungu, W.C.; Fri, J.; Clarke, A.M.; Otigbu, A.; Akum Njom, H. Seasonal Variation in Antimicrobial Activity of Crude Extracts of *Psammaplysilla* sp. 1 from Phillips Reef, South Africa. *International Journal of Microbiology*, **2021**, 2021. https://doi.org/10.1155/2021/7568493

Kim, N.K.; Park, H.M.; Lee, J.; Ku, K.M.; Lee, C.H. Seasonal variations of metabolome and tyrosinase inhibitory activity of *Lespedeza maximowiczii* during growth periods. *Journal of Agricultural and Food Chemistry*, **2015**, 63, 8631-8639.

Koek, M.; Jellema, R.; Greef, J.; Tas, A.; Hankemeier, T. Quantitative metabolomics based on gas chromatography mass spectrometry: Status and perspectives. *Metabolomics,* **2011**, 7**,** 307-328.

Koparde, A.A.; Doijad, R.C.; Magdum, C.S. Natural products in drug discovery: In pharmacognosy-medicinal plants. *IntechOpen*, **2019**.

Lautie, E.; Russo, O.; Ducrot, P.; Boutin, J.A. Unraveling plant natural chemical diversity for drug discovery purposes. *Frontiers in Pharmacology*, **2020**, 11, 397.

Li, X.; Zhang, X.; Ye, L.; Kang, Z.; Jia, D.; Yang, L.; Zhang, B. LC-MS-based metabolomic approach revealed the significantly different metabolic profiles of five commercial truffle species. *Frontiers in Microbiology*, **2019**, 10, 2227.

Lubbe, A.; Gude, H.; Verpoorte, R.; Choi, Y.H. Seasonal accumulation of major alkaloids in organs of pharmaceutical crop Narcissus Carlton. *Phytochemistry*, **2013**, 88, 43-53.

Maegawa, H.; Nakamura, T.; Saito, K. Regulation of traditional herbal medicinal products in Japan. *Journal of Ethnopharmacology,* **2014**, 158, 511-515.

Malviya, N.; Malviya, S. Bioassay guided fractionation-an emerging technique influence the isolation, identification and characterization of lead phytomolecules. *International Journal of Hospital Pharmacy*, **2017**, 2, 5.

Martens, J.; Berden, G.; van Outersterp, R.E.; Kluijtmans, L.A.; Engelke, U.F.; van Karnebeek, C.D.; Wevers, R.A.; Oomens, J. Molecular identification in metabolomics using infrared ion spectroscopy. *Scientific Reports*, **2017**, 7, 1-5.

Mothibe, M.E.; Sibanda, M. African traditional medicine: South African perspective. *Traditional and Complementary Medicine*, **2019**, 1-27.

Mück, J.E.; Ünal, B.; Butt, H.; Yetisen, A.K. Market and patent analyses of wearables in medicine. *Trends in Biotechnology*, **2019**, 37, 563-566.

Mulaudzi, R.B.; Ndhlala, A.R.; Kulkarni, M.G.; Finnie, J.F.; Van Staden, J. Anti-inflammatory and mutagenic evaluation of medicinal plants used by Venda people against venereal and related diseases. *Journal of Ethnopharmacology*, **2013**, 146, 173-179.

Nchabeleng, L.; Mudau, F.N.; Mariga, I.K. Effects of chemical composition of wild bush tea (*Athrixia phylicoides* DC.) growing at locations differing in altitude, climate and edaphic factors. *Journal of Medicinal Plants Research*, **2012**, 6, 1662-1666.

Ncube, B.; Finnie, J.F.; Van Staden, J. Seasonal variation in antimicrobial and phytochemical properties of frequently used medicinal bulbous plants from South Africa. *South African Journal of Botany*, **2011**, *77*, 387-396.

Ndhlala, A. R.; Stafford, G.I.; Finnie, J.F.; Van Staden, J. Commercial herbal preparations in KwaZulu-Natal, South Africa. The urban face of traditional medicine. *South African Journal of Botany*, **2011**, 77, 830-843.

Newman D. Screening and identification of novel biologically active natural compounds. *F1000Research*, **2017**, 6, 783.

Ngarivhume, T.; van't Klooster, C.I.; de Jong, J.T.; Van der Westhuizen, J.H. Medicinal plants used by traditional healers for the treatment of malaria in the Chipinge district in Zimbabwe. *Journal of Ethnopharmacology*, **2015**, 159, 224-237.

Okada, T.; Mochamad Afendi, F.; Altaf-Ul-Amin, M.; Takahashi, H.; Nakamura, K.; Kanaya, S. Metabolomics of medicinal plants: the importance of multivariate analysis of analytical chemistry data. *Current Computer-aided Drug Design*, **2010**, 6, 179-196.

Pan, S.Y.; Zhou, S.F.; Gao, S.H.; Yu, Z.L.; Zhang, S.F.; Tang, M.K.; Sun, J.N.; Ma, D.L.; Han, Y.F.; Fong, W.F.; Ko, K.M. New perspectives on how to discover drugs from herbal medicines: CAM's outstanding contribution to modern therapeutics. *Evidence-Based Complementary and Alternative Medicine*, **2013**.

Patti, G. J., Yanes, O.; Siuzdak, G. Innovation: Metabolomics: the apogee of the omics trilogy. *Nature Reviews Molecular Cell Biology*, **2012**, 13, 263-269.

Patwardhan, B.; Vaidya, A. Natural products drug discovery: accelerating the clinical candidate development using reverse pharmacology approaches. *Indian Journal of Experimental Biology*, **2010**, 48**,** 220-227.

Patwardhan, B.; Vaidya, A. D. B.; Chorgghade, M. Ayurveda and natural products drug discovery. *Current Science*, **2004**, 86**,** 789-799.

Regenmortel M. H.V. Reductionism and complexity in molecular biology. Scientists now have the tools to unravel biological and overcome the limitations of reductionism. *EMBO reports*, **2004**, 5, 1016–1020.

Roessner, U.; Bowne, J. What is metabolomics all about. *Biotechniques*, **2009**, 46, 363-365.

Sahoo, N.; Manchikanti, P. Herbal drug regulation and commercialization: An Indian industry perspective. *Journal of Alternative and Complementary Medicine*, **2013**, 19, 957-963.

Sandasi, M.; Kamatou, G. P.; Viljoen, A. M. Chemotaxonomic evidence suggests that *Eriocephalus tenuifolius* is the source of Cape chamomile oil and not *Eriocephalus punctulatus*. *Biochemistry, Biochemical Systematics and Ecology*, **2011**, 39, 328-338.

Sasidharan, S.; Chen, Y.; Saravanan, D.; Sundram, K. M.; Yoga Latha, L. Extraction, isolation and characterization of bioactive compounds from plants' extracts. *African journal of traditional, complementary, and alternative medicines*, **2011**, 8, 1–10.

Scognamiglio, M.; D'Abrosca, B.; Esposito, A.; Fiorentino, A. Chemical composition and seasonality of aromatic mediterranean plant species by NMR-based metabolomics. *Journal of Analytical Methods in Chemistry*, **2015**, 2015. http://doi.org/10.1155/2015/258570

Shafi, A.; Zahoor, I. Metabolomics of medicinal and aromatic plants: Goldmines of secondary metabolites for herbal medicine research. In Medicinal and Aromatic Plants. *Academic Press*, **2021**, 261-287.

Shyur, L.-F.; Yang, N.-S. Metabolomics for phytomedicine research and drug development. *Current Opinion in Chemical Biology*, **2008**, 12, 66-71.

Soner, B. C.; Sahin, A. S.; Sahin, T. K. A survey of Turkish hospital patients' use of herbal medicine. *Europe Journal Integrative Medicine*, **2013**, 5, 547-552.

Soni, U.; Brar, S.; Gauttam, V.K. Effect of seasonal variation on secondary metabolites of medicinal plants. *International Journal of Pharmaceutical Sciences and Research*, **2015**, 6, 3654-3662.

Sowemimo, A.A.; Fakoya, F.A.; Awopetu, I.; Omobuwajo, O.R.; Adesanya, S.A. Toxicity and mutagenic activity of some selected Nigerian plants. *Journal of Ethnopharmacology*, **2007**, 113, 427-432.

Street, R.A.; Prinsloo, G. Commercially important medicinal plants of South Africa: a review. *Journal of Chemistry*, **2013**.

Strohl, W.R. The role of natural products in a modern drug discovery program. *Drug Discovery Today*, **2000**, 5, 39-41.

Sultana, R.; Majid, N.; Nissar, S.; Rather A.M. Seasonal variation of phytochemicals. *International Journal of Pharmacy and Biological Sciences*, **2018**, 8, 987-990.

Tomar, N.S.; Sharma, M.; Agarwal, R.M. Phytochemical analysis of *Jatropha curcas* L. during different seasons and developmental stages and seedling growth of wheat (*Triticum aestivum* L) as affected by extracts/leachates of *Jatropha curcas* L. *Physiology and Molecular Biology of Plants*, **2015**, 21, 83-92.

Van Vuuren, S.F. Antimicrobial activity of South African medicinal plants. *Journal of Ethnopharmacology*, **2008**, 119, 462-472.

Van Wyk, B.E. The potential of South African plants in the development of new medicinal products. *South African Journal of Botany*, **2011**, 77, 812-829.

Veeresham C. Natural products derived from plants as a source of drugs. *Journal of Advanced Pharmaceutical Technology and Research*, **2012**, 3, 200–201.

Verpoorte, R.; Choi, Y. H.; KIM, H. K. Ethnopharmacology and systems biology: A perfect holistic match. *Journal of Ethnopharmacology*, **2005**, 100**,** 53-56.

Wakdikar, S. Global health care challenge: Indian experiences and new prescriptions. *Electronic Journal of Biotechnology*, **2004**, 7, 2-3.

Weller M. G. A unifying review of bioassay-guided fractionation, effect-directed analysis and related techniques. *Sensors (Basel, Switzerland)*, **2012**, 12, 9181–9209.

World Health Organization (WHO). WHO Guidelines on Safety Monitoring of Herbal Medicines in Pharmacovigilance Systems. *Geneva, Switzerland: World Health Organization*, **2004**.

Wurtele, E. S.; Chappell, J.; Jones, A. D.; Celiz, M. D.; Ransom, N.; Hur, M.; Rizshsky, L.; Crispin, M.; Dixon, P.; Liu, J.P.; Widrlechner, M.; Nikolau, B. J. Medicinal plants: a public resource for metabolomics and hypothesis development. *Metabolites*, **2012**, 2, 1031–1059.

Zhang, M.; Aguilera, D.; Das, C.; Vasquez, H.; Zage, P.; Gopalakrishnan, V.; Wolff, J. Measuring cytotoxicity: a new perspective on LC_{50}. *Anticancer Research*, **2007**, 27, 35-38.
Zhang, Y.; Zhang, H.; Chang, D.; Guo, F.; Pan, H.; Yang, Y. Metabolomics approach by ^{1}H-NMR spectroscopy of serum reveals progression axes for asymptomatic hyperuricemia and gout. *Arthritis Research and Therapy*, **2018**, 20, 1-11.

CHAPTER 2 BOTANY, PHYTOCHEMISTRY AND PHARMACOLOGICAL ACTIVITIES OF *BREONADIA SALICINA*

2.1. INTRODUCTION

Breonadia salicina is assigned to the family Rubiaceae. This family comprises about 13 500 species in about 620 genera and is one of the largest families in the angiosperms. There are four subfamilies, viz. Antirheoideae, Cinchonoideae, Ixoroideae, and Rubioideae (Mongrand *et al*., 2005). *Breonadia* is the only genus in the Rubiaceae family consisting of one species, and belongs to the Cinchonoideae subfamily (Mongrand *et al*., 2005). *B. salicina* grows in the tropical and subtropical areas of Africa and Saudi Arabia. In South Africa, it is distributed widely in the northeast of the country, from Limpopo to Mpumalanga and KwaZulu-Natal, growing on the banks or even in the water of permanent watercourses (Beech *et al*., 2017). Preliminary phytochemical investigations have revealed that *B. salicina* contains saponins, tannins, carbohydrates, flavonoids, pentacyclic triterpenoids, phenols, phytosterols and coumarins (Ali *et al*., 2018; Mahlo *et al*., 2013; Nvau *et al*., 2019; Martins and Nunez, 2015). This comprises a wide range of secondary metabolites with reputed medicinal properties such as antioxidant, anti-inflammatory, anti-diabetic, antimicrobial, antiplasmodial, antidiarrheal and antitumor properties (Sibandze *et al*., 2010).

2.2. BOTANICAL DESCRIPTION

Breoanadia salicina (Figure 2.1), called ‘‘Transvaal teak’’ in English, “mingerhout,” “waterboekenhout” or “basterkiaat” in Afrikaans, “mutulume” in tshiVenda, and “matumi” in sePedi, is a tree growing up to 40 m in height. The stem bark is grey to brown in colour, with rough edges. The leaves are generally in spirals of four and are packed at the ends of the twigs. Furthermore, the leaves do not have hair. The veins are light yellow to green and the bulky petioles are up to 20 mm long. The flowers are small, have a light lavender colour and have round axillary heads of up to 40 mm in width on long thin stalks of up to 60 mm long. Moreover, the flowers have a pleasant scent with two leaf-like bracts along their length. They are bisexual, and all floral parts are in fives, spreading into a funnel-shaped throat and five-lobed cup-shaped disc. The stamens are inserted in the throat of the tube bulging from the mouth, and the two-chambered ovary containing light yellow balls develops in the leaf source from November to March.

Furthermore, the fruits are small and have a brown colour with two-lobed capsules which are compactly clustered into round heads which grow in the leaf source, giving a jagged, hard, wart-like appearance. The width of the fruit is 2-3 mm and they are visible during January and February (Coates Palgrave *et al*., 2002).

(a) (b) (c)

Figure 2.1: A typical example of *Breonadia salicina* (a) stem bark, (b) root, and (c) leaves (c). Photographs by D.B. Tlhapi.

2.3. ETHNOMEDICINAL USES

Breonadia salicina is traditionally used in South Africa and some African countries as a medicine. In Tanzania, Ethiopia and South Africa, the root decoctions are taken as a laxative against tachycardia and diarrhoea (Arbonnier, 2004). A mixture of the crushed stem is given to both adults and children in South Africa for the treatment of diarrhoea, vomiting, cancer, diabetes, malaria, inflamed wounds, ulcers, bacterial and fungal infections (Mahlo *et al*., 2013). In South Africa, Zulu people use the bark for stomach complaints, while the Vhavenda use root decoctions for the treatment of tachycardia (Darbyshire *et al*., 2015). A leaf decoction is used in Nigeria to manage, treat, and control yellow fever (Arbonnier, 2004). In Malawi a leaf potion is drunk to inhibit diarrhoea and indigestion, whereas in Madagascar a leaf decoction is drunk to suppress malaria (Arbonnier, 2004). Furthermore, in Malawi the bark is chewed for the treatment of diarrhoea and stomach-ache, and a bark mixture is drunk for the treatment of pneumonia, gastrointestinal illness, fevers, headaches, and arthritis.

In Tanzania bark infusions are used to prevent influenza, for stomach problems and to clean wounds. Dried powdered bark is applied as a wound dressing (Bekele-Tesemma and Tengnäs, 2007). The wood is also suitable for making fruit boxes, kitchen furniture and shelving, as well as heavy construction (including bridges). Household utensils and drums are sometimes carved from it. In southern Tanzania the wood is used widely to make fire, while the twigs are used for cleaning teeth in West Africa. *B. salicina* is often planted as an ornamental tree and sometimes for erosion control and windbreaks. The flowers serve as bee forage. In Madagascar the bark is added in the preparation of local alcoholic drinks ('toaka gasy') to help fermentation (Coates Palgrave *et al*., 2002).

2.4. PHYTOCHEMISTRY

Phytochemicals often exhibit biological or toxicological activities, and are frequently used in the treatment of various ailments (Crozier *et al*., 2008). They are mostly produced for chemical protection against attack by animals, insects, microorganisms (fungi and bacteria), and other plants competing for nutrients and light, but can also serve as a form of chemical store for the plant (Nagel *et al*., 2006). Secondary metabolites are made within the plants, and are the final products of the primary biosynthetic and metabolic pathways for compounds related with plant development (Nagel *et al*., 2006). Natural products can be classified into two main categories: primary metabolites, produced by all living organisms, and secondary metabolites, produced only by plants (Bernhoft *et al*., 2020). Chemically, the secondary plant metabolites can be classified broadly as glycosides, flavonoids, tannins, alkaloids, steroids, saponins, terpenes and phenolic compounds (Bernhoft *et al*., 2020). The family Rubiaceae is a rich source of flavonoids, anthraquinones, coumarins, indole alkaloids, iridoids, quinic acid glycosides, saponins, tannins, terpenoids (diterpenes and triterpenes), and other phenolic derivatives that are found in roots, stem bark and leaves (Martins and Nunez, 2015; Heitzman *et al*., 2005). Many of these compound classes are pharmacologically active, with such properties as antioxidant, anti-inflammatory, anti-diabetic, antimicrobial, antiplasmodial, antidiarrheal and antitumor properties (Sibandze *et al*., 2010), but the phytochemistry and bioactivities of the secondary metabolites of *B. salicina* are not well known or described. Furthermore, most of the biological testing of this plant has been confined to crude organic extracts, and very few pure compounds have been isolated; these include 2,4-dihydroxycinnamic acid, coumarins (such as 7-(*β*-D-apiofuranosyl (1-6)-*β*-D-glucopyranosyl) umbelliferone, 7-hydroxycoumarin and 6-hydroxy-7-methoxycoumarin), pentacyclic triterpenoids (such as *α*-amyrin and ursolic

acid), and a phytosterol (stigmasterol) (Mahlo *et al*., 2013; Nvau *et al*., 2019; Ayo *et al*., 1930). Because the biological activities of most of the pure compounds isolated from *B. salicina* have not yet been assessed, it would be useful to isolate and identify the main phytochemicals from different parts of *B. salicina*, and determine the pharmacological activities responsible for their ethno-traditional use. A short survey of the secondary metabolites previously found in *B. salicina* is presented in the following sections.

2.4.1. Terpenoids

Terpenoids are a ubiquitous group of metabolites comprising linear functionalized hydrocarbons and chiral carbocyclic skeletons decorated with functional groups such as aldehyde, carboxyl, ether, hydroxyl, ketone, and peroxide groups. Furthermore, the structures of terpenes vary from linear to polycyclic molecules, depending on the isoprenoid units (Ludwiczuk *et al*., 2017). Ursolic acid (**1,** Figure 2.2), a pentacyclic triterpenoid, was isolated by Mahlo *et al*. (2013) from the chloroform leaf extract of *B. salicina*. Furthermore, the antifungal potential of ursolic acid (**1**) has been reported before (Mahlo *et al*., 2013). Alpha-amyrin (**2**), another pentacyclic triterpenoid, has been isolated from the crude methanol stem bark extract of *B. salicina* using silica gel column chromatography (Nvau *et al*., 2019). A literature survey shows that the biological activity of α-amyrin (**2**) has not been evaluated yet.

2.4.2. Phenolic acids and phenolic compounds

Phenolic acids are aromatic acids that contain a phenolic ring and a carboxyl functional group. They can be classified into flavonoids and tannins, depending on their structure (Pascual-Teresa *et al*., 2010). Phenolic compounds are complex compounds composed of one or more aromatic rings attached to at least one hydroxyl group (Khoddami *et al*., 2013). Based on the number of phenolic units in the molecule, phenolic compounds can be categorised as phenols or polyphenols (Khoddami *et al*., 2013). Ayo *et al*. (1930) isolated 2,4-dihydroxycinnamic acid (**3**, Figure 2.2) from the ethyl acetate stem bark extract. The compound was obtained with petroleum ether/ethyl acetate (80:20) using preparative thin layer chromatography. A literature survey shows that the biological activity of 2,4-dihydroxycinnamic acid (**3**) has not yet been evaluated.

2.4.3. Phytosterols

The core structure of a sterol comprises a fusion of three cyclohexane rings, one cyclopentane ring, and usually a hydroxyl group at the 3-position of the A-ring, similar to the structure of cholesterol (Fernandes and Cabral, 2007). The functional groups of a sterol may involve unsaturation, a methyl group or an ethyl group (Cabral and Klein, 2017). According to a literature survey, stigmasterol (**4**, Figure 2.2) is the only phytosterol isolated from *Breonadia salicina*. This compound was isolated from a methanol extract of the stem bark of *B. salicina* using silica gel column chromatography (Nvau *et al* (2019). Furthermore, the pharmacological properties of stigmasterol (**4**) have never been reported.

2.4.4. Coumarins

Coumarins are unsaturated lactones which consist of another class of compounds C_6C_3. They exhibit various biological activities, such as anti-hypertension, analgesic, antiseptic, antitumor and toxicity (Matos *et al*., 2015). According to the literature survey, 7-(*β*-D-apiofuranosyl (1-6)-*β*-D-glucopyranosyl) umbelliferone (**5**), 7-hydroxycoumarin (**6**) and 6-hydroxy-7-methoxycoumarin (**7**) were isolated from the crude methanol stem bark extract of *B. salicina* using silica gel column chromatography, as shown in Figure 2.2 (Nvau *et al.*, 2019). The coumarins isolated from the plant have not been associated with any of the medicinal properties of *B. salicina*.

2.5. PHARMACOLOGICAL ACTIVITIES

2.5.1. Antifungal activity

Mahlo *et al.* (2013) found that chloroform extracts of the leaf of *B. salicina* had the highest antifungal activity against the fungal species *Penicillium expansum*, *Penicillium janthinellum* and *Fusarium oxysporum*, with a MIC of 0.16 mg/mL using bioautography. However, the positive control, amphotericin B (AmpB) had a MIC of <0.02 mg/mL; and had the highest activity than *Penicillium expansum*, *Penicillium janthinellum* and *Fusarium oxysporum* fungal species.

2.5.2. Antibacterial activity

Al-Qurainy *et al.* (2013) reported that *B. salicina* also has antibacterial activities. They found that the inhibition zone for the methanolic leaf extract (per disk; 30 µL) was 3.0 mm against *Bacillus subtilis* (ATCC 10400), *Escherichia coli* (ATCC 442), *Shigella sonnei* (ATCC 11060), *Pseudomonas aeruginosa* (ATCC 27853) and *Staphylococcus aureus*. Furthermore, the inhibition zone for the aqueous leaf extract (per disk; 25 µL and 30 µL) was 2.5 mm and 3.0 mm against *Bacillus subtilis* (ATCC 10400), *Escherichia coli* (ATCC 442), *Shigella sonnei* (ATCC 11060), *Pseudomonas aeruginosa* (ATCC 27853) and *Staphylococcus aureus*, respectively.

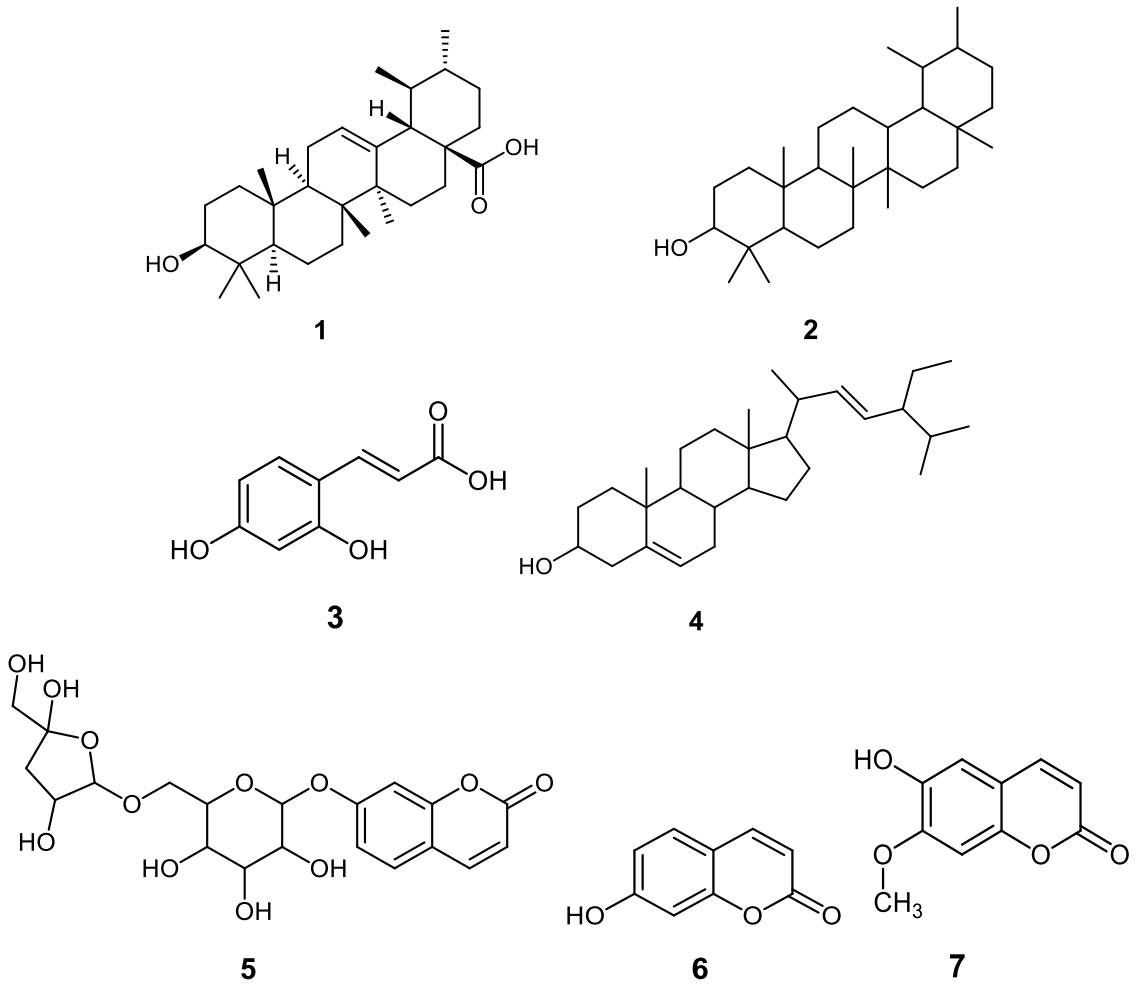

Figure 2.2: Structures of ursolic acid (**1**), α-amyrin (**2**), 2,4-dihydroxycinnamic acid (**3**), stigmasterol (**4**), 7-(β-D-apiofuranosyl (1-6)-β-D-glucopyranosyl) umbelliferone (**5**), 7-hydroxycoumarin (**6**) and 6-hydroxy-7-methoxycoumarin (**7**).

2.5.3. Antioxidant activity

Sibandze (2009) reported the antioxidant activities of extracts of *B. salicina* stem bark and leaves. They also showed that the stem bark and leaf extracts had the highest antioxidant activity against DPPH, with an IC_{50} value of 24.9 ± 13.14 µg/mL and 25.86 ± 2.86 µg/mL, respectively. However, ascorbic acid had higher antioxidant activity than the dichloromethane/methanol (1:1) stem bark and leaf extracts, with an IC_{50} value of 5.61 ± 1.13 µg/mL against DPPH.

2.5.4. Antimalarial activity

Sibandze (2009) found that a dichloromethane/methanol (1:1) stem bark extract had antimalarial activity, with an IC_{50} value of 7.41 ± 1.37 µg/mL, against the asexual stages of the 3D7 strain of *Plasmodium falciparum*, determined using the tritiated hypoxanthine incorporation assay. However, the reference drugs chloroquine and quinine were more active than the dichloromethane/methanol (1:1) stem bark extract, with IC_{50} values of 0.052 ± 0.003 µg/mL and 0.13 ± 0.01 µg/mL, respectively.

2.5.5. Antitrypanosomal activity

Ali *et al.* (2018) reported that the 70 % hydro-ethanolic leaf extract and the 100 % ethanolic leaf extract had antitrypanosomal activities against *Trypanosoma brucei brucei* at concentrations of 0.5 mg/mL, 2.5 mg/mL, 5 mg/mL and 10 mg/mL at 10 min using *in-vitro* antitrypanosomal assay against *T. b. brucei* (Federe stain). However, the control showed the same response, indicating no motile parasites after treatment with somarin at concentrations of 0.5 mg/mL, 2.5 mg/mL, 5 mg/mL and 10 mg/mL at 10 min for both 70 % hydro-ethanolic and 100 % ethanolic leaf extracts

2.5.6. Cytotoxic activity

Mahlo *et al.* (2013) also showed that the chloroform extracts of the leaf of *B. salicina* were less toxic against Vero monkey kidney cells, with a LC_{50} value of 82 µg/mL at the tested concentration of 200 µg/mL, using the MTT (3-(4,5-dimethylthiazol)-2,5-diphenyl tetrazolium bromide) assay. Moreover, Sibandze (2009) reported that the crude methanol/dichloromethane (1:1) stem bark and leaf extracts did not affect the human kidney epithelial cells, with IC_{50} values of 70.84 ± 2.72 µg/mL and 182.66 ± 12.44 µg/mL, respectively; using the 3-(4,5-dimethylthiazol-2yl)-2,5-diphenyltetrazolium bromide (MTT) assay. Therefore, *Breonadia*

salicina is a potential source for the isolation of safe and effective compounds for the treatment of various diseases.

2.6. References

Ali, S.; Umar, A.Z.; Asmau, M.; Deepa, S.; Milli, J.; Fatima, H. In vitro antitrypanosomal activity of *Breonadia salicina* on *Trypanosoma brucei brucei*. *International Journal of Pharmaceutical Sciences and Research*, **2018**, 9, 975-9492.

Al-Qurainy, F.; Gaafar, A.Z.; Khan, S.; Nadeem, M.; Tarroum, M.; Alaklabi, A.; Thomas, J. Antibacterial activity of leaf extract of *Breonadia salicina* (Rubiaceae), an endangered medicinal plant of Saudi Arabia. *Genetics and Molecular Research*, **2013**, 12, 3212-9.

Arbonnier, M. Trees, shrubs and lianas of West African dry zones. *Quae*, **2004**.

Ayo, S.G.; Habila, J.D.; Achika, J.I.; Akinwande, O.O. Isolation and characterization of 2,4-dihydroxycinnamic acid from the stem bark of *Adina microcephala* Delile. *Chemical Society of Nigeria*, **1930**, 47BCC70.

Bekele-Tesemma, A.; Tengnäs, B. Useful trees and shrubs of Ethiopia: identification, propagation, and management for 17 agroclimatic zones. Nairobi, Kenya: RELMA in ICRAF Project, World Agroforestry Centre, Eastern Africa Region, **2007**, 552.

Beech, E.; Rivers, M.; Oldfield, S.; Smith, P.P. Global Tree Search: The first complete global database of tree species and country distributions. *Journal of Sustainable Forestry*, **2017**, 36, 454-489.

Bernhoft, A. Bioactive Compounds in Plants: Benefits and Risks for Man and Animals: Proceedings from a Symposium Held in Norwegian Academy of Science and Letters, Oslo, **2010**, 13-14.

Cabral, C. E.; Klein, M. Phytosterols in the Treatment of Hypercholesterolemia and Prevention of Cardiovascular Diseases. *Arquivos Brasileiros de Cardiologia*, **2017**, 109, 475–482.

Coates Palgrave, K.; Drummond, R.B.; Moll, E.J.; Palgrave, M.C. Trees of Southern Africa. Cape Town: Struik, **2002**.

Crozier, A.; Clifford, M.N.; Ashihara, H. Plant secondary metabolites: occurrence, structure and role in the human diet. New York: John Wiley and Sons, **2008**.

Darbyshire, I.; Kordofani, M.; Farag, I.; Candiga, R.; Pickering, H.A. The plants of Sudan and South Sudan: an annotated checklist. *Royal Botanical Gardens, Kew*, **2015**.

Fernandes, P.; Cabral, J.M.S., 2007. Phytosterols: applications and recovery methods. *Bioresource Technology*, **2007**, 98, 2335-2350.

Khoddami, A.; Wilkes, M.A.; Roberts, T.H. Techniques for analysis of plant phenolic compounds. *Molecules*, **2013**, 18, 2328-2375.

Heitzman, M.E.; Neto, C.C.; Winiarz, E.; Vaisberg, A.J.; Hammond, G.B. Ethnobotany, phytochemistry and pharmacology of *Uncaria* (Rubiaceae). *Phytochemistry*, **2005**, 66, 5-29.

Ludwiczuk, A.; Skalicka-Woźniak, K.; Georgiev, M.I. Terpenoids, *Pharmacognosy*, **2017**.

Mahlo, S.M.; McGaw, L.J.; Eloff, J.N. Antifungal activity and cytotoxicity of isolated compounds from leaves of *Breonadia salicina*. *Journal of Ethnopharmacology*, **2013**, 148, 909-913.

Matos, M.J.; Santana, L.; Uriarte, E.; Abreu, O.A.; Molina, E.; Yordi, E.G. Coumarins—an important class of phytochemicals. *Phytochemicals-Isolation, Characterisation and Role in Human Health*, **2015**, 25, 533-538**.**

Martins, D.; Nunez, C.V. Secondary metabolites from Rubiaceae species. *Molecules*, **2015**, 20, 13422-13495.

Mongrand, S., Badoc, A.; Patouille, B.; Lacomblez, C.; Chavent, M.; Bessoule, J.J. Chemotaxonomy of the Rubiaceae family based on leaf fatty acid composition. *Phytochemistry*, **2005**, 66, 549-559.

Nagle, A.; Hur, W.; Gray, N.S. Antimitotic agents of natural origin. *Current Drug Targets*, **2006**, 7, 305-326.

Nvau, B.J.; Sami, B.; Ajibade, O.S.; Gray, I.A.; Igoli, J.O. Adicardin and Other Coumarins from *Breonadia salicina* (Vahl) Hepper. *Tropical Journal of Natural Product Research*, **2019**, 3, 298-301.

Pascual-Teresa, D.; Moreno, D.A.; García-Viguera, C. Flavanols and anthocyanins in cardiovascular health: a review of current evidence. *International Journal of Molecular Sciences*, **2010**, 11, 1679-1703.

Sibandze, G.F. Pharmacological properties of Swazi medicinal plants. MSc Thesis, University of Witwatersrand, Johannesburg, South Africa, **2009**.

Sibandze, G.F.; van Zyl, R.L.; van Vuuren, S.F. The anti-diarrhoeal properties of *Breonadia salicina*, *Syzygium cordatum* and *Ozoroa sphaerocarpa* when used in combination in Swazi traditional medicine. *Journal of Ethnopharmacoogy*, **2010**, 132, 506-511.

CHAPTER 3 ISOLATION AND CHARACTERISATION OF COMPOUNDS FROM *BREONADIA SALICINA*

3.1. ISOLATION OF PLANT METABOLITES

3.1.1. Introduction

Natural products continue to play an important role in the discovery and development of new pharmaceuticals as clinically useful drugs, as starting materials to produce synthetic drugs, or as lead compounds from which new drugs can be designed and synthesized (Atanasov *et al*., 2021). Higher plants have been an extremely popular source of natural products over time; therefore, compounds isolated and identified from medicinal plants will undoubtedly continue to make important contributions to modern therapeutics (Lahlou, 2013). The study and structure elucidation of natural products makes use of a combination of spectroscopic techniques. The most common techniques for analysing natural products include nuclear magnetic resonance (NMR) spectroscopy, to determine connectivities, mass spectrometry (MS), to ascertain the accurate molecular mass of the isolated compounds (Havlicek and Jaroslav, 2014), and infrared (IR) spectroscopy, to evaluate the presence of functional groups (Huck, 2015). Therefore, this chapter explores the distribution of the chemical constituents in the various plant parts (leaf, stem bark and root). Although the methods for isolating phytochemicals from various parts of *B. salicina* have been previously reported (Mahlo *et al*., 2013; Nvau *et al*., 2019; Ayo *et al*., 1930), the isolation methodology has not been published, and is therefore difficult to repeat. Thus, biomarkers of different plant parts of *B. salicina* need to be isolated and purified, so that they can then be used as standards.

3.2. MATERIALS AND METHODS

3.2.1. Sampling and extraction

The leaves, stem bark, and root samples were gathered in October 2019 at Fondwe, a village in Limpopo Province at 22°55′31.9″ South latitude and 30°15′45.0″ East longitude. The samples were identified at the Department of Botany, University of Venda, by Prof. Peter Tshisikhawe. Voucher sample BD 02 was placed in the Department's herbarium. After four weeks' air-drying, the samples were ground with a hammer mill (NETZSCH, Selb, Germany).

The ground stem bark (about 1.74 kg) and 1.01 kg ground root samples were soaked each in 2 L MeOH for 48 hours at ambient temperature. After filtration and evaporation at 45 °C in a rotary evaporator (BÜCHI Labortechnik AG, Flawil, Switzerland), 95.57 g crude ground stem bark extract and 68.82 g crude root extract (Figure 3.1) were obtained. Furthermore, about 1.12 kg ground *B. salicina* leaves were soaked successively at room temperature in 2 L dichloromethane (DCM) followed by MeOH, each for 48 hours. After filtration and evaporation at 45 °C, 20.52 g crude DCM extract and 66.43g crude MeOH extract were obtained (Figure 3.2). The evaporated extracts were each subjected to gradient elution column chromatography over silica gel (Kieselgel 60, Merck), starting with hexane as mobile phase and gradually increasing the polarity with ethyl acetate (EtOAc) and finally MeOH (Maryadele and Neil, 2006).

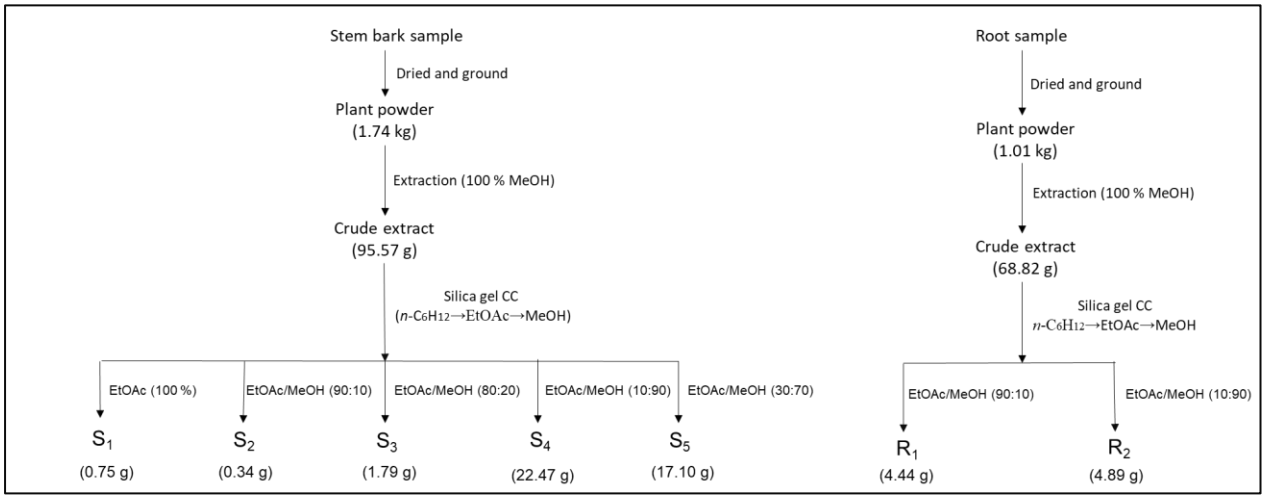

Figure 3.1. Extraction and fractionation of the root and stem bark of *B. salicina*.

3.2.2. Fractionation

Crude MeOH stem bark extract (75.04 g) was reconstituted in a small quantity of MeOH and adsorbed on 199.82 g silica gel. After drying, the adsorbed extract was loaded on a 65 cm x 4.0 cm silica gel column (Kieselgel 60, Merck), that was slurry packed with hexane/EtOAc 50:50. Five fractions coded S_1-S_5 were eluted with EtOAc (100 %), followed by EtOAc/MeOH 90:10, EtOAc/MeOH 80:20, EtOAc/MeOH 10:90, and finally EtOAc/MeOH 30:70, yielding 0.75 g of S_1, 0.34 g of S_2, 1.79 g of S_3, 22.47 g of S_4, and 17.10 g of S_5 (Figure 3.1). Similarly, 50.69 g crude MeOH root extract was re-dissolved in MeOH, adsorbed on 215.42 g silica gel, and after drying the sample was loaded on a silica gel column packed in hexane/EtOAc 50:50. Two root extract fractions were eluted, coded R_1 and R_2. Fraction R_1 (4.44 g) was eluted with

EtOAc/MeOH 90:10, and 4.89 g of fraction R_2 was eluted with EtOAc/MeOH 10:90 (Figure 3.1). Similarly, 15.52 g of the crude DCM leaf extract was chromatographed to yield three fractions coded LD_1-LD_3. Consequently, 1.74 g of LD_1 was obtained with hexane/DCM 80:20, 1.69 g of fraction LD_2 was eluted with DCM, and EtOAc yielded 3.82 g of LD_3 (Figure 3.2).

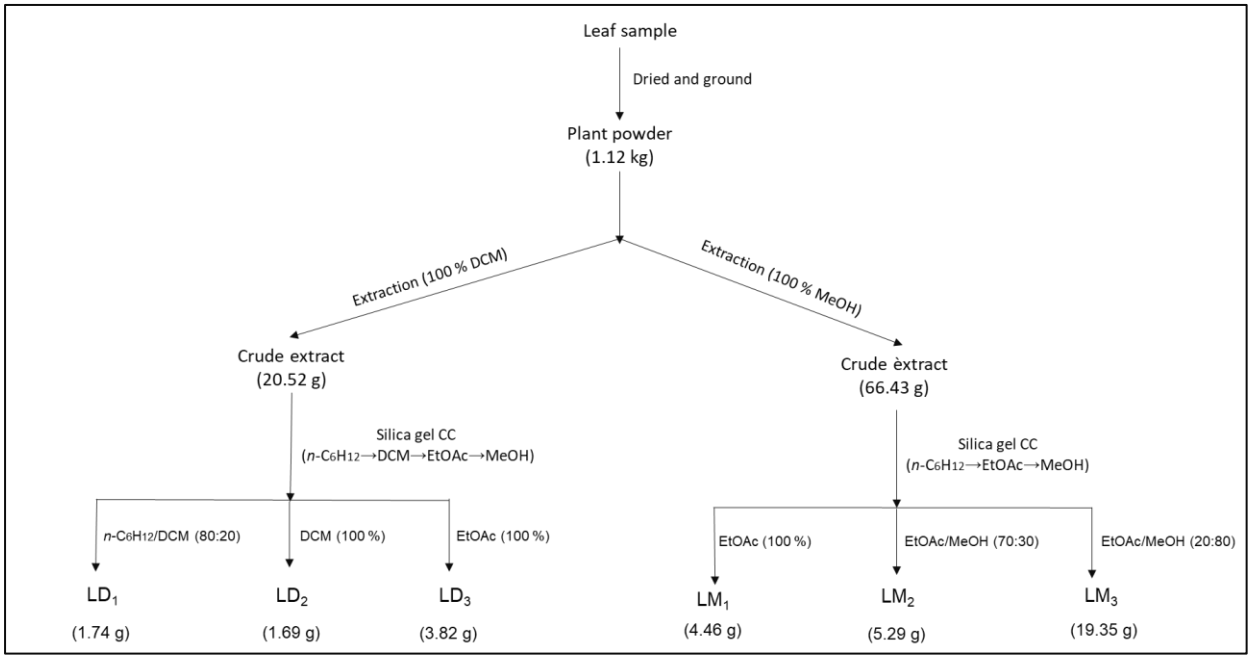

Figure 3.2. Extraction and fractionation of the leaf of *B.salicina*.

Finally, 50.37 g of crude MeOH leaf extract similarly produced three fractions coded LM_1-LM_3. EtOAc eluted 4.46 g of fraction LM_1, EtOAc/MeOH 70:30 yielded 5.29 g of fraction LM_2, and EtOAc/MeOH 20:80 yielded 19.35 g of fraction LM_3 (Figure 3.2). The collection of each crude extract fraction was followed by TLC using chloroform/ethyl acetate/formic acid (32:4:4) as solvent. The compounds with visualized by spraying with a solution of 1 g diphenylboronic acid dissolved in 100 mL MeOH, combined with 5 mL PEG 400 in 95 mL ethanol (EtOH).

3.2.3. Purification of fractions

Preparative normal phase TLC of 0.5 g of Fraction S_1 yielded 0.34 g of compound **1**. The small amount (0.34 g) of fraction S_2 could not be further purified. Preparative normal phase TLC of 0.5 g of fraction S_3 produced 0.36 g of compound **2**. Silica gel column chromatography of 4 g of fraction S_4 with DCM/MeOH 50:50 followed by a DCM/MeOH gradient up to 90:10, yielded 0.27 g of compound **3**. Fraction R_2 was pure compound **4**. Fraction LM_1 was pure compound **5**. Silica gel column chromatography of 5 g of fraction LM_3 with DCM/EtOAc 50:50 was followed by gradient elution with DCM/EtOAc/MeOH mixtures to yield 0.96 g of compound **6**. Fraction LD_1 was pure compound **7**. Silica gel column chromatography of 2 g of Fraction LD_3 with DCM/EtOAc 50:50 and then with DCM/EtOAc/MeOH mixtures, yielded 0.13 g of compound **8**. Fractions S_5, R_1, LM_2, and LD_2 were intractable mixtures that could not be purified further.

3.2.4. Nuclear magnetic resonance (NMR) spectroscopy

The ^{1}H-NMR and ^{13}C-NMR spectra were measured on an Avance 400 spectrometer (Bruker, Fällanden, Switzerland) at 400 MHz and 100 MHz, respectively, with residual undeuterated solvent as internal standard. Chemical shifts are reported as parts per million (ppm). Deuterochloroform ($CDCl_3$), deuterated methanol (CD_3OD), and dimethyl sulfoxide-d_6 (DMSO-d_6) were the solvents used for NMR spectroscopy. The following 2D experiments were also performed: heteronuclear multiple bond correlation (HMBC), heteronuclear single quantum correlation (HSQC), and homonuclear correlation spectroscopy (COSY).

3.2.5. Ultra-performance liquid chromatography-Quadrupole time of flight-Mass spectrometry (UPLC-QTOF-MS)

A Waters Acquity UPLC (Waters, Milford, MA, USA) was connected to a high resolution Waters Synapt G2 Quadrupole time-of-flight (QTOF) MS (Thermo Fisher Scientific) using direct injection (Figure 3.3). A 1 µL sample was injected into a stream consisting of a 60:40 mixture of acetonitrile and 0.1 % aqueous formic acid. The QTOF-MS data was obtained applying both positive and negative electrospray ionisation, with cone voltage 15 V, desolvation temperature 275°C, and desolvation gas flow 650 L/h.

Figure 3.3. UPLC-QTOF-MS instrument. Photograph taken by B.D. Tlhapi.

3.2.6. FTIR analysis of pure compounds

A Bruker Alpha FTIR spectrometer (Fällanden, Switzerland) (Figure 3.4) was used to record attenuated total reflection (ATR) IR spectra.

Figure 3.4. Bruker FTIR spectrometer. Photograph taken by B.D. Tlhapi.

3.2.7. Spectroscopic data

Kaempferol 3-*O*-(2''-*O*-galloyl)-glucuronide (1): Yellow powder, m.p. 215–217 °C (lit. not reported). ^{1}H-NMR (400 MHz, DMSO-d_6): δ_H: 3.19 (1H, t, *J* = 8.4 Hz, 3'''-H), 3.21 (1H, dd, *J* = 9.2 Hz, 2'''-H), 6.25 (1H, d, *J* = 2.3 Hz, 8-H), 6.39 (1H, d, *J* = 2.3 Hz, 6-H), 6.70 (2H, d, *J* = 8.8 Hz, 3'-H, 5'-H), 7.00 (2H, s, 2''-H, 6''-H), 8.25 (2H, d, *J* = 8.8 Hz, 2'-H, 6'-H) ppm. ^{13}C-NMR (100 MHz, DMSO-d_6): δ_C: 71.2 (C-4'''), 74.0 (C-2'''), 79.2 (C-5'''), 79.4 (C-3'''), 94.2 (C-8), 99.4 (C-6), 106.3 (C-1'''), 109.1 (C-2'',6''), 115.4 (C-3',5'), 121.0 (C-1', C-1''), 130.2 (C-2',6'), 132.8 (C-3), 140.9 (C-4''), 146.0 (C-3'', C-5''), 148.4 (C-2), 156.8 (C-5), 163.8 (C-7), 168.0 (C-7'') ppm. HRMS [M-H]$^-$: *m/z* 613.08; calcd. for $C_{28}H_{22}O_{16}$: 613.08129.

3β-Lup-20(29)-en-3-ol (2) (lupeol): White powder, m.p. 217–218 °C (lit. 216–218 °C; Muktar *et al*., 2018). IR: ν_{max} (KBr): 3400 (O-H), 2920.18 (CH_2), 2850.91 (CH_3) cm^{-1}. ^{1}H-NMR (400 MHz, CD_3OD): δ_H: 0.74 (3H, s, 24-H), 0.77 (3H, s, 28-H), 0.87 (3H, s, 25-H), 0.96 (3H, s, 27-H), 0.98 (3H, s, 23-H), 1.02 (3H, s, 26-H), 1.30 (1H, m, 9-H), 1.43 (1H, m, 18-H), 1.52 (1H, m, 2-H), 1.71 (3H, s, 30-H), 1.91 (1H, m, 21-H), 2.23 (1H, m, 19-H), 3.02 (1H, m, *J* = 10.8 Hz, 3-H), 4.61 (1H, s, 29b-H), 4.72 (1H, s, 29a-H) ppm. ^{13}C-NMR (100 MHz, CD_3OD): δ_H: 13.0 (C-27), 13.7 (C-24), 14.6 (C-26), 17.9 (C-28), 18.0 (C-6), 20.1 (C-30), 22.3 (C-11), 25.0 (C-12), 27.9 (C-15), 29.3 (C-2), 30.2 (C-23), 31.6 (C-21), 34.1 (C-7), 36.0 (C-16), 36.2 (C-10), 37.3 (C-13), 38.2 (C-1), 38.5 (C-4), 40.5 (C-8), 42.1 (C-14), 48.2 (C-18), 50.5 (C-9), 56.1 (C-5), 78.2 (C-3), 108.7 (C-29), 150.5 (C-20) ppm. HRMS [M-H]$^-$: *m/z* 455.72; calcd. for $C_{28}H_{22}O_{16}$: 455.3618.

D-Galactopyranose (3): Brown sticky oil. ^{1}H-NMR (400 MHz, CD_3OD): δ_H: 3.32 (1H, m, 3β-H), 3.71 (1H, m, 5β-H), 3.89 (1H, d, 6-H), 3.91 (1H, overlap, 2α-H), 4.10 (1H, overlap, 5α-H), 4.41 (1H, m, 4β-H), 4.52 (1H, dd, 1β-H), 5.16 (1H, d, 1α-H) ppm. ^{13}C-NMR (100 MHz, CD_3OD): δ_C: 62.7 (C-6α), 63.1 (C-6β), 69.7 (C-5α), 70.3 (C-4β), 70.3 (C-3α), 70.3 (C-4α), 71.7 (C-2α), 73.4 (C-2β), 74.1 (C-3β), 76.4 (C-5β), 92.4 (C-1α), 97.8 (C-1β) ppm. HRMS [M-H]$^-$: *m/z* 179.156; calcd. for $C_6H_{12}O_6$: 179.0557.

3-*O*-β-D-Xylopyranosyl-2α,23-dihydroxy-olean-12-en-28-oic acid 28-*O*-α-L-rhamnopyranosyl-(1→2)-β-D-glucopyranoside (4) (bodinioside Q): Brown amorphous solid, m.p. 203–205 °C (lit. not reported). ^{1}H-NMR (400 MHz, CD_3OD): δ_H: 0.82 (3H, s, 29-H), 0.86 (3H, s, 30-H), 0.92 (1H, m, 5-H), 0.95 (3H, s, 24-H), 1.04 (3H, s, 25-H), 1.14 (3H, s, 26-H), 1.19 (3H, s, 27-H), 1.27 (1H, m, 21-H), 1.30 (2H, m, 7-H), 1.46 (1H, m, 6-H), 1.62 (1H, m, 22-H), 1.70 (1H, m, 19-H), 1.95 (1H, m, 9-H), 2.20 (1H, m, 15-H), 2.29 (1H, m, 16-H), 2.85 (1H, d, *J* = 8.8 Hz, 18-H), 3.12 (1H, m, 3-H), 4.48 (1H, m, 23-H), 5.27 (1H, br. s, 12-H) ppm; 3-*O*-sugar: Xyl: 3.80 (1H, overlap, 2'-H), 4.10 (1H, overlap, 3'-H), 4.62 (1H, overlap, 5'-H), 5.12 (1H, d, *J* = 3.6 Hz, 1'-H) ppm; 28-*O*-sugar: Glc: 4.05 (1H, t, *J* = 6.8 Hz, 2''-H), 4.12 (1H, overlap, 5''-H), 4.14 (1H, t, *J* = 7.2 Hz, 4''-H) ppm; Rha: 1.67 (1H, d, *J* = 3.2 Hz, 6'''-H) ppm. ^{13}C-NMR (100 MHz, CD_3OD): δ_C: 13.0 (C-24), 17.4 (C-26), 17.6 (C-25), 20.6 (C-6), 22.7 (C-16), 23.0 (C-30), 23.9 (C-11), 29.1 (C-15), 30.2 (C-20), 30.4 (C-27), 33.5 (C-7, 22, 29), 34.5 (C-21), 37.6 (C-10), 41.3 (C-8), 41.6 (C-4), 42.0 (C-18), 44.5 (C-14), 45.8 (C-19), 46.2 (C-5), 46.7 (C-1), 50.7 (C-9,17), 63.7 (C-23), 68.2 (C-2), 92.5 (C-3), 108.5 (C-28), 122.0 (C-12), 145.1 (C-13) ppm; 3-*O*-sugar: Xyl 68.0 (C-5'), 71.5 (C-4'), 76.0 (C-2'), 81.8 (C-3'), 107.8 (C-1') ppm; 28-*O*-sugar: Glc 61.4 (C-6''), 70.4 (C-4''), 75.6 (C-2''), 81.8 (C-5''), 82.8 (C-3''), 96.7 (C-1'') ppm; Rha 19.4 (C-6'''), 69.8 (C-5'''), 72.4 (C-2'''), 73.5 (C-3'''), 74.8 (C-4'''), 101.7 (C-1''') ppm. HRMS $[M-H]^-$: *m/z* 487 [M–Glc–Rha–Xyl–H]$^-$; calcd. for $C_{47}H_{76}O_{18}$: *m/z*: 487.3448 [M–Glc–Rha–Xyl–H]$^-$.

5-*O*-Caffeoylquinic acid (5): Greenish powder, m.p. 207–209 °C (lit. 209 °C; Gil and Wianowska, 2017). ^{1}H-NMR (400 MHz, CD_3OD): quinic moiety δ_H: 1.51-1.70 (1H, m, 2-H), 1.93-2.29 (1H, m, 6-H), 3.32 (1H, m, 4-H), 3.66 (1H, m, 3-H), 5.24 (1H, m, 5-H) ppm; caffeoyl moiety δ_H: 6.21 (1H, d, 7'-H), 6.79 (1H, d, 5'-H), 6.95 (1H, dd, 6'-H), 7.06 (1H, d, 2'-H), 7.52 (1H, d, 8'-H) ppm. ^{13}C-NMR (100 MHz, CD_3OD): quinic moiety δ_C: 36.6 (C-2), 41.8 (C-6), 68.8 (C-3), 70.7 (C-4), 74.3 (C-5), 76.4 (C-1) ppm; caffeoyl moiety δ_C: 113.6 (C-8'), 113.6 (C-2'), 115.1 (C-5'), 121.6 (C-6'), 126.2 (C-1'), 145.4 (C-7'), 145.8 (C-3'), 148.5 (C-4'), 166.5 (C-9'), 180.2 (COO-) ppm. HRMS $[M-H]^-$: *m/z* 367.311; calcd. for $C_{16}H_{18}O_9$: 367.1107.

***O*-α-D-Glucopyranosyl-(1→2)-β-D-fructofuranoside (6) (sucrose):** Brown sticky solid. ^{1}H-NMR (400 MHz, CD_3OD): δ_H: 3.39 (1H, t, 4-H), 3.50 (1H, dd, *J* = 11.2 Hz, 2-H), 3.63 (2H, s, *J* = 9.2 Hz, 1´-H), 3.72 (1H, t, *J* = 10.2 Hz, 3-H), 3.80 (2H, d, 6´-H), 3.81 (2H, d, *J* = 5.2 Hz, 6-H), 3.83 (1H, m, 5-H), 3.86 (1H, m, 5´-H), 4.02 (1H, t, 4´-H), 4.14 (1H, d, 3'-H), 5.41 (1H,

d, *J* = 3.2 Hz, 1-H) ppm. ^{13}C-NMR (100 MHz, CD_3OD): δ_C: 60.7 (C-6), 61.2 (C-1), 62.5 (C-6'), 67.9 (C-4), 70.2 (C-2), 72.0 (5), 72.2 (C-3), 72.9 (C-4'), 77.8 (C-3'), 81.6 (C-5'), 92.2 (C-1), 103.8 (C-2') ppm. HRMS $[M-H]^-$: *m/z* 341.30; calcd. for $C_{12}H_{22}O_{11}$: 341.1073.

Hexadecane (7): White crystals, m.p. 16–18 °C (lit. 18 °C; Alay *et al*., 2010). ^{1}H-NMR (400 MHz, $CDCl_3$): δ_H: 0.89 (6H, t, 1-H, 16-H), 1.28 (28H, m, 2-H – 15-H) ppm. ^{13}C-NMR (100 MHz, $CDCl_3$): δ_C: 14.1 (C-1,16), 22.7 (C-2,15), 29.3–29.7 (C-4 – C-13), 31.9 (C-3,14) ppm.

Palmitic acid (8): Greenish amorphous solid, m.p. 61–62 °C (lit. 63 °C; Hudson, 2003). IR: ν_{max} (KBr): 3436.00 (O-H), 2917.27 (CH_2), 2849.51 (CH_3), and 1703.71 (C=O) cm^{-1}. ^{1}H-NMR (400 MHz, $CDCl_3$): δ_H: 0.83 (3H, t, 16-H), 1.23 (22H, m, 4-H–14-H), 1.57 (2H, m, 3-H), 1.98 (2H, q, 15-H), 2.27 (2H, t, 2-H) ppm. ^{13}C-NMR (100 MHz, $CDCl_3$): δ_C: 14.1 (C-16), 22.6 (C-15), 24.7 (C-14), 29.0–29.6 (C-4–C-13), 31.9 (C-3), 34.0 (C-2), 178.4 (C-1) ppm. HRMS $[M-H]^-$: *m/z* 255.40; calcd. for $C_{16}H_{32}O_2$: 255.23295.

3.3. RESULTS AND DISCUSSION

3.3.1. Structure elucidation of the isolated compounds

3.3.1.1. Spectroscopic data of Compound 1

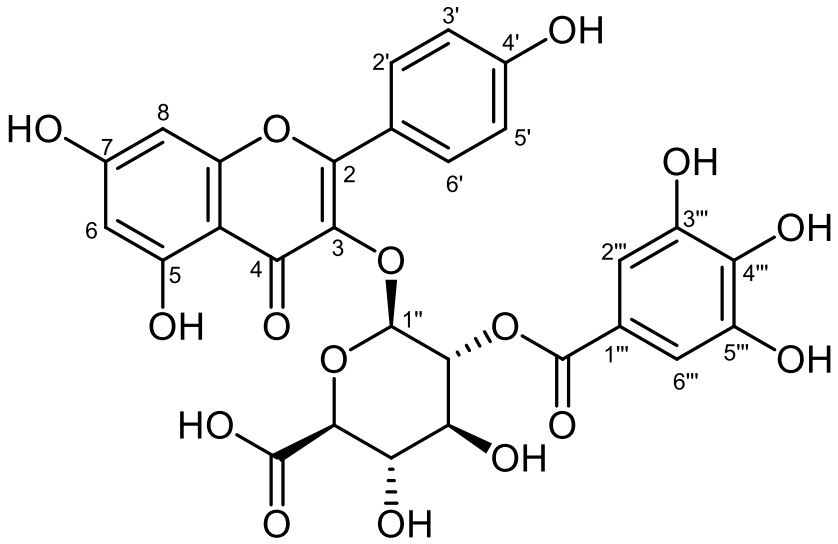

Figure 3.5. Structure of kaempferol 3-*O*-(2''-*O*-galloyl)-glucuronide (**1**).

The HRMS spectrum (Appendix 1) revealed a $[M-H]^-$ peak at *m/z* 613.08129, corresponding to the molecular formula $C_{28}H_{22}O_{16}$. The ^{1}H-NMR spectrum (Appendix 2A) had six aromatic signals at δ_H 6.25 (1H, d, *J* = 2.3 Hz, 8-H), 6.39 (1H, d, *J* = 2.3 Hz, 6-H), 6.706 (2H, d, *J* = 8.8 Hz, 3'-H, 5'-H), and 8.25 (2H, d, *J* = 8.8 Hz, 2'-H, 6'-H) ppm respectively. The ^{13}C-NMR (Appendix 3) and DEPT135 (Appendix 4) spectra showed the presence of 11 methine carbons at δ_C 71.2 (C-4'''), 74.0 (C-2'''), 79.2 (C-5'''), 79.4 (C-3'''), 79.4 (C-3'''), 99.4 (C-6), 106.3 (C-1'''), 109.1 (C-2",6"), 115.4 (C-3',5'), and 121.0 (C-1") ppm. Furthermore, the HSQC spectrum (Appendix 5) showed correlations between δ_H 6.70 ppm (2H, d, 3'-H, 5'-H) and δ_C 115.4 ppm (C-3',5'); between δ_H 7.00 (2H, s, 2"-H, 6"-H) and δ_C 109.1 ppm (C-2",6"); and between δ_H 3.19 (1H, t, 3'''-H) and δ_C 71.2 ppm (C-4'''), respectively. Moreover, the HMBC spectrum (Appendix 6) displayed correlations between δ_H 6.70 (2H, d, 3'-H, 5'-H) and δ_C 130.2 ppm (C-2',6'), as shown in Scheme 3.1. The spectroscopic data for kaempferol 3-*O*-(2"-*O*-galloyl)-glucuronide (Table 3.1) are similar to the published data for this compound (Yoshimura *et al*., 2008). This is the first report of the flavonoid **1** from *B. salicina*.

Table 3.1: ^{1}H-NMR (400 MHz) and ^{13}C-NMR (100 MHz) data of kaempferol 3-*O*-(2"-*O*-galloyl)-glucuronide isolated in this study (exp) compared with literature data (lit) (Yoshimura *et al.*, 2008).

Position	^{1}H-NMR (δ_H ppm, *J* in Hz) (exp)	^{1}H-NMR (δ_H ppm, *J* in Hz) (lit)	^{13}C-NMR (δ_C ppm) (exp)	^{13}C-NMR (δ_C ppm) (lit)
2	-	-	148.4	157.7
3	-	-	132.8	133.8
4	-	-	-	178.3
5	-	-	156.8	157.8
6	6.39 (1H, d, *J* = 2.3 Hz)	6.22 (1H, d, *J* = 2.5 Hz)	99.4	99.5
7	-	-	163.8	165.2
8	6.25 (1H, d, *J* = 2.3 Hz)	6.44 (1H, d, *J* = 2.5 Hz)	94.2	94.5
1'	-	-	121.0	122.0
2'	8.25 (2H, d, *J* = 8.8 Hz)	8.08 (2H, d, *J* = 9.0 Hz)	130.2	131.9
3'	6.70 (2H, d, *J* = 8.8 Hz)	6.95 (2H, d, *J* = 9.0 Hz)	115.4	116.1
4'	-	-	-	162.4
5'	6.70 (2H, d)	6.95 (2H, d)	115.4	116.1
6'	8.25 (2H, d)	8.08 (2H, d)	130.2	131.9
1"	-		121.0	122.0

2''	7.00 (2H, s)	7.22 (2H, s)	109.1	110.2
3''	-	-	146.0	145.9
4''	-	-	140.9	139.0
5''	-	-	146.0	145.9
6''	7.00 (2H, s)	7.22 (2H, s)	109.1	110.2
7''	-	-	168.0	166.6
1'''	-	6.00 (1H, d, *J* = 8.0 Hz)	106.3	99.7
2'''	3.21 (1H, dd, *J* = 9.2 Hz)	5.21 (1H, dd, *J* = 8.0 Hz and 9.5 Hz)	74.0	74.8
3'''	3.19 (1H, t, *J* = 8.4 Hz)	3.89 (1H, t, *J* = 9.5 Hz)	79.4	74.9
4'''	-	3.80 (1H, t, *J* = 9.5 Hz)	71.2	72.8
5'''	-	3.94 (1H, t, *J* = 9.5 Hz)	79.2	76.5
6'''	-	-	-	170.6

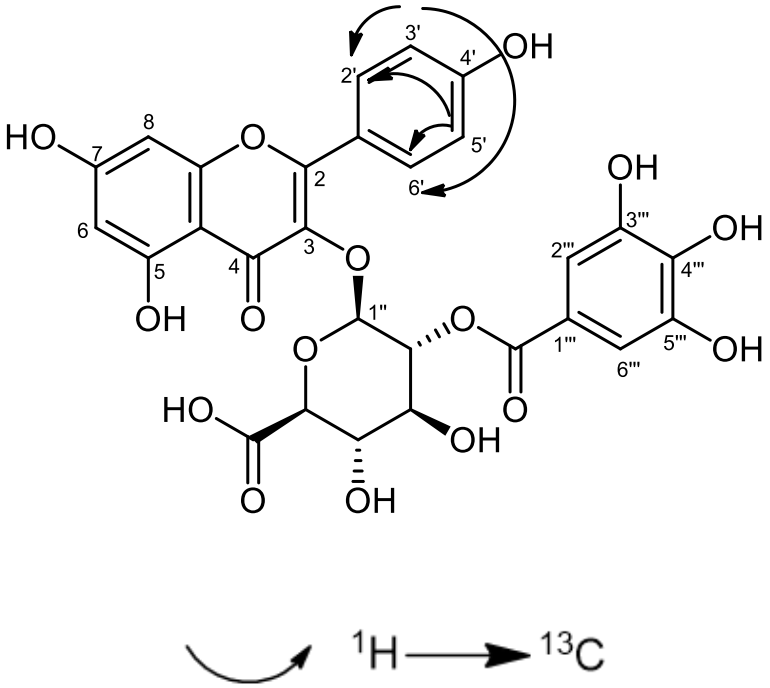

Scheme 3.1: The HMBC correlations of kaempferol 3-*O*-(2''-*O*-galloyl)-glucuronide (**1**).

3.3.1.2 Spectroscopic data for Compound 2

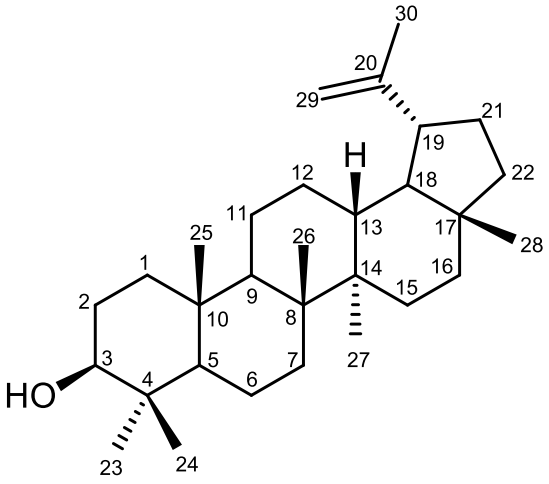

Figure 3.6. Structure of 3β-lup-20(29)-en-3-ol (**2**), lupeol.

The HRMS (Appendix 7) displayed a $[M-H]^-$ peak at *m/z* 455.3618, corresponding to the molecular formula $C_{30}H_{50}O$. The IR spectrum (Appendix 8) of Compound **2** had bands at 3400 cm^{-1} (O-H stretch), 2920.18 cm^{-1} (C-H stretch, $-CH_2-$), and 2850.91 cm^{-1} (C-H stretch, $-CH_3$). The ^{1}H-NMR spectrum (Appendix 9) of Compound **2** revealed the presence of seven methyl groups at δ_H 0.74 (3H, s, 24-H), 0.77 (3H, s, 28-H), 0.87 (3H, s, 25-H), 0.96 (3H, s, 27-H), 0.98 (3H, s, 23-H), 1.02 (3H, s, 26-H), and 1.71 ppm (3H, s, 30-H). A one-proton multiplet at δ_H 2.23 ppm (1H, m) was assigned to 19-H, while the 3-H proton was observed as a multiplet at δ_H 3.02 ppm (1H, m, J = 10.8 Hz). Two broad singlets at δ_H 4.72 (1H, s) and 4.61 ppm (1H, s) were suggestive of the olefinic protons of 29a-H and 29b-H. This indicated the presence of a double bond between a methylene carbon (C-29) and a quaternary carbon (C-20). The HSQC spectrum (Appendix 10) correlated 29a-H (δ_H 4.72 ppm) and 29b-H (δ_H 4.61 ppm) with C-29 (δ_C 108.7 ppm), proving that 29a-H and 29b-H are bound to C-29. The methine signal at δ_H 3.02 ppm (3-H) correlated with a carbon at δ_C 78.2 ppm (C-3). Furthermore, the HSQC spectrum (Appendix 10) revealed the presence of five quaternary carbons at δ_C 36.2 (C-10), 38.5 (C-4), 40.5 (C-8), 42.1 (C-14), and 150.5 (C-20) ppm. The HMBC spectrum (Appendix 11) showed the correlation between the methyl peak at 23-H (δ_H 0.98 ppm) and C-24 (δ_C 13.7 ppm) and C-3 (δ_C 78.2 ppm), respectively. The two broad singlets of the olefinic protons at 29b-H (δ_H 4.61 ppm) and 29a-H (δ_H 4.72 ppm) correlated with the methyl signal for C-30 (δc 20.1 ppm) (Scheme 3.2). The ^{13}C-NMR spectrum (Appendix 12A and 12B) displayed 30 carbon signals. Moreover, the carbon atoms at C-29 and C-20 (δc 108.7 and 150.5 ppm, respectively), revealed the presence of a C=C group. Furthermore, the carbon signal at δc 78.2 ppm (Appendix 12A) was attributed to C-3. Finally, comparing these data (Table 3.2) with

literature data (Mouffok *et al.*, 2012) confirmed the structure of lupeol, a pentacyclic triterpenoid. This is the first reported isolation of the pentacyclic triterpenoid lupeol from *B. salicina*.

Table 3.2: ^{1}H-NMR (400 MHz) and ^{13}C-NMR (100 MHz) data for lupeol (**2**) obtained in this study (exp) and reported in the literature (lit) (Mouffok *et al.*, 2012).

Position	^{1}H-NMR (δ_H ppm, *J* in Hz) (exp)	^{1}H-NMR (δ_H ppm, *J* in Hz) (lit)	^{13}C-NMR (δ_C ppm) (exp)	^{13}C-NMR (δ_C ppm) (lit)
1	-	1.64 (1H, m, 1b-H) 0.94 (1H, m, 1a-H)	38.2	38.7
2	1.52 (1H, m)	1.61 (1H, m)	29.3	27.5
3	3.02 (1H, m, *J* = 10.8 Hz)	3.18 (1H, dd, *J* = 11.0 Hz and 5.3 Hz)	78.2	79.3
4	-	-	38.5	39.8
5	-	0.69 (1H, m)	56.1	55.5
6	-	1.52 (1H, m, 6a-H) 1.39 (1H, m, 6b-H)	18.0	19.0
7	-	1.38 (1H, m)	34.1	34.2
8	-	-	40.5	41.1
9	1.30 (1H, m)	1.30 (1H, m)	50.5	50.9
10	-	-	36.2	37.2
11	-	1.43 (1H, m, 11a-H) 1.29 (1H, m, 11b-H)	20.3	21.2
12	-	1.70 (1H, m, 12a-H) 1.10 (1H, m, 12b-H)	25.0	25.3
13	-	1.62 (1H, m)	38.3	38.5
14	-	-	42.1	42.8
15	-	1.61 (1H, m, 15a-H) 0.96 (1H, m, 15b-H)	27.9	27.2
16	-	1.48 (1H, m)	36.0	35.9
17	-	-	-	43.2
18	1.43 (1H, m)	1.39 (1H, m)	48.2	48.5
19	2.23 (1H, m)	2.38 (1H, m)	-	47.8
20	-	-	150.5	151.2
21	1.91 (1H, m)	1.27 (1H, m)	31.6	30.1
22	-	1.19 (1H, m)	-	40.3
23	0.98 (3H, s)	0.97 (1H, s)	30.2	28.4
24	0.74 (3H, s)	0.77 (1H, s)	13.7	15.6
25	0.87 (3H, s)	0.84 (1H, s)	-	16.2
26	1.02 (3H, s)	1.04 (1H, m)	14.6	16.1
27	0.96 (3H, s)	0.96 (1H, s)	13.0	14.8

28	0.77 (3H, s)	0.80 (1H, s)	17.9	18.1
29	4.72 (1H, s, 29a-H) & 4.61 (1H, s, 29b-H)	4.68 (1H, s, 29a-H) & 4.56 (1H, s, 29b-H)	108.7	109.5
30	1.71 (3H, s)	1.70 (1H, s*l*)	20.1	19.8

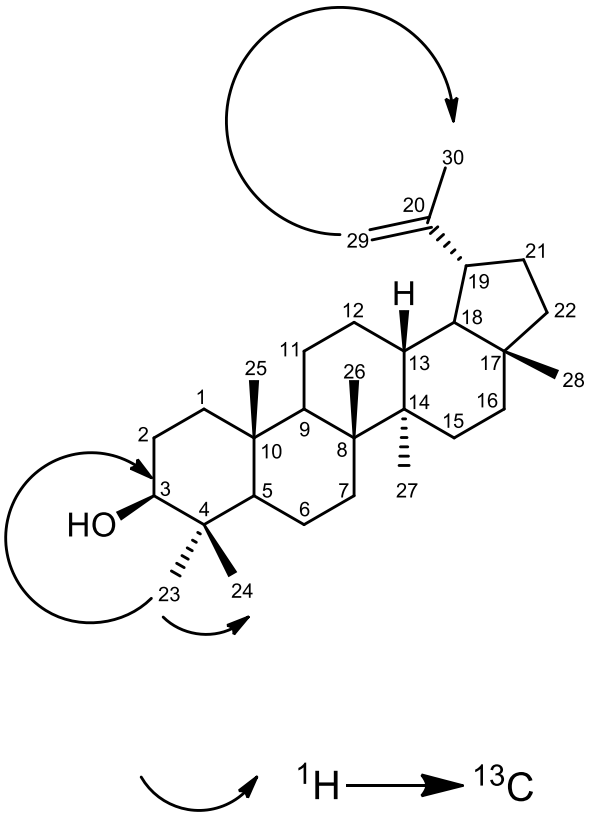

Scheme 3.2: The HMBC correlations of lupeol (**2**).

3.3.1.3. Spectroscopic data for Compound 3

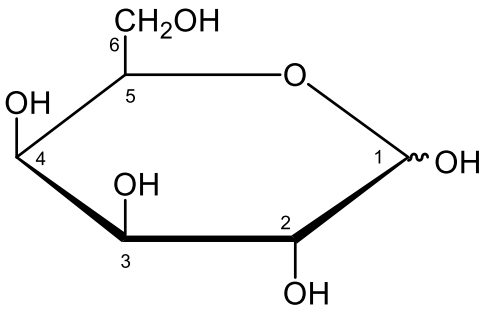

Figure 3.7. Structure of D-galactopyranose (**3**).

The HRMS spectrum of Compound **3** (Appendix 13) had a $[M-H]^-$ peak at *m/z* 179.0557 consistent with the molecular formula $C_6H_{12}O_6$. The ^{1}H-NMR spectrum (Appendix 14) displayed the anomeric proton at δ_H 4.52 (1β-H) and 5.16 (1α-H) ppm. The signal of the α anomeric proton of D-sugars is normally found between δ_H 4.9 and 5.5 ppm, while the β proton signal is usually found between δ_H 4.3 and 4.7 ppm (Ogawa *et al*., 1993). The ^{13}C-NMR (Appendix 15) and DEPT135 (Appendix 16) spectra revealed eight methines at δ_C 69.7 (C-5α), 70.3 (C-3α, 4α, 4β), 71.7 (C-2α), 73.4 (C-2β), 74.1 (C-3β), and 75.59 (C-5β) ppm; two methylene signals at δ_C 63.1 (C-6β) and 63.2 ppm (C-6α); and two anomeric carbons at δ_C 92.4 (C-1α) and 97.8 ppm (C-1β). Moreover, the HSQC spectrum (Appendix 17) correlated 1α-H at δ_H 5.16 ppm with C-1α at δ_C 92.4 ppm ; 1β-H at δ_H 4.52 ppm with C-1β at δ_C 97.8 ppm; and 4β-H at δ_H 4.41 ppm with C-5β (δ_C 76.4 ppm), respectively. Comparing these data (Table 3.3) with literature data (Ogawa *et al*., 1993) confirmed the structure of D-galactopyranose. This is the first report of the isolation of the monosaccharide D-galactopyranose from *B. salicina*.

Table 3.3: ^{1}H-NMR (400 MHz) and ^{13}C-NMR (100 MHz) data of D-galactopyranose obtained in this study (exp) and from the literature (lit) (Ogawa *et al*., 1994).

Position	^{1}H-NMR (δ_H ppm) (exp)	^{1}H-NMR (δ_H ppm) (lit)	^{13}C-NMR (δ_C ppm) (exp)	^{13}C-NMR (δ_C ppm) (lit)
1	5.16 (1H, d, 1α-H) & 4.52 (1H, dd, 1β-H)	5.24 (1α-H) & 4.57 (1β-H)	92.4 (C-1α) & 97.8 (C-1β)	93.6 (C-1α) & 97.9 (C-1β)
2	3.91 (1H, overlap, 2α-H)	2.82 (2α-H) & 3.50 (2β-H)	71.7 (C-2α) & 73.4 (C-2β)	69.8 (C-2α) & 73.4 (C-2β)
3	3.32 (1H, m, 3β-H)	3.51 (3α-H) &	70.3 (C-3α) &	70.7 (C-3α) &

		3.32 (3β-H)	74.1 (C-3β)	74.3 (C-3β)
4	4.41 (1H, m, 4β-H)	4.24 (4α-H) & 4.19 (4β-H)	70.3 (C-4α) & 70.3 (C-4β)	70.8 (C-3α) & 70.2 (C-3β)
5	4.10 (1H, overlap, 5α-H) & 3.71 (1H, m, 5β-H)	4.05 (5α-H) & 3.6 (5β-H)	69.7 (C-5α) & 76.4 (C-5β)	72.0 (C-5α) & 76.6 (C-5β)
6	3.89(1H, d, 6-H)	3.7 (6α-H) & 3.7 (6β-H)	62.7 (C-6α) & 63.1 (C-6β)	62.7 (C-6α) & 62.5 (C-6β)

3.3.1.4. Spectroscopic data for Compound 4

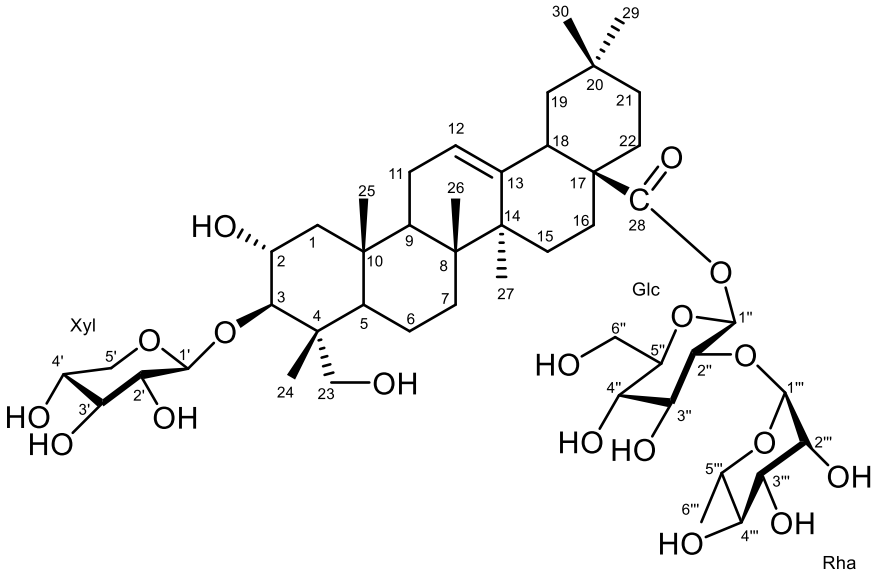

Figure 3.8. Structure of 3-*O*-β-D-xylopyranosyl-2α,23-dihydroxy-olean-12-en-28-oic acid 28-*O*-α-L-rhamnopyranosyl-(1→2)-β-D-glucopyranoside (**4**), bodinioside Q.

The HRMS spectrum of Compound **4** (Appendix 18) displayed a $[M-H]^-$ peak at *m/z* 487.3448 $[M\text{-Glc-Rha-Xyl-H}]^-$, agreeing with the molecular formula $C_{47}H_{76}O_{18}$. The ^{1}H-NMR spectrum (Appendix 19A) showed six methyl signals at δ_H 0.82 (3H, s), 0.82 (3H, s), 0.95 (3H, s), 1.04 (3H, s), 1.14 (3H, s), and 1.19 (3H, s) ppm. Furthermore, the $J_{H1,H2}$ coupling constants of the two anomeric proton signals at δ_H 5.12 ppm (1H, d, J = 3.6 Hz, 1'-H) revealed the β configuration of the xylopyranosyl moiety (Appendix 19B). Moreover, in the HSQC spectrum (Appendix 20) there was clear correlation of carbons C-24 at δ_C 13.0 ppm, C-26 at 17.4, C-25 at 17.6, and C-30 at 23.0 ppm with protons assigned to δ_H 24-H at 0.95, 26-H at 1.14, 25-H at

1.04, and 30-H at 0.86 ppm, respectively. Additionally, the HMBC signal at δ_H 5.27 ppm (1H, br s), assigned to carbon C-12 at δ_C 122.0 ppm (Appendix 21), was coupled to C-13 at δ_C 144.1 ppm, indicating a C=C double bond (Scheme 3.3). These spectroscopic data led to the conclusion that Compound **4** has an olean-12-ene skeleton. The HMBC spectrum (Appendix 21) also revealed correlations of the anomeric carbon signal at position C-1' (δ_C 107.8 ppm) with 2'-H (δ_H 3.80 ppm), and 5'-H (δ_H 4.62 ppm), suggesting D-xylopyranose as part of Compound 4. The ^{13}C-NMR (Appendix 22A,B,C) and DEPT135 (Appendix 23A,B,C) spectra revealed the presence of 15 methines at δ_C 52.9 (C-9), 67.9 (C-2), 68.2 (C-5'), 69.8 (C-5'''), 71.5 (C-4'), 72.4 (C-2'''), 73.4 (C-3'''), 74.8 (C-4''), 75.3 (C-2''), 76.0 (C-2'), 81.8 (C-3',5''), 82.8 (C-3''), 92.5 (C-3), 96.7 (C-1''), and 122.0 (C-12) ppm; eleven methylenes at δ_C 17.7 (C-6), 22.5 (C-16), 22.7 (C-11), 29.3 (C-15), 31.9 (C-22), 32.2 (C-7), 33.4 (C-21), 45.8 (C-19), 46.4 (C-1), 61.3 (C-6''), and 63.0 (C-23) ppm; six methyl groups at δ_C 12.4 (C-24), 16.1 (C-26), 16.4 (C-25), 19.4 (C-6'''), 25.1 (C-30), and 32.4 (C-29) ppm; and five quaternary carbon atoms at δ_C 41.2 (C-8), 46.7 (C-14), 52.9 (C-17), 145.1 (C-28) and 180.5 (C-13) ppm, respectively. Comparing these data (Table 3.4) with literature data (Yang *et al*., 2020) supported the structure of the oleanane triterpenoid saponin, bodinioside Q. This is the first reported isolation of bodinioside Q (**4**) from *B. salicina.*

Table 3.4: ^{1}H-NMR (400 MHz) and ^{13}C-NMR (100 MHz) data for bodinioside Q obtained in this study (exp) and from the literature (lit) (Yang *et al*., 2020).

Position	^{1}H-NMR (δ_H ppm, *J* in Hz) (exp)	^{1}H-NMR (δ_H ppm, *J* in Hz) (lit)	^{13}C-NMR (δc ppm) (exp)	^{13}C-NMR (δc ppm) (lit)
1	-	1.17 (overlap)	46.7	47.9
2	-	4.21 (m)	68.2	66.8
3	3.12 (1H, m)	3.30 (m)	92.5	88.2
4	-	-	41.6	41.9
5	0.92 (1H, m)	0.93 (m)	46.2	47.2
6	1.46 (1H,m)	1.52 (m)	20.2	18.6
7	1.30 (2H, m)	1.36 (m)	33.5	33.0
8	-	-	41.3	41.9
9	1.95 (1H, m)	1.82 (m)	50.7	48.1
10	-	-	37.6	37.7
11	-	1.98 (m)	23.9	23.9
12	5.27 (1H, br. s)	5.42 (br. s)	122.0	122.4
13	-	-	145.1	144.1
14	-	-	46.5	44.6

15	2.20 (1H, m)	2.13 (m)	29.1	28.5
16	2.29 (1H, m)	2.33 (m)	22.7	23.3
17	-	-	50.7	48.1
18	2.85 (1H, d, *J* = 8.8 Hz)	3.08 (d, *J* = 13.6 Hz)	42.0	42.2
19	1.70 (1H, m)	1.70 (m)	45.8	46.2
20	-	-	30.2	30.6
21	1.27 (1H, m)	1.31 (m)	34.5	33.9
22	1.62 (1H, m)	1.66 (m)	33.5	33.0
23	4.48 (1H, m)	4.34 (m)	63.7	63.4
24	0.95 (3H, s)	0.96 (s)	13.0	14.6
25	1.04 (3H, s)	1.03 (s)	17.6	17.4
26	1.14 (3H, s)	1.10 (s)	17.6	17.4
27	1.19 (3H, s)	1.15 (s)	30.4	30.6
28	-	-	108.5	176.3
29	0.82 (3H, s)	0.83 (3H, s)	33.5	33.0
30	0.82 (3H, s)	0.78 (3H, s)	25.0	25.7
1'	5.12 (1H, d, *J* = 3.6 Hz)	5.02 (d, *J* = 7.3 Hz)	107.8	106.3
2'	3.80 (1H, overlap)	4.04 (overlap)	76.0	75.6
3'	4.10 (1H, overlap)	4.14 (overlap)	81.8	78.5
4'	-	4.21 (overlap)	71.5	71.2
5'	4.62 (1H, overlap)	4.33 (overlap) 3.61 (overlap)	68.0	67.2
1"	-	6.19 (d, *J* = 8.1 Hz)	96.7	94.8
2"	4.05 (1H, t, *J* = 6.8 Hz)	4.04 (t, *J* = 8.6 Hz)	75.6	75.3
3"	-	4.20 (t, *J* = 8.2 Hz)	82.8	79.7
4"	4.14 (1H, t, *J* = 7.2 Hz)	4.18 (t, *J* = 9.0 Hz)	70.4	70.7
5"	4.12 (1H, overlap)	4.17 (overlap)	81.8	78.9
6"	-	4.49 (6a-H, overlap) 4.41 (dd, 6b-H, *J* = 12.1 Hz and *J* = 2.0 Hz)	61.4	61.9
1'"	-	6.11 (br. s)	101.7	101.4
2'"	-	4.40 (dd, *J* = 3.2 Hz and *J* = 1.5 Hz)	72.4	72.2
3'"	-	4.56 (overlap)	73.5	72.4
4'"	-	4.42 (t, *J* = 9.0 Hz)	74.8	73.8
5'"	-	4.55 (overlap)	69.8	69.7
6'"	1.67 (1H, d, *J* = 3.2 Hz)	1.75 (d, *J* = 6.1 Hz)	19.4	16.6

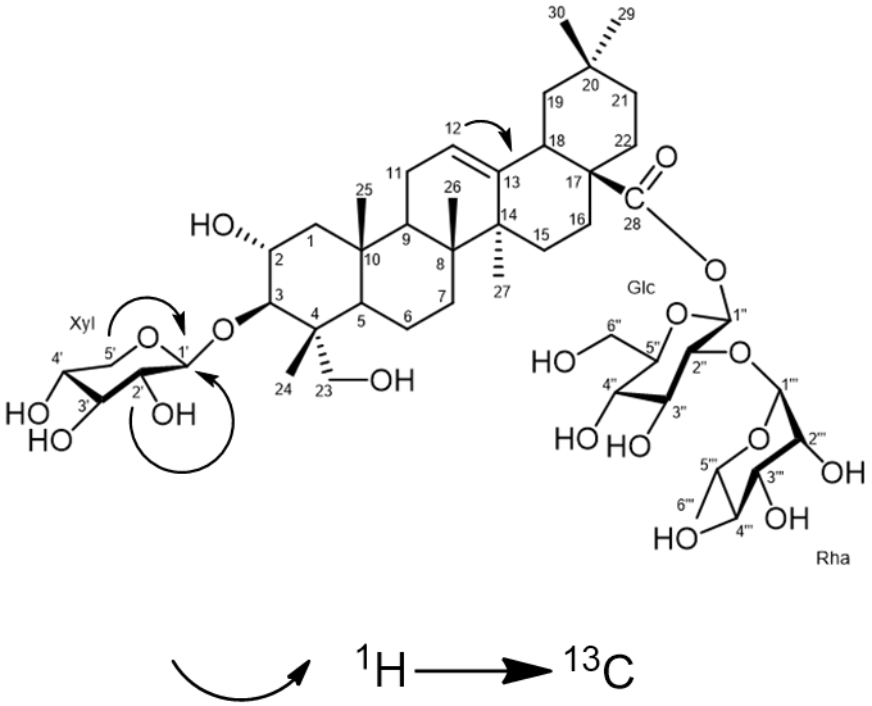

Scheme 3.3: The HMBC correlations of bodinioside Q (**4**).

3.3.1.5. Spectroscopic data for Compound 5

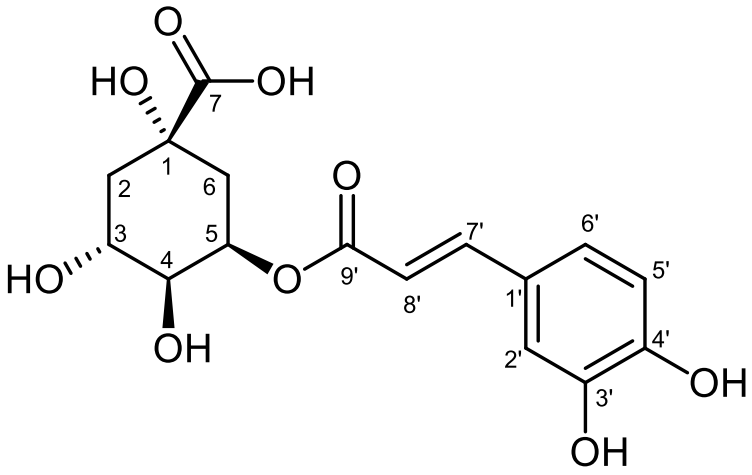

Figure 3.9. Structure of 5-*O*-caffeoylquinic acid (**5**).

The molecular ion peak appearing at *m/z* 367.1107 in the HRMS (Appendix 24) of Compound **5** is consistent with the molecular formula $C_{16}H_{18}O_9$. The presence of 16 carbons is in agreement with the ^{13}C-NMR spectrum. The ^{13}C-NMR spectrum (Appendix 25) of Compound **5** revealed the presence of two carbonyl groups at δ_C 145.4 and 166.5 ppm, corresponding to carbons at positions 7 and 9', respectively. Moreover, the ^{13}C-NMR spectrum (Appendix 25)

also showed two aromatic carbons bonded to hydroxyl groups at δ_C 145.8 and 148.5 ppm, corresponding to carbons at positions 3' and 4', respectively; two olefinic carbons at δ_C 113.6 and 180.2 ppm, corresponding to carbons at positions 8' and 7, respectively. Moreover, the ^{13}C-NMR spectrum (Appendix 25) displayed four aromatic carbons at δ_C 113.6, 115.1, 121.6, and 126.2 ppm, identified as C-2', C-5', C-6', and C-1', respectively; three carbons bonded to hydroxyl groups at δ_C 68.8, 70.7, and 76.4 ppm, assigned to C-3, C-4, and C-1, respectively; one carbon bonded to an ester group at δ_C 74.3 ppm, corresponding to a carbon at position 5; and two methylenes assigned as C-2 and C-6 at δ_C 36.6 ppm and δ_C 41.8 ppm, respectively. The ^{13}C-NMR (Appendix 25) and DEPT135 (Appendix 26) spectra showed the presence of six methines at δ_C 20.1 (C-6'), 74.3 (C-5), 113.6 (C-8'), 115.1 (C-2'), 121.6 (C-5'), and 145.4 (C-7') ppm; and two methylenes at δ_C 36.6 (C-2) and 41.8 (C-6) ppm. The ^{1}H-NMR spectrum (Appendix 27A) revealed two doublets at δ_H 6.79 and δ_H 6.95 ppm that were ortho-coupled, corresponding to aromatic protons at positions 5' and 6'. The broad singlet at δ_H 7.06 ppm was allocated to a proton at position 2', confirming the presence of a trisubstituted aromatic ring. Furthermore, the ^{1}H-NMR (Appendix 27A) showed two doublets, assigned to protons at δ_H 6.21 and 7.52 ppm at positions 7' and 8', consistent with a *trans*-disubstituted ethylene moiety in Compound **5**. Finally, the data for Compound **5** agree with published NMR data of 5-*O*-caffeoylquinic acid isolated by Suárez-Quiroz *et al*. (2013), as shown in Table 3.5. This is the first reported isolation of 5-*O*-caffeoylquinic acid from *B. salicina*.

Table 3.5: ^{1}H-NMR (400 MHz) and ^{13}C-NMR (100 MHz) data for 5-*O*-caffeoylquinic acid (**5**) obtained in this study (exp) and from the literature (lit) (Suárez-Quiroz *et al*., 2014).

Position	^{1}H-NMR (δ_H ppm) (exp)	^{1}H-NMR (δ_H ppm) (lit)	^{13}C-NMR (δc ppm) (exp)	^{13}C-NMR (δ_C ppm) (lit)
1	-	-	76.4	74.7
2	1.70-1.51 (1H, m)	2.02 (br. t) 2.22 (br. t)	36.6	37.3
3	3.66 (1H, m)	5.31 (t)	68.8	70.5
4	3.32 (1H, m)	3.71 (d)	70.7	72.0
5	5.24 (1H, m)	4.15 (br.s)	74.3	70.5
6	2.29-1.93 (1H, m)	2.05 (br. d) 2.14 (d)	41.8	36.7
7	-	-	145.4	175.6
1'	-	-	126.2	126.3
2'	7.06 (1H, d)	7.027 (br. s)	113.6	113.8
3'	-	-	145.8	145.3

4'	-	-	148.5	148.1
5'	6.79 (1H, d)	6.94 (d)	115.1	115.0
6'	6.95 (1H, dd)	6.75 (d)	121.6	121.5
7'	6.21 (1H, d)	7.56 (d)	145.4	145.6
8'	7.52 (1H, d)	6.22 (d)	113.6	113.7
9'	-	-	166.5	167.2

3.3.1.6. Spectroscopic data for Compound 6

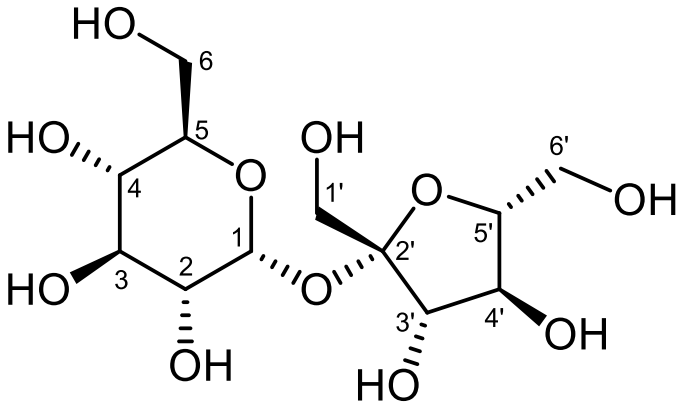

Figure 3.10. Structure of 3*O*-α-D-glucopyranosyl-(1→2)-β-D-fructofuranoside (sucrose).

The structure elucidation of Compound **6** was achieved using ^{1}H-NMR (Appendix 28A,B), ^{13}C-NMR (Appendix 29) and HRMS (Appendix 30). Furthermore, the HRMS spectrum (Appendix 32) displayed a molecular ion peak at *m/z* 341.1073, agreeing with the formula $C_{12}H_{22}O_{11}$. Analysis of both the ^{13}C-NMR (Appendix 29) and the DEPT (Appendix 31) spectra allowed the identification of eight methines at δ_C 67.9 (C-4), 70.2 (C-2), 72.0 (C-5), 72.2 (C-3), 72.9 (C-4'), 77.8 (C-3'), 81.6 (C-5'), and 92.2 (C-1) ppm; three methylenes at δ_C 60.7 (C-6), 61.2 (C-1), and 62.5 (C-6') ppm; and one quaternary carbon at δ_C 103.8 ppm (C-2'). The COSY spectrum (Appendix 32) revealed coupling of protons 3-H (δ_H 3.72 ppm) with 2-H (3.50 ppm) and 4-H (3.39 ppm), 2-H (3.50 ppm) and 1-H (5.41 ppm), respectively. The only coupling constant obtained for the fructoside protons was for 4'-H (δ_H 4.02 ppm) with 5-H' (3.86 ppm) and 6'-H (3.80 ppm). Moreover, the HMBC spectrum (Appendix 33) showed correlations between 1'-H (δ_H 3.63 ppm) and C-5' (δ_C 81.6 ppm), 4'-H (δ_H 4.02 ppm) with C-6' (δ_C 62.5 ppm), 1-H (δ_H 5.41) with C-3 (δ_C 72.2 ppm), and 5'-H (δ_H 3.86 ppm) with C-2' (δ_C 103.8 ppm), respectively, as shown in Scheme 3.4. Furthermore, the glucopyranosyl 1'-H (δ_H 3.63 ppm) correlated strongly with the fructosyl C-2 (δ_C 70.2 ppm), establishing the linkage between the glucopyranosyl anomeric carbon and that of the fructoside anomeric carbon. Lastly, comparing

these data with literature data confirmed the identity of Compound **6** as sucrose (Ben Youssed*et al*., 2016), as shown in Table 3.6. This is the first reported isolation of the disaccharide sucrose from *B. salicina*.

Table 3.6: ^{1}H-NMR (400 MHz) and ^{13}C-NMR (100 MHz) data for sucrose obtained in this study (exp) and from the literature (lit) (Ben Youssed *et al*., 2016).

Position	^{1}H-NMR (δ_H ppm, *J* in Hz) (exp)	^{1}H-NMR (δ_H ppm, *J* in Hz) (lit)	^{13}C-NMR (δ_C ppm) (exp)	^{13}C-NMR (δ_C ppm) (lit)
1	5.41 (d, 1H, *J* = 3.6 Hz)	5.23 (d, *J* = 3.3)	92.2	89.9
2	3.50 (dd, 1H, *J* = 11.2 Hz)	5.28 (dd, *J* = 3.3 and *J* = 11.3)	70.2	68.4
3	3.72 (t, 1H, *J* = 10.2 Hz)	5.16 (dd, *J* = 3.2 and *J* = 10.3)	72.2	70.2
4	3.39 (t, 1H)	5.48 (m)	67.9	68.1
5	3.83 (m, 1H)	4.27 (m)	72.0	69.6
6	3.81 (d, 2H, *J* = 5.2 Hz)	4.02 (dd, *J* = 4.5 and *J* = 9.2) & 4.26 (m)	60.7	61.7
1'	3.63 (s, 2H, *J* = 9.2 Hz)	4.15 (dd, *J* = 2.9 and *J* = 9.5)	61.2	62.8
2'	-	5.37 (dd, *J* = 3.0 and *J* = 3.4)	103.8	103.9
3'	4.14 (d, 1H)	5.33 (m)	77.8	75.6
4'	4.02 (t, 1H)	5.31 (m)	72.9	74.9
5'	3.86 (m, 1H)	5.43 (m)	81.6	79.1
6'	3.80 (d, 2H)	5.41 (m)	62.5	63.6

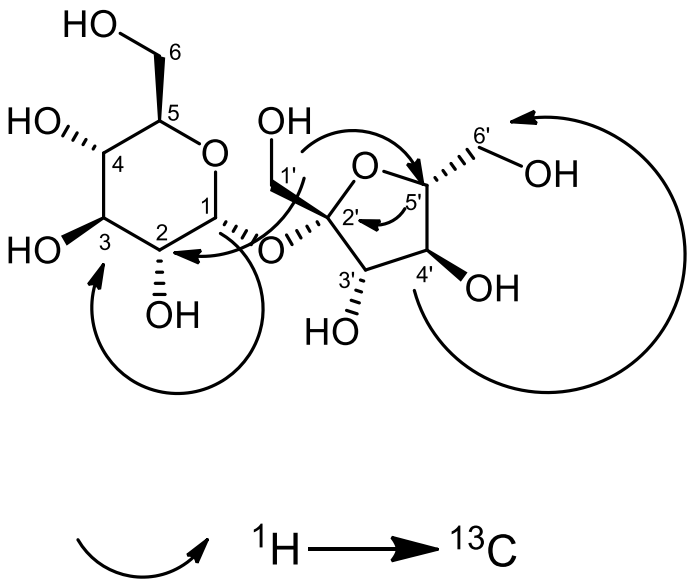

Scheme 3.4: The HMBC correlations of sucrose (**6**).

3.3.1.7. Spectroscopic data of Compound 7

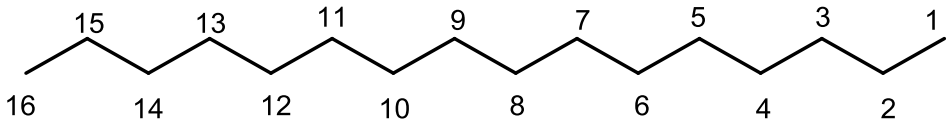

Figure 3.11. Structure of hexadecane (**7**).

The ^{1}H-NMR spectrum of Compound **7** (Appendix 34) exhibited an intense peak of overlapping multiplets at δ_H 1.28 ppm, corresponding to the protons on positions 2 to 15 of the long chain. A single peak at δ_C 29.3–29.7 ppm appeared for carbons 4 to 13 in the ^{13}C-NMR spectrum (Appendix 35). The DEPT 135 (Appendix 36) spectra indicated methylenes at δ_C 31.96 ppm (C-3,14), 29.42-29.74 ppm (C-4 to C-13), 22.73 ppm (C-2,15); and methyls at δ_C 14.12 ppm (C-1,16), respectively. Moreover, the COSY spectrum (Appendix 37) showed correlations between the protons at δ_H 1.283 ppm (2-H to 15-H) with δ_H 0.891 ppm (H-1,16). Compound **7** crystallized as white crystals with a melting point of 16–18 °C. Therefore, comparison of spectroscopic data and melting with literature date confirmed the identity of Compound **7** as hexadecane, as shown in Table 3.7 (Li *et al*., 2015). This is the first reported isolation of the saturated hydrocarbon hexadecane from *B. salicina.*

Table 3.7: ^{1}H-NMR (400 MHz) and ^{13}C-NMR (100 MHz) data for hexadecane obtained in this study (exp) and from the literature (lit) (Li *et al*., 2015).

Position	^{1}H-NMR (δ_H ppm) (exp)	^{1}H-NMR (δ_H ppm) (lit)	^{13}C-NMR (δ_C ppm) (exp)	^{13}C-NMR (δ_C ppm) (lit)
1, 16	0.89 (6H, t)	0.81 (6H, t)	14.1	14.1
2, 15	1.28 (4H, m)	1.03-1.37 (4H, m)	22.7	22.7
3, 14	1.28 (4H, m)	1.03-1.37 (4H, m)	31.9	31.9
4-13	1.28 (20H, m)	1.03-1.37 (20H, m)	29.3-29.7	29.8-28.9

3.3.1.8. Spectroscopic data of Compound 8

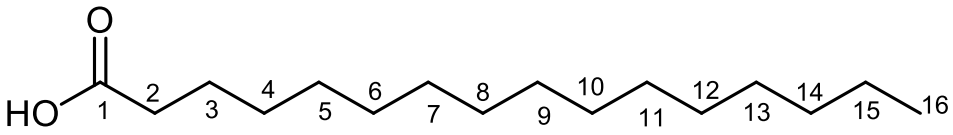

Figure 3.12. Structure of palmitic acid (**8**).

The IR spectrum of Compound **8** (Appendix 38) revealed characteristic O-H stretching absorption at 3436.00 cm^{-1}, aliphatic (CH_3) stretching at 2849.51 cm^{-1}, carbonyl (C=O) stretching at 1703.71 cm^{-1}, and long chain $(CH_2)_n$ bending overtones at 2917.27 cm^{-1}. The molecular formula, $C_{16}H_{32}O_2$ was confirmed by HRMS (Appendix 39), m/z: 255.23295. The ^{1}H-NMR spectrum (Appendix 40) showed an intense single peak encompassing the multiplets of protons at positions 4-H to 13-H at δ_H 1.23 ppm. Furthermore, triplets at δ_H 2.27 (2H, t) and 0.83 (3H, t) ppm corresponded to the protons at positions 2 and 16, respectively. The ^{13}C-NMR (Appendix 41) showed a quaternary carbon (for –COOH) at δ_C 178.4 ppm assigned to C-1, and a methyl carbon for C-16 at δ_C 14.1 ppm. A single intense peak at δ_C 29.0 ppm appeared for C-4 to C-13, while the alpha and beta carbons appeared at δ_C 31.9 ppm (C-3) and 34.0 ppm (C-2), respectively. Moreover, C-14 and C-15 appeared as doublets at δ_C 24.7 and 22.6 ppm, respectively. The DEPT 135 (Appendix 42) spectrum also displayed sixteen carbon signals, including fourteen methylenes at δ_C 22.67 (C-15), 24.75 (C-14), 29.09 (C-4), 29.25 (C-5), 29.33 (C6), 29.44 (C-7), 29.59 (C-8), 29.63 (C-9), 29.67 (C-10, C-11, C-12, C-13), 31.92 (C-3), and 34.01 (C-2) ppm; one methyl at δ_C 14.11 (C-16) and one quaternary carbon at 178.43 (C-1) ppm. Lastly, comparison of these data with the literature confirmed the identity of Compound

8 as palmitic acid, as shown in Table 3.8 (Bulama1 *et al*., 2014). This is the first reported isolation of the saturated fatty acid palmitic acid, from *B. salicina.*

Table 3.8: ^{1}H-NMR (400 MHz) and ^{13}C-NMR (100 MHz) data for palmitic acid obtained in this study (exp) and from the literature (lit) (Bulamal *et al*., 2014).

Position	^{1}H-NMR (δ_H ppm) (exp)	^{1}H-NMR (δ_H ppm) (lit)	^{13}C-NMR (δ_C ppm) (exp)	^{13}C-NMR (δ_C ppm) (lit)
1	-	-	178.4	177.3
2	2.27 (2H, t)	2.23	34.0	36.1
3	1.57 (2H, m)	1.56	31.9	31.9
4-13	1.23 (20H, m)	1.29	29.0-29.6	29.7
14	-	-	24.7	24.8
15	1.98 (2H, q)	1.33	22.6	22.8
16	0.83 (3H, t)	0.96	14.1	14.1

3.4. Summary

The following conclusions can be made:

- Eight compounds were isolated from different parts of *B. salicina.*
- A new method for the isolation of these 8 compounds was developed.
- Compounds **1**, **2**, and **3** were isolated from the stem bark. This is the first reported isolation of kaempferol 3-*O*-(2"-*O*-galloyl)-glucuronide (**1**), lupeol (**2**), and D-galactopyranose (**3**) from the genus *Breonadia* Ridsdale and *B. salicina* species.
- Bodinioside Q (**4**), an oleanane triterpenoid saponin, was isolated for the first time from the roots of *Breonadia salicina.*
- Compounds **5**, **6**, **7**, and **8** were isolated for the first time from the DCM and MeOH leaf extracts of *B. salicina*.

3.5. References

Alay, S.; Göde, F.; Alkan, C. Preparation and characterization of poly (methylmethacrylate-coglycidyl methacrylate)/n-hexadecane nanocapsules as a fiber additive for thermal energy storage. *Fibers and Polymers*, **2010**, 11, 1089–1093.

Atanasov, A.G.; Zotchev, S.B.; Dirsch, V.M.; Supuran, C.T. Natural products in drug discovery: Advances and opportunities. *Nature Reviews Drug Discovery*, **2021**, 1-17.

Ayo, S.G.; Habila, J.D.; Achika, J.I.; Akinwande, O.O. Isolation and characterization of 2,4-dihydroxycinnamic acid from the stem bark of *Adina microcephala* Delile. *Chemical Society of Nigeria*, **1930**, 47BCC70.

Ben Youssef, S.; Fakhfakh, J.; Tchoumtchoua, J.; Halabalaki, M.; Allouche, N. Efficient purification and complete NMR characterization of galactinol, sucrose, raffinose, and stachyose isolated from *Pinus halepensis* (Aleppo pine) seeds using acetylation procedure. *Journal of Carbohydrate Chemistry*, **2016**, 35, 224-237.

Bulama, J.; Dangoggo, S.; Halilu, M.; Tsafe, A.I.; Hassan, S.W. Isolation and characterization of palmitic acid from ethyl acetate extract of root bark of *Terminalia glaucescens*. *Chemistry and Materials Research*, **2014**, 6, 140-3.

Gil, M.; Wianowska, D. Chlorogenic acids–their properties, occurrence and analysis. *Annales Universitatis Mariae Curie-Sklodowska, sectio AA – Chemia*, **2017**, 72, 61.

Havlicek, V.; Jaroslav, S. Natural products analysis: instrumentation, methods, and applications. *Natural Products Analysis*, **2014**, 1.

Huck, C.W. Advances of infrared spectroscopy in natural product research. *Phytochemistry Letters*, **2015**, 11, 384-393.

Hudson, B.J.F. Fatty acids properties, Encyclopedia of Food Sciences and Nutrition, *Academic Press*, **2003**, 2297–2300.

Lahlou, M. The success of natural products in drug discovery, **2013**.

Li, X.Y.; Shang, R.; Fu, M.C.; Fu, Y. Conversion of biomass-derived fatty acids and derivatives into hydrocarbons using a metal-free hydrodeoxygenation process. *Green Chemistry*, **2015**, 17, 2790-2793.

Mahlo, S.M.; McGaw, L.J.; Eloff, J.N. Antifungal activity and cytotoxicity of isolated compounds from leaves of *Breonadia salicina*. *Journal of Ethnopharmacology*, **2013**, 148, 909–913Maryadele, J.N.; Neil, P. The Merck Index—An Encyclopedia of Chemicals, Drugs, and Biologicals. Merck and Co. Inc.: Whitehouse Station, NJ, USA, **2006**.

Maryadele, J.N.; Neil, P. *The Merck Index—An Encyclopedia of Chemicals, Drugs, and Biologicals*; Merck and Co. Inc.: Whitehouse Station, NJ, USA, **2006**.

Mouffok, S.; Haba, H.; Lavaud, C.; Long, C.; Benkhaled, M. Chemical constituents of Chemical constituents of *Centaurea omphalotricha Coss. & Durieu ex Batt. & Trab. Records of Natural Products*, **2012**, 6, 292-5.

Muktar, B.; Bello, I.A.; Sallau, M.S. Isolation, characterization and antimicrobial study of lupeol acetate from the root bark of *Fig-Mulberry* Sycamore (Ficus sycomorus LINN). *Journal Applied Sciences and Environmental Management*, **2018**, 22, 1129–1133.

Nvau, B.J.; Sami, B.; Ajibade, O.S.; Gray, I.A.; Igoli, J.O. Adicardin and Other Coumarins from *Breonadia salicina* (Vahl) Hepper. *Tropical Journal of Natural Product Research*, **2019**, 3, 298-301.

Ogawa, K.; Yamamura, M.; Maruyama, I. Isolation and identification of 3-*O*-methyl-D-galactose as a constituent of neutral polysaccharide of *Chlorella vulgaris. Bioscience, Biotechnology, and Biochemistry*, **1994**, 58, 942-944.

Suarez-Quiroz, M.L.; Campos, A.A.; Alfaro, G.V.; González-Ríos, O.; Villeneuve, P.; Figueroa-Espinoza, M.C. Isolation of green coffee chlorogenic acids using activated carbon. *Journal of Food Composition and Analysis*, **2014**, 33, 55-58.

Yang, L.; Zhang, L.; Du, J.; Shao, L.; Yu, F.; Li, R.; Zhong, J. Two new oleanane triterpenoid saponins from Elsholtzia bodinieri. *Natural Product Research*, **2020**, 1-9.

Yoshimura, M.; Ito, H.; Miyashita, K.; Hatano, T.; Taniguchi, S.; Amakura, Y.; Yoshida, T. Flavonol glucuronides and C-glucosidic ellagitannins from *Melaleuca squarrosa*. *Phytochemistry*, **2008**, 69, 3062-3069.

Zhao, D.; Ding, X.; Hou, Y.; Hou, W.; Liu, L.; Xu, T.; Yang, D. Structural characterization, immune regulation and antioxidant activity of a new heteropolysaccharide from *Cantharellus cibarius* Fr. *International Journal of Molecular Medicine*, **2018**, 41, 2744-2754.

CHAPTER 4 METABOLOMIC PROFILING OF *B. SALICINA* USING ^{1}H-NMR AND UPLC-QTOF-MS ANALYSIS

4.1. INTRODUCTION

Plant metabolomics is widely recognized as a tool for quality assurance of plant-derived therapeutic materials as a large assortment of phytochemicals can be analysed in a single extract (Valentino *et al*., 2020). Currently, plant metabolomics is used mainly to analyse bioactive plant materials for their biochemical structures and metabolic pathways (Xiao *et al*., 2022). Moreover, metabolomics are an advanced technique for drug discovery and can be helpful in determining new compound structures in natural products research (Salem *et al*., 2020). In the case of *Breonadia salicina*, only a few secondary metabolites have been isolated, identified and investigated for their medicinal potential. Thus, comprehensive chemical profiling could be useful for quality assurance purposes. A combination of analytical methods, such as ^{1}H-NMR and ^{13}C-NMR spectroscopy, and high-performance liquid chromatography, can be used to chemically profile (Tan *et al*., 2018) interesting compounds found in medicinal plants (Dayrit *et al*., 2017). This chapter reports the evaluation of the chemical components of crude extracts and chromatographic fractions of the stem bark, roots and leaves of *B. salicina* collected during spring of 2019 and the comparison with the different parts of *B. salicina* collected the following year (2020) during autumn, winter, summer and spring. The metabolomic study intended to explore the metabolites produced over these seasons and to explore the phytochemistry of the species.

4.2. MATERIALS AND METHODS

4.2.1. Sampling and extraction

4.2.1.1. The root, leaf, and stem bark samples collected in the spring of 2019

The detailed method is described in Chapter 3, section **3.2.1**

4.2.1.2. Seasonal samples collected in 2020

The roots, leaves, and stem bark samples were again collected at Fondwe during March, 2020 (Autumn), July, 2020 (Winter), October, 2020 (Spring), and December, 2020 (Summer), and

were identified at the Department of Botany, University of Venda, by Prof. Peter Tshisikhawe. A voucher specimen numbered BD 001-012 was placed in the herbarium. After four weeks' air-drying, the samples were ground with a hammer mill, and approximately 1 kg of each was soaked in 2 L methanol at ambient temperature for 48 hours. The individual supernatants were filtered and each concentrated at 45 °C with a rotatory evaporator (BÜCHI Labortechnik AG) to yield dry extracts, as shown in Figure 4.1. The ground leaf samples were soaked successively in 2 L dichloromethane followed by 2 L methanol, each for 48 hours at ambient temperature. These supernatants were also filtered and concentrated, as shown in Figure 4.1.

The percentage yield of seasonal extracts was calculated using the following equation:

$$Yield\ \% = \frac{mass\ of\ the\ dry\ extract\ (g)}{mass\ of\ the\ dry\ plant\ (g)} X\ 100$$

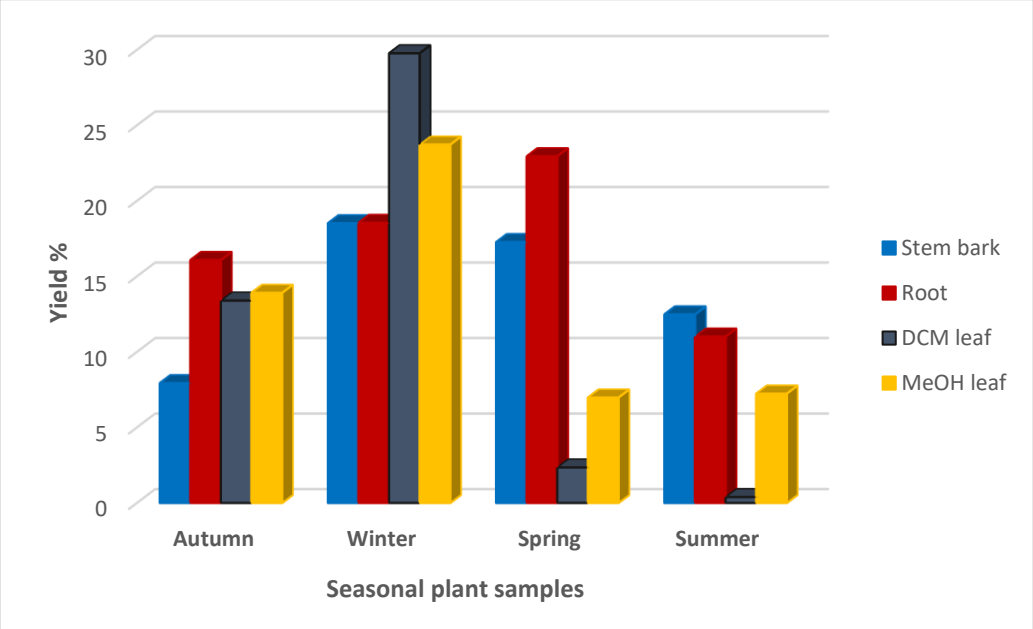

Figure 4.1. Percentage yields of seasonal plant samples of *B. salicina.*

4.2.2. Fractionation

The detailed method is reported in Chapter 3, section **3.2.2**.

4.2.3. Proton NMR spectroscopy

The ^{1}H-NMR spectra were recorded at 400 MHz with a Bruker Avance 400 spectrometer using residual undeuterated solvent as the internal standard. The ^{1}H-NMR chemical shifts are reported as parts per million (ppm). Deuterochloroform ($CDCl_3$), CD_3OD, and DMSO-d_6 were used as solvents.

4.2.4. UPLC-QTOF-MS analysis

Ultra-performance liquid chromatography-MS (UPLC-MS) was executed on a Waters Acquity UPLC (Waters, Milford, MA, USA) fitted with a photodiode array detector (Waters, Milford, MA, USA) and a Waters Synapt G2 Quadrupole time-of-flight MS (Thermo Fisher Scientific). A Waters Acquity BEH C18 column (150 mm x 2.1 mm i.d., particle size 1.7 µm) was used at 40˚C with 2.0 µL injection volume, using full-loop injection. Gradient elution with a mobile phase consisting of a gradient of 0.1 % formic acid (Solvent A) and HPLC grade acetonitrile (Solvent B) was used at a flow rate of 0.3 mL/min. The initial A:B ratio was 9:1 maintained for 4 min, changing to 5:5 maintained for 6 min, increasing to 5:95 over 2.5 min, maintained for 0.5 min, and finally reverting to the initial ratio over 0.5 min. Before every run, the system was equilibrated for 2 minutes. The MS analysis used both positive and negative electrospray ionization (ESI) modes.

4.3. RESULTS AND DISCUSSION

4.3.1. Extraction yield

While all the root and stem bark samples were extracted with 100 % methanol, the leaf samples were extracted successively with 100 % dichloromethane followed by methanol. In autumn, the highest yield was observed from the root extract (16.08 %), while the lowest yield was observed from the stem bark extract (7.93 %, as shown in Fig. 4.1). Furthermore, in winter the highest yield was found in the dichloromethane leaf extract (29.77 %), followed by the methanol leaf extract (23.72 %), root extract (18.54 %) and stem bark extract (18.51 %). In spring, the root extract produced the highest yield (22.95 %) compared to the stem bark (17.26 %), methanol leaf (6.97 %) and dichloromethane leaf (2.35 %) extracts. Finally, the stem bark extract produced the highest yield (12.48 %) in summer, followed by the root (11.01 %), methanol leaf (7.23 %) and dichloromethane leaf (0.39 %) extracts (Fig. 4.1).

4.3.2. The ^{1}H-NMR spectra of *B. salicina* crude extracts and fractions

All the crude extracts and their chromatographic fractions were analysed by ^{1}H-NMR spectroscopy and the chemical shifts of the resulting spectra were compared to those of compounds found in the literature (Ogawa *et al*., 1994; Mouffok *et al*., 2012; Desai *et al*., 2014; Suarez-Quiroz *et al*., 2014; Li *et al*., 2015; Ben Youssef *et al*., 2016). Known secondary metabolites such as sugars (monosaccharides), fatty acids, phenols, quinic acids, and triterpenoids were identified (Table 4.1). Stem bark extract fraction S_1 showed catechin signals in the aromatic region at δ_H 5.94, 5.86, 6.72-6.85, and 7.05 ppm, respectively, as presented in Appendix 43A. Fraction S_2 also displayed the catechin aromatic signals at δ_H 5.87, 5.94, 6.72-6.86, and 7.06 ppm, respectively, as shown in Appendix 44A. The crude stem bark extract did not reveal the presence of catechin, probably because the catechin signals of the crude extract were lost in those of other compounds in the crude extract. The signals of the pentacyclic triterpenoid lupeol appeared in the ^{1}H-NMR spectra of the crude root extract (R.crude, Appendix 45), fraction S_1 (Appendix 43B), and fraction S_2 (Appendix 44B), respectively, at δ_H 0.71 (3H, s), 0.83 (3H, s), 0.92 (3H, s), 0.96 (3H, s), 1.04 (3H, s), and 1.30 (1H, m) ppm; δ_H 0.77 (3H, s), 0.87 (3H, s), 0.96 (3H, s), 0.98 (3H, s), 1.02 (3H, s), 1.56 (1H, m), 1.61 (1H, m), 1.71 (3H, s), 1.91 (1H, m), 2.23 (1H, m), 3.12 (1H, m), 4.60 (1H, s), and 4.72 (1H, s) ppm; and δ_H 0.77 (3H, s), 0.87 (3H, s), 0.96 (3H, s), 0.98 (3H, s), 1.02 (3H, s), and 1.36 (1H, m) ppm. ^{1}H-NMR signals due to 5-*O*-caffeoylquinic acid appeared in the spectra of the crude MeOH leaf extract (LM.crude, Appendix 46), fraction LM_2 (Appendix 47), and fraction LM_3 (Appendix 48), respectively, at δ_H 6.30 (1H, d), 6.79 (1H, d), 6.96 (1H, dd), 7.60 (1H, d), and 7.67 (1H, d) ppm; δ_H 6.79 (1H, d), 6.96 (1H, dd), 7.06 (1H, d), and 7.52 (1H, d) ppm; and δ_H 6.30 (1H, d), 6.79 (1H, d), 6.95 (1H, dd), 7.07 (1H, d), and 7.61 (1H, d) ppm. ^{1}H-NMR signals of hexadecane appeared in the crude dichloromethane leaf extract (LD.crude, Appendix 49), root extract fraction R_1 (Appendix 50), and fraction LD_3 (Appendix 51), respectively, at δ_H 0.90 (6H, t) - 1.69 (28H, m) ppm; δ_H 0.84 (6H, t) - 1.27 (28H, m) ppm; and δ_H 0.87 (6H, t) - 1.27 (28H, t) ppm. ^{1}H-NMR signals of sugars such as fructose, α-glucose, and β-glucose were seen in the crude root extract (R.crude, Appendix 45), crude stem bark extract (S.crude, Appendix 52), crude MeOH leaf extract (LM.crude, Appendix 46) and leaf extract fraction LM_3 (Appendix 48).

Table 4.1. ^{1}H-NMR (δ_H ppm) signals of metabolites identified in *B. salicina* extracts and chromatographic fractions.

Metabolites	^{1}H-NMR (δ_H ppm)	Samples	References
Catechin	5.94 (1H, s), 5.86 (1H, s), 6.72-6.85 (1H, dd), 7.05 (1H, d).	fraction S_1	Desai *et al*., 2014
	4.57 (1H, d), 5.87 (1H, s), 5.94 (1H, s), 6.72-6.86 (1H, dd), 7.06 (1H, d).	fraction S_2	
Lupeol (**2**)	0.71 (3H, s), 0.83 (3H, s), 0.92 (3H, s), 0.96 (3H, s), 1.04 (3H, s), 1.30 (1H, m).	R.crude	Mouffok *et al*., 2012
	0.77 (3H, s), 0.87 (3H, s), 0.96 (3H, s), 0.98 (3H, s), 1.02 (3H, s), 1.56 (1H, m), 1.61 (1H, m), 1.71 (3H, s), 1.91 (1H, m), 2.23 (1H, m), 3.12 (1H, m), 4.60 (1H, s), 4.72 (1H, s).	fraction S_1	
	0.77 (3H, s), 0.87 (3H, s), 0.96 (3H, s), 0.98 (3H, s), 1.02 (3H, s), and 1.36 (1H, m).	fraction S_2	
5-*O*-Caffeoylquinic acid (**5**)	6.30 (1H, d), 6.79 (1H, d), 6.96 (1H, dd), 7.60 (1H, d), 7.67 (1H, d).	LM.crude	Suarez-Quiroz *et al*., 2014
	6.79 (1H, d), 6.96 (1H, dd), 7.06 (1H, d), 7.52 (1H, d).	fraction LM_2	
	6.30 (1H, d), 6.79 (1H, d), 6.95 (1H, dd), 7.07 (1H, d), 7.61 (1H, d).	fraction LM_3	
Hexadecane (**7**)	0.90 (6H, t) - 1.69 (28H, m).	LD.crude fraction R_1	Li *et al*., 2015
	0.84 (6H, t) - 1.27 (28H, m).		
	0.87 (6H, t) - 1.27 (28H, t).	fraction LD_3	
α-Glucose	5.12 (d).	R.crude	Ogawa *et al*., 1994
	5.12 (d).	S.crude	
	5.13 (d).	LM.crude	

	5.13 (d).	fraction LM_3	
β-Glucose	3.12 (m), 4.48 (d). 3.13 (m), 4.49 (d). 3.01 (m). 3.01 (m), 4.50 (d).	R.crude S.crude LM.crude fraction LM_3	Ogawa *et al*., 1994
Glucose and fructose	3.63-3.80 (m). 3.62-3.80 (m). 3.61-3.80 (m). 3.69-3.81 (m).	R.crude S.crude LM.crude fraction LM_3	Ben Youssef *et al*., 2016

4.3.3. Characterization of components from *B. salicina* using UPLC-QTOF-MS analysis

Twenty-five metabolites were detected in the extracts and fractions of the root, stem bark, and leaves of *B. salicina* and were characterised tentatively by comparison of their spectra with reported literature data. Full UPLC-QTOF-MS data for the identified peaks found in the different sample chromatograms, namely their fragment ions, retention times, and molecular ions $[M-H]^-$, are presented in Table 4.2. Peak 1 (Appendix 53, *m/z* 377.08633 $[M-H]^-$) with molecular structure $C_{18}H_{18}O_9$ produced fragments ions at *m/z* 341, 215 and 160, similar to those published of caffeic acid derivatives (Toth *et al*., 2014). Peak 2 (Appendix 54, *m/z* 461.07350 $[M-H]^-$), peak 3 (Appendix 55, *m/z* 300.99929 $[M-H]^-$), peak 4 (Appendix 56, *m/z* 447.05763 $[M-H]^-$) and peak 5 (Appendix 57, *m/z* 289.07225 $[M-H]^-$) were unequivocally confirmed as 4'-*O*-methylellagic acid-3-*O*-α-L-rhamnopyranoside, ellagic acid, ellagic acid-rhamnopyranoside isomer I, and catechin, respectively. Moreover, peaks 2, 3, 4 and 5 yielded significant fragment ions at *m/z* 315, 299; *m/z* 242, 174; *m/z* 300.99898 and *m/z* 245.08155, respectively (Wu *et al*., 2017; Singh *et al*., 2016; Liu, *et al*., 2021). Peak 6 (Appendix 58, *m/z* 485.32825 $[M-H]^-$), peak 7 (Appendix 59, *m/z* 458.33667 $[M-H]^-$), peak 8 (Appendix 60, *m/z* 499.34385 $[M-H]^-$), peak 9 (Appendix 61, *m/z* 453.33834 $[M-H]^-$) and peak 10 (Appendix 62, *m/z* 499.37155 $[M-H]^-$) were identified as hydroxyglycyrrhetinic acid ($C_{30}H_{46}O_5$), neotigogenin acetate ($C_{29}H_{46}O_4$), 25-hydroxy-3-epi-dehydrotumulosic acid ($C_{31}H_{48}O_5$), micromeric acid ($C_{30}H_{46}O_3$) and 3-acetylursolic acid ($C_{32}H_{50}O_4$), respectively. The MS-MS spectra of peaks 6, 7, 8 and 10 produced fragment ions at *m/z* 485, 441; *m/z* 503, 457; *m/z* 455.35408 and *m/z* 497.36498, respectively. Comparison with literature data confirmed the identities of these compounds (Xiang, *et al*., 2011; Pei *et al*., 2021; Wang *et al*., 2015; Borrás-Linares *et al*., 2014; Asteggiano *et al*., 2021).

Peak 11 (Rt = 1.876 min), peak 12 (Rt = 4.728 min) and peak 13 (Rt = 11.530 min) were respectively assigned to (epi)gallocatechin (Appendix 63, *m/z* 305.06698 $[M-H]^-$), 4-*O*-

methylgallic acid (Appendix 64, *m/z* 183.02975 [M-H]$^-$), and myricetin 3-*O*-glucoside (Appendix 65, *m/z* 479.08529 [M-H]). The MS-MS spectra of peaks 12 and 13 had fragment ions at *m/z* 184.03304 and *m/z* 480.08721, respectively (Kardel *et al*., 2013; Peng *et al*., 2019; Tang *et al*., 2020). Comparison with literature data enabled identification of peak 14 (Appendix 66, *m/z* 455.35397 [M-H]$^-$) and peak 15 (Appendix 67, *m/z* 487.33699 [M-H]$^-$) as ursolic acid ($C_{30}H_{48}O_3$) and asiatic acid ($C_{30}H_{48}O_5$), respectively, while peak 15 also had a fragment ion at *m/z* 485.32825 (Liu *et al*., 2015; Velamuri *et al*., 2020). Peak 16 (Rt = 12.569 min) was identified unequivocally by comparison with literature data as ellagic acid pentoside ($C_{19}H_{14}O_{12}$, Appendix 68, *m/z* 433.04194 [M-H]$^-$); and peak 17 (Rt = 1.140, $C_7H_6O_5$) as gallic acid (Appendix 69, *m/z* 170.01742 [M-H]$^-$) (Singh *et al*., 2016; Minh *et al*., 2019). Peak 18 had a retention time of 0.663 min and exhibited an [M-H]$^-$ ion at *m/z* 533.17341 (Appendix 70), corresponding to the molecular formula $C_{19}H_{34}O_{17}$ (Zhumakanova *et al*., 2021). Peak 19 (Appendix 71, *m/z* 353.08839 [M-H]$^-$) was identified as chlorogenic acid because of its characteristic fragment ion at *m/z* 191.05585 [quinic acid-H] (Peeters *et al*., 2020**).** Furthermore, peak 20 (Rt = 8.421 min), peak 21 (Rt = 10.819 min), peak 22 (Rt = 10.181 min), peak 23 (Rt = 12.918 min), peak 24 (Rt = 14.242 min), and peak 25 (Rt = 0.671 min) with [M-H]$^-$ ions at *m/z* 389.10941 (Appendix 72), *m/z* 367.10424 (Appendix 73), *m/z* 451.10412 (Appendix 74), *m/z* 609.14777 (Appendix 75), *m/z* 515.12070 (Appendix 76) and *m/z* 191.05581 (Appendix 77), respectively, were tentatively identified as deacetyl asperuloside acid ($C_{16}H_{22}O_{11}$), 5-methyl caffeoylquinic acid ($C_{17}H_{20}O_9$), cinchonain I isomer ($C_{24}H_{20}O_9$), rutin ($C_{27}H_{30}O_{16}$), di-*O*-caffeoylquinic acid ($C_{25}H_{24}O_{12}$), and quinic acid ($C_7H_{12}O_6$), respectively. Peaks 20 and 21, 22, 23 and 24 also produced fragment ions at *m/z* 390.11317; *m/z* 174.95588; *m/z* 341.06822; *m/z* 463, 447 and *m/z* 353.08946 (Li *et al*., 2015; Ruan *et al*., 2019; Wu *et al*., 2017; El-Askary *et al*., 2019; Sun *et al*., 2019). Comparison with literature data confirmed the identities of these compounds. The stem bark samples solely contained many of these metabolites. This is the first study identifying and reporting these metabolites from *B. salicina*.

Table 4.2. Identification of constituents from *Breonadia salicina* by UPLC-QTOF-MS.

Peak No.	Rt (min)	Theoretical Mass $[M-H]^-$ (*m/z*)	Observed Mass $[M-H]^-$ (*m/z*)	Molecular Formula	MS/MS fragment ions (*m/z*)	Compound Name	Compound Class	Samples	References
1	0.661	377.0878	377.08633	$C_{18}H_{18}O_9$	341,215,160	Caffeic acid derivative	Hydroxycinnamic acid	S.crude	Toth *et al*., 2014
2	14.908	461.0720	461.07350	$C_{21}H_{18}O_{12}$	315,299	4'-*O*-methyellagic acid-3-*O*-α-L-rhamnopyranoside	Polyphenol	S.crude	Wu *et al*., 2017
3	12.782	300.999	300.99929	$C_{14}H_6O_8$	242,174	Ellagic acid	Polyphenol	S.crude	Singh *et al*., 2016
4	13.002	447.0569	447.05763	$C_{20}H_{16}O_{12}$	300.99898	Ellagic acid-rhamnopyranoside isomer I	Hydrolysable tannin	S.crude, fraction S_5	Singh *et al*., 2016
5	5.460	289.0707	289.07225	$C_{15}H_{14}O_6$	245.08155	Catechin	Flavonoid	fraction S_1, fraction S_2, fraction S_3	Liu *et al*., 2021
6	21.504	485.3271	485.32825	$C_{30}H_{46}O_5$	485,441	Hydroxyglycyrrhetinic acid	Triterpenoid	fraction S_1	Xiang *et* al., 2011
7	21.767	458.3396	458.33667	$C_{29}H_{46}O_4$	503,457	Neotigogenin acetate	Triterpenoid	fraction S_1	Pei *et al*., 2021
8	22.507	499.3424	499.34385	$C_{31}H_{48}O_5$	455.35408	25-hydroxy-3-epi-dehydrotumulosic acid	Triterpenoid	fraction S_1	Wang *et al*., 2015
9	23.373	453.3347	453.33834	$C_{30}H_{46}O_3$	-	Micromeric acid	Triterpenoid	fraction S_1	Borrás-Linares *et al*., 2014
10	24.467	499.3736	499.37155	$C_{32}H_{50}O_4$	497.36498	3-Acetylursolic acid	Triterpenoid	fraction S_1, fraction S_2	Asteggiano *et al*., 2021
11	1.876	305.0	305.06698	$C_{15}H_{14}O_7$	-	(Epi)gallocatechin	Flavan-3-ol	fraction S_2	Kardel *et al*., 2013
12	4.728	183.0299	183.02975	$C_8H_8O_5$	184.03304	4-*O*-Methylgallic acid	Phenolic acid	fraction S_2	Peng *et al*., 2019
13	11.530	479.0831	479.08529	$C_{21}H_{20}O_{13}$	480.08721	Myricetin 3-*O*-glucoside	Flavonoid	fraction S_3, fraction S_4	Tang *et al*., 2020
14	22.882	455.35412	455.35397	$C_{30}H_{48}O_3$	-	Ursolic acid	Triterpenoid	S.crude, fraction S_1	Liu *et al*., 2015
15	21.610	487.35	487.33699	$C_{30}H_{48}O_5$	485.32825	Asiatic acid	Triterpenoid	fraction S_3, fraction R_1	Velamuri *et al*., 2020

Peak No.	Rt (min)	Theoretical Mass $[M-H]^-$ (*m/z*)	Observed Mass $[M-H]^-$ (*m/z*)	Molecular Formula	MS/MS fragment ions (*m/z*)	Compound Name	Compound class	Samples	References
16	12.569	433.0412	433.04194	$C_{19}H_{14}O_{12}$	300.99929	Ellagic acid pentoside	Polyphenol	R.crude	Singh *et al.*, 2016
17	1.140	170	170.01742	$C_7H_6O_5$	-	Gallic acid	Phenolic acid	fraction R_1	Minh *et al.*, 2019
18	0.663	533.1738	533.17341	$C_{19}H_{34}O_{17}$	191.05605	Quinic acid + $hexose_2$	Quinic acids and derivatives + Monosaccharide	LM.crude, fraction LM_3	Zhumakanova *et al.*, 2021
19	6.415	353.08685	353.08839	$C_{16}H_{18}O_9$	191,707	Chlorogenic acid [3.4-dihydroxycinnamoylquinic acid; 5-Caffeoylquinic acid]	Quinic acids	LM.crude	Peeters *et al.*, 2020
20	8.421	389.1088	389.10941	$C_{16}H_{22}O_{11}$	390.11317	Deacetyl asperuloside acid	Monoterpenoid	LM.crude	Li *et al.*, 2015
21	10.819	367.10346	367.10424	$C_{17}H_{20}O_9$	174.95588	5-Methyl caffeoylquinic acid	Quinic acid	LD.crude, fraction LM_2	Ruan *et al.*, 2019
22	10.181	451.1029	451.10412	$C_{24}H_{20}O_9$	341.06822	Cinchonain I isomer	Flavonolignan	LM.crude	Wu *et al.*, 2017
23	12.918	609.1464	609.14777	$C_{27}H_{30}O_{16}$	463,447	Rutin	Flavonoid glycoside	LM.crude, fraction LM_3	El-Askary *et al.*, 2019
24	14.242	515.5	515.12070	$C_{25}H_{24}O_{12}$	353.08946	Di-*O*-caffeoylquinic acid	Quinic acid	LM.crude, fraction LM_3	Sun *et al.*, 2019
25	0.671	191.1	191.05581	$C_7H_{12}O_6$	-	Quinic acid	Quinic acids and derivatives	LD.crude, fraction LM_2	Sun *et al.*, 2019

4.3.4. Identification of Components of the seasonal Crude Stem Bark, Root and Leaf Extracts by UPLC-QTOF-MS Analysis

Nineteen metabolites of the crude stem bark, root and leaf extracts collected during autumn, winter, spring, and summer, were isolated and tentatively identified by comparison of their spectra with literature values. The complete UPLC-QTOF-MS data for the peaks found in the different sample chromatograms, including their fragment ions, retention times, and molecular ions $[M-H]^-$ are reported in Table 4.3. Peak 1 (Appendix 78, *m/z* 533.17426 $[M-H]^-$), peak 2 (Appendix 79, *m/z* 353.08943 $[M-H]^-$), peak 3 (Appendix 80, *m/z* 390.11424 $[M-H]^-$), peak 4 (Appendix 81, *m/z* 403.12695 $[M-H]^-$) and peak 5 (Appendix 82, *m/z* 515.12236 $[M-H]^-$) and peak 6 (Appendix 83, *m/z* 537.16508 $[M-H]^-$) were identified as quinic acid + hexose$_2$ ($C_{19}H_{34}O_{17}$), chlorogenic acid [3,4-dihydroxycinnamoylquinic acid; 5-caffeoylquinic acid] ($C_{16}H_{18}O_9$), *trans*-resveratroloside ($C_{20}H_{22}O_8$), oleoside 11-methylester ($C_{17}H_{24}O_{11}$), 3,4-dicaffeoylquinic acid ($C_{25}H_{24}O_{12}$), and 4,8,4',8'-tetramethoxy-(1,1'-biphenanthrene)-2,7,2',7'-tetrol ($C_{32}H_{26}O_8$), respectively. The MS-MS spectra of peaks 1, 2, 3, 4 and 5 yielded fragment ions at *m/z* 191.05626; *m/z* 191.05672; *m/z* 389.11129; *m/z* 404.13018 and *m/z* 353,191, respectively. Comparison with literature data allowed identification of these compounds (Zhumakanova *et al*., 2021; Peeters *et al*., 2020; Goufo *et al*., 2020; Tang *et al*., 2020; Kramberger *et al*., 2020; Luo *et al*., 2021). Peaks 7 (Rt = 12.670 min), 8 (Rt = 0.746 min), 9 (Rt = 8.735 min), and 10 (Rt = 0.760 min) with $[M-H]^-$ ions at *m/z* 439.32578 (Appendix 84), *m/z* 369.08500 (Appendix 85), *m/z* 455.31978 (Appendix 86), and *m/z* 191.05725 (Appendix 87), were tentatively identified as pfaffic acid ($C_{29}H_{44}O_3$), ferulic acid 4-*O*-glucuronide ($C_{16}H_{18}O_{10}$), ursolic acid ($C_{30}H_{48}O_3$), and quinic acid ($C_7H_{12}O_6$), respectively (Rodrigues *et al*., 2013; Tang *et al*., 2020; Liu *et al*., 2015; Sun *et al*., 2019). Peak 8 also produced fragment ions at *m/z* 161 and 353, whereas peaks 7, 9, and 10 did not produce significant fragment ions. Peak 11 (Rt = 5.218, $C_{16}H_{22}O_{11}$) was identified unequivocally as deacetyl asperuloside acid (Appendix 88, *m/z* 389.11215 $[M-H]^-$), peak 12 (Rt = 7.005, $C_{27}H_{30}O_{16}$) as rutin (Appendix 89, *m/z* 609.15209 $[M-H]^-$), and peak 13 (Rt = 13 7.290, $C_{25}H_{24}O_{12}$) as di-*O*-caffeoylquinic acid (Appendix 90, *m/z* 515.12463 $[M-H]^-$) (Li *et al*., 2015; El-Askary *et al*., 2019; Sun *et al*., 2019). The MS-MS spectra of peaks 11, 12 and 13 also showed fragment ions at *m/z* 390.11531; *m/z* 463,447 and *m/z* 353.09154, respectively. Peak 14 (Appendix 91, *m/z* 327.22003 $[M-H]^-$), was identified as trihydroxy-octadecadienoic acid, peak 15 (Appendix 92, *m/z* 271.23033 $[M-H]^-$) as 15-hydroxyhexadecanoic acid, peak 16 (Appendix 93, *m/z* 490.36367 $[M-H]^-$) as 3-α,24*R*,25-trihydroxytirucall-8-en-21-oic acid, peak

17 (Appendix 94, *m/z* 433.13824 $[M-H]^-$) as 6-α-hydroxyforsythide dimethyl ester, peak 18 (Appendix 95, *m/z* 578.27461 $[M-H]^-$) as atractyloside G 2-*O*-β-D-glucopyranoside, and peak 19 (Appendix 96, *m/z* 547.36888 $[M-H]^-$) as sibiricose A6 (Yan *et al*., 2015; Zhang *et al*., 2018; Liu and Abreu, 2006; Reidah and Ibrahim, 2013; Kitajima *et al*., 2003; Sun *et al*., 2020). The MS-MS spectra of peaks 14, 15, 16, 17, 18 and 19 also showed fragment ion signals at *m/z* 301.20403; *m/z* 161.02552; *m/z* 489.36367; *m/z* 191,377,403; *m/z* 577.27461 and *m/z* 369,443, respectively. Finally, the identities of these compounds were confirmed by comparison with literature data.

The UPLC-QTOF-MS profiles showed that different plant parts of *B. salicina,* collected in 2019 and 2020, produced both similar and dissimilar phytochemicals during different seasons. The crude stem bark, root and leaf extracts collected in 2019 contained 3-acetylursolic acid, asiatic acid, a caffeic acid derivative, 5-*O*-caffeoylquinic acid, catechin, cinchonain I isomer, ellagic acid, ellagic acid pentoside, ellagic acid-rhamnopyranoside isomer I, (epi)gallocatechin, fructose, gallic acid, α-glucose, β-glucose, hexadecane, 25-hydroxy-3-epi-dehydrotumulosic acid, hydroxyglycyrrhetinic acid, lupeol, 5-methyl caffeoylquinic acid 4'-*O*-methylellagic acid-3-*O*-α-L-rhamnopyranoside, 4-*O*-methylgallic acid, micromeric acid, myricetin 3-*O*-glucoside, and neotigogenin acetate. However, these phytochemicals did not appear in the crude extracts of the leaves, stem bark, and roots collected in 2020. On the other hand, atractyloside G 2-*O*-β-D-glucopyranoside, ferulic acid 4-*O*-glucuronide, 6-α-hydroxyforsythide dimethyl ester, 15-hydroxyhexadecanoic acid, oleoside 11-methylester, pfaffic acid, *trans*-resveratroloside, sibiricose A6, 4,8,4',8'-tetramethoxy-[1,1'-biphenanthrene]-2,7,2',7'-tetrol, trihydroxy-octadecadienoic acid, and 3-α,24*R*,25-trihydroxytirucall-8-en-21-oic acid were only identified in the crude stem bark, root and leaf extracts collected in 2020, and these phytochemicals were not detected in the stem bark, root and leaf extracts collected in 2019. On the other hand, the crude stem bark, leaf, and root extracts of both years revealed the presence of 5-caffeoylquinic acid, di-*O*-caffeoylquinic acid, deacetyl asperuloside acid, 3,4-dihydroxycinnamoylquinic acid, quinic acid, quinic acid + $hexose_2$, rutin, and ursolic acid.

Table 4.3. Identification of constituents from the seasonal crude extracts of *Breonadia salicina* by UPLC-QTOF-MS.

Peak No.	Rt (min)	Theoretical Mass $[M-H]^-$ (*m/z*)	Observed Mass $[M-H]^-$ (*m/z*)	Molecular formula	MS/MS fragment ions (*m/z*)	Compound Name	Compound Class	Autumn extracts	Winter extracts	Spring extracts	Summer extracts	References
1	0.702	533.1738	533.17426	$C_{19}H_{34}O_{17}$	191.05626	Quinic acid + hexose$_2$	Quinic acids and derivatives + Monosaccharide	Stem, root	Stem, root	Stem, root, MeOH leaf	Stem, root	Zhumakanova *et al*., 2021
2	5.351	353.08685	353.08943	$C_{16}H_{18}O_9$	191.05672	Chlorogenic acid [3.4-Dihydroxycinnamoylquinic acid; 5-Caffeoylquinic acid]	Quinic acids	Stem, root, leaf (MeOH & DCM)	Stem, root	Stem, root, leaf (MeOH & DCM)	Stem, root, leaf (MeOH & DCM)	Peeters *et al*., 2020
3	5.204	390.388	390.11424	$C_{20}H_{22}O_8$	389.11129	*trans*-Resveratroloside	Monomers	Stem	Stem	Stem	Stem	Goufo *et al*., 2020
4	6.416	403.1319	403.12695	$C_{17}H_{24}O_{11}$	404.13018	Oleoside 11-methylester	Tyrosols	Stem, root	Stem, root	Stem, root	Stem, root	Tang *et al*., 2020
5	7.210	515.1189	515.12236	$C_{25}H_{24}O_{12}$	353,191	Dicaffeoyl quinic acid isomer: 3,4−diCQA	Quinic acids	Stem, root	Stem, root	Stem, root	Stem, root	Kramberger *et al*., 2020
6	7.723	537.1529	537.16508	$C_{32}H_{26}O_8$	-	4,8,4',8'-Tetramethoxy-[1,1'-biphenanthrene]-2,7,2',7'-tetrol	Biphenanthrene derivatives	Stem, root	Stem, root	Stem, root	Stem, root	Luo *et al*., 2021
7	12.67	439	439.32578	$C_{29}H_{44}O_3$	-	Pfaffic acid	Nortriterpene	Stem	Stem	Stem	Stem	Rodrigues *et al*., 2013
8	0.746	369.0833	369.08500	$C_{16}H_{18}O_{10}$	161,353	Ferulic acid 4-*O*-glucuronide	Phenolic glycosides	Stem, root	Stem, root	Root	Root	Tang *et al*., 2020
9	17.08	455.35412	455.31978	$C_{30}H_{48}O_3$	-	Ursolic acid	Triterpenoid	Root, DCM leaf	Root, DCM leaf	Root	Root	Liu *et al*., 2015
10	0.760	191.1	191.05725	$C_7H_{12}O_6$	-	Quinic acid	Quinic acids and derivatives	MeOH & DCM leaf	MeOH & DCM leaf	DCM leaf	MeOH & DCM leaf	Sun *et al*., 2019
11	5.218	389.1088	389.11215	$C_{16}H_{22}O_{11}$	390.11531	Deacetyl asperuloside acid	Monoterpenoid	Stem, leaf (MeOH & DCM)	Stem, MeOH leaf	Stem, leaf (MeOH & DCM)	Stem, leaf (MeOH & DCM)	Li *et al*., 2015

12	7.005	609.1464	609.15209	$C_{27}H_{30}O_{16}$	463,447	Rutin	Flavonoid glycoside	MeOH & DCM leaf	MeOH & DCM leaf	MeOH leaf	MeOH leaf	El-Askary *et al*., 2019
13	7.290	515.5	515.12463	$C_{25}H_{24}O_{12}$	353.09154	Di-*O*-Caffeoylquinic acid	Quinic acid	MeOH & DCM leaf	MeOH & DCM leaf	MeOH & DCM leaf	MeOH leaf	Sun *et al*., 2019
14	16.80	327.2209	327.22003	$C_{18}H_{32}O_5$	301.20403	Trihydroxy-octadecadienoic acid	Fatty acid	DCM leaf	DCM leaf	DCM leaf	DCM leaf	Yan *et al*., 2015
15	16.22	271.2351	271.23033	$C_{16}H_{32}O_3$	161.02552	15-Hydroxyhexadecanoic acid	Fatty acid	DCM leaf	DCM leaf	DCM leaf	DCM leaf	Zhang *et al*., 2018
16	16.65	490.3658	490.36367	$C_{30}H_{50}O_5$	489.36367	3-α,24R,25-Trihydroxytirucall-8-en-21-oic acid	Triterpenes	DCM leaf	DCM leaf	DCM leaf	DCM leaf	Liu and Abreu, 2006
17	6.071	433.1424	433.13824	$C_{18}H_{26}O_{12}$	191,377,403	6-α-Hydroxyforsythide dimethyl ester	Iridoid glucosides	Root	Root	Root	Root	Reidah and Ibrahim, 2013
18	14.23	578.2938	578.27461	$C_{27}H_{46}O_{13}$	577.27461	Atractyloside G 2-*O*-β-D-glucopyranoside	Sesquiterpenoid	MeOH leaf	MeOH leaf	MeOH leaf	MeOH leaf	Kitajima *et al*., 2003
19	14.44	547.1631	547.36888	$C_{23}H_{32}O_{15}$	369,443	Sibiricose A6	Oligosaccharide ester	DCM leaf	-	DCM leaf	DCM leaf	Sun *et al*., 2020

4.3.5. Comparison of constituents identified in the crude leaf, root, and stem bark extracts of *B. salicina* samples collected in spring 2019 and spring 2020.

The UPLC-QTOF-MS and ^{1}H-NMR profiles shown in Table 4.4 reveal that 3-acetylursolic acid, asiatic acid, a caffeic acid derivative, 5-*O*-caffeoylquinic acid, catechin, cinchonain I isomer, ellagic acid, ellagic acid pentoside, ellagic acid-rhamnopyranoside isomer I, (epi)gallocatechin, fructose, gallic acid, α-glucose, β-glucose, hexadecane, hydroxyglycyrrhetinic acid, 25-hydroxy-3-epi-dehydrotumulosic acid, lupeol, 5-methyl caffeoylquinic acid, 4'-*O*-methyellagic acid-3-*O*-α-L-rhamnopyranoside, 4-*O*-methylgallic acid, micromeric acid, myricetin 3-*O*-glucoside, and neotigogenin acetate, were found only in the root, stem bark, and leaf extracts of samples collected in Spring 2019. These metabolites were not recorded in the extracts of samples collected in Spring 2020. Moreover, atractyloside G 2-*O*-β-D-glucopyranoside, ferulic acid 4-*O*-glucuronide, 15-hydroxyhexadecanoic acid, 6-α-hydroxyforsythide dimethyl ester, oleoside 11-methylester, pfaffic acid, *trans*-resveratroloside, sibiricose A6, 4,8,4’,8’-tetramethoxy-(1,1’-biphenanthrene)-2,7,2’,7’-tetrol, trihydroxy-octadecadienoic acid, and 3-α,24*R*,25-trihydroxytirucall-8-en-21-oic acid were found only in the crude extracts of the stem bark, roots and leaves collected in Spring 2020. These metabolites were not found in the crude extracts of samples collected in the Spring of 2019. Lastly, the chemical profiles show that the stem bark, root and leaf extracts collected in both years also produced several shared metabolites such as 5-caffeoylquinic acid, deacetyl asperuloside acid, di-*O*-caffeoylquinic acid, 3,4-dihydroxycinnamoylquinic acid, gallic acid, quinic acid, quinic acid + hexose$_2$, rutin, and ursolic acid. This study also shows that several compounds were mostly found in the stem bark in both years (Table 4.4).

Table 4.4. Constituents identified from the crude extracts of parts of *Breonadia salicina* collected in Spring 2019 and Spring 2020.

Compound Name	Year 2019	Year 2020	Compound class
Caffeic acid derivative	S.crude	-	Hydroxycinnamic acid
4'-*O*-methyellagic acid-3-*O*-α-L-rhamnopyranoside	S.crude	-	Polyphenol
Ellagic acid	S.crude	-	Polyphenol
Ellagic acid-rhamnopyranoside isomer I	S.crude, fraction S_5	-	Hydrolysable tannin
Catechin	fraction S_1, fraction S_2, fraction S_3	-	Flavonoid
Hydroxyglycyrrhetinic acid	fraction S_1	-	Triterpenoid
Neotigogenin acetate	fraction S_1	-	Triterpenoid
25-hydroxy-3-epi-dehydrotumulosic acid	fraction S_1	-	Triterpenoid
Micromeric acid	fraction S_1	-	Triterpenoid
3-Acetylursolic acid	fraction S_1, fraction S_2	-	Triterpenoid
(Epi) gallocatechin	fraction S_2	-	Flavan-3-ol
4-*O*-Methylgallic acid	fraction S_2	-	Phenolic acid
Myricetin 3-*O*-glucoside	fraction S_3, fraction S_4	-	Flavonoid
Ursolic acid	S.crude, fraction S_1	Root, DCM leaf	Triterpenoid
Asiatic acid	fraction S_3, fraction R_1	-	Triterpenoid
Ellagic acid pentoside	R.crude	-	Polyphenol
Gallic acid	fraction R_1	-	Phenolic acid
Quinic acid + hexose$_2$	LM.crude, fraction LM_3	Stem, root, MeOH leaf	Quinic acids and derivatives + Monosaccharide
Chlorogenic acid [3,4-dihydroxycinnamoylquinic acid; 5-Caffeoylquinic acid]	LM.crude	Stem, root, leaf (MeOH & DCM)	Quinic acids
Deacetyl asperuloside acid	LM.crude	Stem, leaf (MeOH & DCM)	Monoterpenoid
5-Methylcaffeoylquinic acid	LD.crude, fraction LM_2	-	Quinic acid
Cinchonain I isomer	LM.crude	-	Flavonolignan
Hexadecane (**7**)	LD.crude, fraction R_1, fraction LD_3	-	Fatty acid
Lupeol (**2**)	R.crude, fraction S_1, fraction S_2	-	Triterpenoid
5-*O*-caffeoylquinic acid (**5**)	LM.crude, fraction LM_2, fraction LM_3	-	Quinic acids
Rutin	LM.crude, fraction LM_3	MeOH leaf	Flavonoid glycoside

β-Glucose	R.crude, S.crude, LM.crude fraction LM_3	-	Monosaccharide
Glucose and fructose	R.crude, S.crude, LM.crude, fraction LM_3	-	Disaccharide
Di-*O*-caffeoylquinic acid	LM.crude, fraction LM_3	Stem, root, leaf (MeOH & DCM)	Quinic acid
Quinic acid	LD.crude, fraction LM_2	DCM leaf	Quinic acids and derivatives
trans-Resveratroloside	-	Stem	Monomers
Oleoside 11-methylester	-	Stem, root	Tyrosols
4,8,4',8'-Tetramethoxy-[1,1'-biphenanthrene]-2,7,2',7'- tetrol	-	Stem, root	Biphenanthrene derivatives
Pfaffic acid	-	Stem	Nortriterpene
Ferulic acid 4-*O*-glucuronide	-	Root	Phenolic glycosides
Trihydroxy-octadecadienoic acid	-	DCM leaf	Fatty acid
15-Hydroxyhexadecanoic acid	-	DCM leaf	Fatty acid
3-α,24R,25-Trihydroxytirucall-8-en-21-oic acid	-	DCM leaf	Triterpenes
6-α-Hydroxyforsythide dimethyl ester	-	Root	Iridoid glucosides
Atractyloside G 2-*O*-β-D-glucopyranoside	-	MeOH leaf	Sesquiterpenoid
Sibiricose A6	-	DCM leaf	Oligosaccharide ester

4.4. Summary

To conclude:

- Seven metabolites (5-*O*-caffeoylquinic acid, catechin, fructose, α-glucose, β-glucose, hexadecane, and lupeol) were tentatively identified by ^{1}H-NMR profiling.
- Forty-four metabolites were identified tentatively by UPLC-QTOF-MS profiling.
- Fifty-one metabolites were tentatively identified in the crude extracts, fractions and seasonal samples of *B. salicina* by ^{1}H-NMR and UPLC-QTOF-MS profiling.
- Flavonoids, polyphenols and triterpenoids were found mostly in the root and stem bark samples collected in both years.
- Quinic acids and fatty acids were mostly found in the leaf samples collected in both years.
- Similar and dissimilar metabolites were produced in different plant parts in each season.
- Autumn produced the most compounds, followed by spring, summer and winter.
- In Spring of both years, the stem bark produced more metabolites than the leaf and root samples.
- The results of this study show that the metabolomics approach is potentially a superior method compared to classical methods. Moreover, classical methods are time-consuming and often inefficient in the exploration of chemical constituents, unlike the metabolomics approach.
- This is the first report on the chemical variability of the metabolites found in *B. salicina* stem bark, root and leaf, collected in the same season for two years using a metabolomics approach.

4.5 References

Asteggiano, A.; Occhipinti, A.; Capuzzo, A.; Mecarelli, E.; Aigotti, R.; Medana, C. Quali–Quantitative Characterization of Volatile and Non-Volatile Compounds in *Protium heptaphyllum* (Aubl.) Marchand Resin by GC–MS Validated Method, GC–FID and HPLC–HRMS2. *Molecules*, **2021**, 26, 1447.

Ben Youssef, S.; Fakhfakh, J.; Tchoumtchoua, J.; Halabalaki, M.; Allouche, N. Efficient purification and complete NMR characterization of galactinol, sucrose, raffinose, and stachyose isolated from *Pinus halepensis* (Aleppo pine) seeds using acetylation procedure. *Journal of Carbohydrate Chemistry*. **2016**, *35*, 224-237.

Borrás-Linares, I.; Stojanović, Z.; Quirantes-Piné, R.; Arráez-Román, D.; Švarc-Gajić, J.; Fernández-Gutiérrez, A.; Segura-Carretero, A. *Rosmarinus officinalis* leaves as a natural source of bioactive compounds. *International Journal of Molecular Sciences*, **2014**, 15, 20585-20606.

Dayrit, F.M.; Lagurin, L.G.; Magsalin, J.D.J.; Zosa, A.R. Chemical profiling and chemical standardization of *Vitex negundo* using ^{13}C-NMR. *Journal of Medicinal Plants Research*, **2017**, 11, 11-21.

Desai, S.; Tatke, P.; Gabhe, S. Isolation of catechin from stem bark of *Albizia lebbeck*. *International Journal of Analytical, Pharmaceutical and Biomedical Sciences*, **2014**, 3, 31-35.

El-Askary, H.; Handoussa, H.; Badria, F.; El-Khatib, A.H.; Alsayari, A.; Linscheid, M.W.; Abdel Motaal, A. Characterization of hepatoprotective metabolites from *Artemisia annua* and *Cleome droserifolia* using HPLC/PDA/ESI/MS–MS. *Revista Brasileira de Farmacognosia*, **2019**, 29, 213-220.

Goufo, P.; Singh, R.K.; Cortez, I. A reference list of phenolic compounds (including stilbenes) in grapevine (*Vitis vinifera* L.) roots, woods, canes, stems, and leaves. *Antioxidants*, **2020**, 9, 398.

Kardel, M.; Taube, F.; Schulz, H.; Schütze, W.; Gierus, M. Different approaches to evaluate tannin content and structure of selected plant extracts–review and new aspects. *Journal of Applied Botany and Food Quality*, **2013**, 86, 154-166.

Kitajima, J.; Kamoshita, A.; Ishikawa, T.; Takano, A.; Fukuda, T.; Isoda, S.; Ida, Y. Glycosides of *Atractylodes lancea*. *Chemical and Pharmaceutical Bulletin*, **2003**, 51, 673-678.

Kramberger, K.; Barlič-Maganja, D.; Bandelj, D.; Baruca Arbeiter, A.; Peeters, K.; Miklavčič Višnjevec, A.; Jenko Pražnikar, Z. HPLC-DAD-ESI-QTOF-MS determination of bioactive compounds and antioxidant activity comparison of the hydroalcoholic and water extracts from two *Helichrysum italicum* species. *Metabolites*, **2020**, 10, 403.

Li, L.; Wang, Z.; Peng, Y.; Fu, X.; Wang, Y.; Xiao, W.; Song, S. Screening and identification of multi-components in Re Du Ning injections using LC/TOF-MS coupled with UV-irradiation. *Journal of Chromatographic Science*, **2015**, 53, 778-786.

Li, X.Y.; Shang, R.; Fu, M.C.; Fu, Y. Conversion of biomass-derived fatty acids and derivatives into hydrocarbons using a metal-free hydrodeoxygenation process. *Green Chemistry*, **2015**, 17, 2790-2793.

Liu, W.; Huang, J.; Zhang, F.; Zhang, C-C.; Li, R-S.; Wang, Y-L.; Wang,C-R.; Liang, X-M.; Zhang, W-D.; Yang, L.; Liu, P.; Ge, G-B. Comprehensive profiling and characterization of the absorbed components and metabolites in mice serum and tissues following oral administration of Qing-Fei-Pai-Du decoction by UHPLC-Q-Exactive-Orbitrap HRMS. *Chinese Journal of Natural Medicines*, **2021**, 19, 305-320.

Liu, M.; Zhao, S.; Wang, Y.; Liu, T.; Li, S.; Wang, H.; Tu, P. Identification of Multiple Constituents in Chinese Medicinal Prescription Shensong Yangxin Capsule by Ultra-Fast

Liquid Chromatography Combined with Quadrupole Time-of-Flight Mass Spectrometry. *Journal of Chromatographic Science*, **2015**, 53, 240-252.

Liu, Y.; Abreu, P. Tirucallane triterpenes from the roots of Ozoroa insignis. *Phytochemistry*, **2006**, 67, 1309-1315.

Luo, Y.; Wang, J.; Li, S.; Wu, Y.; Wang, Z.; Chen, S.; Chen, H. Discovery and identification of potential anti-melanogenic active constituents of Bletilla striata by zebrafish model and molecular docking, **2021**.

Minh, T.N.; Xuan, T.D.; Tran, H.D.; Van, T.M.; Andriana, Y.; Khanh, T.D.; Quan, N.V.; Ahmad, A. Isolation and purification of bioactive compounds from the stem bark of *Jatropha podagrica. Molecules*, **2019**, 24, 889.

Mouffok, S.; Haba, H.; Lavaud, C.; Long, C.; Benkhaled, M. Chemical constituents of Chemical constituents of *Centaurea omphalotricha Coss. & Durieu ex Batt. & Trab. Records of Natural Products*. **2012**, *6*, 292-5.

Ogawa, K.; Yamamura, M.; Maruyama, I. Isolation and identification of 3-*O*-methyl-d-galactose as a constituent of neutral polysaccharide of *Chlorella vulgaris. Bioscience, Biotechnology, and Biochemistry*, **1994**, 58, 942-944.

Pei, H.; Su, W.; Gui, M.; Dou, M.; Zhang, Y.; Wang, C.; Lu, D. Comparative Analysis of Chemical Constituents in Different Parts of Lotus by UPLC and QToF-MS. *Molecules*, **2021**, 26, 1855.

Peng, D.; Zahid, H.F.; Ajlouni, S.; Dunshea, F.R.; Suleria, H.A. Lc-esi-qtof/ms profiling of australian mango peel by-product polyphenols and their potential antioxidant activities. *Processes*, **2019**, 7, 764.

Peeters, L.; Van der Auwera, A.; Beirnaert, C.; Bijttebier, S.; Laukens, K.; Pieters, L.; Hermans, N.; Foubert, K. Compound characterization and metabolic profile elucidation after in vitro gastrointestinal and hepatic biotransformation of an *Herniaria hirsuta* extract using unbiased dynamic metabolomic data analysis. *Metabolites*, **2020**, 10, 111.

Reidah, I.M.A.; Ibrahim, M. Characterization of phenolic compounds in highly-consumed vegetable matrices by using advanced analytical techniques. *Editorial de la Universidad de Granada*, **2013**.

Rodrigues, M.V.N.; Vedovello, A.; Rodrigues, R.A.F.; Montanari Junior, I.; Rehder, V.L.G. Improved method to obtain pfaffic acid as a marker for quality control. *Química Nova*, **2013**, 36, 725-728.

Ruan, J.; Yan, J.; Zheng, D.; Sun, F.; Wang, J.; Han, L.; Zhang, Y.; Wang, T. Comprehensive chemical profiling in the ethanol extract of *Pluchea indica* aerial parts by liquid chromatography/mass spectrometry analysis of its silica gel column chromatography fractions. *Molecules*, **2019**, 24, 2784.

Salem, M.A.; Perez de Souza, L.; Serag, A.; Fernie, A.R.; Farag, M.A.; Ezzat, S.M.; Alseekh, S. Metabolomics in the context of plant natural products research: From sample preparation to metabolite analysis. *Metabolites*, **2020**, 10, 37.

Singh, A.; Bajpai, V.; Kumar, S.; Sharma, K.R.; Kumar, B. Profiling of gallic and ellagic acid derivatives in different plant parts of *Terminalia arjuna* by HPLC-ESI-QTOF-MS/MS. *Natural Product Communications*, **2016**, 11, 1934578-1601100227.

Suarez-Quiroz, M.L.; Campos, A.A.; Alfaro, G.V.; González-Ríos, O.; Villeneuve, P.; Figueroa-Espinoza, M.C. Isolation of green coffee chlorogenic acids using activated carbon. *Journal of Food Composition and Analysis*. **2014**, *33*, 55-58.

Sun, L.; Tao, S.; Zhang, S. Characterization and quantification of polyphenols and triterpenoids in thinned young fruits of ten pear varieties by UPLC-Q TRAP-MS/MS. *Molecules*, **2019**, 24, 159.

Sun, Y.; Feng, G.; Zheng, Y.; Liu, S.; Zhang, Y.; Pi, Z.; Song, F.; Liu, Z. Putative multiple reaction monitoring strategy for the comparative pharmacokinetics of postoral administration Renshen–Yuanzhi compatibility through liquid chromatography–tandem mass spectrometry. *Journal of Ginseng Research*, **2020**, 44, 105-114.

Tan, J.; Zheng, M.; Duan, S.; Zeng, Y.; Zhang, Z.; Cui, Q.; Zhang, J.; Hong, T.; Bai, J.; Du, S., 2018. Chemical profiling and screening of the marker components in the fruit of *Cassia fistula* by HPLC and UHPLC/LTQ-Orbitrap MSn with chemometrics. *Molecules*, **2018**, 23, 1501.

Tang, J.; Dunshea, F.R.; Suleria, H.A. Lc-esi-qtof/ms characterization of phenolic compounds from medicinal plants (hops and juniper berries) and their antioxidant activity. *Foods*, **2020**, 9, 7.

Toth, A.; Toth, G.; Kery, A. Polyphenol composition and antioxidant capacity of three *Lysimachia* species. *Natural Product Communications*, **2014**, 9, 1934578-1400901017.

Valentino, G.; Graziani, V.; D'Abrosca, B.; Pacifico, S.; Fiorentino, A.; Scognamiglio, M. NMR-based plant metabolomics in nutraceutical research: an overview. *Molecules*, **2020**, 25, 1444.

Velamuri, R.; Sharma, Y.; Fagan, J.; Schaefer, J. Application of UHPLC-ESI-QTOF-MS in phytochemical profiling of sage (*Salvia officinalis*) and rosemary (*Rosmarinus officinalis*). *Planta Medica International Open*, **2020**, 7, 133-144.

Wang, P.; Wang, B.; Xu, J.; Sun, J.; Yan, Q.; Ji, B.; Zhao, Y.; Yu, Z. Detection and chemical profiling of Ling-Gui-Zhu-Gan decoction by ultra-performance liquid chromatography-hybrid linear ion trap-orbitrap mass spectrometry. *Journal of Chromatographic Science*, **2015**, 53, 263-273.

Wu, J.; Fang, X.A.; Yuan, Y.; Dong, Y.; Liang, Y.; Xie, Q.; Ban, J.; Chen, Y.; Lv, Z. UPLC/Q-TOF-MS profiling of phenolics from *Canarium pimela* leaves and its vasorelaxant and antioxidant activities. *Revista Brasileira de Farmacognosia*, **2017**, 27, 716-723.

Xiang, C.; Qiao, X.; Wang, Q.; Li, R.; Miao, W.; Guo, D.; Ye, M. From single compounds to herbal extract: a strategy to systematically characterize the metabolites of licorice in rats. *Drug Metabolism and Disposition*, **2011**, 39, 1597-1608.

Xiao, Q.; Mu, X.; Liu, J.; Li, B.; Liu, H.; Zhang, B.; Xiao, P. Plant metabolomics: a new strategy and tool for quality evaluation of Chinese medicinal materials. *Chinese Medicine*, **2022**, 17, 1-19.

Yan, G.; Zou, D.; Zhang, A.; Tan, Y.; Sun, H.; Wang, X. UPLC-Q-TOF-MS/MS fingerprinting for rapid identification of the chemical constituents of *Ermiao Wan*. *Analytical Methods*, **2015**, 7, 846-862.

Zhang, Y.D.; Li, P.; Zheng, N.; Jia, Z.W.; Meruva, N.; Ladak, A.; Cleland, G.; Wen, F.; Li, S.L.; Zhao, S.G.; Wang, J.Q. A metabolomics approach to characterize raw, pasteurized, and ultra-high temperature milk using ultra-performance liquid chromatography–quadrupole time-of-flight mass spectrometry and multivariate data analysis. *Journal of Dairy Science*, **2018**, 101, 9630-9636.

Zhumakanova, B.S.; Korona-Głowniak, I.; Skalicka-Woźniak, K.; Ludwiczuk, A.; Baj, T.; Wojtanowski, K.K.; Józefczyk, A.; Zhaparkulova, K.A.; Sakipova, Z.B.; Malm, A. Phytochemical Fingerprinting and In Vitro Antimicrobial and Antioxidant Activity of the Aerial Parts of *Thymus marschallianus* Willd. and *Thymus seravschanicus* Klokov Growing Widely in Southern Kazakhstan. *Molecules*, **2021**, 26, 3193.

CHAPTER 5 EFFECT OF SEASONAL VARIATION ON THE SECONDARY METABOLITES OF *B. SALICINA*

5.1. INTRODUCTION

Many medicinal plants produce active secondary metabolites (phytochemicals) during different seasons. These metabolites have been isolated and derived from different plants and are widely used in modern medicine (Mendoza and Silva, 2018). However, the appearance of various components and growth of medicinal plants are influenced by environmental conditions, such as temperature, height above MSL, rainfall, light intensity, different soil characteristics, humidity and change of season (Vanitha *et al*., 2006; Gololo *et al.*, 2016). These conditions may produce major variations in the bioactive compounds present in the plants (Geetha and Geetha 2014). Therefore, these environmental conditions should be taken into consideration for plant collection purposes, to ensure a reproducible quantity of bioactive compounds (Vanitha *et al*., 2006). Metabolomics is used in many different study areas of traditional medicine as a method for drug discovery (Putri *et al*., 2013; Heyman and Meyer 2012; Heyman *et al.*, 2015). Such studies usually apply spectroscopic techniques and chemometrics to characterize, categorise and validate different medicinal plant species or to study the impact of the seasons, storage, developmental stages, drying, geographic locations, harvesting, processing and growth environment on the occurrence of certain secondary metabolites, and their quality and efficacy (Fan *et al.*, 2014; Farag *et al*., 2014; Scognamiglio *et al*., 2015). In order to study the influence of seasonal variation on the phytochemical constituents of *Breonadia salicina,* analysis by UPLC-QTOF-MS and integrated multivariate analysis, was used. Metabolomics were effective in determining the chemical composition and efficacy of the leaves, roots, and stem bark of *B. salicina* collected during the different seasons (spring, summer, autumn, and winter).

Metabolomics is a term denoting the wide-ranging quantitative and qualitative analysis of a group of metabolites (targeted approach) or all metabolites (untargeted approach), classifying and quantifying biomarkers in a complex matrix (Rosli *et al*., 2021; Seneviratne *et al*., 2020). While the targeted approach focuses on analysing for a group of known metabolites, the untargeted approach involves identification of numerous unexpected metabolites (Liang *et al*., 2020). Identification and quantitation of secondary plant metabolites is supported mostly by liquid chromatography and gas chromatography coupled to mass spectrometry, NMR

spectroscopy, and FTIR spectroscopy (Li *et al*., 2019; Zhang *et al*., 2018; Martens *et al*., 2017). However, liquid chromatography-mass spectrometry (LC-MS) is the most frequently used technology in metabolomics for the analysis of more polar constituents (Nalbantoglu, 2019). Furthermore, GC-MS is also a commonly used technique in metabolomics, used to detect trace quantities of targeted or untargeted metabolites that are non-polar, volatile or highly volatile (Wang, 2015; Fiehn, 2016). Moreover, NMR spectroscopy is normally used as an analytical tool for plant metabolomics, to identify and characterize structures of compounds (Emwas *et al*., 2019). Several atoms are NMR active, such as ^{1}H, ^{13}C and ^{31}P; proton (^{1}H) NMR spectroscopy is the most commonly applied technique in metabolomics (Lee *et al*., 2016). The complete characterization of a compound is achieved with 2D-NMR (Emwas *et al*., 2019). Multivariate analysis is a tool used to determine the metabolomic fingerprinting of chromatographic or spectroscopic datasets, and is performed using principal component analysis (PCA), which is used to convert datasets in the untargeted approach. Other methods are partial least squares-discriminant analysis (PSL-DA), requiring supervised methods or a targeted approach; discriminant analysis by orthogonal projection of latent structures (OPLS-DA), which involves using known information of the samples with supervision; and hierarchical cluster analysis (HCA), which reveals the differences amongst groups or classes without using the unsupervised or untargeted approach (Worley and Powers, 2013). In the previous chapter (Chapter 4) we described how the chemical profiles of the seasonal samples were explored and compared with the chemical profiles of the samples that were collected during Spring of the previous year, since phytochemical analysis and the biological activities might be limited to the chemistry of the plant collected in one season (spring). Therefore, we now discuss the chemometric study used to mine the data provided by the UPLC-QTOF-MS analysis to display the chemical variability of the leaves, roots, and stem bark of *B. salicina*, collected during four consecutive seasons (spring, summer, autumn, and winter).

5.2. MATERIALS AND METHODS

5.2.1. Plant sampling and extraction of seasonal samples

Chapter 4, section **4.2.1.2** describes the methodology in detail.

5.2.2. UPLC-QTOF-MS analysis

A 1 mg/mL working solution was prepared in HPLC grade methanol (Merck, Darmstadt, Germany) for UPLC-QTOF-MS analysis. Samples (n = 48) were prepared and analysed in triplicate (Table 5.1). The detailed UPLC-QTOF-MS methodology is reported in Chapter 4, section **4.2.4**.

Table 5.1. Seasonal plant samples and codes for *B. salicina* in triplicate (n = 48).

Seasonal samples	Codes
Autumn	
Stem bark	Sa1, Sa2 and Sa3
Root	Ra1, Ra2 and Ra3
DCM leaf	Lda1, Lda2 and Lda3
MeOH leaf	Lma1, Lma2 and Lma3
Winter	
Stem bark	Sb1, Sb2 and Sb3
Root	Rb1, Rb2 and Rb3
DCM leaf	Ldb1, Ldb2 and Ldb3
MeOH leaf	Lmb1, Lmb1 and Lmb1
Spring	
Stem bark	Sc1, Sc2 and Sc3
Root	Rc1, Rc2 and Rc3
DCM leaf	Ldc1, Ldc1 and Ldc1
MeOH leaf	Lmc1, Lmc1 and Lmc1
Summer	
Stem bark	Sd1, Sd1 and Sd1
Root	Rd1, Rd1 and Rd1
DCM leaf	Ldd1, Ldd1 and Ldd1
MeOH leaf	Lmd1, Lmd1 and Lmd1

5.2.3. Chemometric Analysis of LC-MS Data

The UPLC-MS analysis of 48 seasonal samples provided data that was exported to Microsoft Excel (Sandasi *et al*., 2011) and successively imported into MetaboAnalyst 5.0, a free metabolomics data analytical tool available online (www.metaboanalyst.ca/MetaboAnalyst/home.xhtml). Principal component analysis (PCA), partial least squares discriminant analysis (PLS-DA) and a loading score plot were obtained with Pareto scaling method. Hierarchical cluster analysis (HCA) was based on the PCA model and the resulting dendrogram was used to evaluate sample groupings and trends in the *Breonadia salicina* dataset.

5.3. RESULTS AND DISCUSSION

5.3.1. Using UPLC-MS for quality assurance

5.3.1.1. Untargeted UPLC-MS analysis

The UPLC-MS data were used to construct the principal component analysis (PCA) model, using the fingerprints of the leaf, root, and stem bark samples collected during the four different seasons to assess the trends within the analysis results. The scores plot was established using the first (39.5 %) and second (18.4 %) components, explaining 57.9 % of the variation in the data. The colours of the scores plot were based on the samples of the three plant parts (leaf, root, and stem bark), as shown in Figure 5.1. Largely, the two major clusters observed are related to the leaf, root, and stem bark samples. The largest group encompassing the leaves, was separated along negative PC1 while the stem and root samples were clustered along positive PC1. There was a clear separation of the dichloromethane and methanol leaf extracts along PC2. The PLS-DA analysis (Figure 5.2) enabled identification of the compounds contributing to the different dendrogram clusters. A scores plot was constructed using the first (39.3 %) and second (11.3 %) components, contributing 50.6 % of the variation (as shown in Figure 5.2). Branch red (X), which consists of the stem bark and root samples was separated along negative PC1; and branch blue (Y), which consists of the methanol leaf and dichloromethane leaf samples was distributed on the positive PC1. Furthermore, there was a clear separation of the dichloromethane and methanol leaf extracts along PC2. In addition, separation of the stem bark and root samples can be observed along PC1. There was also a clear separation of the root samples; the autumn samples (Ra1, Ra2, Ra3) were further separated from the other seasons, indicating that the chemistry of the autumn root samples differs from that of the other seasons (as shown in Figure 5.2). A dendrogram (Figure 5.3) was constructed from the hierarchical cluster analysis (HCA), to explore the chemical variability within the samples. The dendrogram (Figure 5.3) obtained revealed three major branches, like the PCA plot. Branch X (red) consists of stem and root samples, while branch Y consists of leaf samples. In branch X, the stem and root samples were further separated indicating distinct chemistry that was not visible in the PCA plot. The first branch X (red, Figure 5.3) displayed clusters of all the different seasons: summer (Sd1, Sd2, Sd3), winter (Sb1, Sb2, Sb3), autumn (Sa1, Sa2, Sa3), and spring (Sc1, Sc2, Sc3) in the stem bark samples, respectively. However, the root samples revealed clusters of all four seasons: spring (Rc1, Rc2, Rc3), winter (Rb1, Rb2, Rb3), summer (Rd1, Rd2, Rd3) and autumn (Ra1, Ra2, Ra3), respectively, as presented in Figure 5.3. Moreover, the second branch Y (blue) comprising the leaf samples showed a

clear separation between the MeOH leaf extracts and DCM leaf extracts, as shown in Figure 5.3. Furthermore, the second branch Y (blue) showed clusters of the methanol leaf extracts of all the different seasons. The dichloromethane extracts also exhibited clusters for spring (Ldc1, Ldc2, Ldc3), autumn (Lda1, Lda2, Lda3), summer (Ldd1, Ldd2, Ldd3), and winter (Ldb1, Ldb2, Ldb3), respectively. Therefore, the second branch Y (blue) of the dendrogram points to the different chemistries of the MeOH leaf extracts and the DCM leaf extracts. In addition, the chemistry of the leaf extracts differs from that of the root and stem bark samples. The constituents contributing to most of the discrimination shown in the loadings plot (Figure 5.4) were identified using the VIP scores. The marker compounds were identified as follows: leaf sample: ursolic acid (*m/z* 455.35/Rt 17.08 min), rutin (*m/z* 609.14/Rt 6.99 min) and *m/z* 505.35 (Rt 14.80 min); root samples: *m/z* 793.43 (Rt 12.07 min), quinic acid + hexose$_2$ (*m/z* 533.17/Rt 0.70 min), pfaffic acid (*m/z* 439.31/Rt 12.67 min), 4,8,4',8'-tetramethoxy-[1,1'-biphenanthrene]-2,7,2',7'-tetrol (*m/z* 537.15/Rt 7.72 min) and *m/z* 967.62 (Rt 12.66 min); stem bark samples: 4,8,4',8'-tetramethoxy-[1,1'-biphenanthrene]-2,7,2',7'-tetrol (*m/z* 537.15/Rt 7.72 min), ferulic acid 4-*O*-glucuronide (*m/z* 369.08/Rt 0.74 min) and quinic acid + hexose$_2$ (*m/z* 533.17/Rt 0.70 min). According to the heatmap (Figure 5.5), the concentrations of rutin and ursolic acid were moderate in the leaf samples. However, the concentration of an unidentified compound with molecular ion *m/z* 501.31 (Rt 15.50 min) was very high in the autumn dichloromethane leaf samples. Furthermore, the concentrations of ferulic acid 4-*O*-glucuronide, oleoside 11-methylester, pfaffic acid, 4,8,4',8'-tetramethoxy-[1,1'-biphenanthrene]-2,7,2',7'-tetrol, di-*O*-caffeoylquinic acid and quinic acid + hexose$_2$ were very low in the leaf samples; however the concentrations of these compounds were moderate in the root and stem bark extracts.

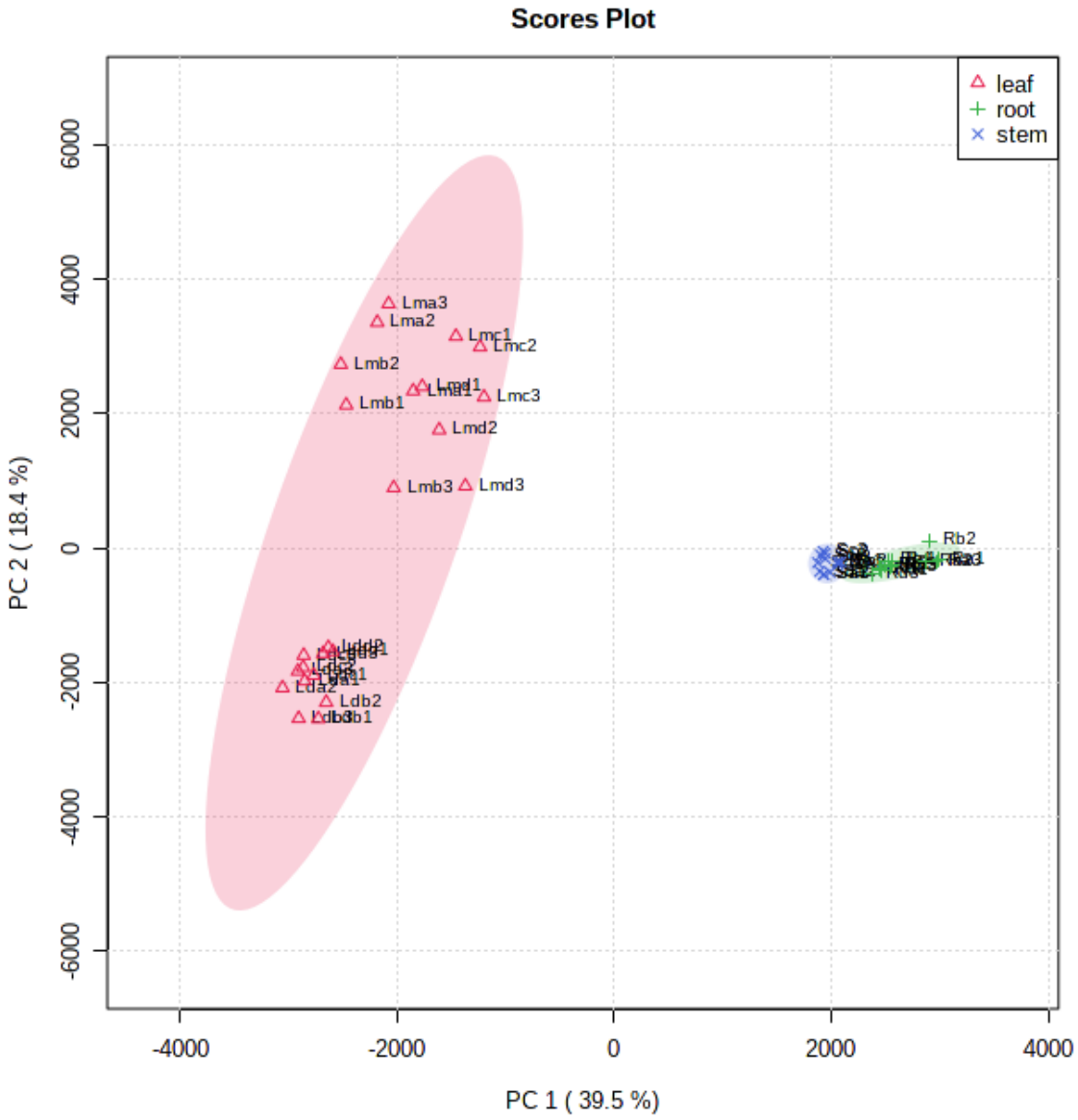

Figure 5.1. Principal component analysis (PCA) of clusters of crude leaf, root, and stem bark extracts of samples collected in autumn, winter, spring, and summer.

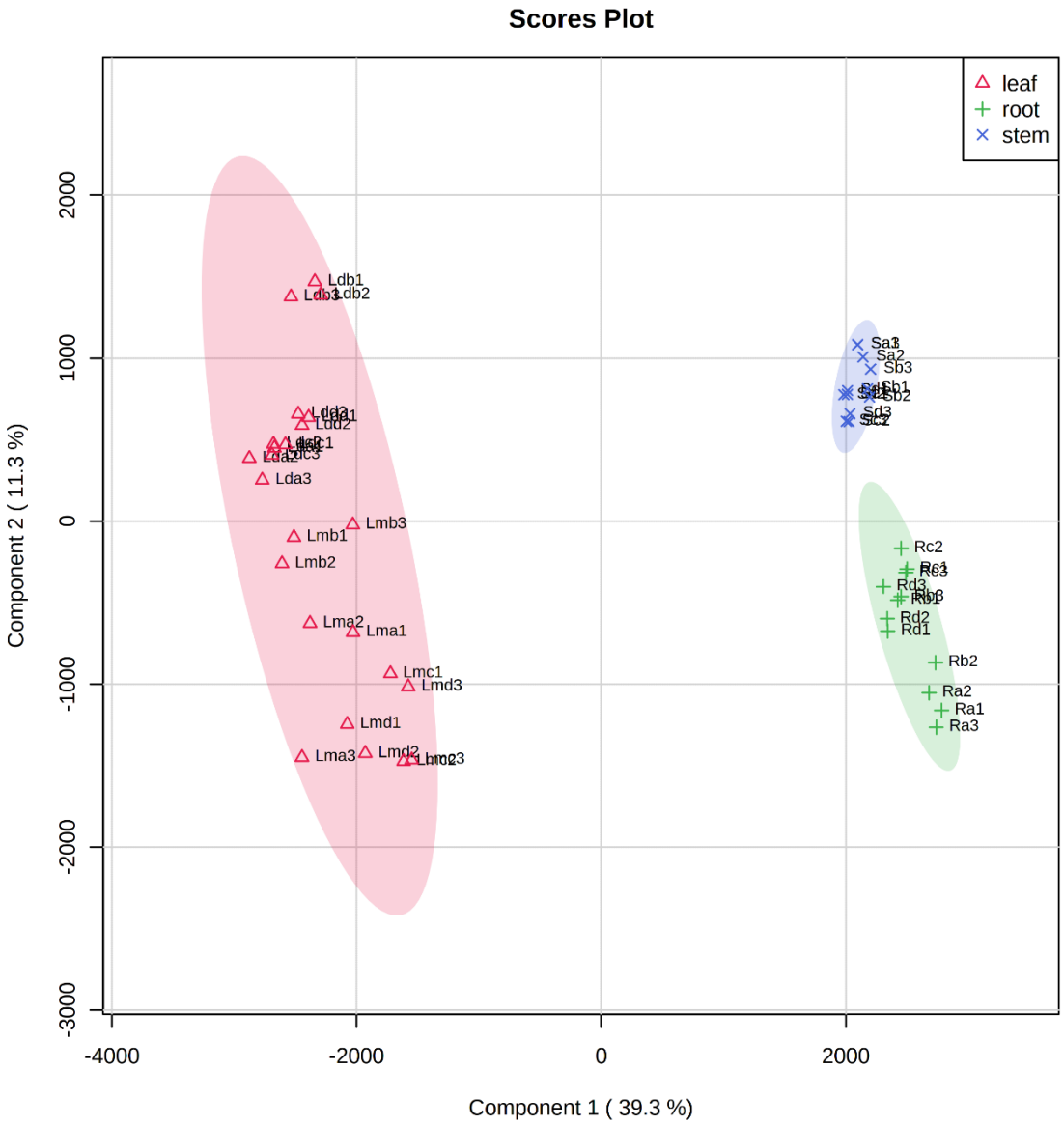

Figure 5.2. PLS-DA of clusters of the dendrogram.

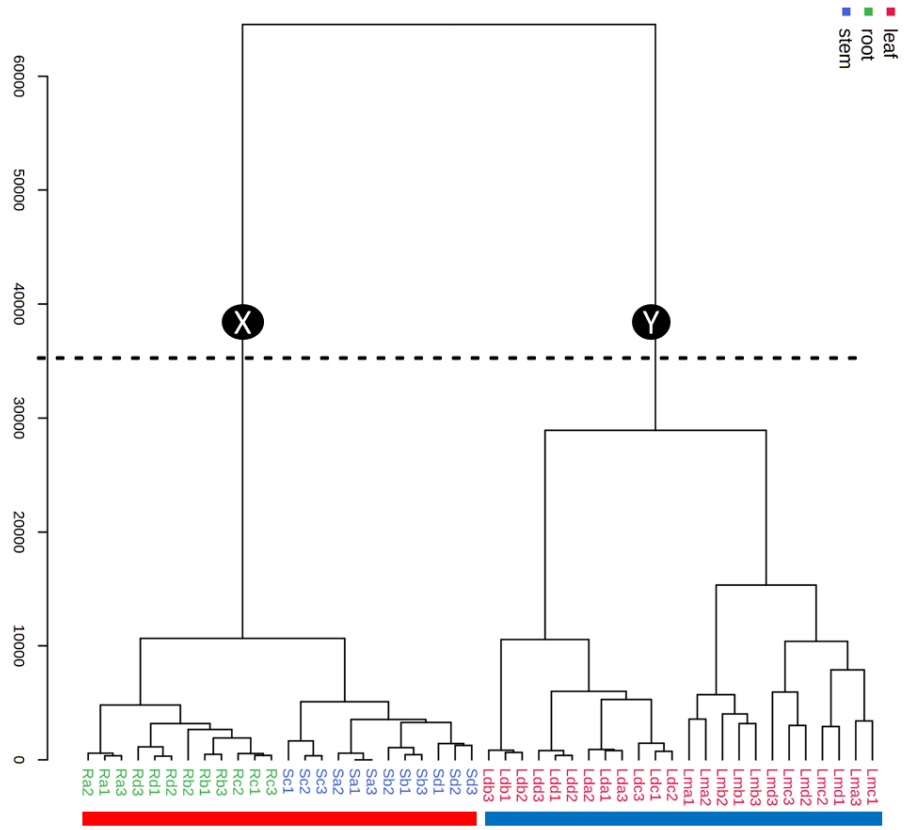

Figure 5.3. HCA dendrogram of the LCMS data (n = 48) acquired from the leaf, stem bark and root samples from four different seasons. Branch X (red): samples of the stem bark and root; branch Y (blue): samples of MeOH and DCM leaf extracts.

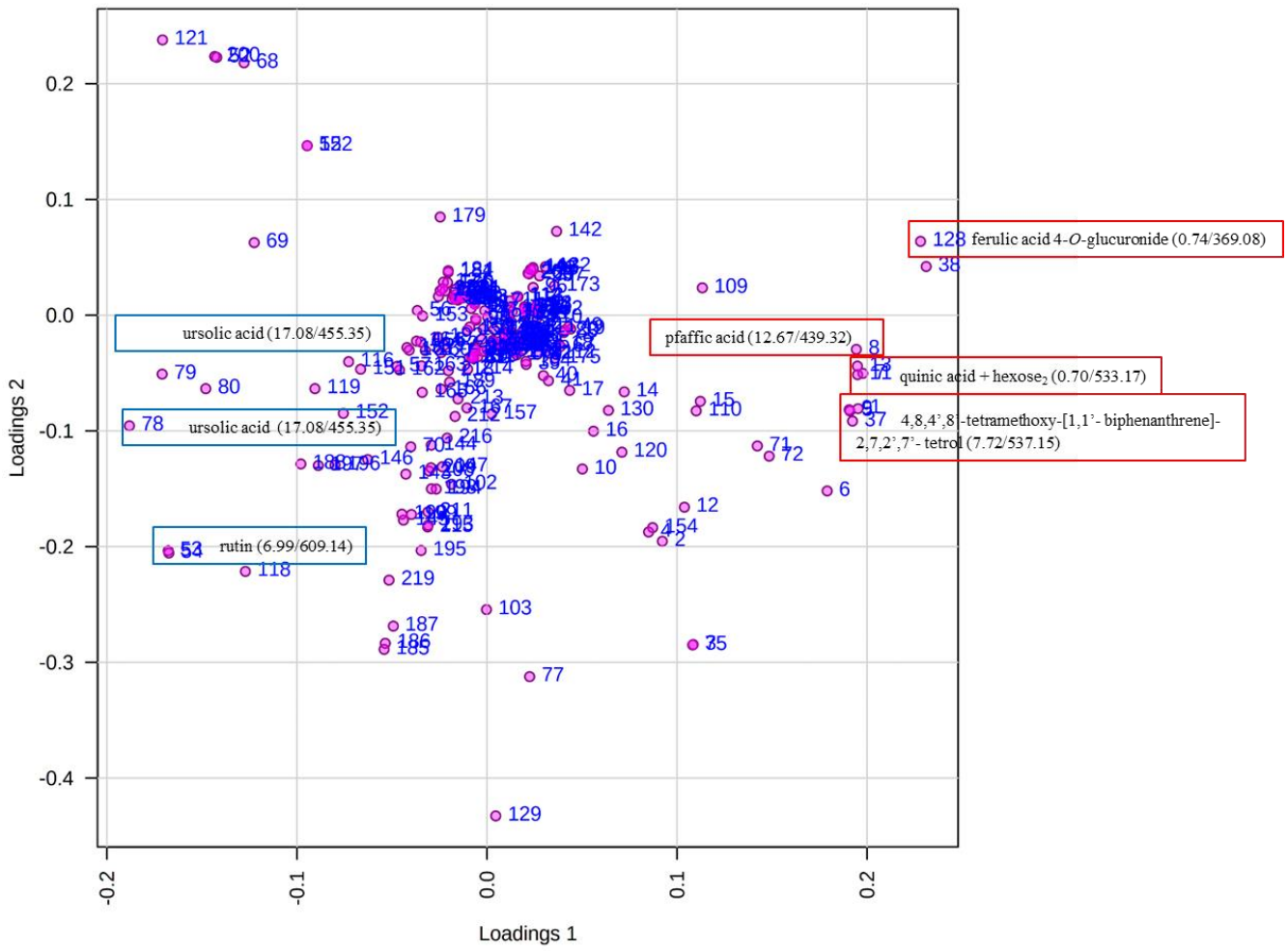

Figure 5.4. Loadings score plot obtained from constituents shown as red (root) and red (stem bark) rectangles contributing to the Branch X (red) cluster. Compounds in the blue (leaf) rectangles contributed to Branch Y (blue) clustering. The constituent indicated by a red rectangle (ferulic acid 4-*O*-glucuronide: 0.74/369.08) was the first variable shown by the VIP plot.

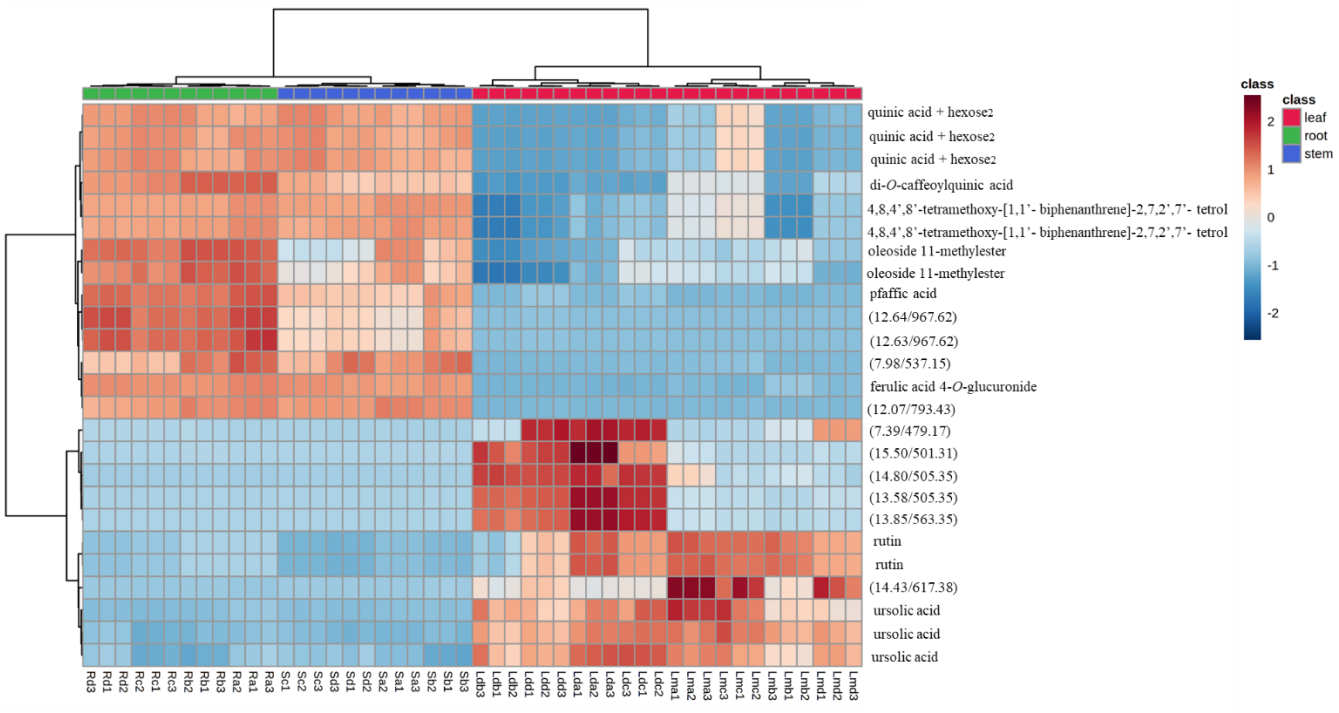

Figure 5.5. Heatmap of 25 peaks in 48 samples of *B. salicina* stem bark, root and leaf.

5.4. Summary

In conclusion:

- The hierarchical cluster analysis showed that the metabolites identified by UPLC-QTOF-MS analysis of the seasonal leaf, stem bark, and root samples could be categorised into two main groups, implying significantly different chemical compositions.
- In the dendrogram, the root and stem bark extracts contributed to the clustering in branch red (X); whereas the leaf samples were clustered in branch blue (Y).
- The data showed that the chemistries of the leaf, stem and root samples are different; it further showed that the root and stem samples have similar chemistry.
- The chemistry of the methanol and dichloromethane leaf samples is different. In addition, the dendrogram showed that the chemistry of the leaf samples differs from that of the root and stem bark extracts.
- The heatmap and the variable importance for project (VIP) plot showed that rutin and ursolic acid contribute to the clustering of the leaf samples; and ferulic acid 4-*O*-glucuronide, oleoside 11-methylester, pfaffic acid, 4,8,4',8'-tetramethoxy-[1,1'-biphenanthrene]-2,7,2',7'-tetrol, di-*O*-caffeoylquinic acid and quinic acid + hexose$_2$ contribute to the clustering of the root and stem bark extracts.
- This is the first seasonal study of *Breonadia salicina* using a metabolomics approach, chemometrics and UPLC-QTOF-MS analysis.

5.5. References

Emwas, A.H.; Roy, R.; McKay, R.T.; Tenori, L.; Saccenti, E.; Gowda, G.A.; Raftery, D.; Alahmari, F.; Jaremko, L.; Jaremko, M.; Wishart, D.S. NMR spectroscopy for metabolomics research. *Metabolites*, **2019**, 9, 123.

Fan, G.; Luo, W.Z.; Luo, S.H.; Li, Y.; Meng, X.L.; Zhou, X.D.; Zhang, Y. Metabolic discrimination of *Swertia mussotii* and *Swertia chirayita* known as "Zangyinchen" in traditional Tibetan medicine by ^{1}H NMR-based metabolomics. *Journal of Pharmaceutical and Biomedical Analysis*, **2014**, 98, 364-370.

Farag, M.A.; Gad, H.A.; Heiss, A.G.; Wessjohann, L.A. Metabolomics driven analysis of six Nigella species seeds via UPLC-qTOF-MS and GC–MS coupled to chemometrics. *Food Chemistry*, **2014**, 151, 333-342.

Fiehn, O. Metabolomics by gas chromatography–mass spectrometry: combined targeted and untargeted profiling. *Current Protocols in Molecular Biology*, **2016**, 114, 30-34.

Geetha, T.S.; Geetha, N. Phytochemical screening, quantitative analysis of primary and secondary metabolites of *Cymbopogan citratus* (DC) Stapf. leaves from Kodaikanal hills, Tamilnadu. *International Journal of Pharmtech Research*, **2014**, 6, 521-529.

Gololo, S.S.; Shai, L.J.; Agyei, N.M.; Mogale, M.A. Effect of seasonal changes on the quantity of phytochemicals in the leaves of three medicinal plants from Limpopo province, South Africa. *Journal of Pharmacognosy and Phytotherapy*, **2016**, 8, 168-172.

Heyman, H.M.; Meyer, J.J.M. NMR-based metabolomics as a quality control tool for herbal products. *South African Journal of Botany*, **2012**, 82, 21-32.

Heyman, H.M.; Senejoux, F.; Seibert, I.; Klimkait, T.; Maharaj, V.J.; Meyer, J.J.M. Identification of anti-HIV active dicaffeoylquinic-and tricaffeoylquinic acids in *Helichrysum populifolium* by NMR-based metabolomic guided fractionation. *Fitoterapia*, **2015**, 103, 155-164.

Liang, Y.; Ke, X.; Xiao, Z.; Zhang, Y.; Chen, Y.; Li, Y.; Wang, Z.; Lin, L.; Yao, P.; Lu, J. Untargeted Metabolomic Profiling Using UHPLC-QTOF/MS Reveals Metabolic Alterations Associated with Autism. *BioMed Research International*, **2020**, 2020.

Li, X.; Zhang, X.; Ye, L.; Kang, Z.; Jia, D.; Yang, L.; Zhang, B. LC-MS-based metabolomic approach revealed the significantly different metabolic profiles of five commercial truffle species. *Frontiers in Microbiology*, **2019**, 10, 2227.

Lee, S.Y.; Abas, F.; Khatib, A.; Ismail, I.S.; Shaari, K.; Zawawi, N. Metabolite profiling of *Neptunia oleracea* and correlation with antioxidant and α-glucosidase inhibitory activities using ^{1}H-NMR-based metabolomics. *Phytochemistry Letters*, **2016**, 16, 23-33.

Martens, J.; Berden, G.; van Outersterp, R.E.; Kluijtmans, L.A.; Engelke, U.F.; van Karnebeek, C.D.; Wevers, R.A.; Oomens, J. Molecular identification in metabolomics using infrared ion spectroscopy. *Scientific Reports*, **2017**, 7, 1-5.

Mendoza, N.; Silva, E.M.E. Introduction to phytochemicals: secondary metabolites from plants with active principles for pharmacological importance. *Phytochemicals: Source of Antioxidants and Role in Disease Prevention*, **2018**, 25. http://dx.doi.org/10.5772/intechopen.78226

Nalbantoglu, S. Metabolomics: basic principles and strategies. *Molecular Medicine*, **2019**, 10.

Putri, S.P.; Nakayama, Y.; Matsuda, F.; Uchikata, T.; Kobayashi, S.; Matsubara, A.; Fukusaki, E. Current metabolomics: practical applications. *Journal of Bioscience and Bioengineering*, **2013**, 115, 579-589.

Rosli, M.A.F.; Mediani, A.; Azizan, K.A.; Baharum, S.N.; Goh, H.H. UPLC-TOF-MS/MS-Based Metabolomics Analysis Reveals Species-Specific Metabolite Compositions in

Pitchers of *Nepenthes ampullaria*, *Nepenthes rafflesiana*, and Their Hybrid *Nepenthes*× *hookeriana*. *Frontiers in Plant Science*, **2021**, 12.

Sandasi, M.; Kamatou, G.P.; Viljoen, A.M. Chemotaxonomic evidence suggests that *Eriocephalus tenuifolius* is the source of Cape chamomile oil and not *Eriocephalus punctulatus. Biochemical Systematics and Ecology*, **2011**, 39, 328-338.

Scognamiglio, M.; D'Abrosca, B.; Esposito, A.; Fiorentino, A. Chemical composition and seasonality of aromatic mediterranean plant species by NMR-based metabolomics. *Journal of Analytical Methods in Chemistry*, **2015**, 2015. http://doi.org/10.1155/2015/258570

Seneviratne, C.J.; Suriyanarayanan, T.; Widyarman, A.S.; Lee, L.S.; Lau, M.; Ching, J.; Delaney, C.; Ramage, G. Multi-omics tools for studying microbial biofilms: current perspectives and future directions. *Critical Reviews in Microbiology*, **2020**, 46, 759-778.

Tooth, S.; McCarthy, T.S.; Hancox, P.J.; Brandt, D.; Buckley, K.; Nortje, E.; McQuade, S. The geomorphology of the Nyl River and floodplain in the semi-arid Northern Province, South Africa. *South African Geographical Journal*, **2002**, 84, 226-237.

Vanitha, A.; Renganayagi, R.; Prabakaran, R.; Mohammed, S.M. Pharmacognostic studies on *Trichodesma indicum* Linn. (*Boraginaceae*) an ethnobotanically important herb from Tropics. *Pharmacie Globale*, **2015**, 6, 1.

Wang, Y.; Xu, L.; Shen, H.; Wang, J.; Liu, W.; Zhu, X.; Wang, R.; Sun, X.; Liu, L. Metabolomic analysis with GC-MS to reveal potential metabolites and biological pathways involved in Pb and Cd stress response of radish roots. *Scientific Reports*, **2015**, 5, 1-13.

Worley, B.; Powers, R. Multivariate analysis in metabolomics. *Current Metabolomics*, **2013**, 1, 92-107.

Zhang, Y.; Zhang, H.; Chang, D.; Guo, F.; Pan, H.; Yang, Y. Metabolomics approach by ^{1}H-NMR spectroscopy of serum reveals progression axes for asymptomatic hyperuricemia and gout. *Arthritis Research and Therapy*, **2018**, 20, 1-11.

CHAPTER 6 EFFECTS OF SEASONAL VARIATION ON ANTIMALARIAL AND ANTITRYPANOSOMAL ACTIVITIES OF *BREONADIA SALICINA*

6.1. INTRODUCTION

Several environmental conditions, such as seasonal changes, affect metabolite production in plants (Soni *et al*., 2015; Sultan *et al*., 2018). Metabolites might accumulate over a certain period in reaction to seasonal changes. Variations in metabolite formation may lead to noticeable changes in a plant's metabolic fingerprint or profile, thus affecting the quality of the bioactive compound (Sultan *et al*., 2018). The physiological activity, which relies on the compounds present, is subjected to these variations, and various studies have provided evidence of these variations in chemistry and bioactivity of plant extracts (Ncube *et al*., 2011; Kibungu *et al*., 2021; Nndwammbi *et al*., 2018; Soni *et al*., 2015; Sultan *et al*., 2018; Gololo *et al*., 2016; Bhardwaj *et al*., 2019; Demuner *et al*., 2011; Lubbe *et al*., 2013; Tomar *et al*., 2015). Temperature, rainfall, soil humidity, height above MSL, light intensity, and change of season, are all environmental factors that can influence plant growth (Szakiel *et al*., 2011; Ahmad *et al*., 2011). Furthermore, the chemical composition, such as the concentration, availability and bioactivity, determines the biological product. Discrepancy in these physical characteristics in a plant may cause difficulties for the validation of its therapeutic value (Dhami and Mishra 2015). If a natural plant product loses or has no activity, such a plant may cease to be regarded as having any medicinal importance, whereas conditions causing the changes in phytochemical production may have been missed. The traditional herbal market would benefit from plants and herbs with stable and standardized amounts of active secondary metabolites, and less variation in pharmacological activity (Falasca *et al*., 2014). For better quality assurance, it is essential to monitor any discrepancies in the composition and pharmacological activity resulting from environmental conditions affecting the production of phytochemicals. Furthermore, a biotechnology methodology like metabolomics with integrated multivariate data analysis can be used to determine the effects caused by environmental factors, such as seasons, on the production of phytochemicals (Farag *et al*., 2014). Plant metabolomics has been able to accomplish this through its ability to distinguish variations in plant metabolite affected by different environmental factors (Heyman *et al*., 2015). A few studies have provided evidence in the success of the metabolomics technique in exploring seasonal influences on the chemical compounds circulating in significant therapeutic plants (Fan *et al*., 2014;

Scognamiglio *et al*. 2015; Kim *et al*., 2015; Gazim *et al*., 2010; Falasca *et al*., 2014). As shown by ethnobotanical research, *B. salicina* is used widely to treat malaria and trypanosomiasis (Sibandze, 2009; Ali *et al*., 2018), indicating that the plant produces compounds with antimalarial and antitrypanosomal activities. However, no reports could be found describing the phytochemistry and bioactivity of those phytochemicals that could be responsible for the plant's antimalarial and antitrypanosomal activities. Therefore, the isolation of compounds from the different parts of *B. salicina* using reductionist and classical methods was contemplated, to assess their role in the treatment of malaria and trypanosomiasis. A few studies have revealed that the Rubiaceae family possesses phytochemicals such as alkaloids, anthraquinones, coumarins, flavonoids, iridoids, quinic acid glycosides, terpenes, and other phenolic derivatives (Martins and Nunez, 2015). However, nothing is known about the seasonal variation of the chemistry and bioactivity of *Breonadia salicina*. Therefore, the effect of seasonal variation on the bioactivity was explored. In the foregoing chapters (Chapters 4 and 5), the chemical profile and chemical variability of *Breonadia salicina* was explored using a holistic approach. This is because reductionist and classical methods are inadequate to explore the phytochemistry of *B. salicina* and link the phytochemistry to the biological activities. Consequently, in this chapter the changes in chemical and antimalarial and antitrypanosomal activities in response to seasonal changes are evaluated using a metabolomics approach; furthermore, compounds will be isolated to determine their role in the biological activities of the plant parts.

6.2. MATERIALS AND METHODS

6.2.1. Sampling and extraction

The method is described in detail in Chapter 3, section **3.2.1**.

6.2.2. Fractionation

A detailed description of the fractionation methodology is provided in Chapter 3, section **3.2.2**.

6.2.3. Purification of fractions

A detailed description of the purification methodology appears in Chapter 3, section **3.2.3**.

6.2.4. Plant sampling and extraction of seasonal samples

A detailed description of the methodology is provided in Chapter 4, section **4.2.1.2.**

6.2.5. UPLC-QTOF-MS

A detailed description of the method appears in Chapter 4, section **4.2.4**.

6.2.6. Chemometric Analysis of LC-MS Data

A detailed description of the chemometric analysis is given in Chapter 5, section **5.2.3**.

6.2.7. Antiplasmodial activity method

Plasmodium falciparum (3D7 strain) parasites (Manassas, VA, USA) were maintained in an atmosphere comprising 5 % CO_2, 5 % O_2 and 90 % N_2 at 37 °C in RPMI 1640 medium consisting of 5 % Albumax II, 60 µg/mL gentamycin, 20 mM glucose, 2 mM L-glutamine, 25 mM Hepes (Lonza Bioscience), 0.65 mM hypoxanthine, and 2-4 % hematocrit human red blood cells. The crude extracts and fractions (50 µg/mL) and isolated compounds (20 µg/mL) were added in 96-well plates and incubated for 48 hours in a 37 °C CO_2 incubator. After incubation, 20 µL of each culture was transferred to another 96-well plate with a concoction of 125 µL Malstat and Nitroblue tetrazolium (NBT)/Phenazine ethosulphate (PES) solutions (Lunga *et al*., 2018) in each well. The *Plasmodium* lactate dehydrogenase (pLDH) enzyme was used to determine the activity of the measured solutions. The absorbance at 620 nm (Abs_{620}) of the coloured solution was measured using a Spectramax M3 microplate reader (Molecular Dynamics Inc.). From Abs_{620} the percentage parasite viability (%) was calculated and compared to untreated control wells. Dose-response analyses were done as described above, but the parasite cultures were incubated with three serial dilutions of the crude extracts, fractions and seasonal crude extracts (300 µg/mL), while the concentrations of the pure compounds were 200 µg/mL. Graphs of the percentage parasite viability versus the log(sample concentration) were drawn and the plots were used to calculate the IC_{50} values by non-linear regression using GraphPad Prism (GraphPad Software).

6.2.8. Antitrypanosomal activity

The samples were dissolved to yield concentrations of 50 µg/mL for the crude extracts and fractions, and 20 µg/mL for pure compounds, and added to *T. b. brucei* (strain Lister 427) cultures in 96-well plates (triplicate; 2.4 x 10^4 parasites/well). Iscove's Modified Dulbecco's Medium consisting of 25 mM HEPES (4-(2-hydroxyethyl)-1-piperazineethanesulfonic acid) (IMDM; Thermo Fisher Scientific) supplemented with 10 % foetal bovine serum (Biowest), penicillin/streptomycin (Lonza) and HMI-9 supplement was used (Scovill *et al*., 2002). HMI-

9 consists of 1.5 mM cysteine, 0.09 mM cytosine, 1 mM hypoxanthine, 0.05 mM bathocuproine disulfonic acid, 0.014 % 2-mercaptoethanol, 1.25 mM pyruvic acid, 0.16 mM thymidine, and 0.09 mM uracil (Sigma-Aldrich). Incubation at 37˚C for 24 h in a humidified 5 % CO_2 incubator was followed by addition of resazurin (Sigma-Aldrich) to a final concentration of 0.05 mM. After a further 24 h incubation, the fluorescence of the formed resorufin was measured using a Spectramax M3 fluorescence plate reader. The fluorescence was converted to % cell viability, after subtracting blank and background fluorescence. For dose-response analysis, the experiments were done as described above. However, the parasite cultures were incubated with three serial dilutions of 300 µg/mL crude extracts and fractions, while the pure compounds were tested at a concentration of 200 µg/mL. The percentage (%) parasite viability was plotted against the log(sample concentration) and was used to determine the IC_{50} by non-linear regression as above.

6.2.9. Statistical analysis

For the antiplasmodial dose-response tests, the parasite was cultured with three serial dilutions each of fraction S_1, fraction S_2, fraction S_3, kaempferol 3-*O*-(2"-*O*-galloyl)-glucuronide (**1**), palmitic acid (**8**), autumn DCM leaf extract, winter DCM leaf extract, spring DCM leaf extract, and summer DCM leaf extract. As before, the graph of percentage viability against log(sample concentration) was used to calculate IC_{50} values. The antiplasmodial drug chloroquine was used as positive control for antiplasmodial activity. The antitrypanosomal dose-response tests were executed similarly, by culturing the parasite with 3 serial dilutions each of fraction S_1, LM.crude, LD.crude, fraction LD_3, kaempferol 3-*O*-(2"-*O*-galloyl)-glucuronide (**1**), lupeol (**2**), bodinioside Q (**4**), palmitic acid (**8**), autumn MeOH leaf extract, spring MeOH leaf extract, summer MeOH leaf extract, autumn DCM leaf extract, winter DCM leaf extract, spring DCM leaf extract, and summer DCM leaf extract. The graph of percentage viability versus log (sample concentration) permitted calculation of IC_{50} values. The known drug pentamidine was used as positive control.

6.3. RESULTS AND DISCUSSION

6.3.1. Antimalarial activity of *B. salicina*

The *in vitro* antiplasmodial activity of the fractions, crude extracts, and pure compounds was assayed against *Plasmodium falciparum* (3D7 strain) cultures. At 50 µg/mL, the crude extracts and fractions all caused a significant decrease in parasite viability, except for fraction LD_2, which did not decrease the viability of *Plasmodium falciparum* (64.59 ± 4.52 %) (Table 6.1). The presence of the identified and characterized flavanoids, hydrolysable tannin, hydroxycinnamic acids polyphenols, quinic acids, and triterpenoids might have been responsible for the strong antimalarial activities of these samples at a concentration of 50 µg/mL (Table 4.2, Chapter 4). The *Plasmodium* lactate dehydrogenase (pLDH) assay was then repeated at a concentration of 10 µg/mL. As a result, fractions S_1, S_2 and S_3 caused a significant decrease in parasite viability, with viabilities of 16.16 ± 8.63 %, 27.01 ± 4.47 % and 31.07 ± 6.71 % (Table 6.1); and IC_{50} values of 2.19 ± 0.09 µg/mL, 1.91 ± 0.05 µg/mL and 3.02 ± 0.08 µg/mL, respectively (Figure 6.1). However, the crude stem bark extract (S.crude, viability 105.65 ± 3.20 %) from which the fractions S_1, S_2 and S_3 were obtained did not decrease the viability of *Plasmodium falciparum*. This might be because the compounds causing the antimalarial activities of fractions S_1, S_2 and S_3 were in low concentrations in the crude stem bark extract. Furthermore, the presence of catechin, hydroxyglycyrrhetinic acid, neotigogenin acetate, 25-hydroxy-3-epidehydrotumulosic acid, micromeric acid, 3-acetylursolic acid, ursolic acid, (epi)gallocatechin, 4-*O*-methylgallic acid, asiatic acid, and myricetin 3-*O*-glucoside, identified in fractions S_1, S_2 and S_3, might have been responsible for the significant antimalarial activities of these fractions at a concentration of 10 µg/mL (Table 4.2, Chapter 4). According to the literature survey, there are no reports of the *in vitro* and *in vivo* antimalarial activities of these phytochemicals. Therefore, this study provides the first information on the metabolites that could be contributing to the antimalarial activity of *B. salicina*. Furthermore, kaempferol 3-*O*-(2"-*O*-galloyl)-glucuronide (**1**) and palmitic acid (**8**) caused a substantial decrease in parasite viability at a concentration of 50 µg/mL, with viabilities of 29.37 ± 1.29 % and 24.97 ± 5.21 % (Table 6.1); and IC_{50} values of 9.06 ± 0.036 µg/mL and 6.792 ± 0.046 µg/mL at a concentration of 200 µg/mL, respectively (Figure 6.1). Chloroquine was the positive control with an IC_{50} of 0.03 µg/mL (Figure 6.1).

Table 6.1. Antiplasmodial activities of the crude extracts, fractions and pure compounds.

Samples	pLDH (% viability ± SD) 50 µg/mL	pLDH (% viability ± SD) 10 µg/mL
S.crude	35.87 ± 0.52	105.65 ± 3.20
Fraction S_1	17.58 ± 1.13	16.16 ± 8.63
Fraction S_2	14.97 ± 2.90	27.01 ± 4.47
Fraction S_3	10.89 ± 0.58	31.07 ± 6.71
Fraction S_4	30.09 ± 5.21	97.29 ± 4.15
Fraction S_5	12.77 ± 0.24	84.86 ± 1.28
R.crude	42.61 ± 2.99	102.26 ± 4.79
Fraction R_1	14.06 ± 1.23	100.90 ± 2.88
LM.crude	10.82 ± 0.78	105.20 ± 6.39
Fraction LM_2	13.94 ± 2.55	101.81 ± 8.63
Fraction LM_3	16.42 ± 0.46	105.88 ± 3.52
LD.crude	10.88 ± 0.65	99.10 ± 3.52
Fraction LD_2	64.59 ± 4.52	64.59 ± 4.52
Fraction LD_3	15.33 ± 1.70	100.45 ± 0.32
Kaempferol 3-*O*-(2"-*O*-galloyl)-glucuronide (**1**)	29.37 ± 1.29	-
Lupeol (**2**)	60.15 ± 5.93	-
D-Galactopyranose (**3**)	87.70 ± 0.59	-
Bodinioside Q (**4**)	89.42 ± 2.41	-
5-*O*-Caffeoylquinic acid (**5**)	69.19 ± 3.54	-
Sucrose (**6**)	81.80 ± 3.74	-
Hexadecane (**7**)	89.72 ± 9.59	-
Palmitic acid (**8**)	24.97 ± 5.21	-

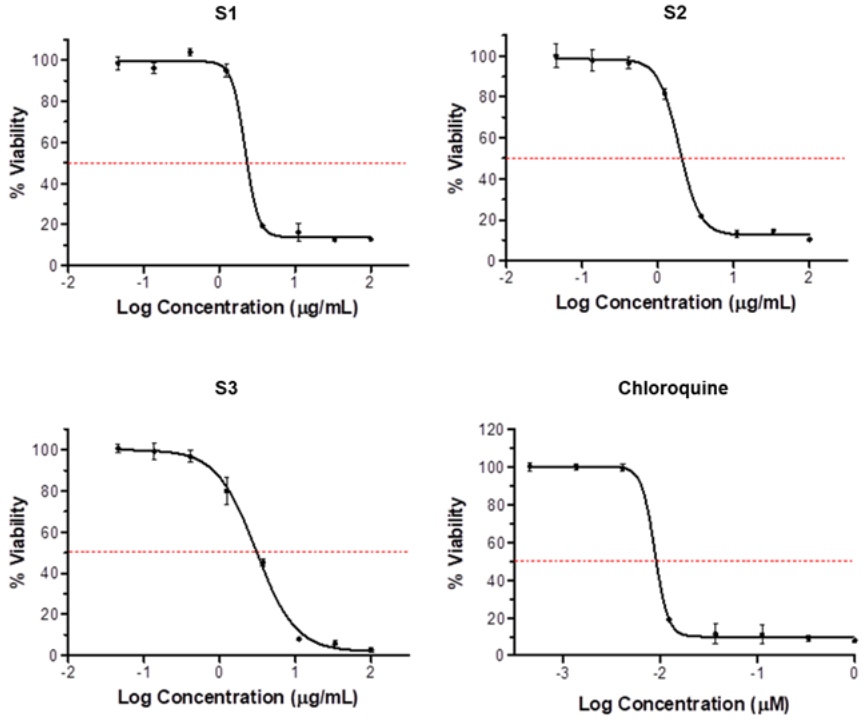

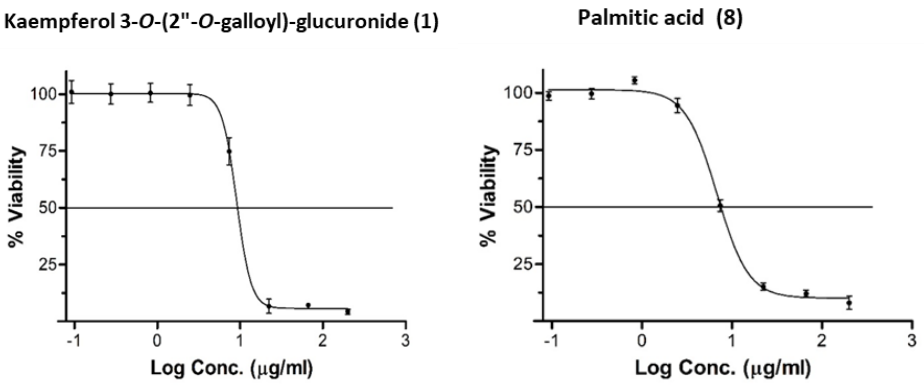

Figure 6.1. Dose-response curves for antimalarial assay: S1—Fraction S_1; S2—Fraction S_2; S3—Fraction S_3; kaempferol 3-*O*-(2"-*O*-galloyl)-glucuronide (**1**) and palmitic acid (**8**) expressed as percentage (%) parasite viability ± standard deviation.

6.3.2. Antitrypanosomal activity of *B. salicina*

The antitrypanosomal activities were determined against *in vitro Trypanosoma brucei brucei* (427 strain) cultures. Fraction S_1 strongly affected the viability of trypanosomes at 50 µg/mL, with a viability of 7.78 ± 0.08 % (Table 6.2) and IC_{50} value 2.0 ± 0.09 µg/mL at a concentration of 300 µg/mL (Figure 6.2). However, there was not a significant decrease (at 90.56 ± 1.55 %) when the parasites were treated with the stem bark extract (S.crude) (Table 6.2). This is probably because of the removal of the active compounds in the stem bark crude extract during fractionation. The MeOH leaf extract (LM.crude) and DCM leaf extract (LD.crude), as well as fraction LD_3 decreased the viability of trypanosomes, with viabilities of 6.74 ± 0.06 %, 6.38 ± 2.15 % and 5.05 ± 0.35 % (Table 6.2); and IC_{50} values of 11.4 ± 0.42 µg/mL, 10.6 ± 0.07 µg/mL and 7.1 ± 0.14 µg/mL, respectively (Figure 6.2). The MeOH and DCM leaf extracts showed greater activity than their respective fractions. This is probably due to the synergistic effect of the compound mixtures in these extracts. Furthermore, the presence of 3-acetylursolic acid, catechin, cinchonain I isomer, 5-caffeoylquinic acid, deacetyl asperuloside acid, di-*O*-caffeoylquinic acid, 3,4-dihydroxycinnamoylquinic acid, 25-hydroxy-3-epidehydrotumulosic acid, hydroxyglycyrrhetinic acid, micromeric acid, neotigogenin acetate, quinic acid, quinic acid + hexose, rutin, and ursolic acid might have increased the activity of crude DCM leaf extract (LD.crude), crude MeOH leaf extract (LM.crude), fraction S_1, and fraction LD_3 (Table 4.2, Chapter 4). The *in vitro* and *in vivo* antitrypanosomal activities of these compounds have not been evaluated (Table 4.2, Chapter 4). Furthermore, bodinioside Q (**4**), lupeol (**2**), kaempferol 3-*O*-(2"-*O*-galloyl)-glucuronide (**1**), and palmitic acid (**8**) exhibited antitrypanosomal activity with viabilities of 20.38 ± 2.35 %, 5.46 ± 0.04 %, 12.99 ± 0.53 %

and 5.83 ± 0.28 % at 20 µg/mL (Table 4); and IC_{50} values of 4.0 ± 0.09 µg/mL, 1.1 ± 0.22 µg/mL, 4.2 ± 0.27 µg/mL and 5.7 ± 0.09 µg/mL at 200 µg/mL, respectively (Figure 6.2). Fraction S_3 had little effect (94.33 ± 0.77 %), possibly because the concentration of lupeol (**2**) was low in fraction S_3. The antitrypanosomal activities of bodinioside Q (**4**), kaempferol 3-*O*-(2''-*O*-galloyl)-glucuronide (**1**), lupeol (**2**), and palmitic acid (**8**) have never been evaluated. The reference drug pentamidine was used as positive control for the crude extracts, fractions and pure compounds; and had an IC_{50} of 10.2 ± 0.07 µg/mL (Figure 6.2). This is the first report on the antitrypanosomal activity of the *B. salicina* extractives.

Table 6.2. Antitrypanosomal activities of the *B. salicina* crude extracts, fractions and pure compounds.

Samples	***T. brucei* (% viability ± SD)**
S.crude	90.56 ± 1.55
Fraction S_1	7.78 ± 0.08
Fraction S_2	99.68 ± 8.23
Fraction S_3	94.33 ± 0.77
Fraction S_4	59.69 ± 0.95
Fraction S_5	95.22 ± 3.34
R.crude	86.51 ± 1.81
Fraction R_1	105.65 ± 1.11
LM.crude	6.74 ± 0.06
Fraction LM_2	104.08 ± 1.87
Fraction LM_3	105.09 ± 2.98
LD.crude	6.38 ± 2.15
Fraction LD_2	56.38 ± 0.98
Fraction LD_3	5.05 ± 0.35
Kaempferol 3-*O*-(2''-*O*-galloyl)-glucuronide (**1**)	20.38 ± 2.35
Lupeol (**2**)	5.46 ± 0.04
D-Galactopyranose (**3**)	92.93 ± 4.46
Bodinioside Q (**4**)	12.99 ± 0.53
5-*O*-Caffeoylquinic acid (**5**)	109.97 ± 2.99
Sucrose (**6**)	103.52 ± 3.43
Hexadecane (**7**)	103.60 ± 2.41
Palmitic acid (**8**)	5.83 ± 0.28

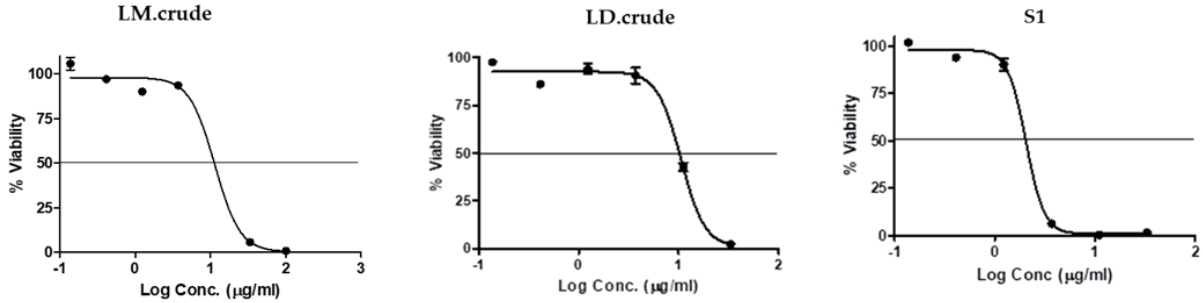

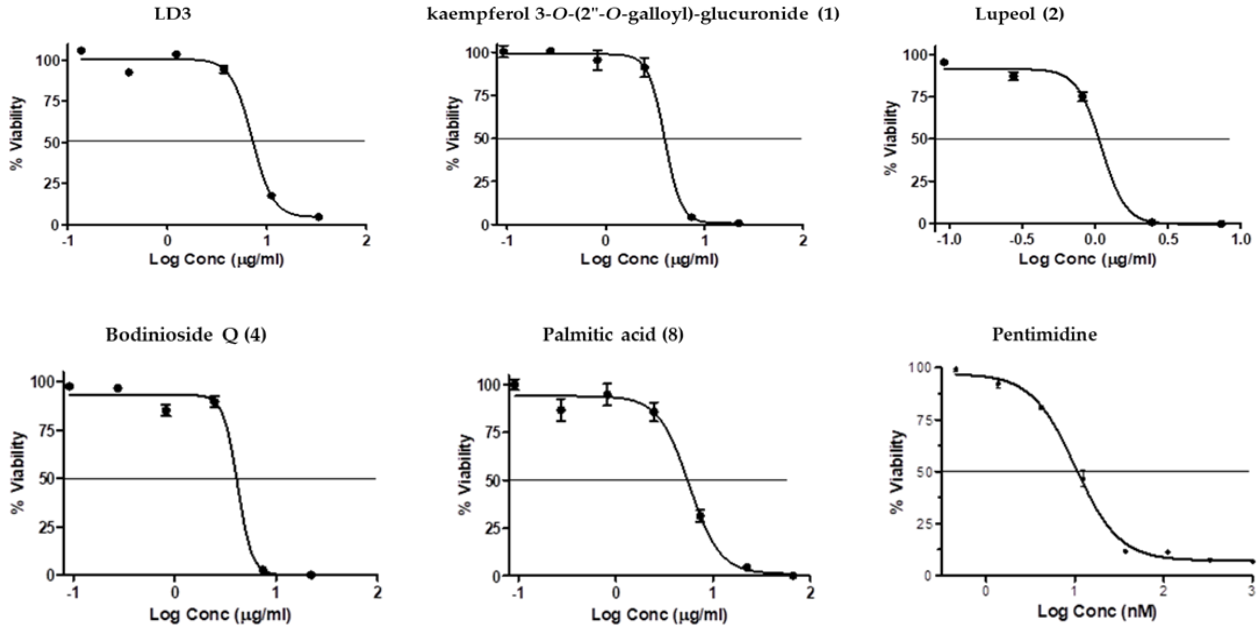

Figure 6.2. Dose-response curves for antitrypanosomal assay: LM.crude—crude MeOH leaf extract; LD.crude—crude DCM leaf extract; S1—Fraction S_1; LD3—Fraction LD_3; bodinioside Q (**4**), kaempferol 3-*O*-(2"-*O*-galloyl)-glucuronide (**1**), lupeol **(2**), and palmitic acid (**8**) are shown as % parasite viability ± standard deviation.

6.3.3. Pharmacological activities of the seasonal extracts

6.3.3.1. Antimalarial activity

The chemical variability of the seasonal plant samples (autumn, winter, spring and summer) was evaluated by comparing the antimalarial activities of the crude extracts of different plant parts collected in the second year with the crude extracts of samples collected in spring of the first year against *Plasmodium falciparum* (3D7 strain) parasites. The extracts of leaves collected in the second year had the highest antimalarial activities compared to the root and stem bark extracts (Figure 6.3). This was different from the activity recorded in the spring of the first year in which the stem bark displayed the highest antimalarial activity (as shown in Table 6.1, Chapter 6). The stem bark and dichloromethane leaf extracts collected in the first and second year produced different metabolites (as shown in Tables 4.2 and 4.3, Chapter 4, respectively). These results indicate that different parts of *B. salicina* produce different metabolites, which contribute to the antimalarial activities of this plant. Furthermore, the dichloromethane extracts of leaves collected in the second year in each season had the highest antimalarial activities, compared with the methanol leaf extracts. However, the dichloromethane leaf extracts recorded in the first year did not have significant antimalarial activity.

This was because 5-methylcaffeoylquinic acid and quinic acid were only present in the dichloromethane extracts of leaves collected in the first year; and were not present in the second year's dichloromethane leaf extracts. Furthermore, deacetyl asperuloside acid, di-*O*-caffeoylquinic acid, trihydroxy-octadecadienoic acid, 15-hydroxyhexadecanoic acid, 3-α,24*R*,25-trihydroxytirucall-8-en-21-oic acid and sibiricose A6 were only found in the dichloromethane leaf extracts of the second year and not found in the dichloromethane leaf extracts of the first year. Therefore, these metabolites might have contributed the strong antimalarial activities of the dichloromethane leaf extracts of *Breonadia salicina* in the second year in each season. In addition, the highest antimalarial activity of the dichloromethane leaf extracts was found in autumn, followed by summer, winter and spring, with viabilities of 18.57 ± 1.99 %, 20.21 ± 5.19 %, 32.07 ± 4.91 % and 38.11 ± 5.07 % at 50 µg/mL (Figure 6.3); and IC_{50} values of 7.903 ± 0.060 µg/mL, 15.26 ± 0,059 µg/mL, 18.15 ± 0,074 µg/mL and 19.40 ± 0,065 µg/mL at 300 µg/mL, respectively (Figure 6.4), while chloroquine had an IC_{50} of 0.03 µg/mL (Figure 6.4). However, there was no significant decrease in the viability of *Plasmodium falciparum* (82.13 ± 7.28 %, 78.07 ± 1.04 %, 77.66 ± 1.25 % and 53.44 ± 6.22 %, respectively) in the 50 µg/mL MeOH autumn, winter, summer and spring leaf extracts (Figure 6.3) compared to the DCM leaf extracts. Moreover, the same trend observed in the biological assays corresponds to the chemistry of the MeOH leaf extracts and the DCM leaf extracts. Chemometric analysis showed that there was a clear separation of the dichloromethane and methanol leaf extracts along PC2 (Figure 5.1, Chapter 5), indicating that the chemistry and bioactivity of the methanol and dichloromethane leaf extracts in each season differ. The variability of the samples in antiplasmodial activities against *P. falciparum* shows how important it is to evaluate antimalarial activities of different seasons' plant samples to explain these chemical deviations. The principal component analysis was done to determine the relationship between the chemistry and bioactivity of the samples, and produced a scores plot with the first and second components explaining 57.9 % of the variation (Figure 5.1, Chapter 5). The active samples (Red) were distributed along PC2 (Figure 5.1, Chapter 5) and the inactive samples (Green and Blue) clustered along PC1 (Figure 5.1, Chapter 5). Furthermore, a VIP plot exposed those compounds contributing considerably to the separation (Figure 5.4, Chapter 5). In addition, the UPLC-QTOF-MS revealed that both the MeOH and DCM leaf extracts produced similar as well as dissimilar compounds in each season.

The chemical profiles of the MeOH and DCM leaf extracts showed the presence of metabolites, including quinic acids (3,4-dihydroxycinnamoylquinic acid, 5-caffeoylquinic acid, di-*O*-

caffeoylquinic acid and quinic acid), monoterpenoid (deacetyl asperuloside acid) and flavonoid glycoside (rutin), as shown in Table 4.3, Chapter 4. However, the presence of metabolites such as trihydroxy-octadecadienoic acid, 15-hydroxyhexadecanoic acid, 3-α,24*R*,25-trihydroxytirucall-8-en-21-oic acid and sibiricose A6 were only found in the dichloromethane leaf extracts but not in the methanol leaf extracts (Table 4.3, Chapter 4). The *in vitro* and *in vivo* antimalarial activities of these metabolites have not been determined before. Therefore, the presence of these fatty acids, triterpenes and oligosaccharide esters might be a factor in the antimalarial activities of the crude dichloromethane leaf extracts in autumn, winter, spring and summer. This is the first study reporting important phytochemicals contributing to the antimalarial activities of *Breonadia salicina* in autumn, winter, spring and summer.

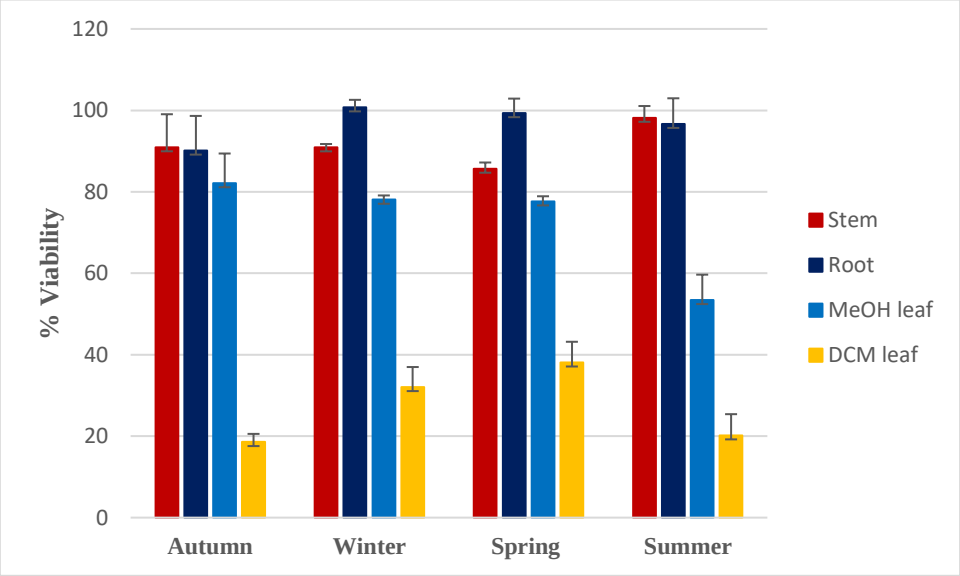

Figure 6.3. Antimalarial activity of the seasonal extracts against *Plasmodium falciparum*: Stem—crude stem bark extract; Root—crude root extract; MeOH leaf—crude methanol leaf extract and DCM leaf—crude dichloromethane leaf extract expressed as % parasite viability ± SD.

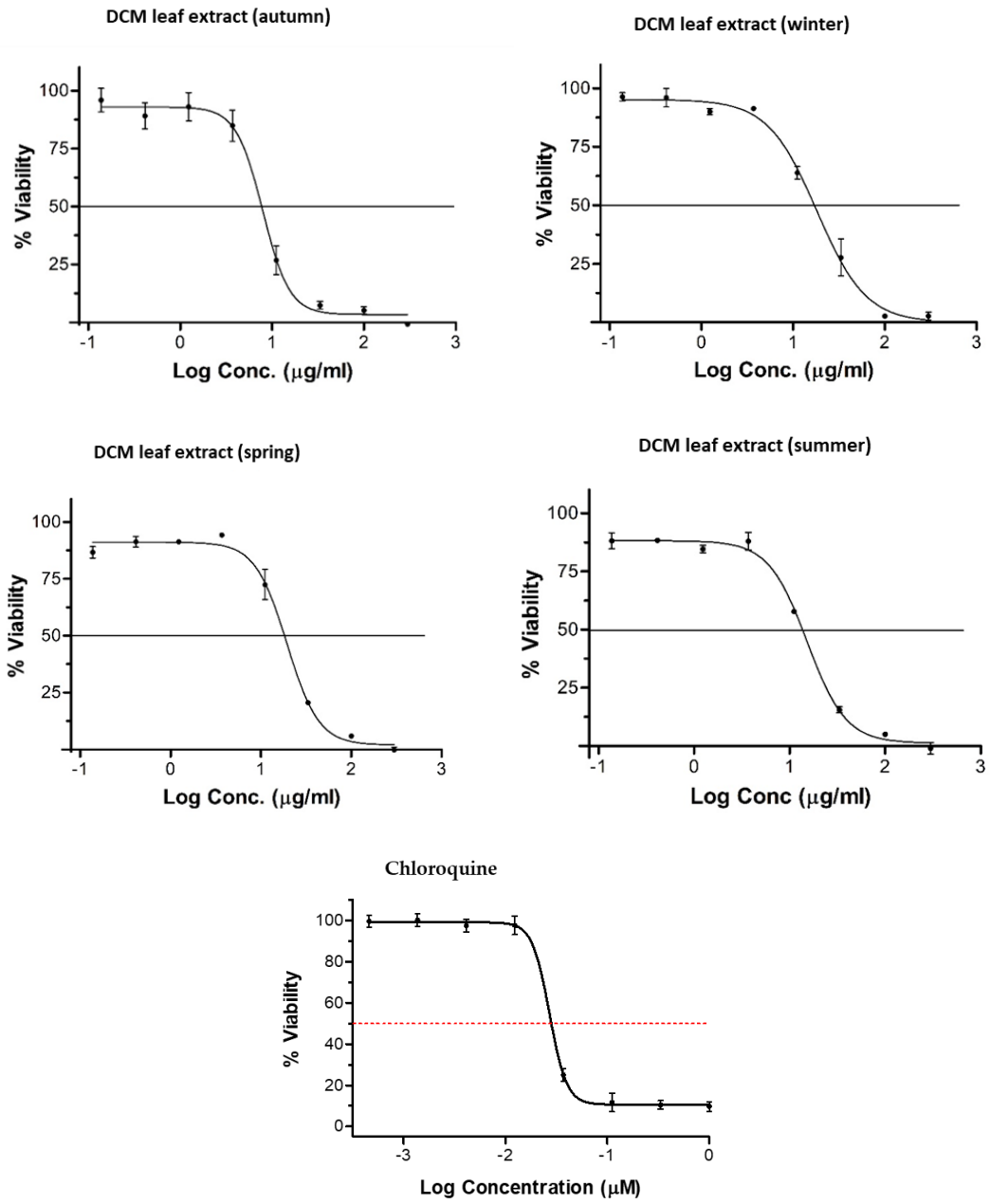

Figure 6.4. Results of the antimalarial assay: The dichloromethane leaf extracts in autumn, winter, spring and summer expressed as percentage (%) parasite viability ± standard deviation.

6.3.3.2. Antitrypanosomal activity

The chemical variability of fresh seasonal samples (autumn, winter, spring, and summer) was evaluated by comparison of the antitrypanosomal activities against *Trypanosoma brucei brucei* (427 strain) of crude extracts collected in the second year with those collected during the first year. The results showed that the extracts of leaves collected in the second year had the highest antitrypanosomal activities, compared to the root and stem bark extracts (Figure 6.5, Chapter 6).

However, the results obtained in the first year's spring were not different from those obtained in the spring of the second year, in which the MeOH and DCM leaf extracts displayed the highest antitrypanosomal activities. The chemical profiles obtained with UPLC-QTOF-MS revealed that the leaf extracts in both years produced the same metabolites, such as 3,4-dihydroxycinnamoylquinic acid, 5-caffeoylquinic acid, deacetyl asperuloside acid, rutin, di-*O*-caffeoylquinic acid and quinic acid (Tables 4.2 and 4.3, Chapter 4, respectively). The antitrypanosomal activities of these metabolites have not been assessed before. This is therefore the first study reporting phytochemicals contributing to the antitrypanosomal activities of the leaves of *Breonadia salicina* in spring. Furthermore, this study shows that both the methanol and dichloromethane leaf extracts in autumn, winter, spring and summer displayed the highest antitrypanosomal activity, except for the methanol leaf extracts in winter. The highest value of antitrypanosomal activity of the methanol leaf extracts was found in autumn season, followed by summer, spring and winter season, with viabilities of 5.84 ± 0.38 %, 9.05 ± 0.80 %, 26.66 ± 3.91 % and 85.56 ± 3.52 % at 50 µg/mL (Figure 6.5); and IC_{50} values of 12.0 ± 0.36 µg/mL, 10.6 ± 0.07 µg/mL, 5.2 ± 0.74 µg/mL at 300 µg/mL, respectively (Figure 6.6); the winter methanol leaf extract did not show any activity. Furthermore, the highest value of antitrypanosomal activity of the dichloromethane leaf extracts was found in autumn season, followed by summer, winter and spring season, with viabilities of 3.50 ± 0.59 %, 3.85 ± 0.10 %, 4.13 ± 0.06 % and 29.47 ± 1.25 % at 50 µg/mL (Figure 6.5); and IC_{50} values of 4.6 ± 1.82 µg/mL, 4.0± 0.08 µg/mL, 5.1 ± 0.30 µg/mL and 5.1 ± 0.72 µg/mL at 300 µg/mL, respectively (Figure 6.6). Moreover, chemometric analysis of the data obtained showed that there was a clear separation of the dichloromethane and methanol leaf extracts along PC2 (Figure 5.1, Chapter 5). Seasonal variations were observed in each plant part in which autumn and winter samples were closely clustered, compared to the spring and summer in the methanol leaf plant parts. The markers identified by the VIP plot and heatmap (Figure 5.4 and Figure 5.5, Chapter 5) indicated that ursolic acid and rutin were found in the methanol leaf samples but not in the stem bark and root samples. The reference drug pentamidine was used as positive controls for all the tested crude extract in autumn, winter, spring and summer, and had an IC_{50} value of 10.2 ± 0.07 µg/mL (Figure 6.6).

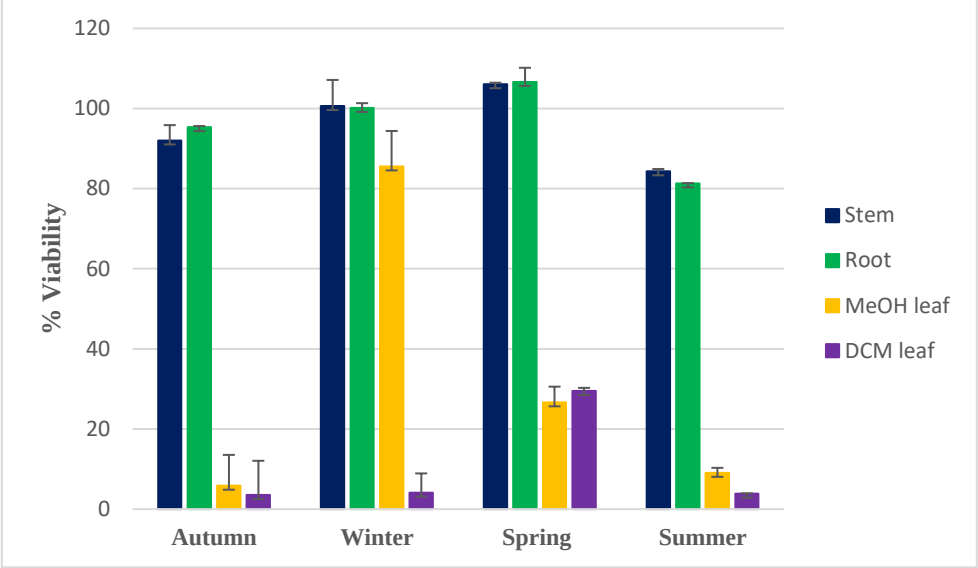

Figure 6.5. Antitrypanosomal activity of the seasonal extracts against *Trypanosoma brucei brucei*: Stem—crude stem bark extract; Root—crude root extract; MeOH leaf—crude methanol leaf extract and DCM leaf—crude dichloromethane leaf extract expressed as % parasite viability ± SD.

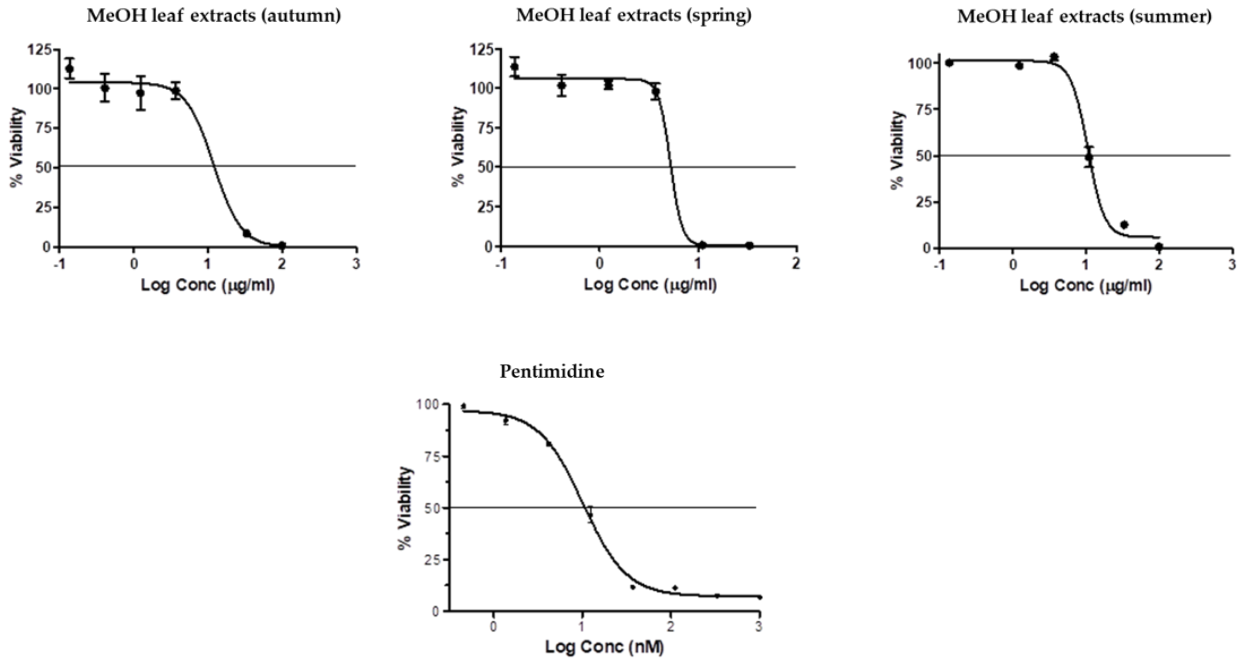

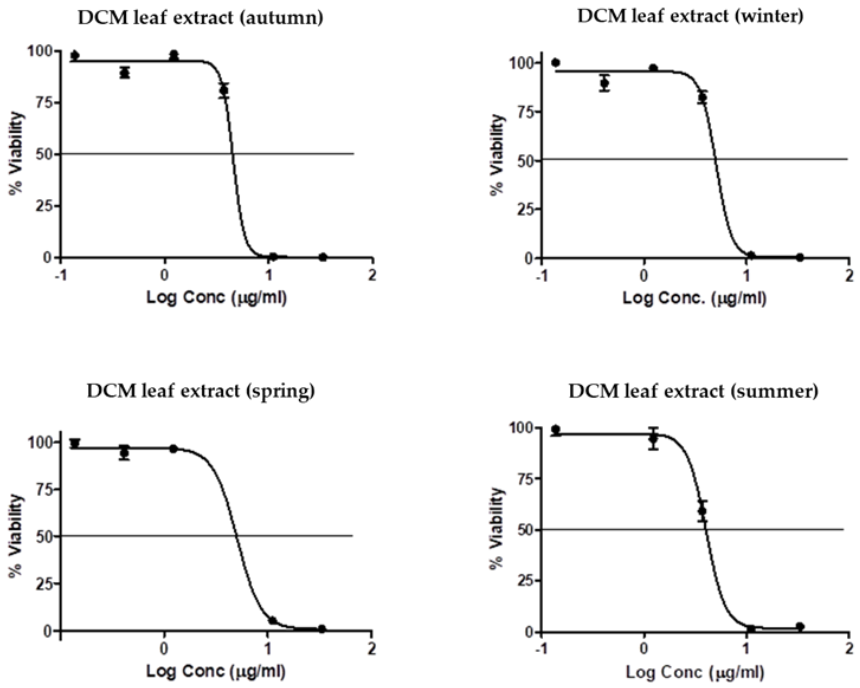

Figure 6.6. Results of antitrypanosomal assay: Crude methanol and dichloromethane leaf extracts in autumn, winter, spring and summer expressed as % parasite viability ± SD.

6.4. Summary

To conclude:

- All the extracts and fractions produced a significant viability decrease against *Plasmodium falciparum* at 50 µg/mL.
- However, fraction S_1, fraction S_2, and fraction S_3 had higher antimalarial activities at 10 µg/mL than that of the initial crude extract from which they were fractionated.
- Fraction LD_3 had the highest antimalarial activity compared to kaempferol 3-*O*-(2''-*O*-galloyl)-glucuronide (**1**, obtained from fraction S_1), palmitic acid (**9**, obtained from fraction LD_3) and the dichloromethane (DCM) leaf extracts in each season.
- The extracts of stem bark collected in the first year's spring had a higher antimalarial activity than the extracts of leaves collected during spring of the second year.
- The stem bark and dichloromethane leaf extracts collected in the first and second years displayed different metabolite profiles. Furthermore, the chemical profile of the stem bark extracts collected in Spring of the first year showed the presence of lupeol, 5-*O*-caffeoylquinic acid, hexadecane, α-glucose, β-glucose, fructose, caffeic acid derivative, 4'-*O*-methyellagic acid-3-*O*-α-L-rhamnopyranoside, ellagic acid, ellagic acid-

rhamnopyranoside isomer I, catechin, hydroxyglycyrrhetinic acid, neotigogenin acetate, 25-hydroxy-3-epi-dehydrotumulosic acid, micromeric acid, 3-acetylursolic acid, (epi)gallocatechin, 4-*O*-methylgallic acid, myricetin 3-*O*-glucoside, ursolic acid and asiatic acid which might have contributed to the antimalarial activity of the extracts of stem bark collected in the first year. However, the chemical profile of the dichloromethane extracts of leaves collected in the second year spring showed the presence of 3,4-dihydroxycinnamoylquinic acid, 5-caffeoylquinic acid, quinic acid, deacetyl asperuloside acid, di-*O*-caffeoylquinic acid, trihydroxy-octadecadienoic acid, 15-hydroxyhexadecanoic acid, 3-α,24*R*,25-trihydroxytirucall-8-en-21-oic acid, ursolic acid and sibiricose A6, which might have been responsible for the antimalarial activity of the dichloromethane leaf extracts collected in the second year.

- Fraction LD_3 had the highest antitrypanosomal activity compared to fraction S_1, crude methanol leaf extract, crude dichloromethane leaf extract, kaempferol 3-*O*-(2"-*O*-galloyl)-glucuronide (**1**), lupeol (**2**), bodinioside Q (**4**), palmitic acid (**8**), crude methanol and dichloromethane leaf extracts in each season.
- The methanol and dichloromethane extracts of leaves collected in the first and second year had the highest antitrypanosomal activity.
- The chemical profiles of the methanol and dichloromethane extracts of leaves collected in the first and second year produced the same metabolites.
- This is the first study to investigate the effects of seasonal variation on phytochemicals contributing to the antimalarial and antitrypanosomal activities of *Breonadia salicina.*

6.5. References

Ahmad, I.; Ahmad, M.S.A.; Ashraf, M.; Hussain, M.; Ashraf, M.Y., 2011. Seasonal variation in some medicinal and biochemical ingredients in *Mentha longifolia* (L.) Huds. *Pakistan Journal of Botany*, **2011**, 43, 69-77.

Ali, S.; Umar, A.Z.; Asmau, M.; Deepa, S.; Milli, J.; Fatima, H. In vitro antitrypanosomal activity of *Breonadia salicina* on *Trypanasoma brucei brucei. International Journal of Pharmaceutical Sciences and Research*, **2018**, 9, 975-9492.

Bhardwaj, S.; Rashmi.; Parcha, V. Effect of seasonal variation on chemical composition and physicochemical properties of *Hedychium spicatum* rhizomes essential oil. *Journal of Essential Oil Bearing Plants*, **2019**, 22, 1593-1600.

Demuner, A.J.; Almeida Barbosa, L.C.; Gonçalves Magalhaes, C.; Da Silva, C.J.; Alvares Maltha, C.R.; Lelis Pinheiro, A. Seasonal variation in the chemical composition and antimicrobial activity of volatile oils of three species of *Leptospermum* (Myrtaceae) grown in Brazil. *Molecules*, **2011**, 16, 1181-1191.

Dhami, N.; Mishra, A.D. Phytochemical variation: how to resolve the quality controversies of herbal medicinal products?. *Journal of Herbal Medicine*, **2015**, 5, 118-127.

Falasca, A.; Melck, D.; Paris, D.; Saviano, G.; Motta, A.; Iorizzi, M. Seasonal changes in the metabolic fingerprint of *Juniperus communis* L. berry extracts by ^{1}H-NMR-based metabolomics. *Metabolomics*, **2014**, 10, 165-174.

Fan, G.; Luo, W.Z.; Luo, S.H.; Li, Y.; Meng, X.L.; Zhou, X.D.; Zhang, Y. Metabolic discrimination of *Swertia mussotii* and *Swertia chirayita* known as "Zangyinchen" in traditional Tibetan medicine by ^{1}H NMR-based metabolomics. *Journal of Pharmaceutical and Biomedical Analysis*, **2014**, 98, 364-370.

Farag, M.A.; Gad, H.A.; Heiss, A.G.; Wessjohann, L.A. Metabolomics driven analysis of six Nigella species seeds via UPLC-qTOF-MS and GC–MS coupled to chemometrics. *Food Chemistry*, **2014**, 151, 333-342.

Gazim, Z.C.; Amorim, A.C.L.; Hovell, A.M.C.; Rezende, C.M.; Nascimento, I.A.; Ferreira, G.A.; Cortez, D.A.G., 2010. Seasonal variation, chemical composition, and analgesic and antimicrobial activities of the essential oil from leaves of *Tetradenia riparia* (Hochst.) Codd in Southern Brazil. *Molecules*, **2010**, 15, 5509-5524.

Gololo, S.S.; Shai, L.J.; Agyei, N.M.; Mogale, M.A. Effect of seasonal changes on the quantity of phytochemicals in the leaves of three medicinal plants from Limpopo province, South Africa. *Journal of Pharmacognosy and Phytotherapy*, **2016**, 8, 168-172.

Heyman, H.M.; Senejoux, F.; Seibert, I.; Klimkait, T.; Maharaj, V.J.; Meyer, J.J.M. Identification of anti-HIV active dicaffeoylquinic-and tricaffeoylquinic acids in *Helichrysum populifolium* by NMR-based metabolomic guided fractionation. *Fitoterapia*, **2015**, 103, 155-164.

Kibungu, W.C.; Fri, J.; Clarke, A.M.; Otigbu, A.; Akum Njom, H. Seasonal Variation in Antimicrobial Activity of Crude Extracts of *Psammaplysilla* sp. 1 from Phillips Reef, South Africa. *International Journal of Microbiology*, **2021**, 2021. https://doi.org/10.1155/2021/7568493

Kim, N.K.; Park, H.M.; Lee, J.; Ku, K.M.; Lee, C.H. Seasonal variations of metabolome and tyrosinase inhibitory activity of *Lespedeza maximowiczii* during growth periods. *Journal of Agricultural and Food Chemistry*, **2015**, 63, 8631-8639.

Lubbe, A.; Gude, H.; Verpoorte, R.; Choi, Y.H. Seasonal accumulation of major alkaloids in organs of pharmaceutical crop Narcissus Carlton. *Phytochemistry*, **2013**, 88, 43-53.

Lunga, M.J.; Chisango, R.L.; Weyers, C.; Isaacs, M.; Taylor, D.; Edkins, A.L.; Khanye, S.D.; Hoppe, H.C.; Veale, C.G. Expanding the SAR of nontoxic antiplasmodial indolyl-3-ethanone ethers and thioethers. *ChemMedChem*, **2018**, 13, 1353-1362.

Martins, D.; Nunez, C.V. Secondary metabolites from Rubiaceae species. *Molecules*, **2015**, 20, 13422-13495.

Ncube, B.; Finnie, J.F.; Van Staden, J. Seasonal variation in antimicrobial and phytochemical properties of frequently used medicinal bulbous plants from South Africa. *South African Journal of Botany*, **2011**, *77*, 387-396.

Nndwammbi, M.; Ligavha-Mbelengwa, M.H.; Anokwuru, C.P.; Ramaite, I.D.I. The effects of seasonal debarking on physical structure, polyphenolic content and antibacterial and antioxidant activities of *Sclerocarya birrea* in the Nylsvley nature reserve. *South African Journal of Botany*, **2018**, 118, 138-143.

Scognamiglio, M.; D'Abrosca, B.; Esposito, A.; Fiorentino, A. Chemical composition and seasonality of aromatic mediterranean plant species by NMR-based metabolomics. *Journal of Analytical Methods in Chemistry*, **2015**, 2015. http://doi.org/10.1155/2015/258570

Scovill, J.; Blank, E.; Konnick, M.; Nenortas, E.; Shapiro, T. Antitrypanosomal activities of *tryptanthrins*. *Antimicrobial Agents and Chemotherapy*, **2002**, 46, 882-883.

Sibandze, G.F. Pharmacological properties of Swazi medicinal plants. MSc Thesis, University of Witwatersrand, Johannesburg, South Africa, **2009**.

Soni, U.; Brar, S.; Gauttam, V.K. Effect of seasonal variation on secondary metabolites of medicinal plants. *International Journal of Pharmaceutical Sciences and Research*, **2015**, 6, 3654-3662.

Sultana, R.; Majid, N.; Nissar, S.; Rather A.M. Seasonal variation of phytochemicals. *International Journal of Pharmacy and Biological Sciences*, **2018**, 8, 987-990.

Szakiel, A.; Pączkowski, C.; Henry, M. Influence of environmental abiotic factors on the content of saponins in plants. *Phytochemistry Reviews*, **2011**, 10, 471-491.

Tomar, N.S.; Sharma, M.; Agarwal, R.M. Phytochemical analysis of *Jatropha curcas* L. during different seasons and developmental stages and seedling growth of wheat (*Triticum aestivum* L) as affected by extracts/leachates of *Jatropha curcas* L. *Physiology and Molecular Biology of Plants*, **2015**, 21, 83-92.

CHAPTER 7 ANTIOXIDANT AND ANTITUBERCULAR ACTIVITY OF *BREONADIA SALICINA* EXTRACTS AND COMPOUNDS

7.1. INTRODUCTION

Tuberculosis (TB) is a leading communicable disease adding to the world's health burden (Izebe *et al*., 2020). In 2018, the World Health Organisation (WHO) estimated that 10.4 million people contracted TB, leading to 1.7 million deaths worldwide (WHO, 2018). Current tuberculosis treatment consists of a long course of a combination of drugs, including isoniazid (INH), rifampicin (RIF), pyrazinamide, ethambutol, and streptomycin. Therefore, designing drugs that could act in synergy with, or replace, previously potent anti-TB drugs remains an important objective (Gowrish *et al*., 2015). Very few studies have been reported on combining natural products extracted from plant materials with synthetic drugs. Studying the phytochemicals from active extracts or compounds contributing to the antitubercular activity of medicinal plants may result in more effective TB treatment (Aro *et al*., 2016). Tuberculosis is mostly linked to oxidative stress due to free radicals (Gowrish *et al*., 2015). Free radicals are highly reactive chemical molecules made when the body cells use oxygen to produce energy (Tauchen *et al*., 2016). Nitrogen oxides (NOs) and reactive oxygen species (ROS) are typical examples. At moderate concentrations these free radicals have helpful effects on cellular responses and immune function, but at high levels they cause oxidative stress. Antioxidants in the human diet play a vital role and potentially have great health benefits (Jiménez-Zamora *et al*., 2016). The ROS and other free radicals accumulating in the body cause oxidative stress, contributing to many degenerative and chronic diseases, such as Alzheimer's disease, atherosclerosis, diabetes, cancer, and inflammation (Tauchen *et al*., 2016). DNA and other biomolecules are protected against oxidation by antioxidants, which reduce the risk of degenerative or chronic disease (Limmongkon *et al*., 2017). Traditional medicinal remedies are often excellent sources of antioxidant, especially those rich in phenolic compounds like flavonoids, flavonols, polyphenols, and proanthocyanidins (Kalaycıoğlu and Erim, 2017). These compounds offer protection against free radical damage (Jayathilake *et al.*, 2016). Anti-tubercular drugs with both anti-tubercular and antioxidant activities would be advantageous in tuberculosis treatment or prevention. Since traditional medicine forms a significant part of TB treatment in several developing countries (Wang, 2015), medicinal plants and plant parts, such as the leaves, roots, and stem bark of *Breonadia salicina* are potential new sources of anti-

tubercular molecules (Kong *et al*., 2009). *B. salicina* is commonly used in South Africa by traditional health practitioners for the treatment of TB and its associated symptoms. Furthermore, the DPPH assay for free radicals (Sibandze, 2009) has revealed the high antioxidant activity of crude extracts of *B. salicina* stem bark. However, root extracts of *B. salicina* have not yet been tested for antioxidant activity. Moreover, compounds that may be responsible for the antioxidant and antitubercular activities of *B. salicina* have not yet been identified. Therefore, there is a need to further investigate and determine the pharmacological properties of *B. salicina.*

7.2. MATERIALS AND METHODS

7.2.1. Antioxidant activities

7.2.1.1. DPPH Free Radical Scavenging

All samples were assayed by an amended spectrophotometric 2,2-diphenyl-1-picrylhydrazyl (DPPH) free radical scavenging test (Motamed and Naghibi, 2010). Distilled water (100 µL) was added to each well of a 96-well plate, and then 100 µL of each crude extract, fraction and pure compound was added in the first three wells, followed by triplicate serial dilutions with a multi-channel micropipette. Lastly, each well received 200 µL of 125 mM methanolic DPPH solution, and after keeping the plate in the dark for up to 30 minutes, the absorbance at 517 nm was measured using a VersaMax™ tuneable microplate reader.

The % radical scavenging was calculated using the formula:

$\%\ \text{Free RSA} = [(A_{DPPH} - A_{sample})/(A_{DPPH})] \times 100$

7.2.1.2. Reducing power

The reducing power of samples was measured using a modified method (Pereira *et al.,* 2013) was employed to measure. Triplicate sample solutions (each 100 µL) and gallic acid and ascorbic acid standards were added to the first three wells of a 96-well plate, each well containing 100 µL deionised water, followed by serial dilution. Sodium phosphate buffer (0.2 M, pH 6.6, 50 µL) was added in all 96 wells, followed by 50 µL 1 % aqueous $K_3Fe(CN)_6$ solution. After 20 minutes' incubation at 45 °C, each well received 50 µL 10 % aqueous trichloroacetic acid solution. After transferring 80 µL of each mixture to another 96-well plate

containing 80 µL distilled water and 16 µL ferric chloride solution (0.1 % w/v) in each well, the absorbance at 700 nm was recorded on a tuneable microplate reader (VersaMax™).

7.2.2. Antitubercular activity

Dose-Response Assay: The antimycobacterial activities of crude extracts and fractions were determined using the modified method of Gupta *et al*. (2010). A 10.0 mM stock solution of each in DMSO was prepared. Further 2-fold serial dilutions with growth medium were added to 96-well round bottom plates, resulting in concentrations from 125 µM to 0.244 µM for every sample. The reference drugs were Isoniazid, Moxifloxacin, and Rifampicin (Rif) at concentration ranges of 125 – 0.244 µM, 6.25 – 0.012 µM, and 0.15 – 0.0002 µM, respectively, and each test plate had growth control standards. A *M. tuberculosis* H37RvMA culture was grown in 7H9_ADC_GLU_TYL to an optical density (OD_{600}) of 0.5- 0.7, and a 500-fold dilution was prepared in fresh media. To each well of each test plate 50 µL or ~ 1 x 10^5 bacilli of the diluted culture was added to a final volume of 100 µL per well. After incubation for 7 days with 5 % CO_2 and humidification at 37 °C, Alamar Blue reagent was added to each well and the plates were re-incubated for 24 hours. On day 8 the fluorescence of each well was measured (excitation 540 nm; emission 590 nm) using a SpectraMax i3x Plate reader (Molecular Devices Corporation). Dotmatics software was used for data analysis. Raw relative fluorescence units (RFU) data were normalized using the minimum and maximum inhibition standards to create a dose-response curve of % inhibition by means of the Levenberg-Marquardt damped least-squares method. The MIC was calculated using the 4-parameter curve fit protocol to yield the lowest drug concentration inhibiting 90 % of bacterial growth. All pathogenic mycobacterial strains were handled in a Biosafety Level III certified and compliant facility.

7.2.3. Statistical analysis

The SPSS statistical package (Chicago, IL, USA) was used to calculate the mean ± SD, while the mean differences of the samples in the antioxidant tests were evaluated using one-way analysis of variance (ANOVA, GraphPad Prism 6); $p < 0.05$ was considered statistically significant.

7.3. RESULTS AND DISCUSSION

7.3.1. Antioxidant Activity

The DPPH analysis showed that the crude MeOH stem bark extract (S.crude) had the highest antioxidant activity with IC_{50} 41.7263 ± 7.6401 µg/mL, while the crude root extract (R.crude) showed the highest reducing power with $IC_{0.5}$ 0.1481 ± 0.1441 µg/mL (Table 7.1). It is likely that the polyphenols and flavonoids identified in the root and stem bark extracts (Chapter 4, Tables 4.1 and 4.2) might have contributed to the antioxidant activity. It is known that a component like ellagic acid (present in S.crude, Table 4.2) has a high DPPH activity of 85.6 % at 30 µg/mL (Kilic *et al.*, 2014). Similarly, the catechin, caffeic acid, and (epi)gallocatechin present in the crude stem bark extract (S.crude, Table 4.2, Chapter 4) have high antioxidant (DPPH) activity and reducing power, with IC_{50} 3.965 ± 0.067 mol TE/mol, 0.965 ± 0.015 mol TE/mol, and 2.939 ± 0.037 mol TE/mol respectively; and $IC_{0.5}$ values of 0.793 ± 0.004 mol TE/mol, 1.018 ± 0.004 mol TE/mol, and 1.032 ± 0.007 mol TE/mol, respectively (Grzesik *et al.*, 2018). Thus, ellagic acid, caffeic acid, catechin, and (epi)gallocatechin must be among the important components responsible for the antioxidant activity of the crude stem bark extract. Moreover, D-galactopyranose (**3**) had the highest antioxidant (DPPH) activity, with IC_{50} value 44.5613 ± 2.6772 µg/mL, while kaempferol 3-*O*-(2"-*O*-galloyl)-glucuronide (**1**) showed the highest reducing power, with $IC_{0.5}$ 3.3742 ± 1.7492 µg/mL (Table 7.1). On the other hand, the parent fraction S_4 was less active than D-galactopyranose **3** (Table 7.1). It is possible that there was a synergistic interaction of D-galactopyranose with other components in the fraction, or else a more active component was removed during further fractionation. The antioxidant activity of D-galactopyranose has not been evaluated before. This is the first study reporting the strong antioxidant activity of the crude extracts, fractions, and pure compounds isolated from *B. salicina.*

Table 7.1. Antioxidant activity of crude extracts, fractions, pure compounds, and positive controls.

Sample	DPPH IC_{50} (µg/mL)	Reducing power $IC_{0.5}$ (µg/mL)
S.crude	41.7263 ± 7.6401[a]	1.0738 ± 1.4316[a]
Fraction S_1	49.3931 ± 0.2657[a]	2.7258 ± 3.5872 [a]
Fraction S_2	49.0216 ± 1.1209[a]	0.9902 ± 0.3556 [a]
Fraction S_3	49.6295 ± 0.1562[a]	0.2499 ± 0 [a]
Fraction S_4	48.2396 ± 0.2007[a]	0.1942 ± 0.0464 [a]
Fraction S_5	46.0939 ± 0.9941[a]	0.2502 ± 0.0003 [a]
R.crude	46.569 ± 1.8444[a,b]	0.1481 ± 0.1441 [a]
Fraction R_1	45.2806 ± 0.7117[a]	12.5572 ± 16.7165 [a]
LM.crude	47.3590 ± 0.7794[a,c]	8.5739 ± 10.1838 [a]
Fraction LM_2	48.4597 ± 0.6525[a]	1.1925 ± 0.0849 [a]
Fraction LM_3	45.4784 ± 1.0390[a]	2.1748 ± 1.3042 [a]
LD.crude	47.3397 ± 1.0680[a,d]	2.4379 ± 1.4826 [a]
Fraction LD_2	45.1968 ± 3.1969[a]	2.5178 ± 1.1822 [a]
Fraction LD_3	49.12 ± 0.5357[a]	4.1584 ± 1.7431 [a]
Kaempferol 3-*O*-(2"-*O*-galloyl)-glucuronide (**1**)	46.9493 ± 0.1388[a]	3.3742 ± 1.7492 [a]
Lupeol (**2**)	95.1091 ± 0.1501[a,b,c,d]	32.3413 ± 0 [a]
D-galactopyranose (**3**)	44.5613 ± 2.6772[a]	9.7237 ± 0.1625 [a]
Bodinioside Q (**4**)	48.9097 ± 0.2266[a]	10.9919 ± 6.3849 [a]
5-*O*-Caffeoylquinic acid (**5**)	48.1673 ± 0.1246[a]	16.7798 ± 0 [a]
Sucrose (**6**)	47.3525 ± 0.0380[a]	7.7263 ± 0 [a]
Hexadecane (**7**)	91.5285 ± 0.1032[a]	32.0310 ± 0.022 [a]
Palmitic acid (**8**)	94.4295 ± 0.9197[a,b,c,d]	31.3131 ± 1.0497 [a]
Ascorbic acid	48.0304 ± 2.6010[a]	3.4143 ± 0.1117 [a]
Gallic acid	49.2369 ± 0.7411[a]	1.2361 ± 0.0352 [a]

Notes: Different superscripts mean significant differences in one-way ANOVA at $p < 0.05$. Data (n=3) reported as mean ± SD. In the DPPH test: [a]—Crude stem bark extract (S.crude) differed significantly from the other samples; [a,b]—Crude root extract (R.crude) differed significantly only from lupeol (**2**) and palmitic acid (**7**); [a,c]—Crude MeOH leaf extract (LM.crude) differed significantly from lupeol (**2**) and palmitic acid (**7**); [a,d]— Crude DCM leaf extract (LD.crude) differed significantly only from lupeol (**2**) and palmitic acid (**7**); and [a,b,c,d]—lupeol (**2**) differed significantly only from palmitic acid (**7**). In the reducing power test: [a]—Crude stem bark extract did not differ significantly from the other samples.

7.3.2. Anti-TB Activity

In this study, the antimycobacterial activity of crude extracts and fractions of different plant parts of *Breonadia salicina* was determined against *Mycobacterium tuberculosis* (H37RvMA strain). None of the tested plant samples produced any significant anti-tuberculosis activity at a concentration of 90 µg/mL. All the samples produced a MIC value of >62.5 µg/mL against 7H9_ADC_GLU_TW, 7H9_ADC_GLU_N_TW and 7H9_ADC_GLY_TW media, respectively, as shown in Table 7.2. Previous studies reported several plants with promising antitubercular activity (Tuyiringire *et al*., 2020; Kahaliw *et al*., 2017), mostly in the different parts of plant species from the Rubiaceae family (Aro *et al*., 2015). However, in the present study it was found that different plant parts from *B. salicina* did not exhibit activity, which contradicts the reports of other studies. No significant activity against *Mycobacterium tuberculosis* (H37RvMA strain) was found for the *B. salicina* crude stem bark, root and leaf extracts and fractions, but they may still be found to be active against slow growing non-tuberculous mycobacteria (NTMs) that are responsive to anti-TB drugs (Low *et al*., 2017).

Table 7.2. Anti-tubercular activity of crude extracts, fractions and control.

	MIC 90		
Samples	7H9_ADC_GLU_TW	7H9_ADC_GLU_N_TW	7H9_ADC_GLY_TW
S.crude	>62.5 µg/Ml	>62.5 µg/mL	>62.5 µg/mL
Fraction S_1	>62.5 µg/Ml	>62.5 µg/mL	>62.5 µg/mL
Fraction S_2	>62.5 µg/mL	>62.5 µg/mL	>62.5 µg/mL
Fraction S_3	>62.5 µg/Ml	>62.5 µg/mL	>62.5 µg/mL
Fraction S_4	>62.5 µg/Ml	>62.5 µg/mL	>62.5 µg/mL
Fraction S_5	>62.5 µg/Ml	>62.5 µg/mL	>62.5 µg/mL
R.crude	>62.5 µg/mL	>62.5 µg/mL	>62.5 µg/mL
Fraction R_1	>62.5 µg/mL	>62.5 µg/mL	>62.5 µg/mL
LM.crude	>62.5 µg/mL	>62.5 µg/mL	>62.5 µg/mL
Fraction LM_2	>62.5 µg/mL	>62.5 µg/mL	>62.5 µg/mL
Fraction LM_3	>62.5 µg/mL	>62.5 µg/mL	>62.5 µg/mL
LD.crude	>62.5 µg/mL	>62.5 µg/mL	>62.5 µg/mL
Fraction LD_2	>62.5 µg/mL	>62.5 µg/mL	>62.5 µg/mL
Fraction LD_3	>62.5 µg/mL	>62.5 µg/mL	>62.5 µg/mL

7.4. Summary

To conclude:

- The crude MeOH stem bark extract had the highest DPPH radical scavenging activity.
- The crude MeOH root extract showed the highest reducing power.
- Of the pure compounds, D-galactopyranose (**3**) had the highest DPPH radical scavenging activity.
- Of the pure compounds, kaempferol 3-*O*-(2''-*O*-galloyl)-glucuronide (**1**) had the highest reducing power.
- From this work it is clear that flavonoids, hydroxycinnamic acids, and polyphenols add antioxidant value to *B. salicina* extracts.
- None of the crude extracts and fractions exhibited antimycobacterial activity against *Mycobacterium tuberculosis* (H37RvMA strain).

7.5. References

Aro, A.O.; Dzoyem, J.P.; Eloff, J.N.; McGaw, L.J. Extracts of six Rubiaceae species combined with rifampicin have good in vitro synergistic antimycobacterial activity and good anti-inflammatory and antioxidant activities. *BMC Complementary and Alternative Medicine*, **2016**, 16, 1-8.

Aro, A.O.; Dzoyem, J.P.; Hlokwe, T.M.; Madoroba, E.; Eloff, J.N.; McGaw, L.J. Some South African Rubiaceae tree leaf extracts have antimycobacterial activity against pathogenic and non-pathogenic mycobacterium species. *Phytotherapy Research*, **2015**, 29, 1004-1010.

Bhatter, P.D.; Gupta, P.D.; Birdi, T.J. Activity of medicinal plant extracts on multiplication of Mycobacterium tuberculosis under reduced oxygen conditions using intracellular and axenic assays. *International Journal of Microbiology*, **2016**. https://doi.org/10.1155/2016/8073079

Gowrish, A.; Vagdevi, H.; Rajashekar, H. In vitro antioxidant and antitubercular activity of Leucas marrubioides Desf. root extracts. *Journal of Applied Pharmaceutical Science*, **2015**, 5, 137-142.

Grzesik, M.; Naparło, K.; Bartosz, G.; Sadowska-Bartosz, I. Antioxidant properties of catechins: Comparison with other antioxidants. *Food Chemistry*, **2018**, 241, 480-492.

Gupta, R.; Thakur, B.; Singh, P.; Singh, H.B.; Sharma, V.D.; Katoch, V.M.; Chauhan, S.V.S. Anti-tuberculosis activity of selected medicinal plants against multi-drug resistant Mycobacterium tuberculosis isolates. *Indian Journal of Medical Research*, **2010**, 131, 809.

Izebe, K.S.; Ibrahim, K.; Onaolapo, J.A.; Oladosu, P.; Ya'aba, Y.; Njoku, M.; Shehu, M.B.; Ezeunala, M.; Ibrahim, Y.K. Evaluation of In-Vitro Anti-Tuberculosis Activity of Tetrapleura tetraptera Crude and Fractions on Multidrug Resistant Mycobacterium tuberculosis. *Journal of Tuberculosis Research*, **2020**, 8, 165-176.

Jiménez-Zamora, A.; Delgado-Andrade, C.; Rufián-Henares, J.A. Antioxidant capacity, total phenols and color profile during the storage of selected plants used for infusion. *Food Chemistry*, **2016**, 199, 339-346.

Kahaliw, W.; Aseffa, A.; Abebe, M.; Teferi, M.; Engidawork, E. Evaluation of the antimycobacterial activity of crude extracts and solvent fractions of selected Ethiopian medicinal plants. *BMC Complementary and Alternative Medicine*, **2017**, 17, 1-9.

Kalaycıoğlu, Z.; Erim, F.B. Total phenolic contents, antioxidant activities, and bioactive ingredients of juices from pomegranate cultivars worldwide. *Food Chemistry*, **2017**, 221, 496-507.

Kilic, I.; Yeşiloğlu, Y.; Bayrak, Y. Spectroscopic studies on the antioxidant activity of ellagic acid. *Spectrochimica Acta Part A: Molecular and Biomolecular Spectroscopy*, **2014**, 130, 447-452.

Kong, D.X.; Li, X.J.; Zhang, H.Y. Where is the hope for drug discovery? Let history tell the future. *Drug Discovery Today*, **2009**, 14, 115-119.

Limmongkon, A.; Janhom, P.; Amthong, A.; Kawpanuk, M.; Nopprang, P.; Poohadsuan, J.; Somboon, T.; Saijeen, S.; Surangkul, D.; Srikummool, M.; Boonsong, T. Antioxidant activity, total phenolic, and resveratrol content in five cultivars of peanut sprouts. *Asian Pacific Journal of Tropical Biomedicine*, **2017**, 7, 332-338.

Low, J.L.; Wu, M.L.; Aziz, D.B.; Laleu, B.; Dick, T. Screening of TB actives for activity against nontuberculous mycobacteria delivers high hit rates. *Frontiers in Microbiology*, **2017**, 8, 1539.

Motamed, S. M.; Naghibi, F. Anti-oxidant activity of some edible plants of the Turkmen Sahra region in northern Iran. *Food Chemistry*, **2010**, 119, 1637-1642.

Pereira, O. R.; Macias, R. I.; Perez, M. J.; Marin, J. J.; Cardoso, S. M. Protective effects of phenolic constituents from *Cytisus multiflorus*, *Lamium album* L. and *Thymus citriodorus* on liver cells. *Journal of Functional Foods*, **2013**, 5, 1170-1179.

Sibandze, G.F. Pharmacological properties of Swazi medicinal plants. MSc Thesis, University of the Witwatersrand, Johannesburg, South Africa, **2009**.

Tauchen, J.; Bortl, L.; Huml, L.; Miksatkova, P.; Doskocil, I.; Marsik, P.; Villegas, P.P.P.; Flores, Y.B.; Damme, P.V.; Lojka, B.; Havlik, J. Phenolic composition, antioxidant and anti-proliferative activities of edible and medicinal plants from the Peruvian Amazon. *Revista Brasileira de Farmacognosia*, **2016**, 26, 728-737.

Tuyiringire, N.; Deyno, S.; Weisheit, A.; Tolo, C.U.; Tusubira, D.; Munyampundu, J.P.; Ogwang, P.E.; Muvunyi, C.M.; Vander Heyden, Y. Three promising antimycobacterial medicinal plants reviewed as potential sources of drug hit candidates against multidrug-resistant tuberculosis. *Tuberculosis*, **2020**, 101987.

Wang, X.Q. Operational guidance: Information needed to support clinical trials of herbal products. *Chinese Journal of Clinical Pharmacology and Therapeutics*, **2005**, 12, 582.

World Health Organisation (WHO). Global tuberculosis report. WHO, France, **2018**.

CHAPTER 8 ANTI-DIABETIC AND ANTI-INFLAMMATORY ACTIVITIES OF *BREONADIA SALICINA*

8.1. INTRODUCTION

Diabetes mellitus is included in a group of chronic metabolic diseases linked to high blood sugar (hyperglycaemia), occurring either when insufficient insulin is produced by the pancreas (type I) or when the body cannot use insulin effectively (type II, Salehi *et al*., 2019). With diabetes currently among the four main causes of death in most industrialized countries (Salehi *et al*., 2019), diabetes prevalence is rising rapidly so that it is now considered to be a global health threat. Worldwide, about 463 million people, or 8.3% of adults were living with diabetes in 2019, and this trend may continue to rise to 548 million by 2045 (Saeedi *et al*., 2019). As many as 374 million people across the world were diagnosed with diabetes in 2020 (IDF, 2020). Moreover, Africa has reportedly the second highest prevalence of undiagnosed diabetes in the world. It has been estimated that about 6 million people in South Africa are living with diabetes, the majority of them undiagnosed (Jeftha *et al*., 2021). Currently, approaches to control diabetes utilize modern synthetic anti-diabetic drugs, insulin injections and life style alteration. Synthetic anti-diabetic drugs include secretagogues like the sulphonylureas, sensitizers such as the biguanides, thiazolidinediones (glitazones) and α-glucosidase inhibitors (Kokil *et al*., 2010). The sulphonylureas stimulate secretion of insulin by blocking the ATP-sensitive potassium-ion channels. Sulphonylureas are prescribed to patients diagnosed with Type II Diabetes, and the side effects include hypoglycaemia and weight gain (Kokil *et al*., 2010). The mode of action of the biguanides is complex; it acts in the presence of insulin by increasing the glucose uptake and utilization by tissues in the skeletal muscle, by decreasing the hepatic glucose production; it decreases hepatic gluconeogenesis. Biguanides lower LDL cholesterol, and possible side effects include nausea, lactate acidosis, diarrhoea, and renal toxicity, excluding hypoglycaemia (Rang and Dale, 2011). Thiazolidinediones increase insulin sensitivity and, accordingly, have a hypoglycaemic effect that increases peripheral glucose utilisation. The precise mode of action is not fully understood yet, but it is well known that thiazolidinediones bind and activate the gamma-peroxisomal proliferator-activated receptors (PPAR-γ), resulting in the hypoglycaemic activity. Their side effects include hepatotoxicity (troglitazone) (Rang and Dale, 2011). The mode of action of the inhibitors of alpha-glucosidase is to reduce and delay the digestive absorption of glucose and decrease postprandial

hyperglycaemia. The alpha-glucosidase drugs are indicated for patients diagnosed with Type I and Type II Diabetes, with possible side effects including malabsorption, flatulence, and diarrhoea (Bradshaw *et al*., 2007). However, synthetic anti-diabetic drugs may have serious side effects, characterised by weight loss or gain, renal damage, stomach upset, hypoglycemic shock, and liver failure (Kane *et al.*, 2005). Furthermore, these drugs are costly and inaccessible to most of the people in rural communities in Africa and other countries across the world. These limitations, together with a sharp rise in the occurrence of undetected diabetes, that are motivating researchers to investigate traditional medicinal plants and their active phytochemicals as potential alternative remedies for diabetes. Such research is motivated by the possibility to develop novel plant-derived anti-diabetic constituents that would relieve complications related to diabetes, since natural plant extracts contain numerous compounds that have been found over time to offset the potentially severe side effects of synthetic drugs. These can be standardized successively and used as medication for the treatment of diabetes mellitus (Suganya *et al*., 2014; Shazhni *et al*., 2018).

Inflammation is predominantly characterized by oedema and pain occurring in response to injury, lipid peroxidation, or by an infection causing swelling, pain, redness, heat, and loss of function of the affected area (Ricciotti and FitzGerald, 2011). These external invaders damage the organ or tissue releasing vasoactive and chemotactic conditions that attract blood towards the site of invasion, causing processes of exudate, diapedesis, and phagocytosis. Treatment, management, and control of these conditions have been a challenge (Cekici *et al*., 2014). The available drugs used to protect an organ or cells due to overreaction cause side effects. Therefore, it is important to discover novel anti-inflammatory drugs from natural products with fewer side effects (Maroon *et al*., 2010; Bhogireddy *et al*., 2013). Medicinal plants are an essential aspect of health-care provision in Africa and elsewhere (Okaiyeto and Oguntibeju, 2021). Several plant products used in Africa and elsewhere as either crude extracts, or active fractions, or pure compounds, have been investigated for their possible anti-inflammatory or anti-diabetic activity. However, very few plants and isolated bioactive compounds with potential anti-diabetic or other medicinal properties have been discovered and few of their anti-diabetic and anti-inflammatory activities have been scientifically proven (Salehi *et al*., 2019). A particular objective of this project was to illuminate the *in vitro* anti-diabetic and anti-inflammatory potentials of *Breonadia salicina*. This plant is used to treat diabetes and inflammation by many people in South Africa and other African countries (Mahlo *et al*., 2013). Therefore, this study should provide information on which part of the plant produces the best

anti-diabetic and anti-inflammatory activity and which compounds are contributing to the biological activities evaluated, since there are no reports in literature regarding this plant.

8.2. MATERIALS AND METHODS

8.2.1. Sampling and extraction

The method is reported in detail in Chapter 3, Section **3.2.1**.

8.2.2. Fractionation

The detailed fractionation methodology appears in Chapter 3, Section **3.2.2**.

8.2.3. Anti-diabetic activity

8.2.3.1. α-Amylase inhibition assay

The crude MeOH stem bark (S.crude), MeOH root (R.crude), MeOH leaf (LM.crude), and DCM leaf (LD.crude) extracts were re-dissolved in DMSO to a concentration of 100 µg/mL. The samples were diluted to 500, 250, 125 and 62.5 µg/mL in assay buffer. Fifteen microliter of each extract was added in 96-well plates in quadruplicate, followed by 5 µL enzyme (Sigma-Aldrich, St. Louis, MO, USA). The 96-well plates were incubated at 37 °C for 10 minutes. After incubation, 20 µL starch solution was added to the 96-well plates. The plates were further incubated at 37 °C for 30 minutes. Ten microliter stop solution and 75 µL iodine reagent (Sigma-Aldrich, St. Louis, MO, USA) were added into the 96-well plates (Tundis *et al*., 2010). Absorbance was measured at 580 nm using a BioTek® PowerWave XS spectrophotometer (Winooski, VT, USA). Enzyme and substrate standards were not included, and the % α-amylase inhibition was calculated as follows:

$$\%\ \alpha\text{–}amylase\ inhibition = \frac{(\text{amylase activity of control} - \text{amylase activity of test sample})}{\text{amylase activity of control}}\ x\ 100$$

where

$$amylase\ activity = A_{580nm}\ without\ enzyme - A_{580nm}\ with\ enzyme.$$

8.2.3.2. α-Glucosidase inhibition assay

The crude MeOH stem bark (S.crude), MeOH root (R.crude), MeOH leaf (LM.crude) and DCM leaf (LD.crude) extracts were re-dissolved in DMSO to a final concentration of 100

µg/mL. The samples were diluted to 500, 250, 125, 62.5 and 31.3 µg/mL in assay buffer. Five microliter of each extract was added into 96-well plates in quadruplicate, followed by 20 µL glucosidase solution (Sigma-Aldrich). Sixty microliter was added to the solution in the 96-well plates and incubated at 37 °C for 5 minutes. After incubation, 10 µL p-NP-Gluc was added. Thereafter, the 96-well plates were incubated at 37 °C for 20 minutes and 25 µL Na_2CO_3 (100 mM, Sigma-Aldrich) was added (Roskar *et al*., 2015; Rose *et al*., 2018). Absorbance was measured at 405 nm using a BioTek® PowerWave XS spectrophotometer (Winooski, VT, USA). No enzyme or substrate controls were included, and % α-glucosidase inhibition was calculated as follows:

$$\%\ \alpha\text{-}glucosidase\ inhibition = \frac{(\text{A405nm of control} - \text{A405nm of test sample})}{\text{A405nm of control}} \text{ x } 100$$

8.2.4 Anti-inflammatory activity

The crude MeOH stem bark (S.crude), MeOH root (R.crude), MeOH leaf (LM.crude) and DCM leaf (LD.crude) extracts were solubilized in DMSO to make a 100 mg/mL stock solution. Aminoguanidine (100 µM; Sigma-Aldrich) was used as a positive control to indicate anti-inflammatory activity. RAW 264.7 cells (Cellonex, South Africa) were seeded in RPMI1640 culture medium supplemented with 10 % FBS (RPMI complete medium; GE Healthcare Life Sciences) into 96-well plates at a density of 1 x 10^5 cells per well and left overnight to allow attachment. The following day, the spent culture medium was removed and 100 µL of each extract (diluted in RPMI complete medium) were added to each well to result in concentrations of 50, 100, and 200 µg/mL. To determine the anti-inflammatory activity, 100 µL of LPS (final concentration 500 ng/mL; Sigma-Aldrich, St. Louise, MO, USA) containing medium was added to the corresponding wells. Aminoguanidine (AG; Sigma-Aldrich) was used as the positive control at 100 µM. After incubation for a further 24 h, NO production was quantified by transferring 50 µL of spent culture medium to a fresh 96-well plate and adding 50 µL Griess reagent (Sigma-Aldrich) (Adebayo *et al*., 2015). The absorbance was measured at 540 nm. The calibration graph was drawn using appropriate amounts of sodium nitrite dissolved in culture medium, and was used to derive the NO concentration in each sample.

8.2.5. Statistical analysis

The α-amylase inhibition data are reported as % α-amylase inhibition ± one standard deviation (SD). Similarly, the α-glucosidase inhibition data are reported as % α-glucosidase inhibition ± SD. The anti-inflammatory activity data for the tested crude extracts are reported as nitric oxide production ± SD. The positive control for α-amylase inhibition was acarbose, epigallocatechin gallate (ECGC) was used for the α-glucosidase inhibition assay, and aminoguanidine for anti-inflammatory activity.

8.3. RESULTS AND DISCUSSION

8.3.1. Antidiabetic activity

The highest antidiabetic activity was shown by the crude stem bark (S.crude) and root (R.crude) extracts. The α-amylase inhibition assay of the crude stem bark (S.crude) and root (R.crude) extracts showed very strong activity at the lowest test concentration of 62.5 µg/mL, with 74.53 ± 0.73 % and 79.1 ± 1.49 % inhibition, respectively (Figure 8.1). The methanol and dichloromethane leaf extracts did not show any noteworthy activity at the lowest test concentration of 62.5 µg/mL, with inhibition of 1.532 ± 0.11 % and 3.864 ± 0.11 % respectively. However, the crude dichloromethane leaf extract showed some inhibition of <20 % observed at 500 µg/mL, as shown in Figure 8.1. The crude stem bark (S.crude) and root (R.crude) extracts inhibited α-glucosidase completely at the lowest test concentration of 31.3 µg/mL at 98.20 ± 0.15 % and 97.98 ± 0.22 %, as shown in Figure 8.2. Furthermore, the crude MeOH leaf extract (LM.crude) exhibited strong inhibition at 125 µg/mL of 95.16 ± 0.41 %. However, the crude dichloromethane leaf extract (LD.crude) displayed low inhibitory activity at a concentration of 125 µg/mL at 27.75 ± 2.39 %, as presented in Figure 8.2. A concentration-dependent increase in inhibitory activity was observed for the dichloromethane leaf extract, with the highest inhibitory activity observed at a test concentration of 500 µg/mL at 73.46 ± 0.52 %, as shown in Figure 8.2. However, the stem bark (S.crude), root (R.crude) and methanol leaf (LM.crude) extracts showed good α-glucosidase inhibition activity at a concentration of 500 µg/mL at 92.66 ± 0.23 %, 90.66 ± 0.33 % and 91.33 ± 0.89 %, respectively, as shown in Figure 8.2. The same trend was evident with the crude stem bark, leaf, and root extracts. The crude root and stem bark and root extracts contained the same metabolites (as shown in Figures 8.3 A and B, respectively). However, the chemical profiles revealed that the methanol and

dichloromethane leaf extracts (Figure 8.3 C and D, respectively) produced metabolites that were completely different from the crude stem bark and root extracts (Figure 8.3 A and B, respectively). Therefore, this study indicates that the chemistry and bioactivity of the crude stem bark and root extracts are the same, but differ from the leaf extracts; which explains the higher anti-diabetic activity exhibited by the root and stem bark extracts. Therefore, it can be concluded that the presence of a hydroxycinnamic acid (caffeic acid), a triterpenoid (ursolic acid), and a polyphenol (ellagic acid) in the crude stem bark (S.crude) and root (R.crude) extracts plays an important role in the antidiabetic activities of these extracts (Table 4.2, Chapter 4). Chiou *et al*. (2017) reported in their study of an *Echinacea purpurea* flower extract that caffeic acid, which in this study appeared in the crude stem bark extract (S.crude, Table 4.2, Chapter 4), had high anti-diabetic activity as measured against α-amylase, with 85.23 % inhibition and IC_{50} 1.81 ± 0.02 mg/mL. On the other hand, Kang *et al*. (2012) reported that ursolic acid, isolated from the EtOAc extracts of *Osmanthus fragrans*, has anti-diabetic activity against α-glucosidase with an IC_{50} value of 3.38 µg/mL. Furthermore, Ramachandran *et al.* (2013) confirmed that the presence of ellagic acid, identified using an HPLC analysis of a crude aqueous extract of the stem bark of *Terminalia paniculata* had high *in vitro* anti-diabetic activity against *α*-amylase and *α*-glucosidase. To the best of our knowledge, there are no published *in vitro* or *in vivo* studies of the possible antidiabetic activity of crude methanol stem bark, methanol root, dichloromethane leaf and methanol leaf extracts of *B. salicina*.

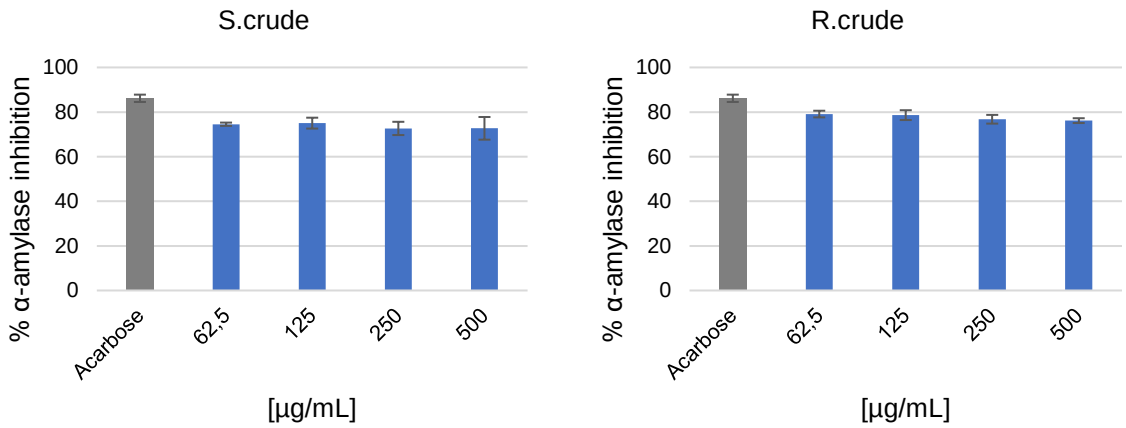

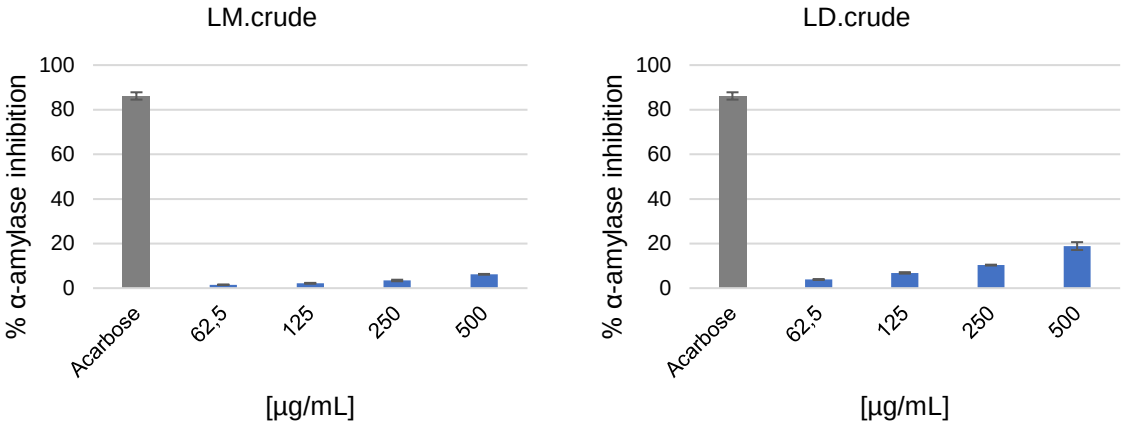

Figure 8.1. α-Amylase inhibition assay: S.crude—crude stem bark extract; R.crude—crude root extract; LM.crude—methanol leaf extract and LD.crude—dichloromethane leaf extract. Data (n = 4) expressed as percentage α-amylase inhibition ± standard deviation.

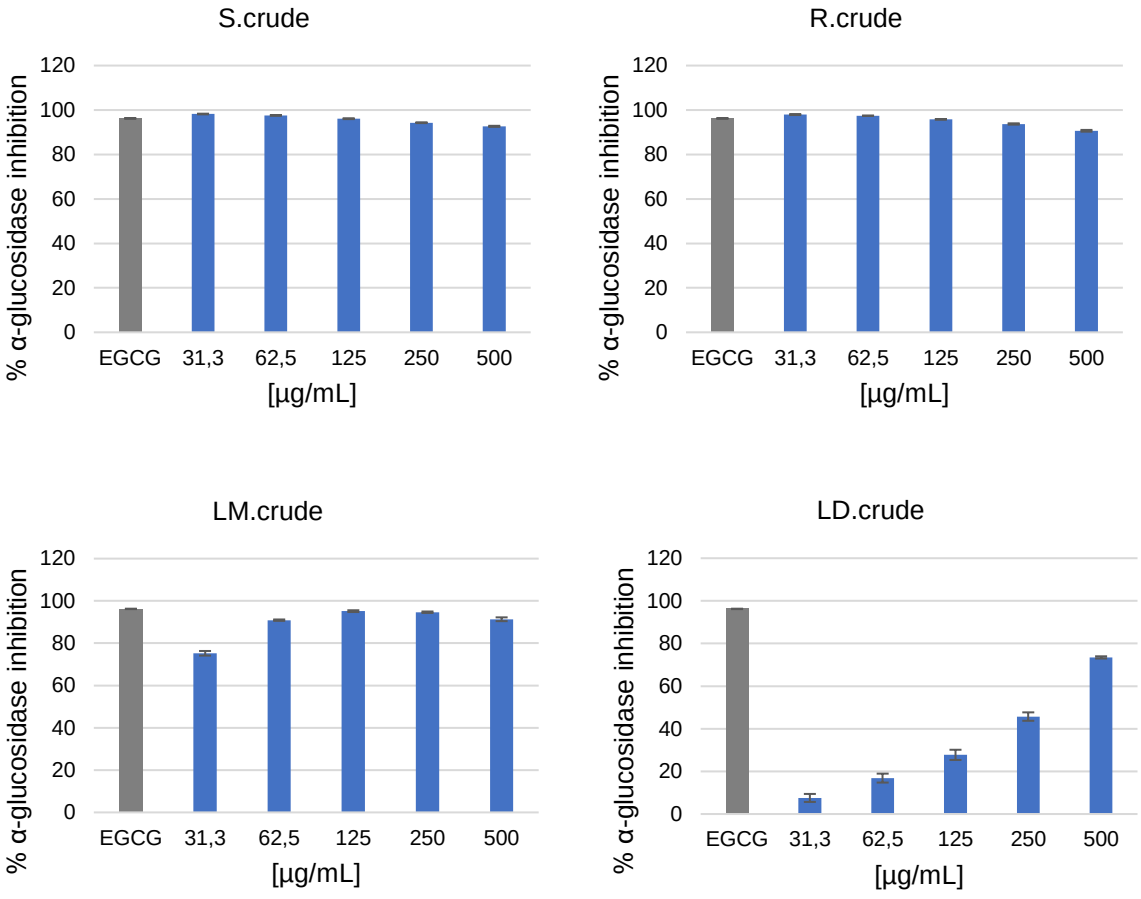

Figure 8.2. α-Glucosidase inhibition assay: S.crude—crude stem bark extract; R.crude—crude root extract; LM.crude—methanol leaf extract and LD.crude—dichloromethane leaf extract. Data (n = 4) expressed as percentage α-glucosidase inhibition ± standard deviation.

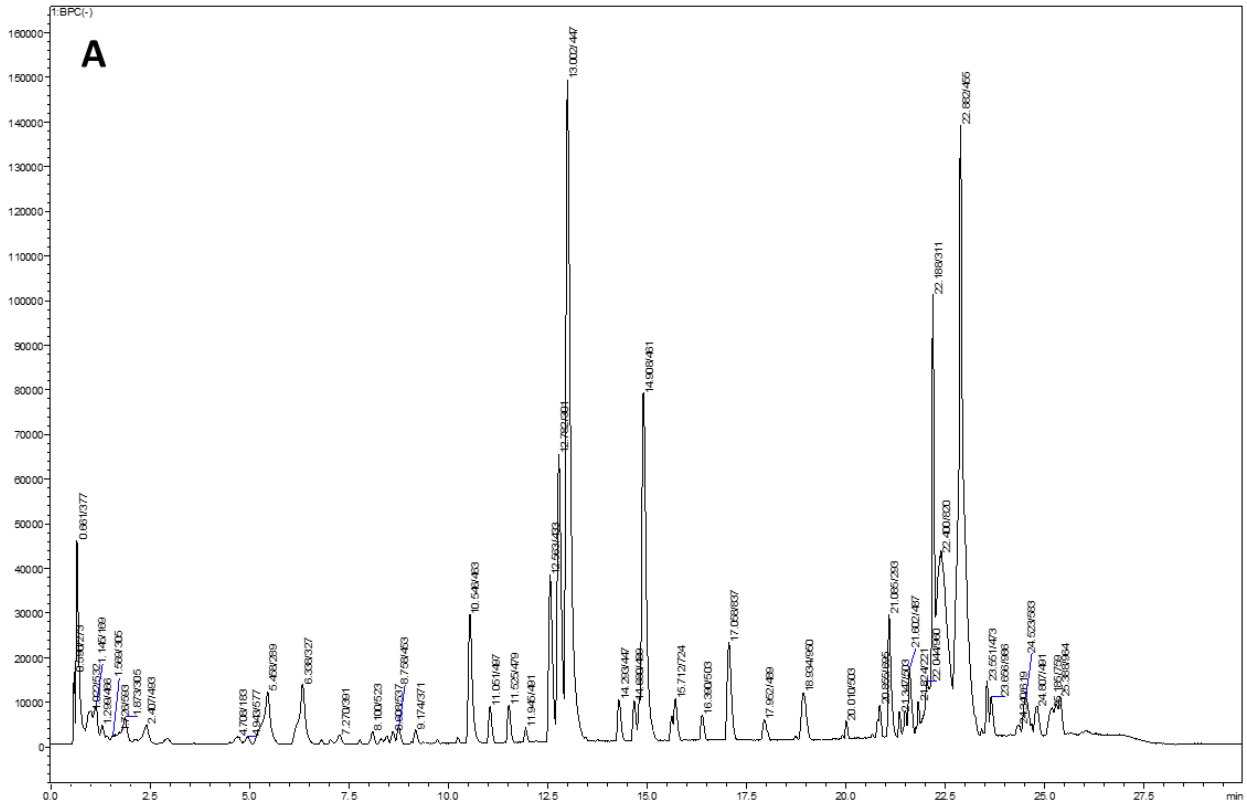

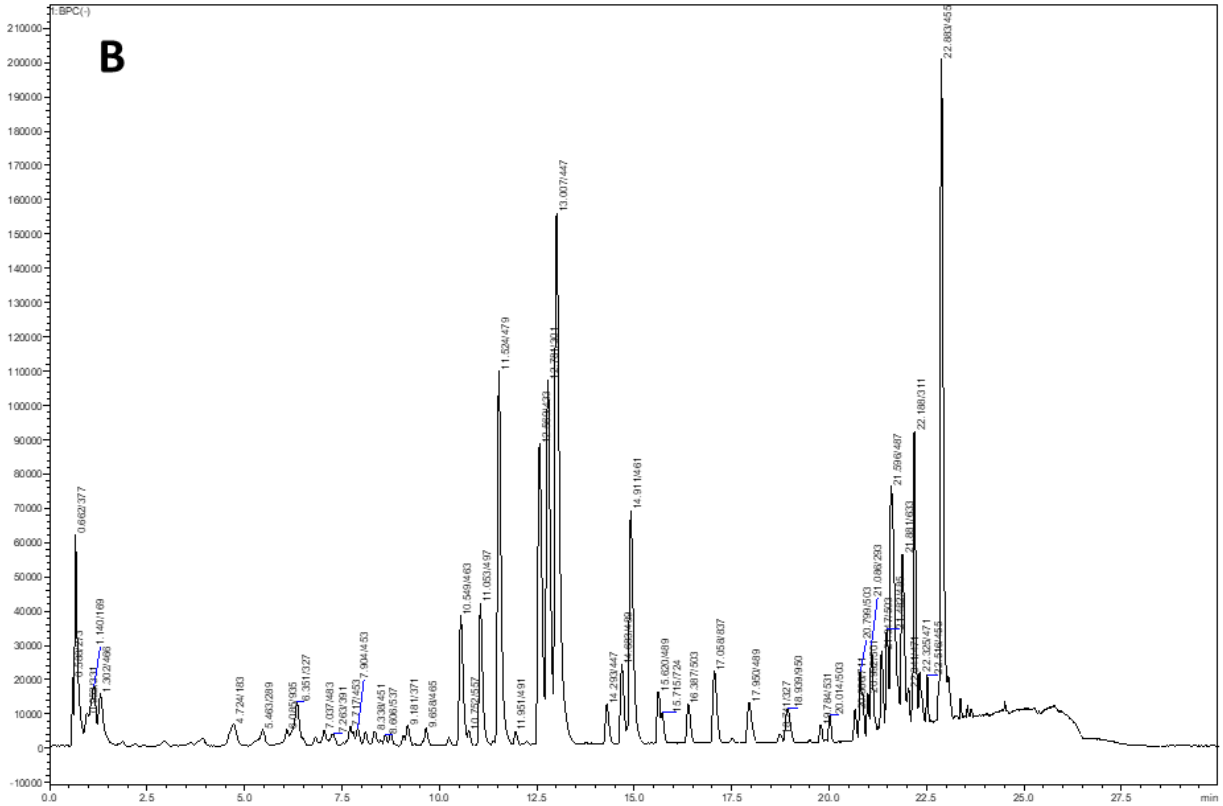

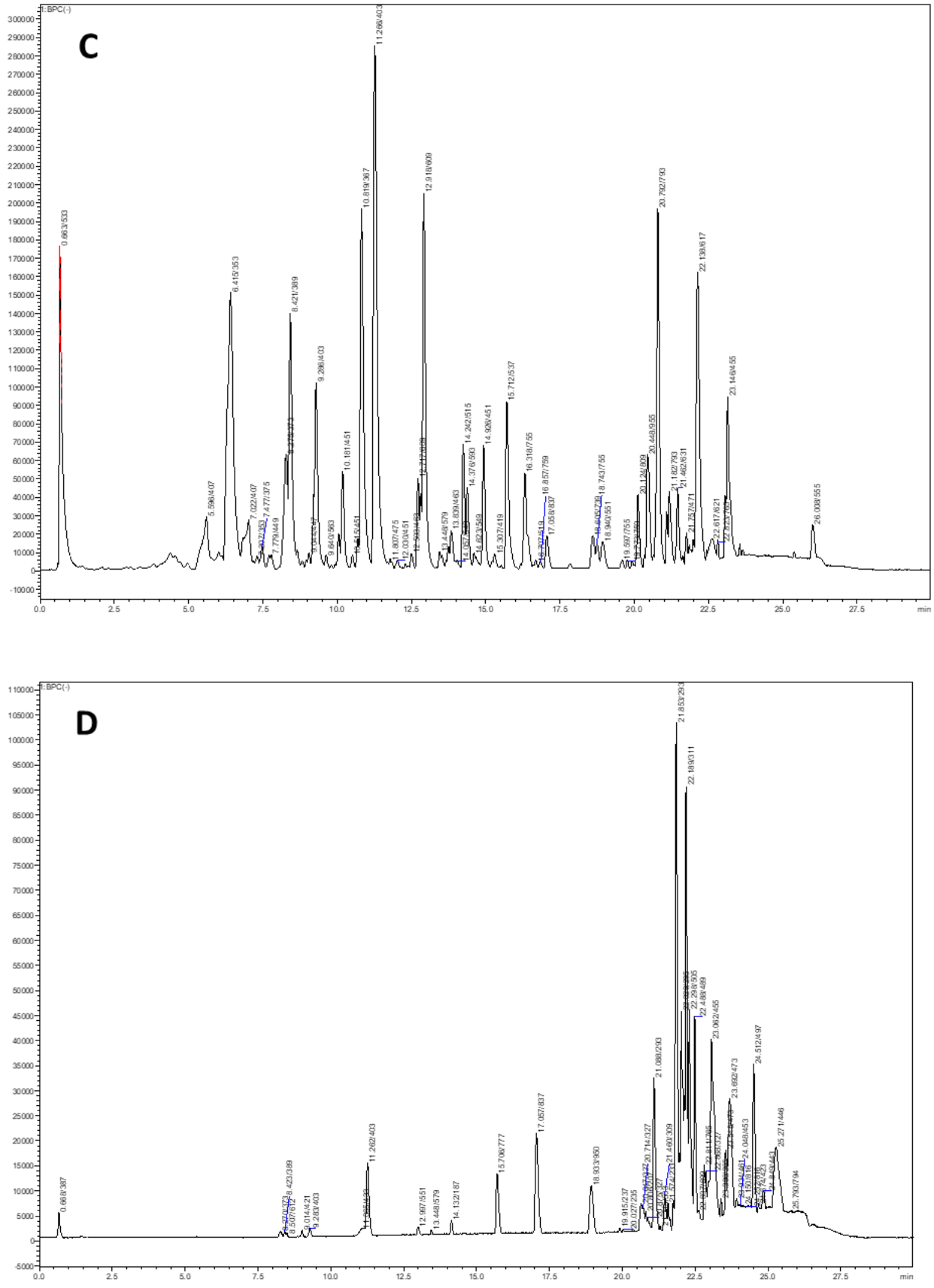

Figure 8.3. UPLC-QTOF-MS chromatograms of: A) S.crude—crude stem bark extract; B) R.crude—crude root extract; C) LM.crude—methanol leaf extract and D) LD.crude—dichloromethane leaf extract.

8.3.2. Anti-inflammatory activity

The crude stem bark (S.crude), root (R.crude), MeOH leaf (LM.crude), and DCM leaf (LD.crude) extracts were analyzed using RAW 264.7 macrophages and the Griess assay. According to the literature survey, different plant parts of *Breonadia salicina* are used to treat inflammation. However, there are no reports on which part of the plant produces the best anti-inflammatory activity; and which metabolites are responsible for the anti-inflammatory activity of *Breonadia salicina*. The leaf extracts had the highest anti-inflammatory activity; more specifically, the dichloromethane leaf (LD.crude) extracts were more active than the methanol leaf (LM.crude) extracts. The crude dichloromethane leaf extract (LD.crude) lowered the nitrite concentration at the highest concentration of 200 µg/mL with a cell viability of 79.06 ± 1.88 % and thus could potentially exhibit anti-inflammatory activity, as shown in Figure 8.4. The chemical fingerprint using UPLC-QTOF-MS showed that the crude dichloromethane leaf (LD.crude) extracts produced metabolites which were different from the methanol leaf, root, and stem bark extracts (as shown in Figure 8.3 D, C, B and A, respectively). Therefore, these different metabolites may make an important contribution to the anti-inflammatory activity of the dichloromethane leaf extracts (Figure 8.3 D). Furthermore, this is the first study to provide preliminary evidence on the plant part that has the highest anti-inflammatory activity; and which metabolites contribute to the anti-inflammatory activity of *Breonadia salicina.*

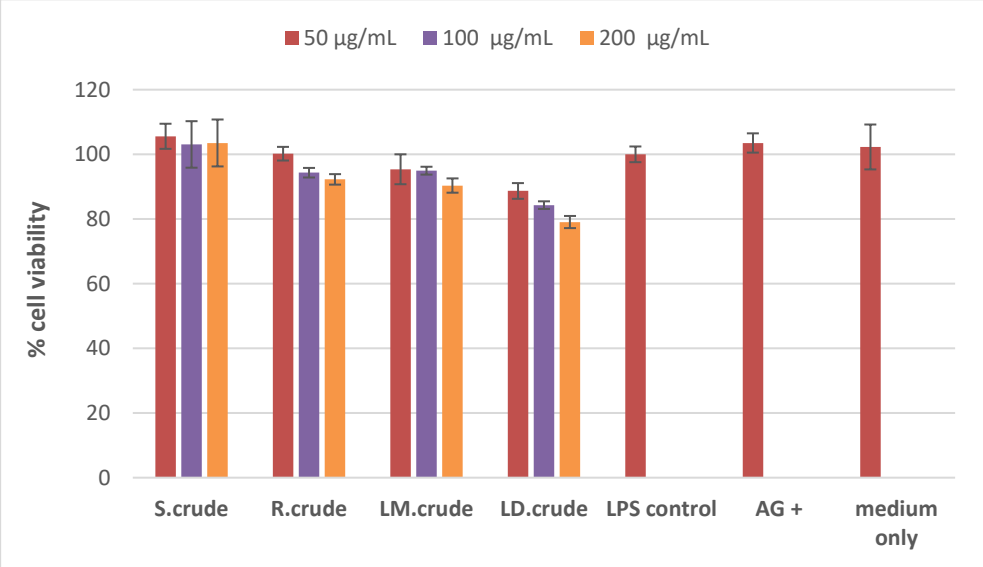

Figure 8.4. Anti-inflammatory activity against RAW 264.7 macrophages: S.crude—crude stem bark extract; R.crude—crude root extract; LM.crude—methanol leaf extract and LD.crude—dichloromethane leaf extract expressed as nitric oxide production ± standard deviation at varying concentrations.

8.4. Summary

In conclusion:

- The crude root and stem bark extracts had high antidiabetic activities compared to the leaf extracts.
- The UPLC-QTOF-MS highlighted the similarities of the crude stem bark and root extract chemical profiles while the leaf extract had a different profile.
- The crude dichloromethane leaf extract had the highest anti-inflammatory activity of all the extracts.
- The chemical profiling fingerprint using UPLC-QTOF-MS revealed that the dichloromethane leaf extract produced metabolites differed from the methanol leaf, stem and root extracts.

8.5. References

Adebayo, S.A.; Dzoyem, J.P.; Shai, L.J.; Eloff, J.N. The anti-inflammatory and antioxidant activity of 25 plant species used traditionally to treat pain in southern African. *BMC Complementary and Alternative Medicine*, **2015**, 15, 1-10.

Bhogireddy, N.; Naga, A.; Ramesh, B.; Pradeep, M.; Reddy, O.V.S.; Gaddaguti, V.; Raj, K.K.; Pola, P.K.; Venkataraman, B. Anti-inflammatory and anti-diabetic activities with their other ethnomedicinal properties of the plants. *Journal of Medicinal Plants Studies*, **2013**, 1, 87-96.

Bradshaw, D.; Norman, R.; Pieterse, D.; Levitt, N.S. Estimating the burden of disease attributable to diabetes South Africa in 2000. *South African Medical Journal*, **2007**, 97, 700-706.

Cekici, A.; Kantarci, A.; Hasturk, H.; Van Dyke, T.E. Inflammatory and immune pathways in the pathogenesis of periodontal disease. *Periodontology 2000*, **2014**, 64, 57-80.

Chiou, S.Y.; Sung, J.M.; Huang, P.W.; Lin, S.D. Antioxidant, antidiabetic, and antihypertensive properties of *Echinacea purpurea* flower extract and caffeic acid derivatives using in vitro models. *Journal of Medicinal Food*, **2017**, 20, 171-179.

International Diabetes Federation (IDF). Diabetes facts and figures, **2020**. https://idf.org

Jeftha, A.; Roberts, T.; Kimmie-Dhansay, F. The effect of periodontal disease on metabolic control in patients with diabetes mellitus in South Africa: Protocol for a Systematic Review. *JMIR Research Protocols*, **2021**, 10, 27471.

Kane, M.P.; Abu-Baker, A.; Busch, R.S. The utility of oral diabetes medications in type 2 diabetes of the young. *Current Diabetes Reviews*, **2005**, 1, 83-92.

Kang, W.; Song, Y.; Gu, X. α-glucosidase inhibitory in vitro and antidiabetic activity in vivo of *Osmanthus fragrans*. *Journal of Medicinal Plants Research*, **2012**, 6, 2850-2856.

Kokil, R.G.; V Rewatkar, P.; Verma, A.; Thareja, S.; Naik, R.S. Pharmacology and chemistry of diabetes mellitus and antidiabetic drugs: a critical review. *Current Medicinal Chemistry*, **2010**, 17, 4405-4423.

Mahlo, S.M.; McGaw, L.J.; Eloff, J.N. Antifungal activity and cytotoxicity of isolated compounds from leaves of *Breonadia salicina. Journal of Ethnopharmacology*, **2013**, 148, 909-913.

Maroon, J.C.; Bost, J.W.; Maroon, A. Natural anti-inflammatory agents for pain relief. *Surgical Neurology International*, **2010**, 1, 80.

Okaiyeto, K.; Oguntibeju, O.O. African Herbal Medicines: Adverse Effects and Cytotoxic Potentials with Different Therapeutic Applications. *International Journal of Environmental Research and Public Health*, **2021**, 18, 5988.

Ramachandran, S.; Rajasekaran, A.; Adhirajan, N. In vivo and in vitro antidiabetic activity of *Terminalia paniculata* bark: an evaluation of possible phytoconstituents and mechanisms for blood glucose control in diabetes. *International Scholarly Research Notices*, **2013**, 2013. http://dx.doi.org/10.1155/2013/484675

Rang, H.P.; Dale, M.M.; Ritter, J.M.; Flower, R.J.; Henderson, G. *Rang and Dale's pharmacology*. *Elsevier Health Sciences*, **2011**. https://books.google.co.za

Ricciotti, E.; FitzGerald, G.A. Prostaglandins and inflammation. *Arteriosclerosis, Thrombosis, and Vascular Biology*, **2011**, 31, 986-1000.

Rose, D.R.; Chaudet, M.M.; Jones, K. Structural studies of the intestinal α-glucosidases, maltase-glucoamylase and sucrase-isomaltase. *Journal of Pediatric Gastroenterology and Nutrition*, **2018**, 66, 11-13.

Roskar, I.; Molek, P.; Vodnik, M.; Stempelj, M.; Strukelj, B.; Lunder, M. Peptide modulators of alpha-glucosidase. *Journal of Diabetes Investigation*, **2015**, 6, 625-631.

Saeedi, P.; Petersohn, I.; Salpea, P.; Malanda, B.; Karuranga, S.; Unwin, N.; Colagiuri, S.; Guariguata, L.; Motala, A.A.; Ogurtsova, K.; Shaw, J.E. Global and regional diabetes prevalence estimates for 2019 and projections for 2030 and 2045: Results from the International Diabetes Federation Diabetes Atlas. *Diabetes Research and Clinical Practice*, **2019**, 157, 107843.

Salehi, B.; Ata, A.; Kumar, A.V.N.; Sharopov, F.; Ramírez-Alarcón, K.; Ruiz-Ortega, A.; Abdulmajid Ayatollahi, S.; Valere Tsouh Fokou, P.; Kobarfard, F.; Amiruddin Zakaria, Z.; Iriti, M. Antidiabetic potential of medicinal plants and their active components. *Biomolecules*, **2019**, 9, 551.

Shazhni, J.A.; Renu, A.; Vijayaraghavan, P. Insights of antidiabetic, anti-inflammatory and hepatoprotective properties of antimicrobial secondary metabolites of corm extract from Caladium x *hortulanum*. *Saudi Journal of Biological Sciences*, **2018**, 25, 1755-1761.

Suganya, G.; Kumar, S.P.; Dheeba, B.; Sivakumar, R. In vitro antidiabetic, antioxidant and anti-inflammatory activity of *Clitoria ternatea* L. *International Journal of Pharmacy and Pharmaceutical Science*, **2014**, 6, 342-347.

Tundis, R.; Loizzo, M.R.; Menichini, F. Natural products as α-amylase and α-glucosidase inhibitors and their hypoglycaemic potential in the treatment of diabetes: an update. *Mini Reviews in Medicinal Chemistry*, **2010**, 10, 315-331.

CHAPTER 9 *IN VITRO* TOXICOLOGY OF *BREONADIA SALICINA*

9.1. INTRODUCTION

Toxicology is predominantly concerned with antagonistic or toxic properties in living organisms from an exposure to a poisonous substance, either a drug or chemical substance (Zhang *et al.*, 2007). One of the World Health Organisation's conditions for traditional herbs to be used in medicine, is that they should be proved to be non-toxic (Chapman *et al*., 2013). Plants frequently used in traditional medicine are assumed to be non-toxic and free of side-effects because they have been used to treat, control and manage various illnesses and infections for a long time (Jennings, 2015; Nasri *et al.*, 2013). However, in addition to the existing prehistoric information about medicinal plant use, a proper toxicological evaluation of herbal plants should be carried out before they are acknowledged as safe medicine (Langman and Kapur, 2006). This is because recent research has revealed that various plants used as food have adverse health problems which are potentially toxic and may cause death (Bonifas *et al*., 2010; Fennell *et al.*, 2004). Therefore, the toxicity of traditional medicinal plants should be tested, preferably by means of a cell culture assay that would use both *in vitro* and *in vivo* models to evaluate their toxicity (Greene *et al*., 2010; Edziri *et al*., 2011). Consequently, in this chapter, the evaluation of possible anti-proliferation, cytotoxic and genotoxic activities of the crude extracts and fractions of *B. salicina* are reported, using the NucRed nuclei dye, MTT (3-(4,5-dimethylthiazol-2-yl)-2,5-diphenyltetrazolium bromide) cell toxicity, and Hoechst 33342/Propidium iodide (PI) dual staining assays to provide information on which part of the plant can be a potential source of safe and effective compounds to treat various diseases.

9.2. MATERIALS AND METHODS

9.2.1. Sampling and extraction

A detailed account of the methodology is provided in Chapter 3, Section **3.2.1**.

9.2.2. Fractionation

The detailed methodology appears in Chapter 3, Section **3.2.2**.

9.2.3. Anti-proliferation activity

To evaluate cytotoxicity, the crude extracts and fractions were incubated at a fixed concentration of 50 µg/mL and 10 µg/mL, respectively, in 96-well plates that had been seeded 24 hours before with HeLa cells (Cellonex; 2 x 10^4 cells per well). The plates were incubated at 37 °C with 5 % CO_2 for 48 hours in a humidified incubator. Dulbecco's modified Eagle's medium (DMEM; Thermo Fisher Scientific) containing the culture medium was added with 10 % foetal bovine serum (Biowest) and penicillin/streptomycin/amphotericin (Lonza). Furthermore, resazurin (Sigma-Aldrich) was added to a final concentration of 0.05 mM, followed by 2 hours incubation. After incubation, the fluorescence at Exc560 and Em590 was measured using a Spectramax M3 (Molecular Devices) plate reader (San Jose, CA, USA) (Stander *et al*., 2009). The % cell viability relative to the untreated control wells was calculated after deducting background readings.

9.2.4. Genotoxic activity

The crude extracts (S.crude, R.crude, LM.crude and LD.crude) were re-dissolved in DMSO to a final concentration of 100 mg/mL and stored at 4°C. The plates were seeded with 3000 cells/well (100 µL each) and kept overnight. Cells were then treated with 15.125, 31.25, 62.5, 125 and 250 µg/mL samples at 37 °C for 48 hours in a 5 % CO_2 atmosphere. Griseofulvin was used as the positive control at a concentration range of 0–50 µM. After incubation, the cells were fixed for 15 minutes with a 4 % formaldehyde solution. A working solution of NucRed was prepared by adding 2 drops of NucRed per mL complete medium. Fixative was aspirated prior to addition of 100 µL NucRed working solution. The cells were stained for 15–30 minutes; thereafter, images were acquired using the Cy5 filter on the ImageXpress Micro XLS Widefield Microscope (Molecular Devices). Live and dead cells were counted using the Multi-Wavelength Cell Scoring Application and MetaXpress software. The acquired data were recorded in an EXCEL spreadsheet and processed (Gertsch, 2009; Luzhna *et al*., 2013; Phillips and Arlt, 2009).

9.2.5. Cytotoxicity

9.2.5.1. MTT assay

To accurately confirm the potential anti-inflammatory activity and the absence of toxicity, the cell viability in the crude extracts (S.crude, R.crude, LM.crude and LD.crude) was assessed using MTT (3-(4,5-dimethylthiazol-2-yl)-2,5-diphenyltetrazolium bromide)) against RAW 264.7 macrophages. The remaining medium and treatments in the 96-well plates were removed and replaced with medium containing 0.5 mg/mL MTT (3-(4,5-dimethylthiazol-2-yl)-2,5-diphenyltetrazolium bromide). Thereafter, the 96-well plates were incubated for 30 minutes at 37°C. After incubation, the MTT was removed and 100 µL DMSO was added to each well to solubilise the formazan crystals (Tolosa *et al*., 2015). The absorbance was measured at 540 nm on a BioTek® PowerWave XS spectrophotometer (Winooski, VT, USA).

9.2.5.2. Hoechst 33342/Propidium iodide (PI) dual staining method

The cytotoxicity of the crude stem bark, root, methanol leaf and dichloromethane leaf extracts was determined using the Hoechst 33342/Propidium iodide (PI) dual staining method. The extracts were re-dissolved in DMSO to a final concentration of 100 mg/mL. Thereafter, 100 µL Vero cells (4000 cells/well) were seeded into 96-well microtiter plates. The microtiter plates were incubated at 37°C and 5 % CO_2, and 100 % relative humidity for 48 hours. Furthermore, 100 µL aliquots of each dilution were added to 100 µL attached cells in the 96-well plate at concentrations of 15.625, 31.25, 62.5, 125, and 250 µg/mL. The plates were incubated for 30 minutes and then 100 µL of the Hoechst 33342 nuclear dye staining solution was added to each well. Finally, 10 µL propidium iodide solution (Carolina *et al*., 2011) was added. Live and dead cells were quantified using the ImageXpress Micro XLS Widefield Microscope (Molecular Devices) with a 10x Plan Fluor objective and DAPI and Texas Red filter cubes. Melphalan (100 mM stock) was used as a positive control at 30 µM.

9.2.6. Statistical analysis

For the anti-proliferation activity, the data for the single concentration and IC_{50} screening was shown as percentage (%) parasite viability ± standard deviation (SD). For dose-response tests,

the organisms were cultured with three serial dilutions of fraction S_2, and a graph of % viability versus log(compound concentration) was drawn to find the IC_{50} values using non-linear regression (in GraphPad Prism v.5.02). The positive control standard for the anti-proliferation activity was the cell apoptosis inducer emetine. For genotoxicity, the data for the cytotoxicity was shown as Vero cell number ± standard deviation at varying concentrations. However, the data for the micro-nucleated cells was shown as percentage micro-nucleated Vero cells ± standard deviation at varying concentrations. Griseofulvin was the positive control for the genotoxicity screening. Furthermore, for the MTT assay, the data for the cytotoxicity was shown as percentage cell viability of LPS activated macrophages ± standard deviation at varying concentrations. Moreover, for the cytotoxicity using the Hoechst 33342/Propidium iodide (PI) dual staining method, the data for the cytotoxicity was shown as average number of live cells ± standard deviation at varying concentrations.

9.3. RESULTS AND DISCUSSION

9.3.1. Anti-proliferation activity

As described earlier, the cytotoxicities of crude extracts and fractions against human cervix adenocarcinoma (HeLa) cells were obtained from the cell toxicity assays. All the samples produced a significant cytotoxic effect against HeLa cells to less than 50 % viability (Figure 9.1) when tested at 50 µg/mL. The cytotoxicity assay was repeated at a lowered concentration of 10 µg/mL. Fraction S_2 still had significant cytotoxicity (Figure 9.1). At this concentration, fraction S_2 had the highest anti-proliferation activity of 35.99 ± 0.09 % viability and IC_{50} value of 8.7 ± 0.27 µg/mL (Figure 9.2). In contrast, at this concentration, the crude methanol stem bark extract (S.crude), from which fraction S_2 had originated, did not show significant cytotoxic effects (89.46 ± 1.11 % viability, Figure 9.1). This may be due to the removal of active components from the crude extract (S.crude) during chromatography, or low concentrations of active components in the crude extract. Furthermore, fraction S_2 was more active than the parent crude methanol stem bark extract (S.crude). This could be due to the synergistic effects of various components in fraction S_2, and these effects may be further influenced by bioactive components being narrowed to components of a particular polarity. Emetine, the positive standard, had an IC_{50} value of 0.022 µM (Figure 9.2). No toxic effects of *Breonadia salicina* have been reported before (Mahlo *et al*., 2013; Sibandze, 2009). Furthermore, the chloroform leaf extract was less toxic to Vero monkey kidney cells (LC_{50} = 82 mg/mL) in the MTT assay

(Mahlo *et al*., 2013). Moreover, a previous study showed that the MeOH/CH_2Cl_2 (1:1) stem bark and leaf extracts did not affect human kidney epithelial cells (70.84 ± 2.72 µg/mL and 182.66 ± 12.44 µg/mL, respectively) using the MTT assay (Sibandze, 2009). These results do not agree with the results of this study, but the difference may be the result of the extraction methodology used in the different studies. It should be taken into consideration that *in vitro* results are not necessarily indicative of what could happen *in vivo*, hence the panel of human cells on which fraction S_2 was tested should be expanded to confirm if it is toxic; moreover, fraction S_2 and the least toxic extracts and fractions should be evaluated in an *in vivo* model for the toxicity of its metabolites. As far as could be ascertained, the anti-proliferation activity of *B. salicina* against HeLa cells has not been assessed before. This is the first report on the potential anti-proliferation activity of *B. salicina* against these cells.

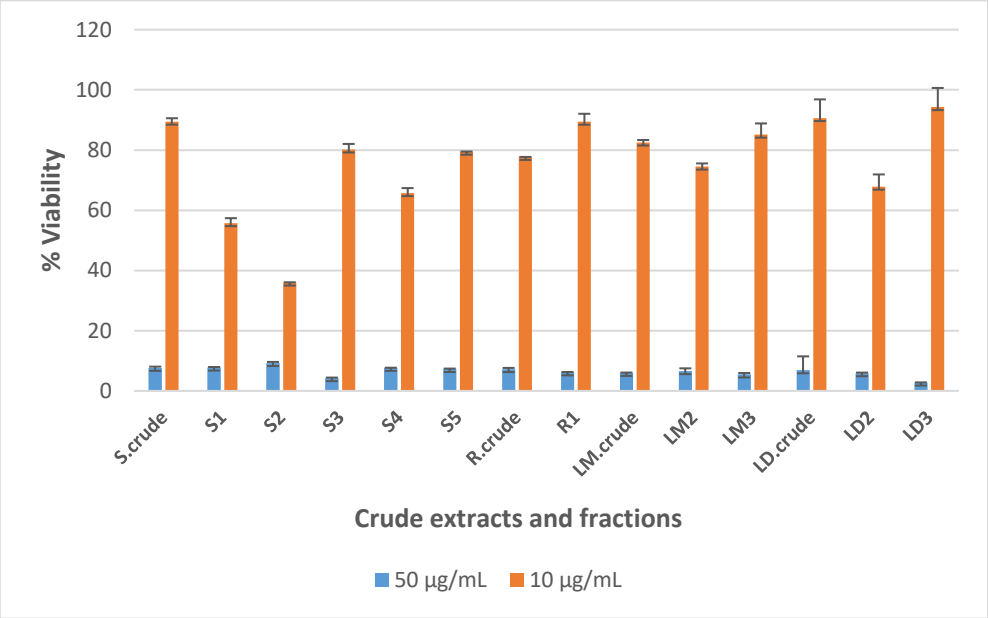

Figure 9.1. Anti-proliferation activity against HeLa cells: S.crude— crude stem bark extract; S1—Fraction S_1; S2—Fraction S_2; S3—Fraction S_3; S4—Fraction S_4; S5—Fraction S_5; R.crude—crude root extract; R1—Fraction R_1; LM.crude—methanol leaf extract; LM2—Fraction LM_2; LM3—Fraction LM_3; LD.crude—dichloromethane leaf extract; LD2—Fraction LD_2 and LD3—Fraction LD_3 – expressed as % parasite viability ± SD.

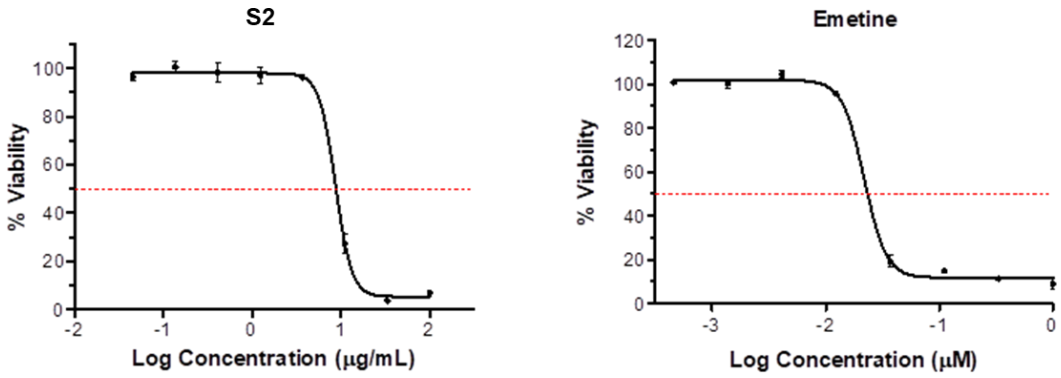

Figure 9.2. Dose-response curves for the cell toxicity assay: S2—Fraction S_2 expressed as % parasite viability ± SD.

9.3.2. Genotoxicity

The crude stem bark (S.crude), root (R.crude) and methanol leaf (LM.crude) extracts were not cytotoxic at 15.125 µg/mL, 31.25 µg/mL, 125 µg/mL and 250 µg/mL, respectively. However, the crude dichloromethane leaf extract (LD.crude) was cytotoxic at 250 µg/mL, but not at lower concentrations of 15.125 µg/mL, 31.25 µg/mL and 125 µg/mL, as shown in Figure 9.3. An increase in the percentage of micronucleated cells was evident with all the crude extracts, indicating their potential genotoxicity, as shown in Figure 9.4. However, no increased toxicity was observed with the crude dichloromethane leaf extract (LD.crude) at 250 µg/mL, as shown in Figure 9.4. The genotoxicity of *Breonadia salicina* to Vero cells has not been determined before. Therefore, this is the first report on the genotoxicity of *B. salicina* against these cells.

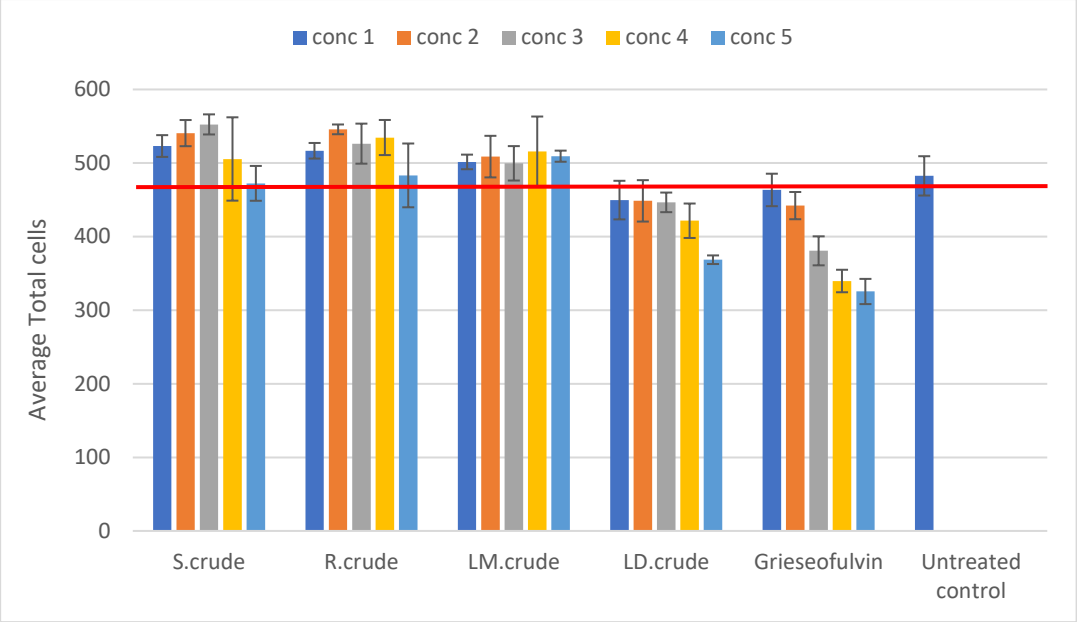

Figure 9.3. Genotoxicity against Vero cells: S.crude—crude stem bark extract; R.crude—crude root extract; LM.crude—methanol leaf extract and LD.crude—dichloromethane leaf extract. Data (n = 4) expressed as total Vero cell number ± standard deviation at different concentrations. The red line indicates the number of total cells in an untreated Vero population, i.e. a nontoxic treatment control. Concentrations: 1 = 15.125, 2 = 31.25, 3 = 62.5, 4 = 125 and 5 = 250 µg/mL.

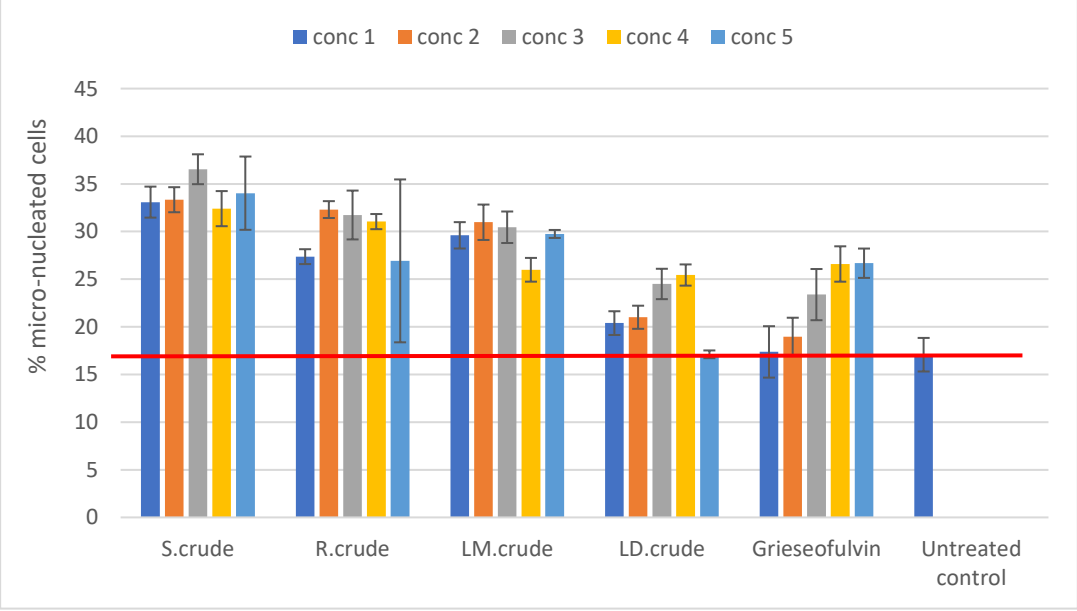

Figure 9.4. Genotoxicity against Vero cells: S.crude—crude stem bark extract; R.crude—crude root extract; LM.crude—methanol leaf extract and LD.crude—dichloromethane leaf extract. Data (n = 4) expressed as percentage micro-nucleated Vero cells ± standard deviation at varying concentrations. The red line indicates % micro-nucleated cells of the untreated Vero control population. Concentrations: 1 = 15.125, 2 = 31.25, 3 = 62.5, 4 = 125 and 5 = 250 µg/mL.

9.3.3. Cytotoxicity

The cytotoxicity of the crude extracts (S.crude, R.crude, LM.crude and LD.crude) was assessed using the Hoechst 33342/Propidium iodide (PI) dual staining method against Vero cells (Figure 9.6). None of the extracts were shown to be cytotoxic at the concentrations of 50 µg/mL, 100 µg/mL and 200 µg/mL against RAW 264.7 macrophages (Figure 9.5). The crude stem bark and root extracts were cytotoxic at 250 µg/mL (Figure 9.6). The cytotoxicity may be the result of synergistic effects of several compounds found in the crude stem bark (S.crude) and root (R.crude) extracts (Table 4.2, Chapter 4). There are no published reports or studies that validate the cytotoxic effects of these compounds occurring in the root and stem bark extracts (Table 4.2, Chapter 4) in other medicinal plants. However, this study provides information on which compounds may be causing the cytotoxic effect of *B. salicina* against Vero cells. Furthermore, the stem bark and root extracts did not show cytotoxic effects at concentrations of 15.625 µg/mL, 31.25 µg/mL, 62.5 µg/mL and 125 µg/mL (as shown in Figure 9.6). Moreover, the crude leaf (methanol and dichloromethane) extracts were not cytotoxic against Vero cells at concentrations of 15.625 µg/mL, 31.25 µg/mL, 62.5 µg/mL, 125 µg/mL and 250 µg/mL (as shown in Figure 9.6). The toxicity of *Breonadia salicina* has not been determined before using Raw 264.7 macrophages. This is the first report on the possible cytotoxic effects of *B. salicina* against these cells.

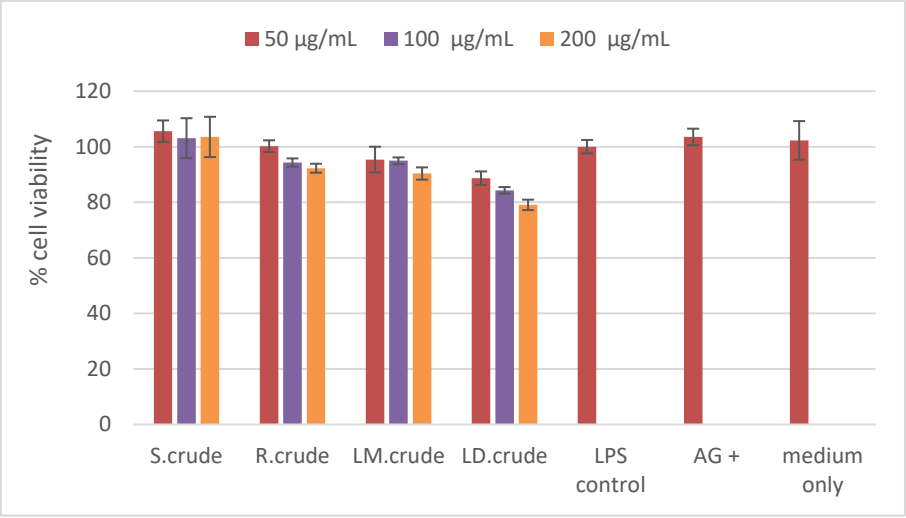

Figure 9.5. Cytotoxicity against Raw 264.7 macrophages: S.crude—crude stem bark extract; R.crude—crude root extract; LM.crude—methanol leaf extract and LD.crude—dichloromethane leaf extract. Data (n = 4) expressed as percentage cell viability of LPS activated macrophages ± SD at 50 µg/mL, 100 µg/mL and 200 µg/mL.

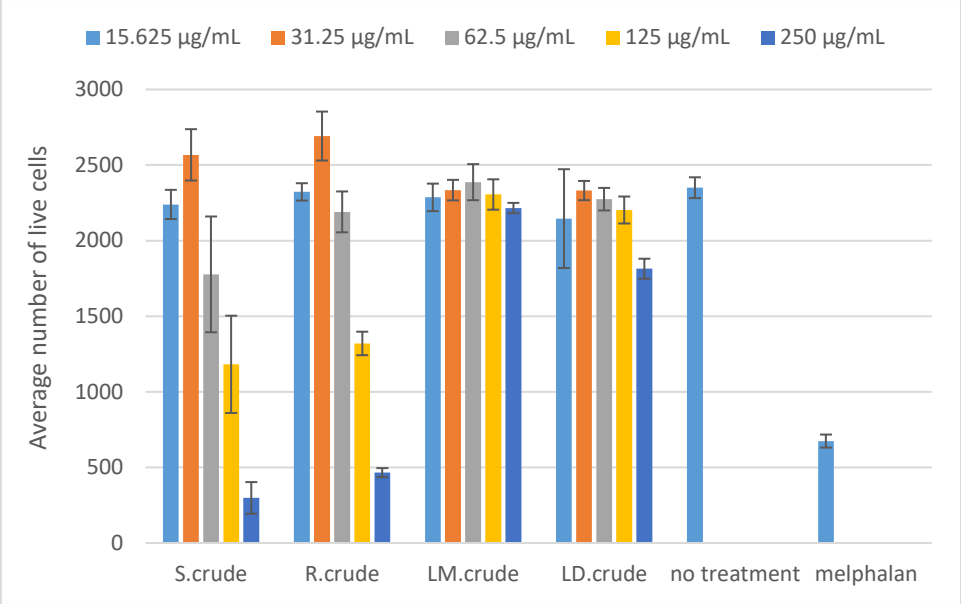

Figure 9.6. Cytotoxicity against Vero cells: S.crude—crude stem bark extract; R.crude—crude root extract; LM.crude—methanol leaf extract and LD.crude—dichloromethane leaf extract. Data (n = 4) expressed as average number of live cells ± SD at 15.625 µg/mL, 31.25 µg/mL, 62.5 µg/mL, 125 µg/mL and 250 µg/mL.

9.4. Conclusion

This study set out to evaluate the possible *in vitro* anti-proliferation activity, cytotoxicity, and genotoxicity of *Breonadia salicina*. According to the literature survey, the safety profile of *B. salicina* has not been fully established. Therefore, in our study different assays were used to ascertain the safety of this plant, and to determine which part of the plant can be a potential source of safe and effective compounds to treat various diseases. This study shows that all the samples tested at a concentration of 50 µg/mL produced a significant cytotoxic effect against HeLa cells to below 50 %. When the cytotoxicity assay was repeated at 10 µg/mL, fraction S_2, obtained from the stem bark (S.crude), exhibited significant cytotoxic effects against HeLa cells, with a viability of 35.99 ± 0.09 % and IC_{50} value of 8.7 ± 0.27 µg/mL. Furthermore, the crude dichloromethane leaf extract (LD.crude) was genotoxic at the highest tested concentration of 250 µg/mL against Vero cells. Moreover, the crude dichloromethane leaf extract (LD.crude) did not increase the percentage of micronucleated Vero cells at a concentration of 250 µg/mL. The crude stem bark and root extracts showed cytotoxic effects against Vero cells at 250 µg/mL in the Hoechst 33342/Propidium iodide (PI) dual staining test. However, none of the extracts (S.crude. R.crude, LM.crude and LD.crude) was found to be cytotoxic at the concentrations of 50 µg/mL, 100 µg/mL and 200 µg/mL against RAW 264.7 macrophages. These results demonstrate the varying cytotoxicity of certain parts of *B. salicina*

against a panel of cells using different methods. However, it should be taken into consideration that *in vitro* results are not necessarily indicative of what could happen *in vivo*. Therefore, all the tested samples should be evaluated using an *in vivo* model to evaluate the toxicity of the metabolites.

9.5. Summary

To conclude:

- The leaf and root samples did not exhibit anti-proliferation activity against HeLa cells; therefore, the safe and effective constituents of these samples could be potential leads for the treatment, control and management of diseases.
- Fraction S_2 showed significant cytotoxic effect against HeLa cells.
- The crude extracts (S.crude, R.crude, LM.crude and LD.crude) were not toxic at lower concentrations.
- The crude extracts (S.crude, R.crude, LM.crude and LD.crude) were not cytotoxic against RAW 264.7 macrophages at 50 µg/mL, 100 µg/mL and 200 µg/mL.
- The crude stem bark and root extracts were cytotoxic at 250 µg/mL against Vero cells.
- This is the first study to determine significant anti-proliferation activity, genotoxicity and cytotoxicity against HeLa cells, RAW 264.7 macrophages and Vero cells.

9.6. References

Bonifas, J.; Hennen, J.; Dierolf, D.; Kalmes, M.; Blömeke, B. Evaluation of cytochrome P450 1 (CYP1) and N-acetyltransferase 1 (NAT1) activities in HaCaT cells: implications for the development of in vitro techniques for predictive testing of contact sensitizers. *Toxicology In Vitro*, **2010**, 24, 973-980.

Carolina, L.E.M.A.; Varela-Ramirez, A.; Aguilera, R.J. Differential nuclear staining assay for high-throughput screening to identify cytotoxic compounds. *Current Cellular Biochemistry*, **2011**, 1, 1.

Chapman, K. L.; Holzgrefe, H.; Black, L. E.; Brown, M.; Chellman, G.; Copeman, C.; Couch, J.; Creton, S.; Gehen, S.; Hoberman, A. Pharmaceutical toxicology: designing studies to reduce animal use, while maximizing human translation. *Regulatory Toxicology and Pharmacology*, **2013**, 66, 88-103.

Edziri, H.; Mastouri, M.; Mahjoub, A.; Anthonissen, R.; Mertens, B.; Cammaerts, S.; Gevaert, L.; Verschaeve, L. Toxic and mutagenic properties of extracts from Tunisian traditional medicinal plants investigated by the neutral red uptake, VITOTOX and alkaline comet assays. *South African Journal of Botany*, **2011**, 77, 703-710.

Fennell, C.; Lindsey, K.; McGaw, L.; Sparg, S.; Stafford, G.; Elgorashi, E.; Grace, O.; Van Staden, J. Assessing African medicinal plants for efficacy and safety: pharmacological screening and toxicology. *Journal of Ethnopharmacology*. **2004**, 94, 205-217.

Gertsch, J. How scientific is the science in ethnopharmacology? Historical perspectives and epistemological problems. *Journal of Ethnopharmacology*, **2009**, 122, 177-183.

Greene, N.; Aleo, M. D.; Louise-May, S.; Price, D. A.;Will, Y. Using an in vitro cytotoxicity assay to aid in compound selection for *in vivo* safety studies. *Bioorganic and Medicinal Chemitsry Letters*, **2010**, 20, 5308-5312.

Jennings, P. The future of *in vitro* toxicology. *Toxicology In Vitro*, **2015**, 29, 1217-1221.

Langman, L. J.; Kapur, B. M. Toxicology: then and now. *Clinical Biochemistry*, **2006**, 39, 498-510.

Luzhna, L.; Kathiria, P.; Kovalchuk, O. Micronuclei in genotoxicity assessment: from genetics to epigenetics and beyond. *Frontiers in Genetics*, **2013**, 4, 131.

Mahlo, S.M.; McGaw, L.J.; Eloff, J.N. Antifungal activity and cytotoxicity of isolated compounds from leaves of *Breonadia salicina*. *Journal of Ethnopharmacology*, **2013**, 148, 909-913.

Nasri, H.; Shirzad, H. Toxicity and safety of medicinal plants. *Journal of Herbal Medicine. Pharmacology*, **2013**, 2, 21-22.

Phillips, D.H.; Arlt, V.M. Genotoxicity: damage to DNA and its consequences. *Molecular, Clinical and Environmental Toxicology*, **2009**, 87-110.

Sibandze, G.F. Pharmacological properties of Swazi medicinal plants. MSc Thesis, University of the Witwatersrand, Johannesburg, South Africa, **2009**.

Stander, A.; Marais, S.; Stivaktas, V.; Vorster, V.; Albrecht, C.; Lottering, M.-L.; Joubert, A.M. *In vitro* effects of Sutherlandia frutescens water extracts on cell numbers, morphology, cell cycle progression and cell death in a tumorigenic and a non-tumorigenic epithelial breast cell line. *Journal of Ethnopharmacology*, **2009**, 124, 45–60.

Tolosa, L.; Donato, M.T.; Gómez-Lechón, M.J. General cytotoxicity assessment by means of the MTT assay. In Vinken **M**., Rogiers V. (eds), *Protocols in in vitro hepatocyte research*, Humana Press, New York, NY, **2015**, 333-348.

Zhang, M.; Aguilera, D.; Das, C.; Vasquez, H.; Zage, P.; Gopalakrishnan, V.; Wolff, J. Measuring cytotoxicity: a new perspective on LC_{50}. *Anticancer Research*, **2007**, 27, 35.

CHAPTER 10 CONCLUSIONS AND RECOMMENDATIONS

10.1. OVERVIEW

The main aim of this study was to investigate the phytochemistry and biological activities of *Breonadia salicina*. All the objectives indicated were achieved as follows:

10.1.1. Phytochemistry

The first objective was to explore the distribution of the chemical constituents in the various plant parts (leaf, stem and root). This was important because the stem and root are not sustainable for conservation purpose. The isolated compounds also served as standards for metabolomic studies and evaluation of the bioactive constituents. A total of eight compounds were isolated and four compounds (5-*O*-caffeoylquinic acid, sucrose, hexadecane and palmitic acid) were found in the leaf, while three compounds (kaempferol 3-*O*-(2"-*O*-galloyl)-glucuronide, lupeol and D-galactopyranose) were found in the stem and one compound (bodinioside Q) was found in the root. Metabolomic profiling of chemical constituents that could not be easily isolated was carried out using UPLC-QTOF-MS and ^{1}H-NMR. The chemical fingerprints further revealed that quinic acids (5-*O*-caffeoylquinic acid, 5-methyl caffeoylquinic acid, di-*O*-caffeoylquinic acid and quinic acid), monosaccharide (hexose$_2$), monoterpenoid (deacetyl asperuloside acid), flavonolignan (cinchonain I isomer) and flavonoid glycoside (rutin) were found in the leaf but not in the stem and root.

The second objective was to explore the effect of seasonal variation on the chemical profile of the plant parts. Fresh seasonal samples (autumn, winter, spring, and summer) were collected in the second year. The samples collected in the first-year spring were used for objective 1. Chemometrics analysis of the data obtained indicated that the chemistry of the stem and root are similar and different from the chemistry of the leaf. Seasonal variations were observed in each plant part in which autumn and winter samples were closely clustered, compared to the spring and summer in the methanol leaf plant parts. The markers identified by the VIP plot and heatmap indicated that di-*O*-caffeoylquinic acid and rutin were found in the leaf samples but not in the stem bark and root samples. Furthermore, quinic acid + hexose$_2$, oleoside 11-methylester, 4,8,4',8'-tetramethoxy-[1,1'-biphenanthrene]-2,7,2',7'-tetrol, pfaffic acid, ferulic

acid 4-*O*-glucuronide and ursolic acid were found in the stem bark and root samples, and but found in the leaf samples.

10.1.2. Biological activity

The third objective was to identify the bioactive antimalarial and antitrypanosomal constituents. Crude extracts, fractions and purified compounds were tested. The flavonoid kaempferol 3-*O*-(2"-*O*-galloyl)-glucuronide and fatty acid palmitic acid were the most active against *Plasmodium falciparum*, while kaempferol 3-*O*-(2"-*O*-galloyl)-glucuronide (**1**), lupeol (**2**), bodinioside Q (**4**), palmitic acid were most active against *Trypanosoma brucei brucei* parasites.

The fourth objective was to evaluate the effect of seasonal variation on the antimalarial and antitrypanosomal activity of the crude extracts. The dichloromethane leaf extracts in each season had the highest antimalarial activity. This was different from the activity recorded in the spring of the first year in which the stem displayed the highest antimalarial activity. Furthermore, the results obtained in this study show that the dichloromethane extracts of leaves collected in each season of the second year had the highest antimalarial activities, compared to the methanol leaf extracts. However, the dichloromethane extracts of leaves collected in the first year did not produce significant antimalarial activity. This was due to the fact that 5-methyl caffeoylquinic acid and quinic acid were only present in the dichloromethane extracts of leaves collected in the first year; and were not present in the dichloromethane extracts of leaves collected in the second year. Furthermore, deacetyl asperuloside acid, di-*O*-caffeoylquinic acid, trihydroxy-octadecadienoic acid, 15-hydroxyhexadecanoic acid, 3-α,24*R*,25-trihydroxytirucall-8-en-21-oic acid and sibiricose A6 were only found in the dichloromethane extracts of leaves collected in the second year but not found in the dichloromethane extracts of leaves collected in the first year. Therefore, these metabolites might have been responsible for the strong antimalarial activities of the dichloromethane leaf extracts of *Breonadia salicina* samples collected in each season of the second year. The chemical profiles of extracts from both years were evaluated to resolve the discrepancy. Moreover, the methanol and dichloromethane extracts of leaves collected in autumn, winter, spring and summer displayed the highest antitrypanosomal activity, except for the methanol leaf extracts in winter. The results obtained in the first year spring were not different from the results obtained in the second year spring, in which the methanol and dichloromethane leaf extracts displayed the highest

antitrypanosomal activity. The chemical profiles revealed that quinic acid + hexose$_2$, 3,4-dihydroxycinnamoylquinic acid, 5-caffeoylquinic acid, deacetyl asperuloside acid and di-*O*-caffeoylquinic acid were found in the methanol and dichloromethane extracts of leaves collected in Spring of the first and second year. Therefore, we can conclude that continuous variations could occur with variations in distribution of metabolites in plant parts.

The fifth objective was to determine which of the chemical constituents were likely responsible for the antioxidant, anti-diabetic, and anti-inflammatory activities of the different plant parts. Since an extensive metabolomic evaluation was carried out earlier, it was easy to determine the class of compound responsible for biological activity. The findings in this work comprehensively show that polyphenols, flavonoids, hydroxycinnamic acids and monosaccharides contribute to the antioxidant activities of the crude stem bark and root extracts against DPPH (2,2-diphenyl-1-picrylhydrazyl) free radical scavenging and reducing power. Furthermore, polyphenols, triterpenoids, hydrolysable tannins, hydroxycinnamic acids, flavonoids and quinic acids were responsible for the anti-diabetic activities of the crude stem bark and root extracts against α-glucosidase and α-amylase enzymes; and quinic acids, monoterpenoids, flavonoid glycosides and flavonolignans contribute to the anti-inflammatory activities of the dichloromethane leaf extracts against RAW 264.7 macrophages.

The sixth objective was to evaluate the antimycobacterial activities of the crude extracts and fractions against *Mycobacterium tuberculosis* (H37RvMA strain). None of the crude extracts and fractions exhibited antimycobacterial activity.

10.1.3. Toxicology

The final objective was to determine the *in vitro* anti-proliferation, cytotoxicity and genotoxicity of *Breonadia salicina* to ascertain and fully establish the safety of this plant. The crude stem bark, root and leaf extracts were not toxic at lower concentrations.

10.1.4. Contributions of the study

This is the first study to establish the distribution of the chemical constituents in different plant parts. It is also the first study to determine the effect of seasonal variation on the chemical profile of the plant parts collected in two different years. The results obtained in this study are

the first to determine the effect of seasonal variations on the antimalarial, antitrypanosomal activities. Furthermore, this study provides important information on which plant parts to collect for best antimalarial, antitrypanosomal, antioxidant, anti-diabetic, anti-inflammatory and anti-proliferation activities; and predicts the chemical constituents responsible for the biological activities of different plant parts evaluated using a metabolomics approach. The results of this study may help researchers involved in exploring *Breonadia salicina* for the isolation of valuable malaria, diabetes, anti-inflammatory and antiprotozoal, chemicals. This is also the first study provide evidence on which part of the plant can be a potential source for the isolation of safe and effective compounds for the treatment of various diseases.

10.2. RECOMMENDATIONS

- Three compound classes were identified in this study from different parts of the plant collected in autumn, winter, spring and summer. Further studies are required that include a greater range of populations, including samples from different locations in Vhembe region in Limpopo Province or spread throughout South Africa. This would allow a comprehensive comparison to be made of the chemical variation within the stem bark, roots and leaves of *B. salicina.*
- Ethnomedicinal and pharmacological studies have indicated that the leaves have antimicrobial activities. Further studies should explore how antimicrobial activities are related or connected to the presence and concentrations of the various metabolites.
- It is important to evaluate the *in vitro* and *in vivo* potential antimycobacterial activity of different plant parts of *B. salicina* using different types of TB drugs and strains at various concentrations.
- Finally, these results indicate that different parts of *B. salicina* are capable or incapable of producing cytotoxic effects against various panels of cells using different in vitro methods. Therefore, all the tested samples should be investigated, using an *in vivo* model, to evaluate the toxicity of the metabolites.

Appendix

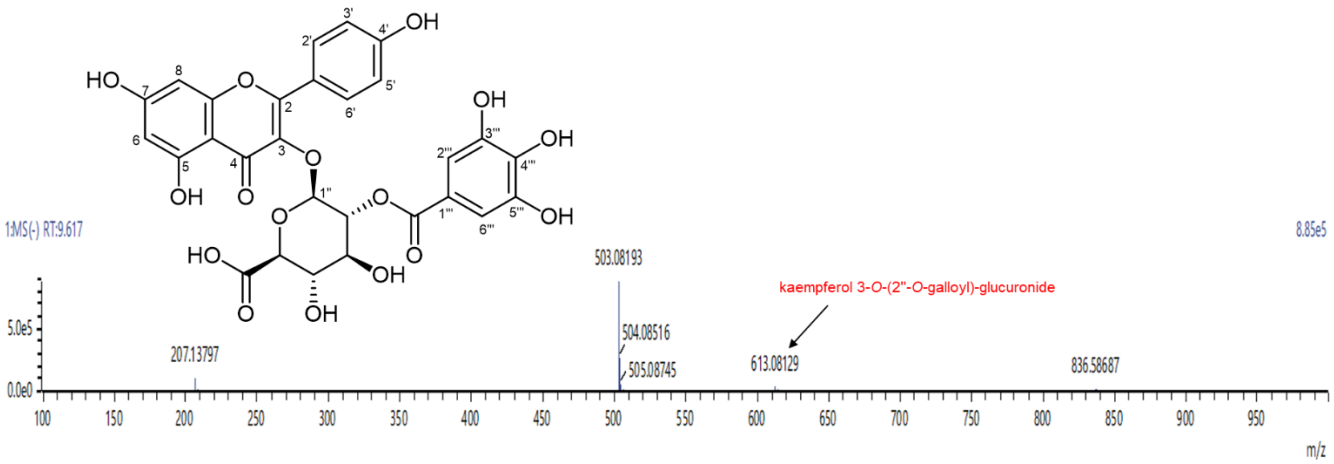

Appendix 1: MS of kaempferol 3-*O*-(2"-*O*-galloyl)-glucuronide (**1**).

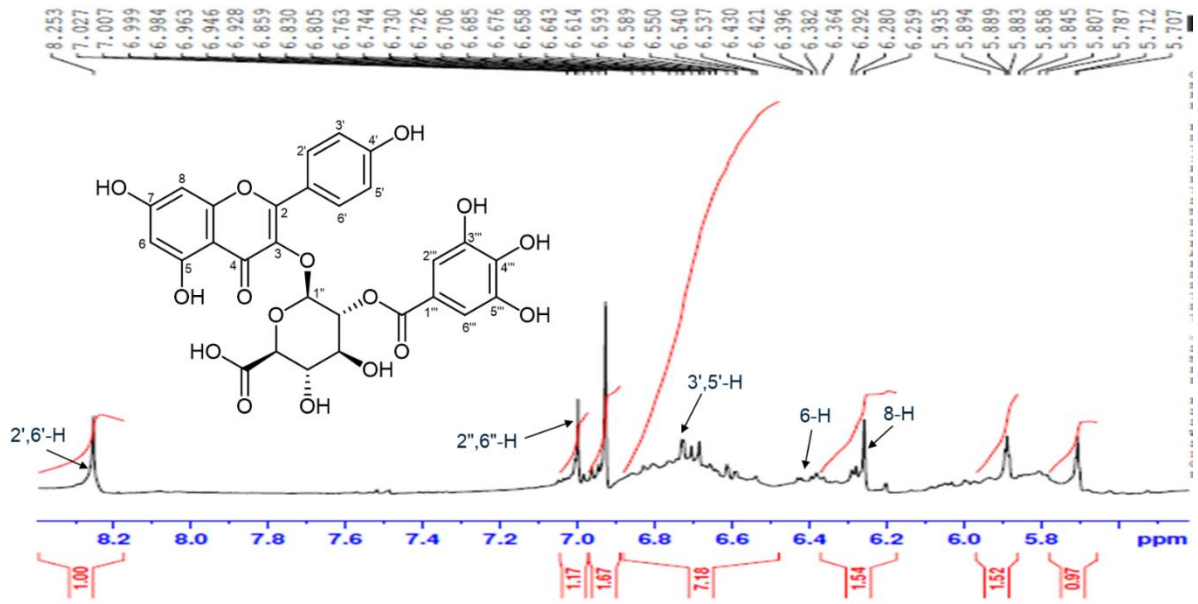

Appendix 2A: ^{1}H-NMR spectrum expansion of kaempferol 3-*O*-(2"-*O*-galloyl)-glucuronide (**1**).

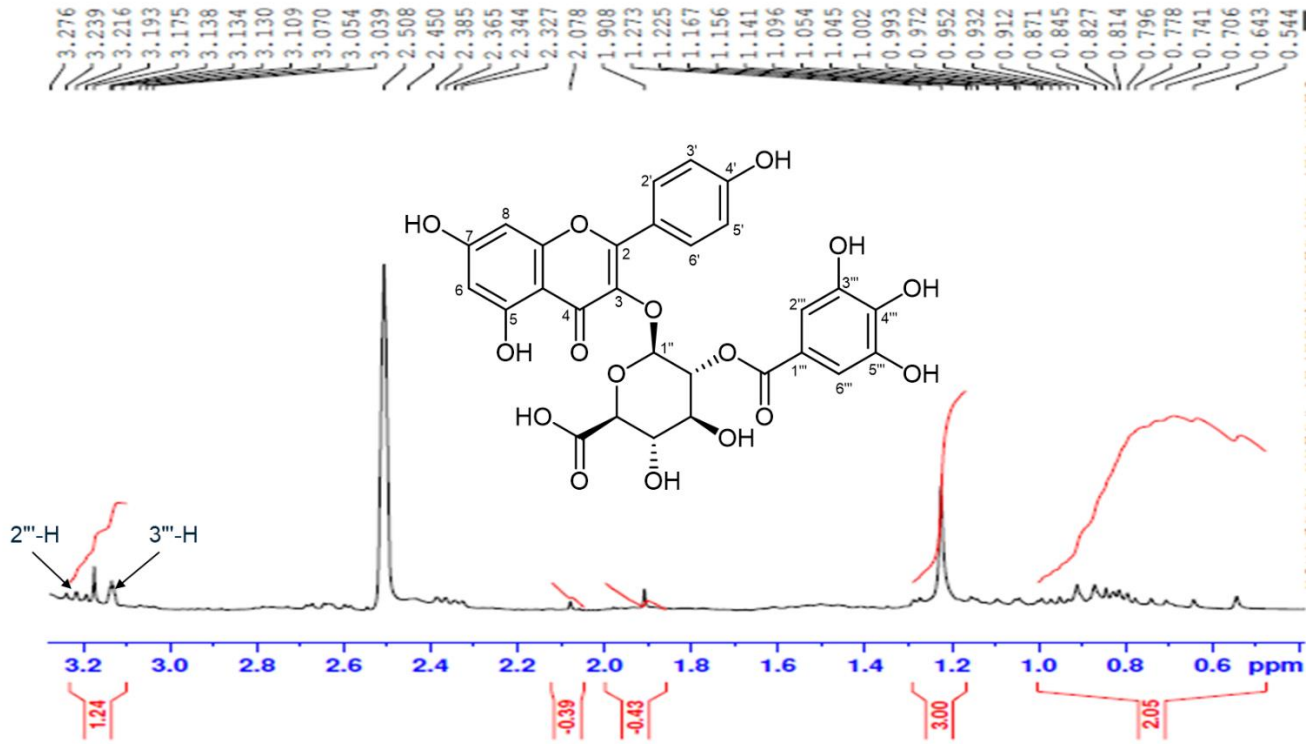

Appendix 2B: [1]H-NMR spectrum expansion of kaempferol 3-*O*-(2"-*O*-galloyl)-glucuronide (**1**).

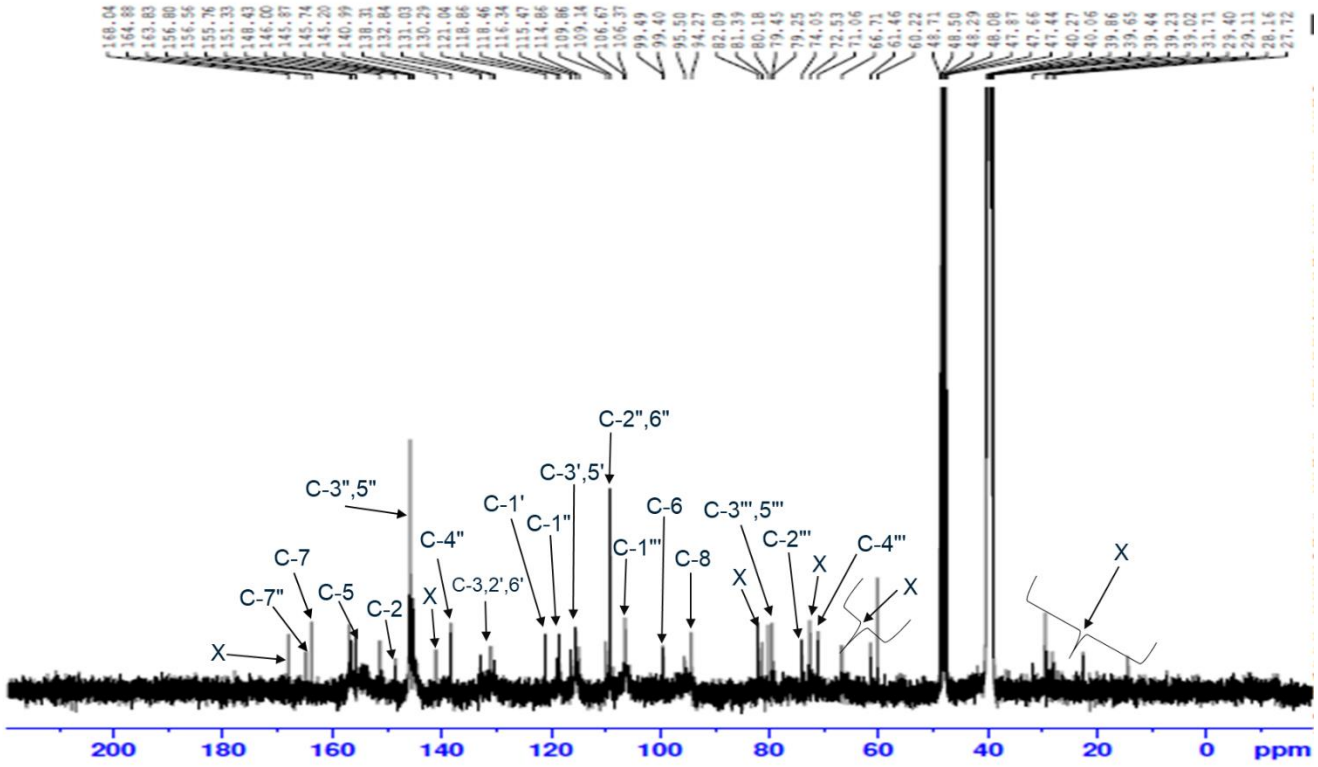

Appendix 3: [13]C-NMR spectrum of kaempferol 3-*O*-(2"-*O*-galloyl)-glucuronide (**1**).

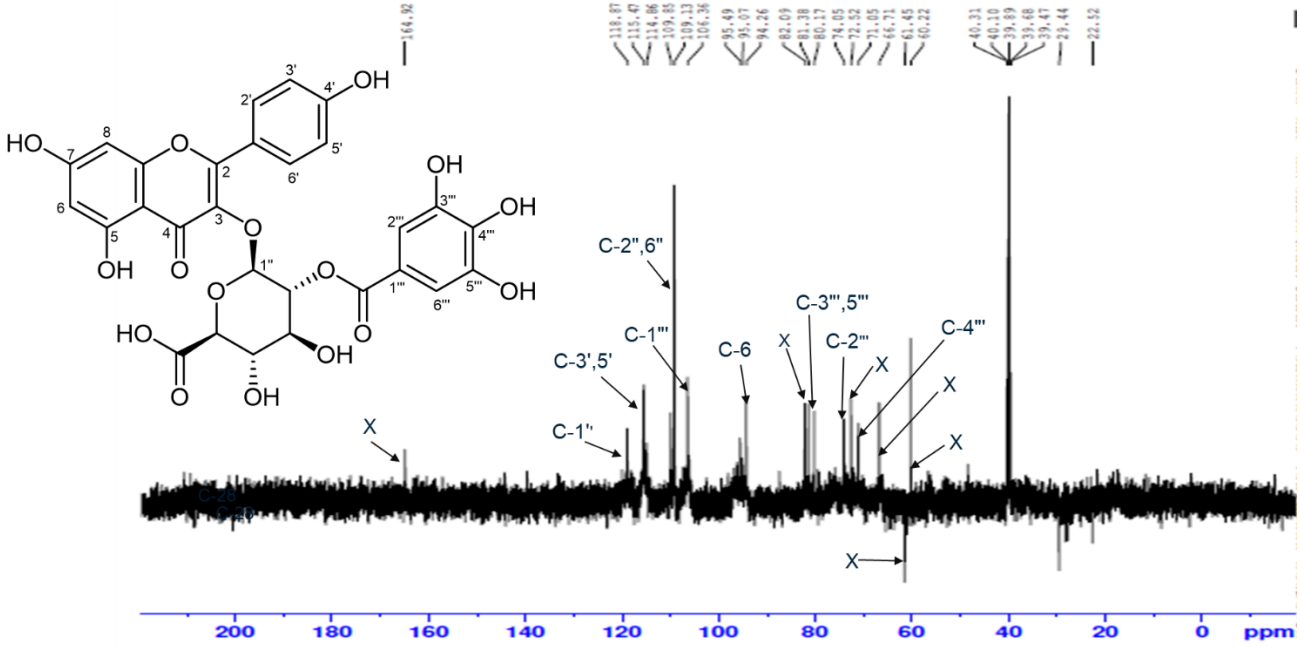

Appendix 4: DEPT 135 spectrum of kaempferol 3-*O*-(2"-*O*-galloyl)-glucuronide (**1**).

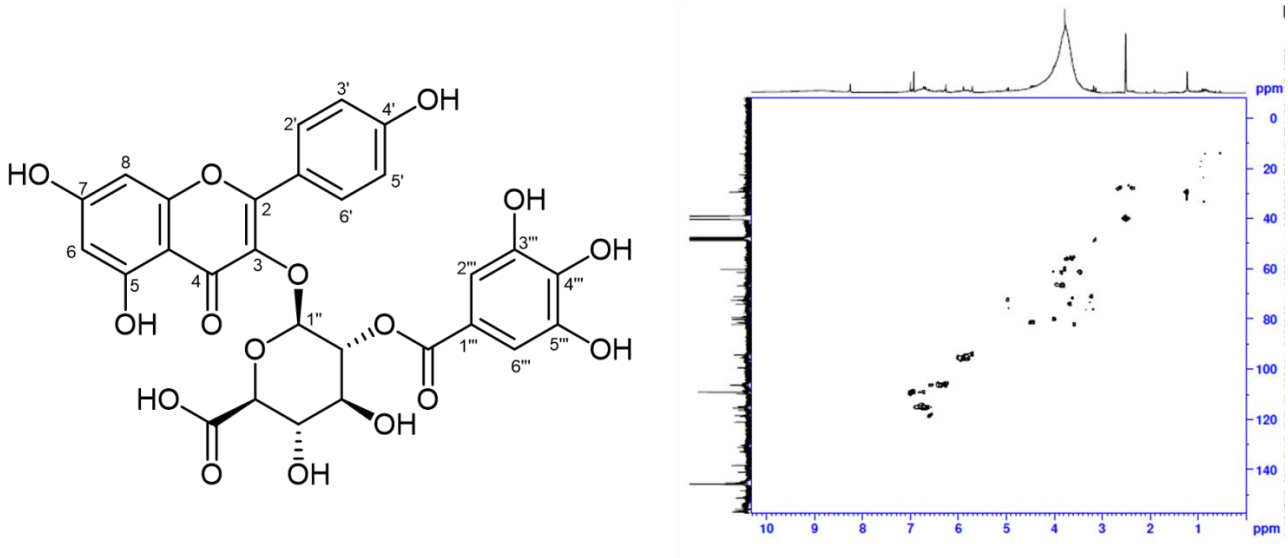

Appendix 5: HSQC spectrum of kaempferol 3-*O*-(2"-*O*-galloyl)-glucuronide (**1**).

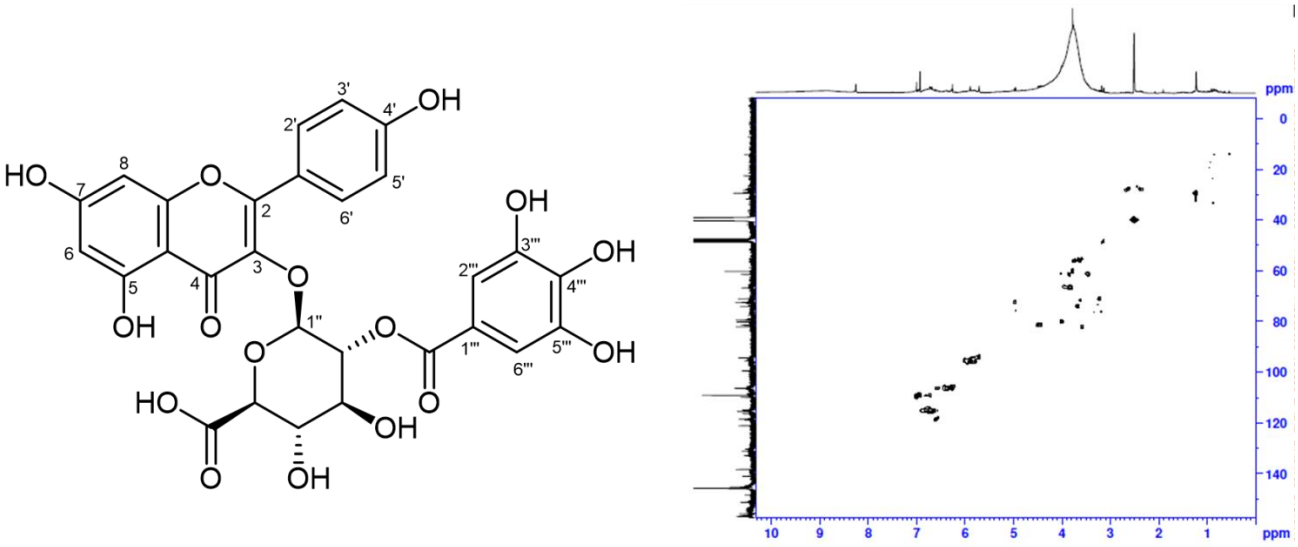

Appendix 6: HMBC spectrum of kaempferol 3-*O*-(2"-*O*-galloyl)-glucuronide (**1**).

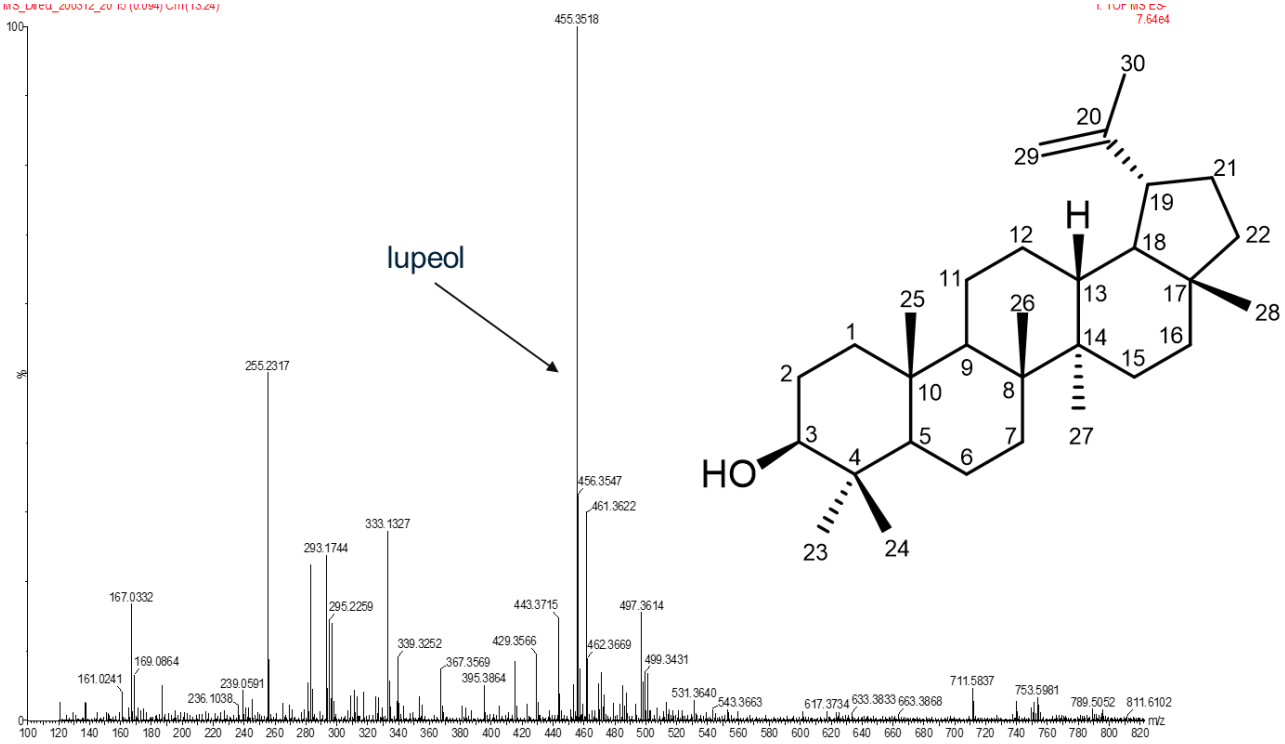

Appendix 7: MS of lupeol (**2**).

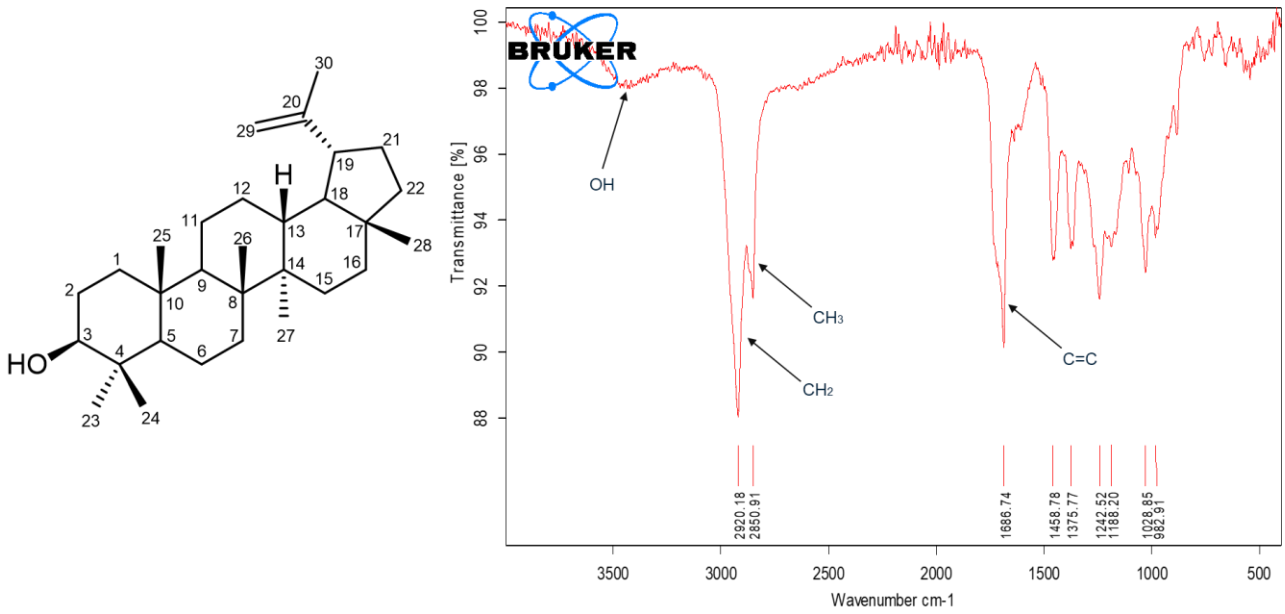

Appendix 8: FTIR spectrum of lupeol (**2**).

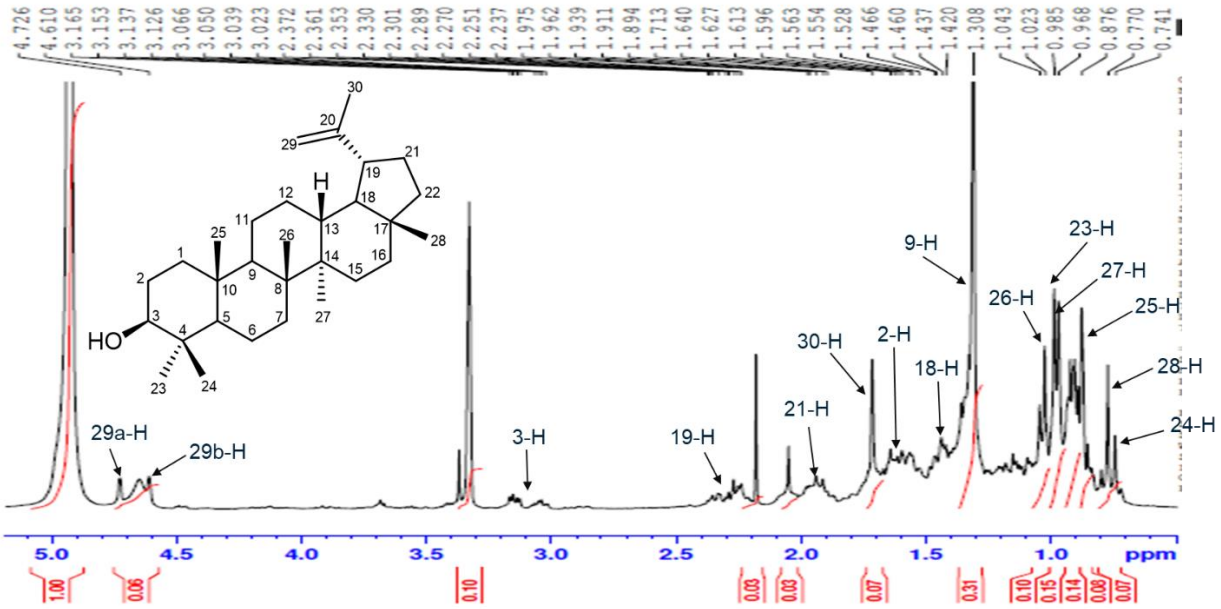

Appendix 9: ^{1}H-NMR spectrum expansion of lupeol (**2**).

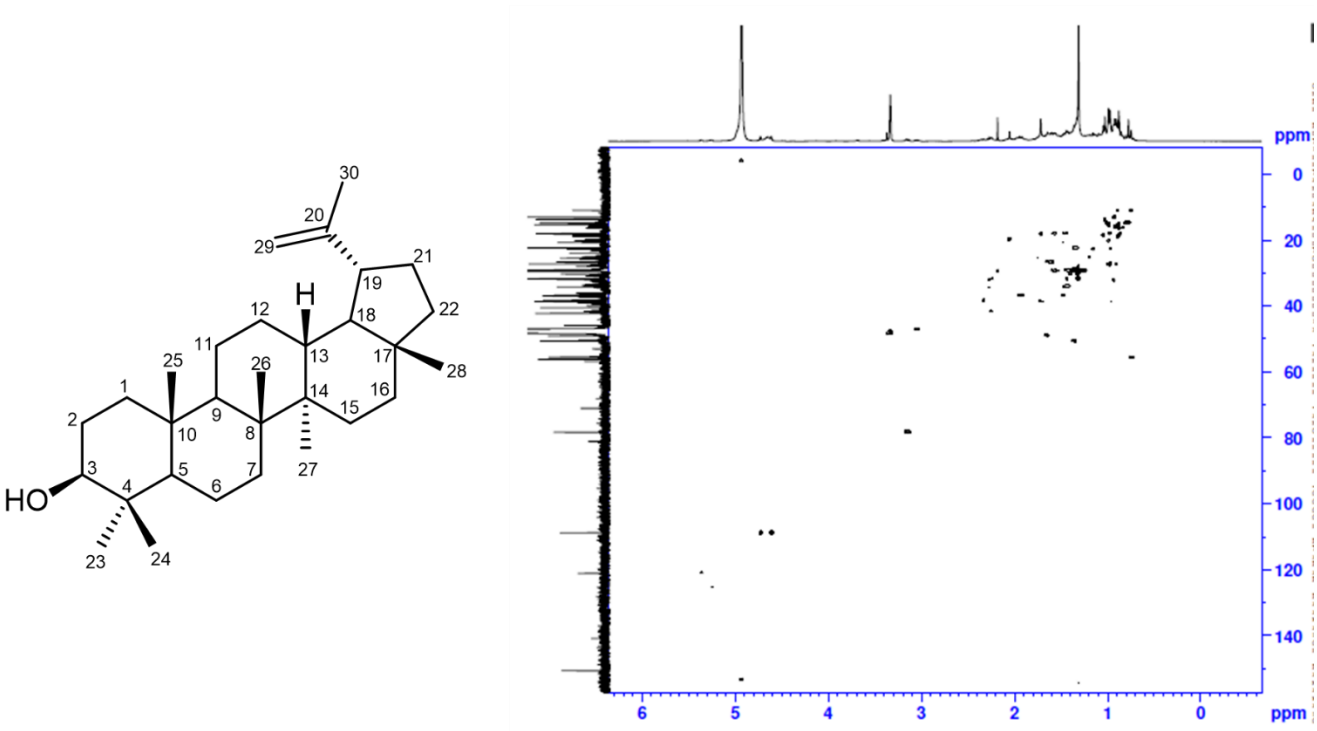

Appendix 10: HSQC spectrum of lupeol (**2**).

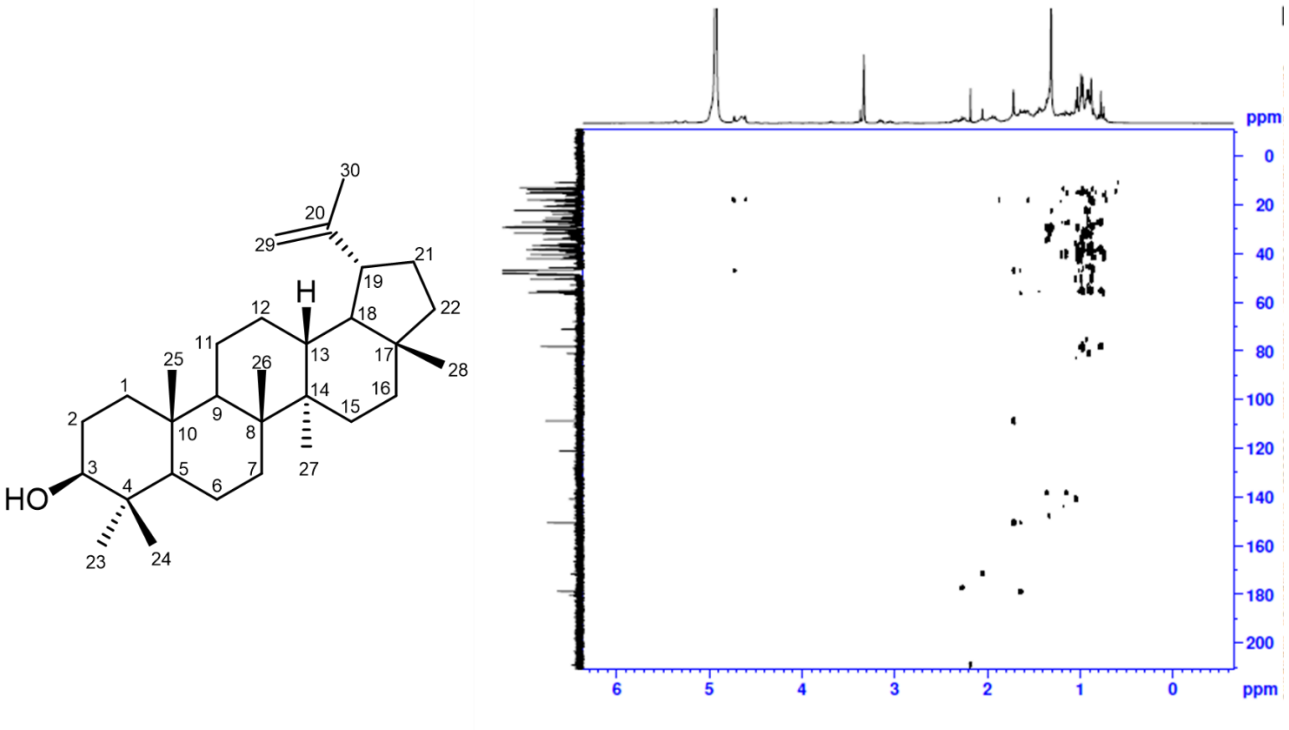

Appendix 11: HMBC spectrum of lupeol (**2**).

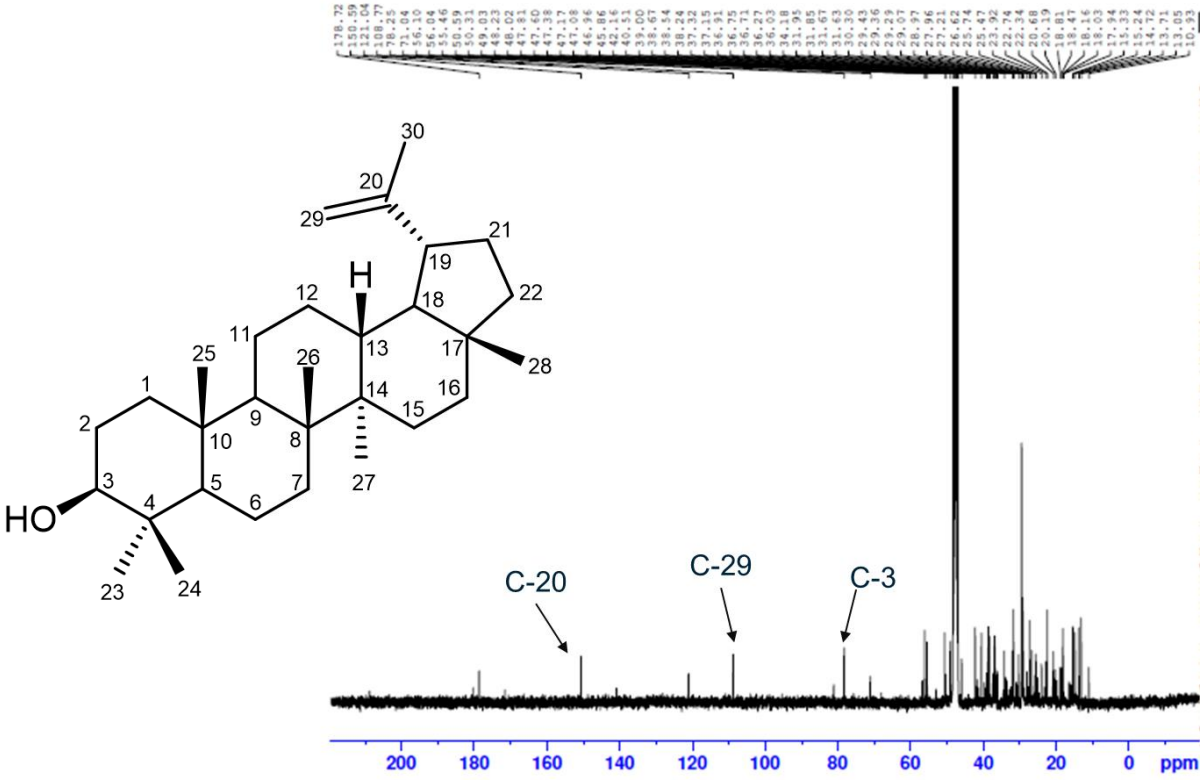

Appendix 12A: ^{13}C-NMR spectrum of lupeol (**2**).

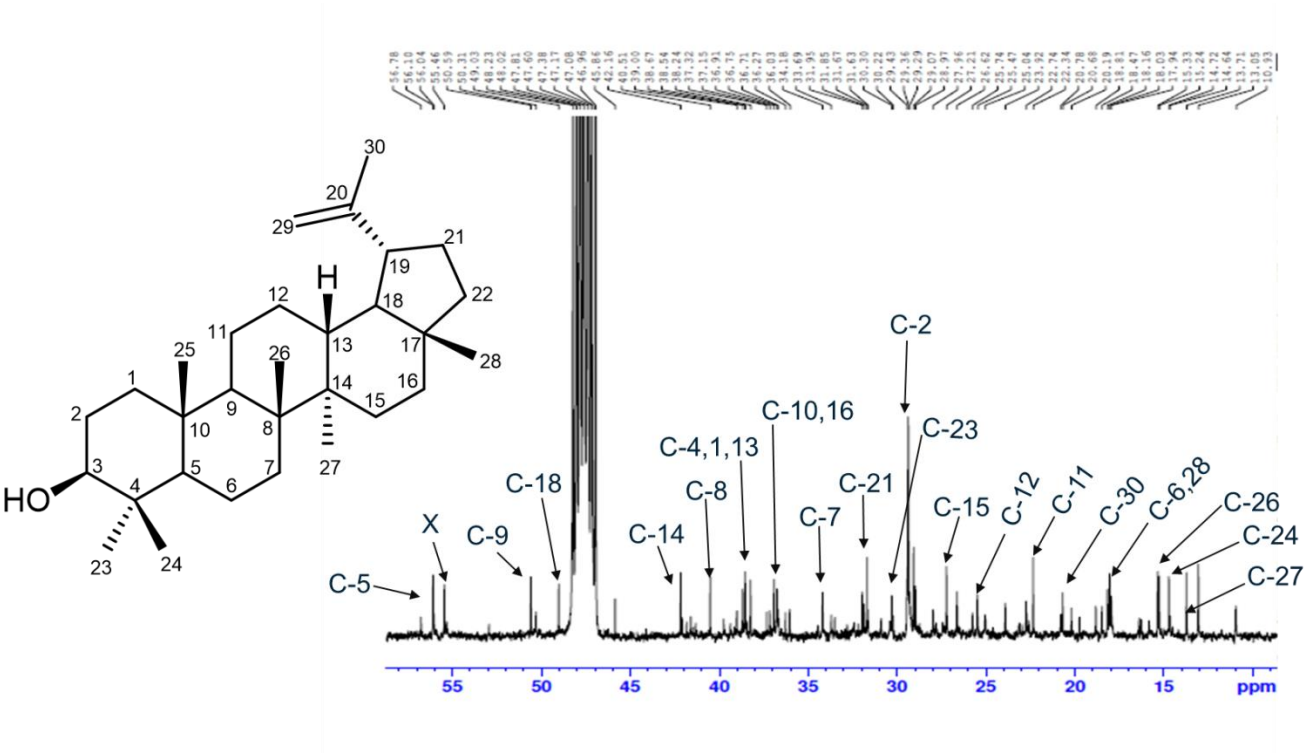

Appendix 12B: ^{13}C-NMR spectrum of lupeol (**2**).

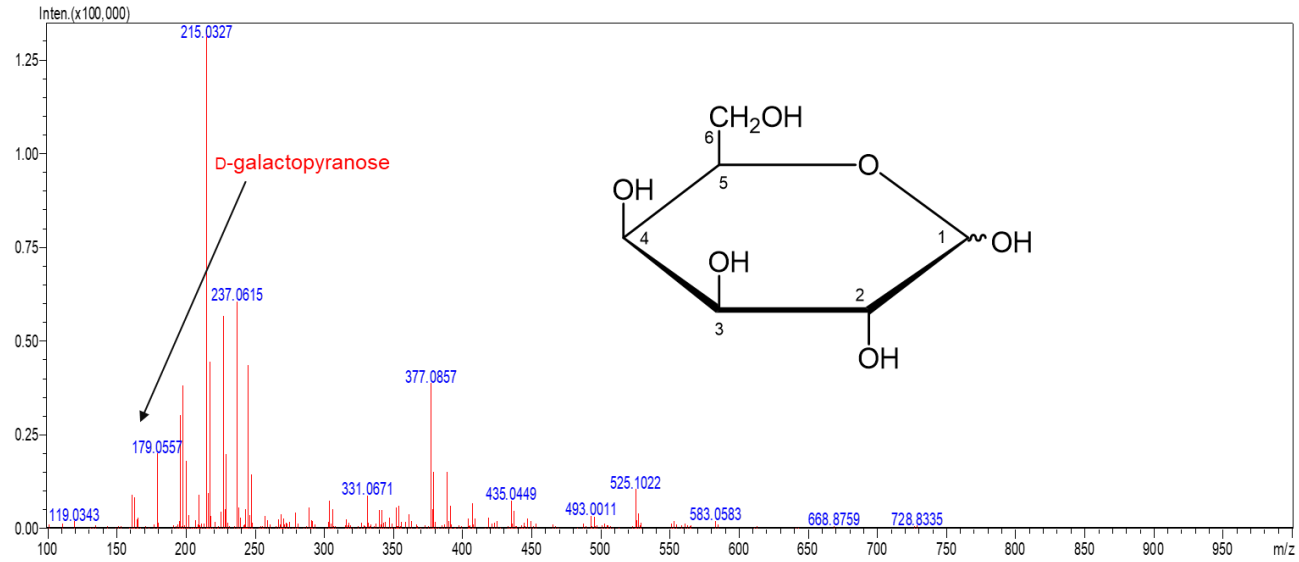

Appendix 13: MS of D-galactopyranose (**3**).

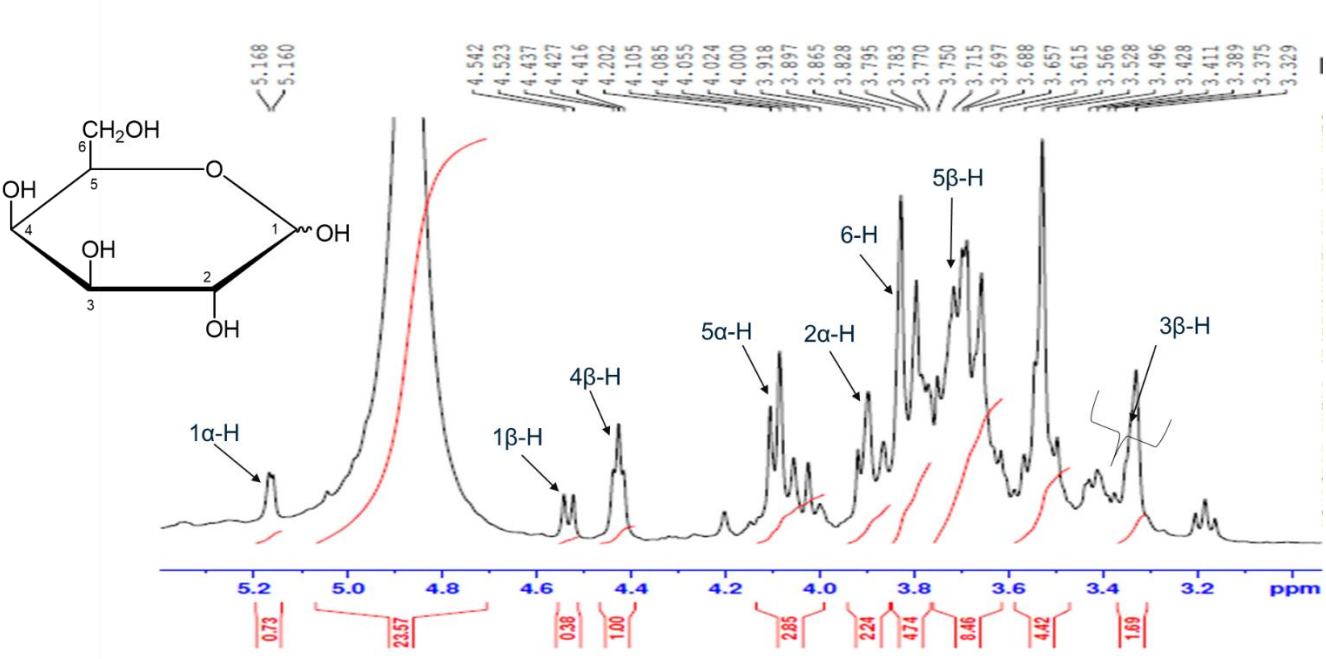

Appendix 14: ^{1}H-NMR spectrum expansion of D-galactopyranose (**3**).

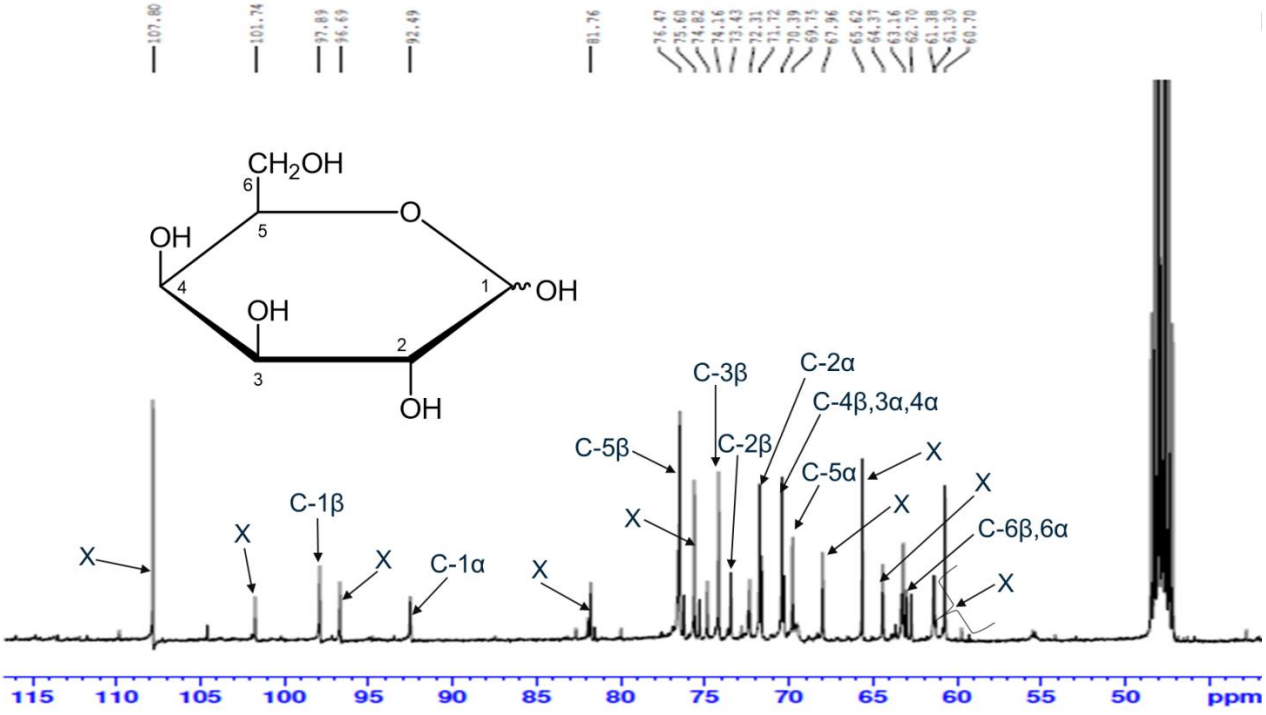

Appendix 15: ^{13}C-NMR spectrum of D-galactopyranose (**3**).

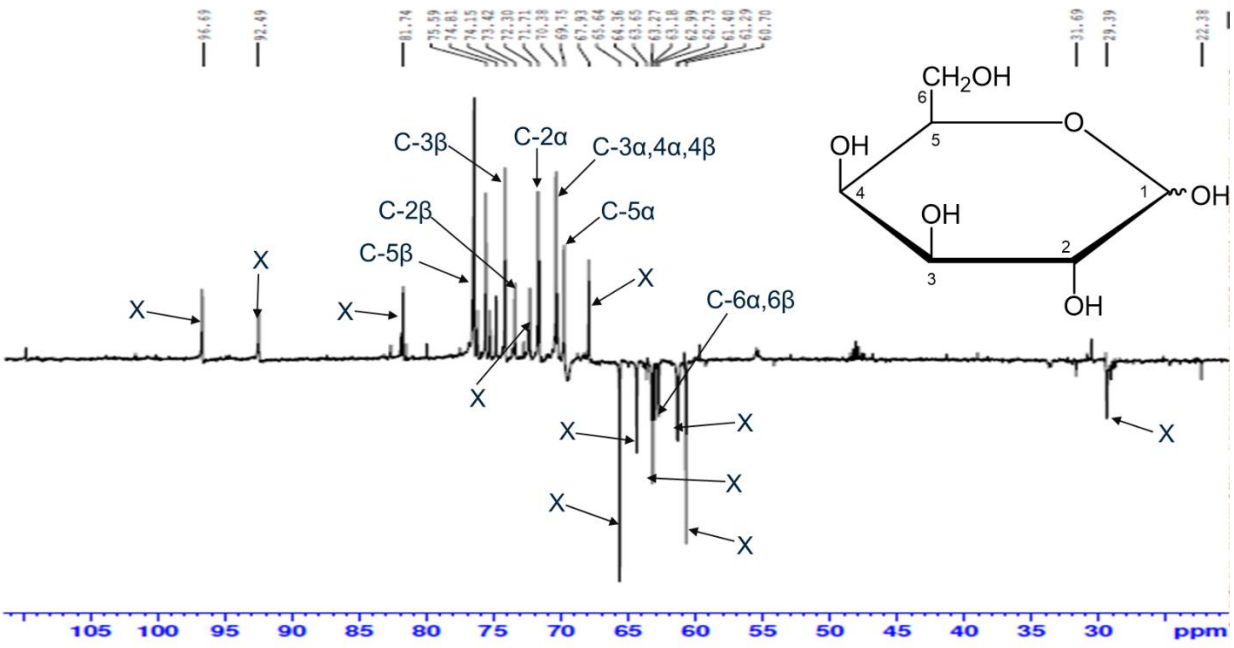

Appendix 16: DEPT 135 spectrum of D-galactopyranose (**3**).

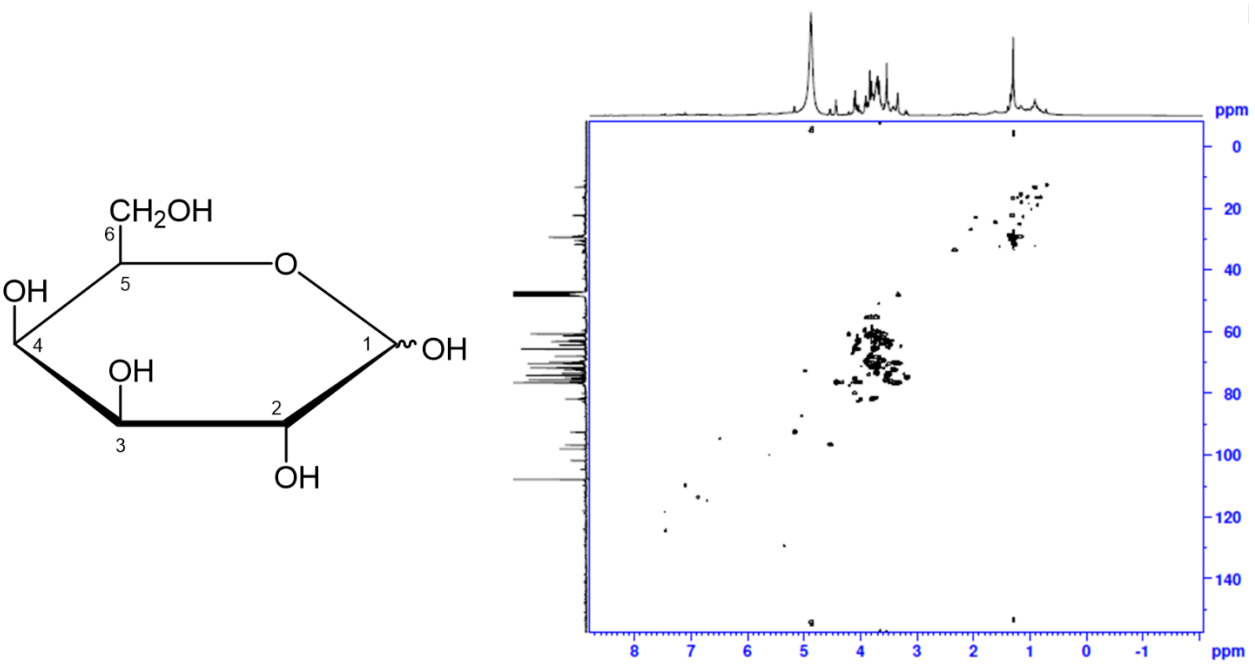

Appendix 17: HSQC spectrum of D-galactopyranose (**3**).

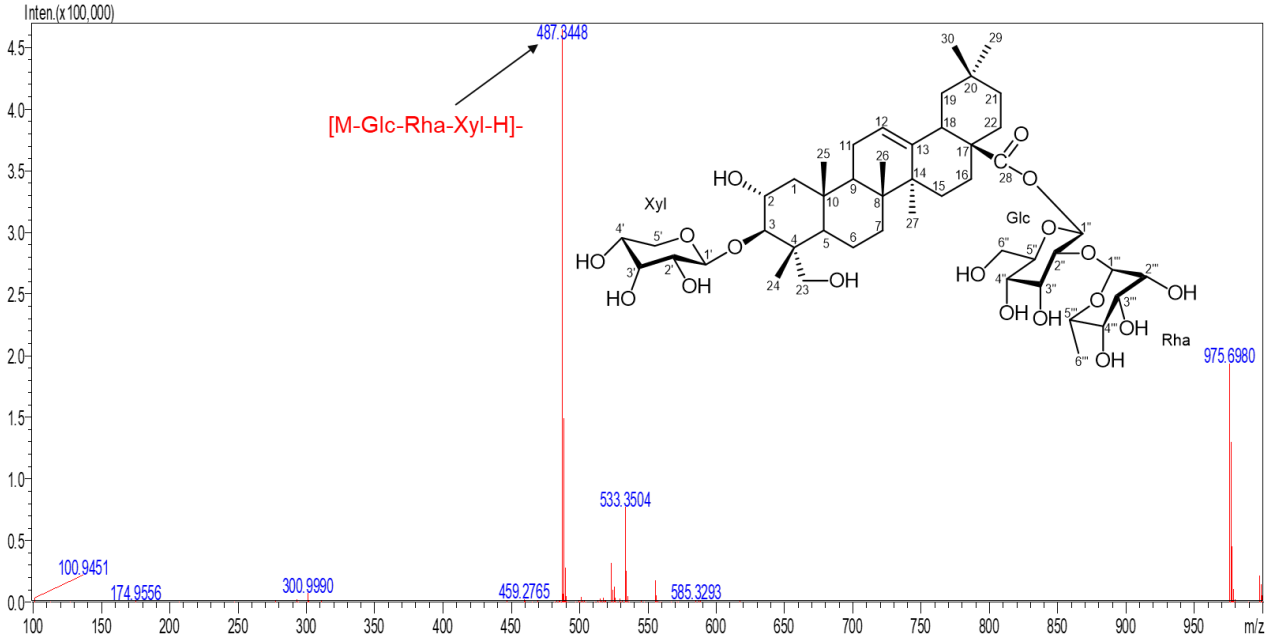

Appendix 18: MS of bodinioside Q (**4**).

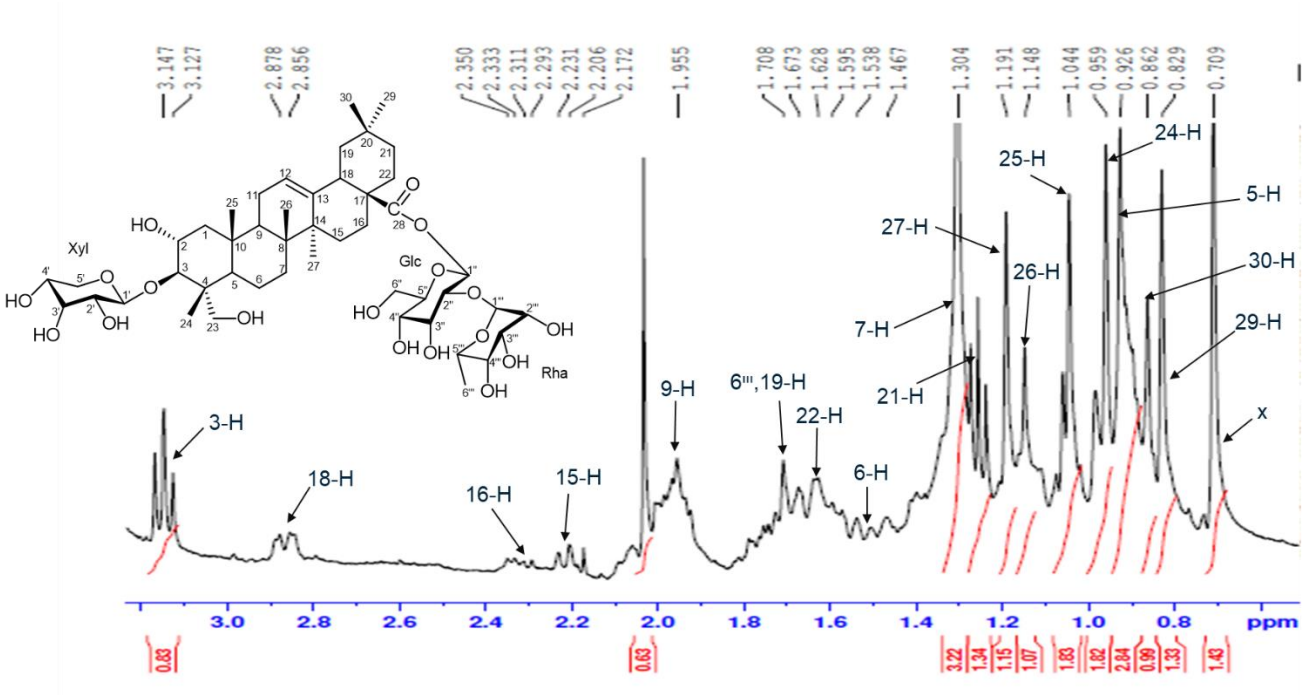

Appendix 19A: ^{1}H-NMR spectrum expansion of bodinioside Q (**4**).

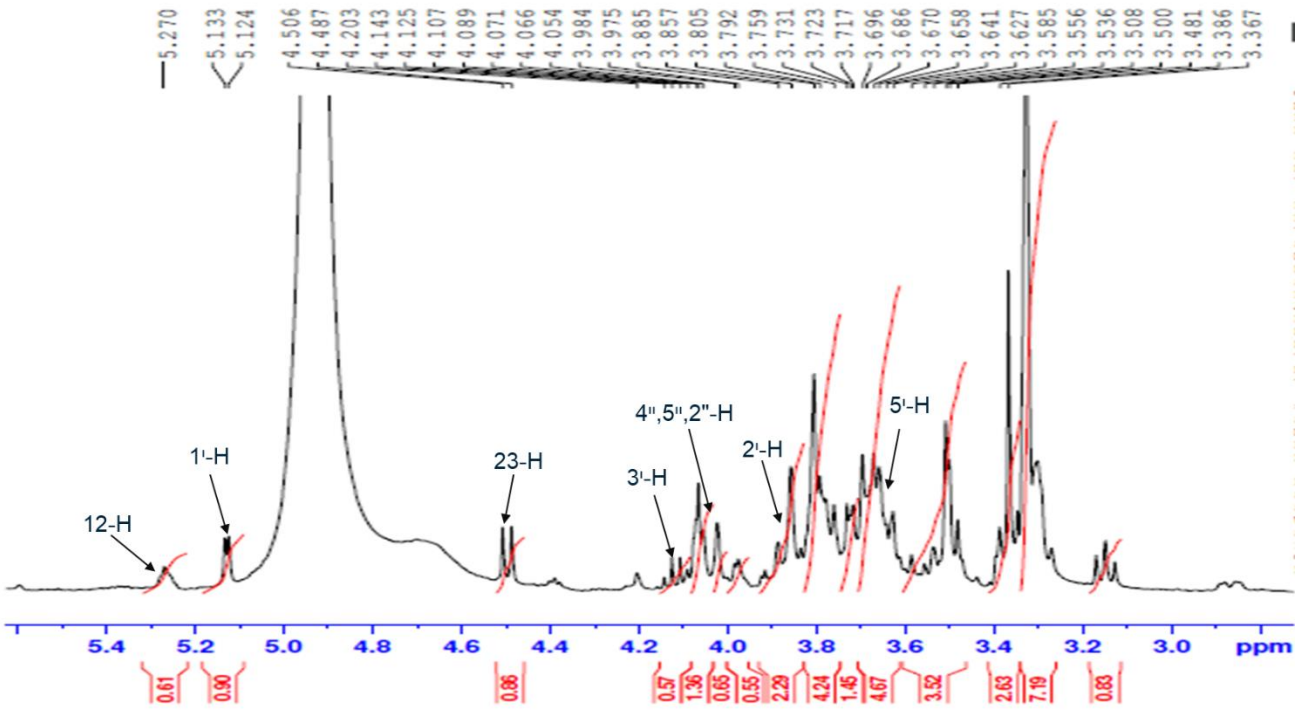

Appendix 19B: ^{1}H-NMR spectrum expansion of bodinioside Q (**4**).

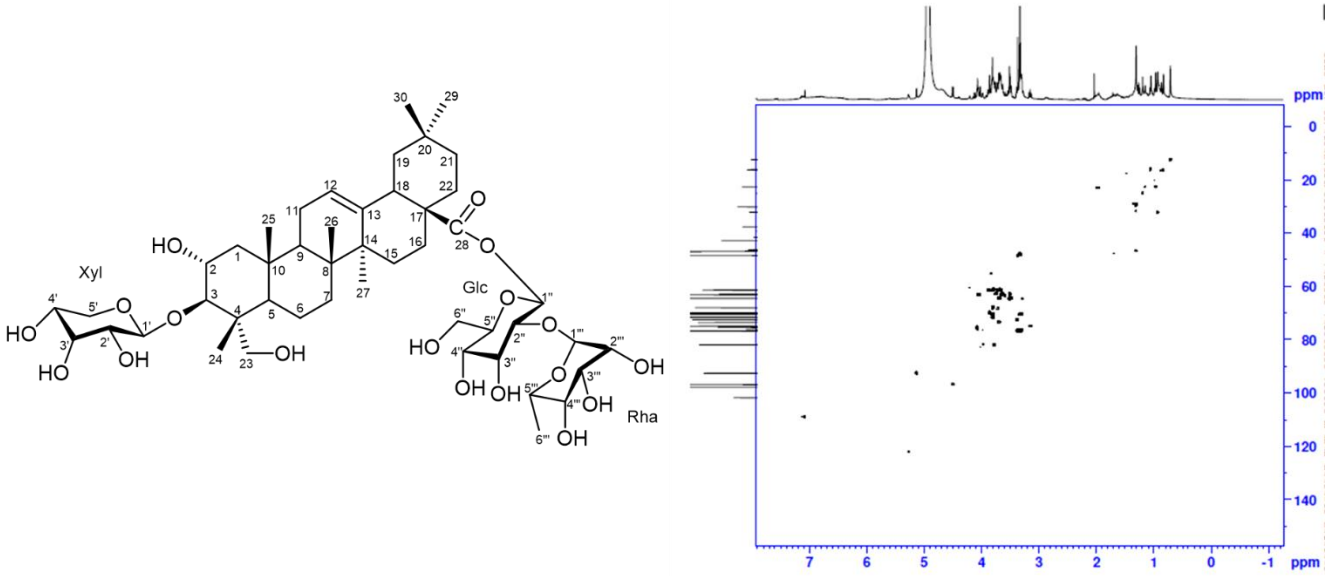

Appendix 20: HSQC spectrum of bodinioside Q (**4**).

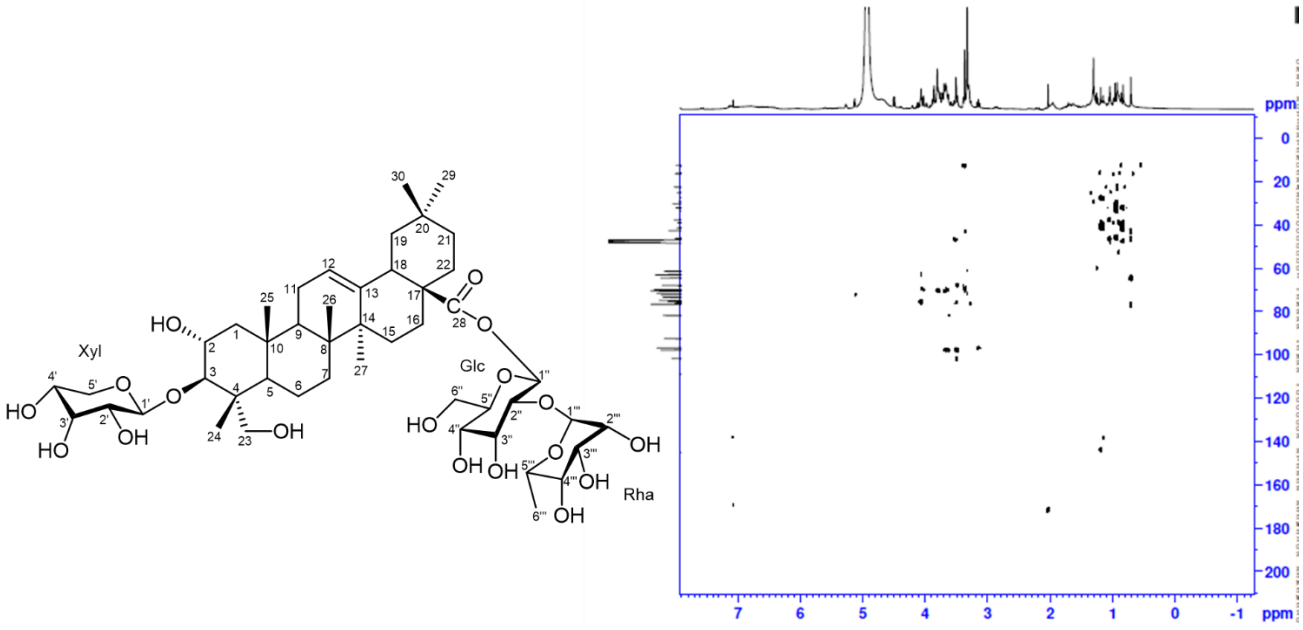

Appendix 21: HMBC spectrum of bodinioside Q (**4**).

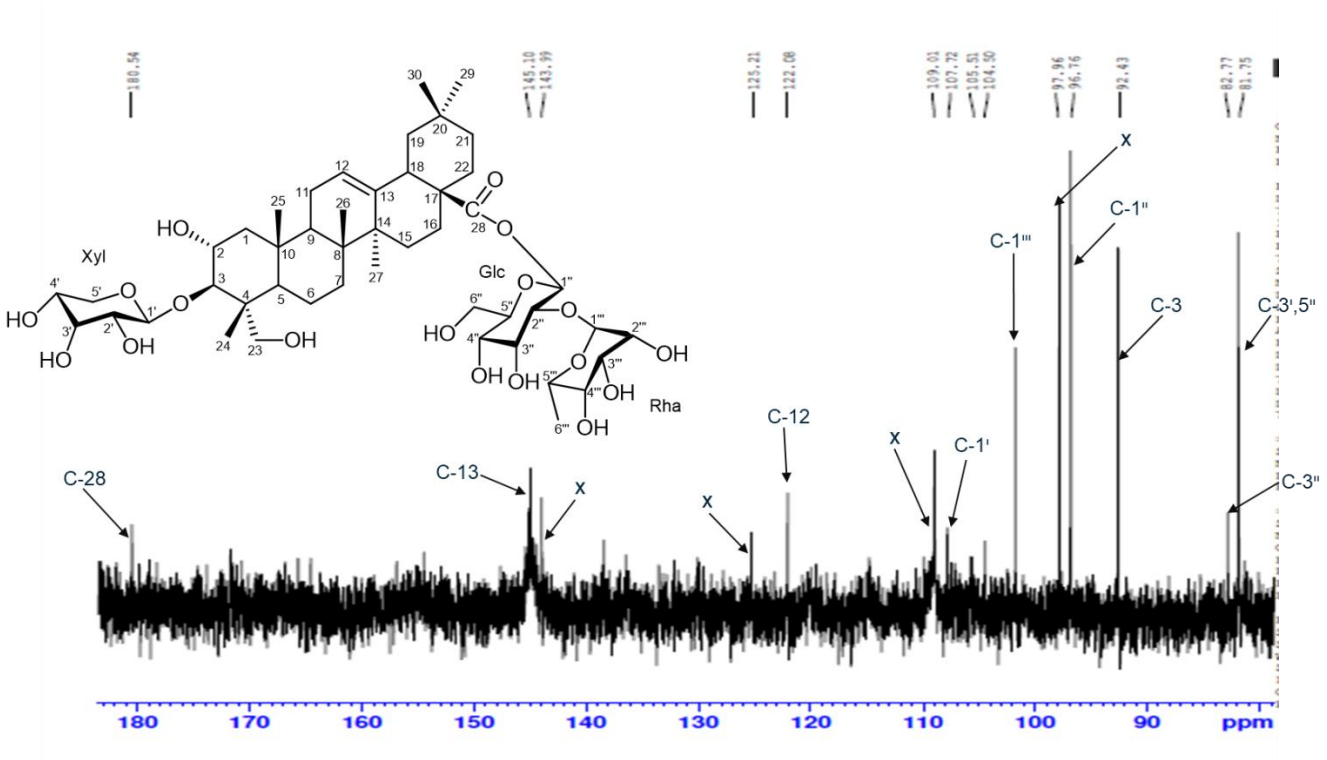

Appendix 22A: ^{13}C-NMR spectrum of bodinioside Q (**4**).

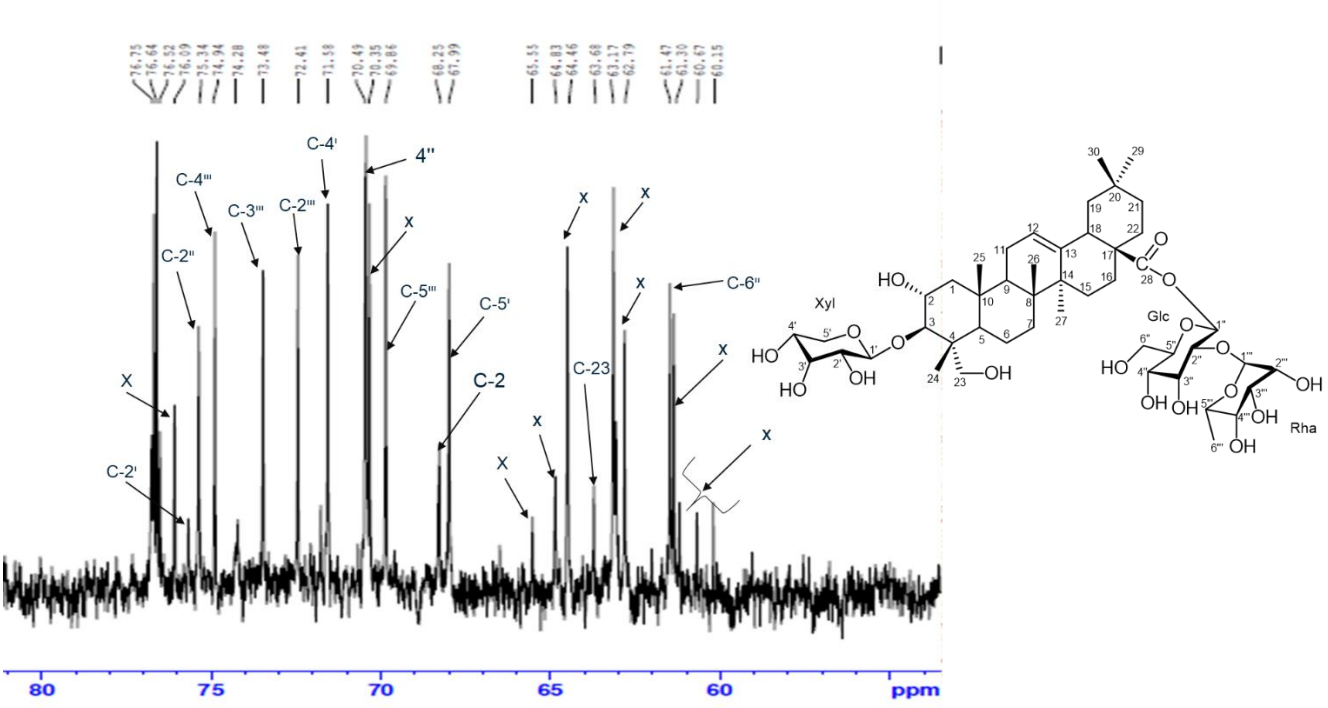

Appendix 22B: ^{13}C-NMR spectrum of bodinioside Q (**4**).

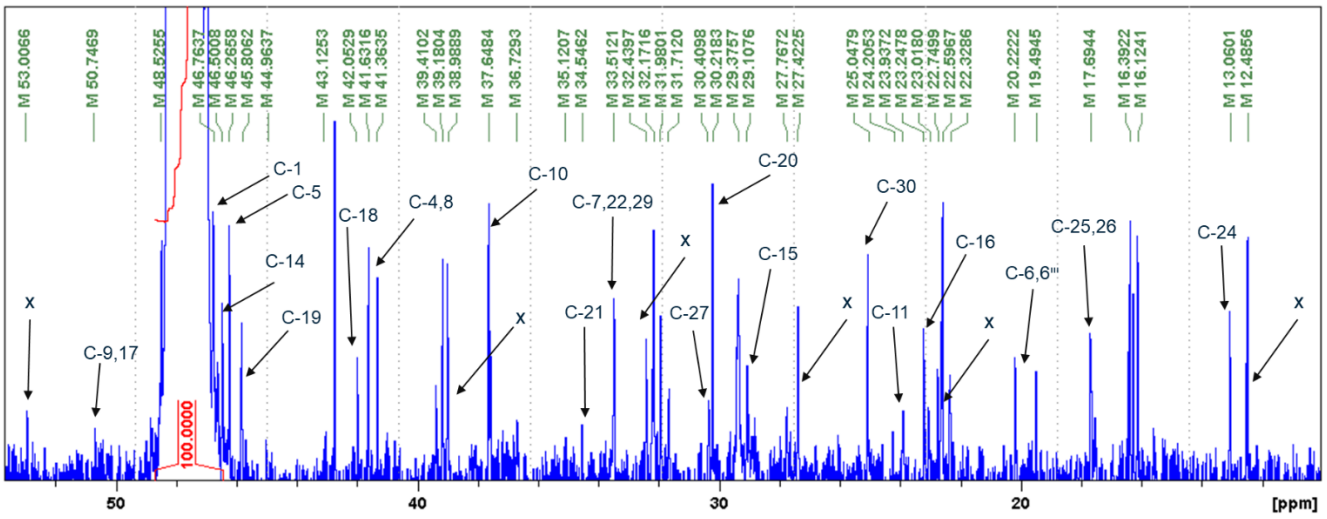

Appendix 22C: ^{13}C-NMR spectrum of bodinioside Q (**4**).

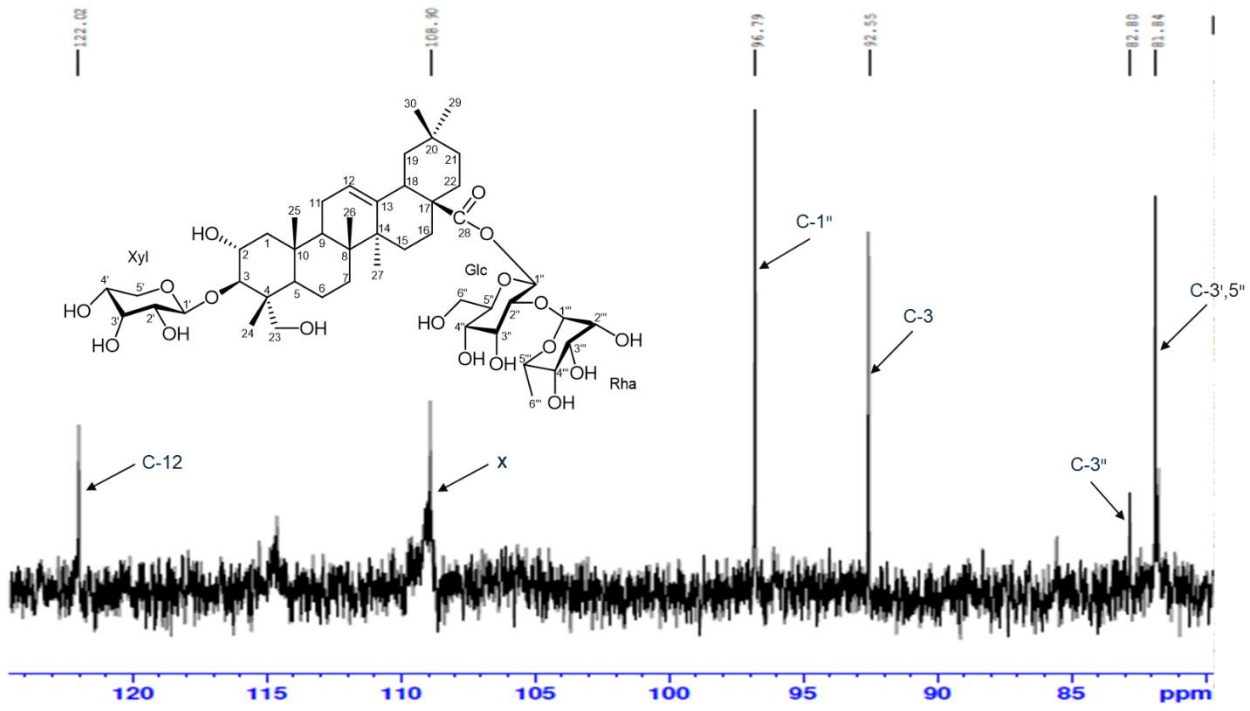

Appendix 23A: DEPT 135 spectrum of bodinioside Q (**4**).

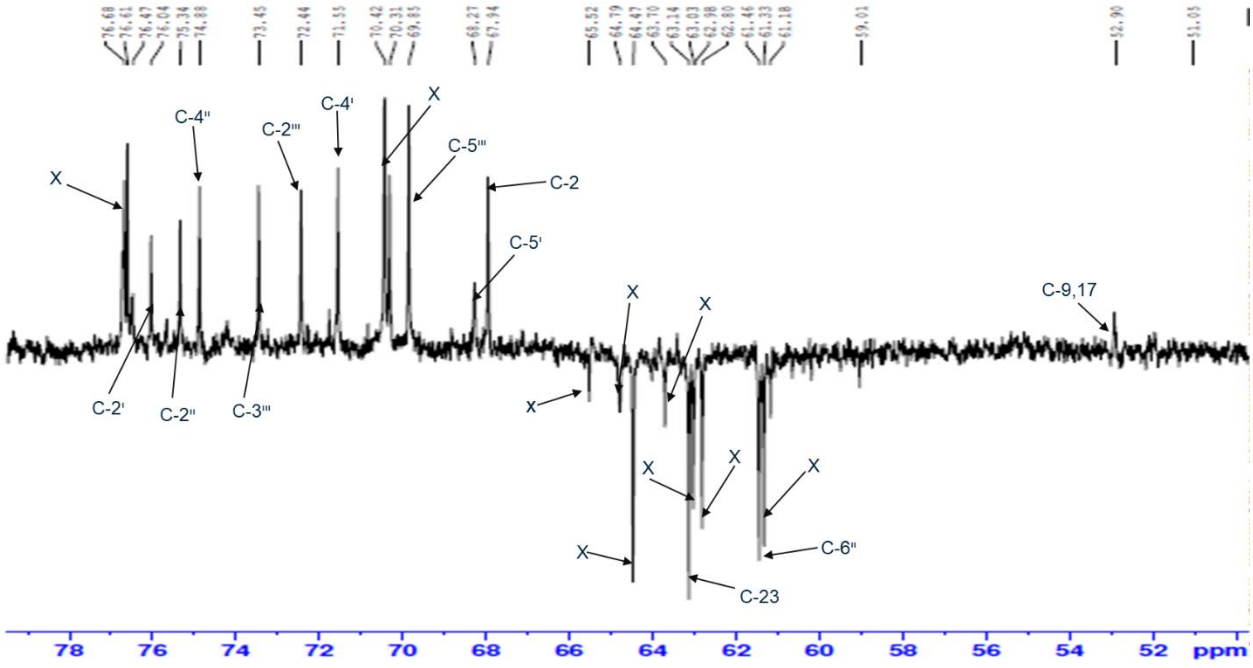

Appendix 23B: DEPT 135 spectrum of bodinioside Q (**4**).

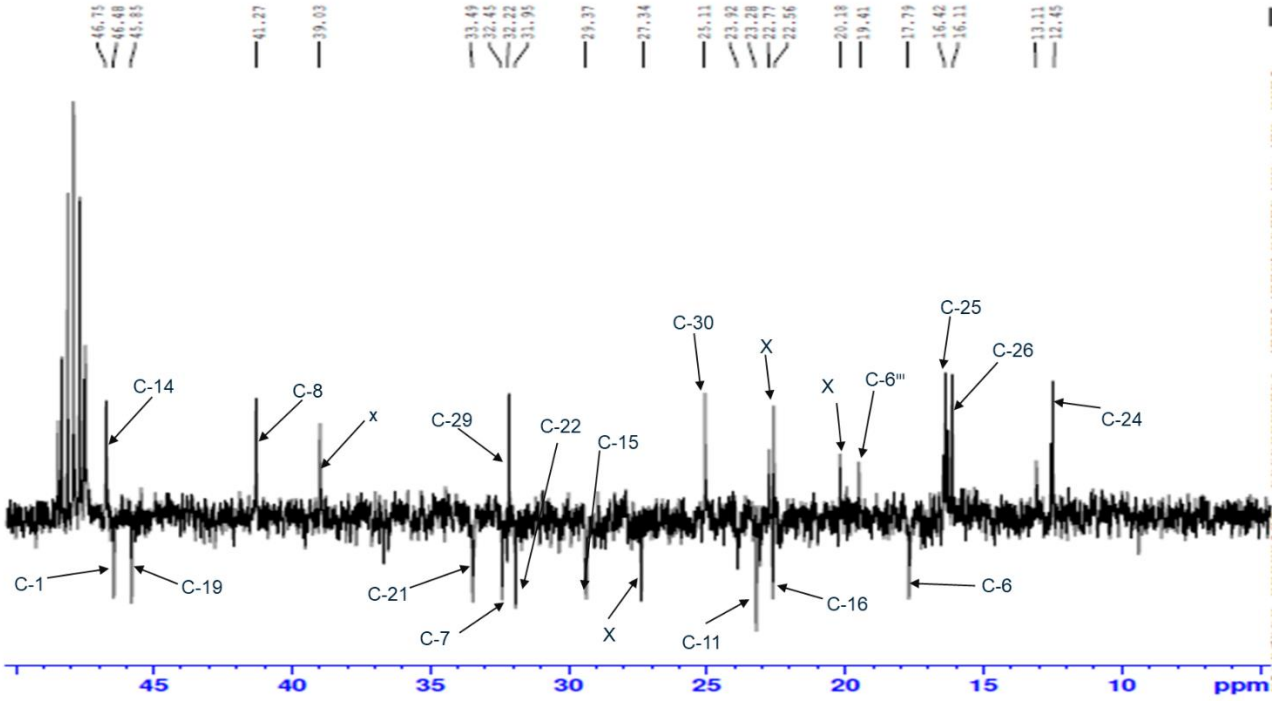

Appendix 23C: DEPT 135 spectrum of bodinioside Q (**4**).

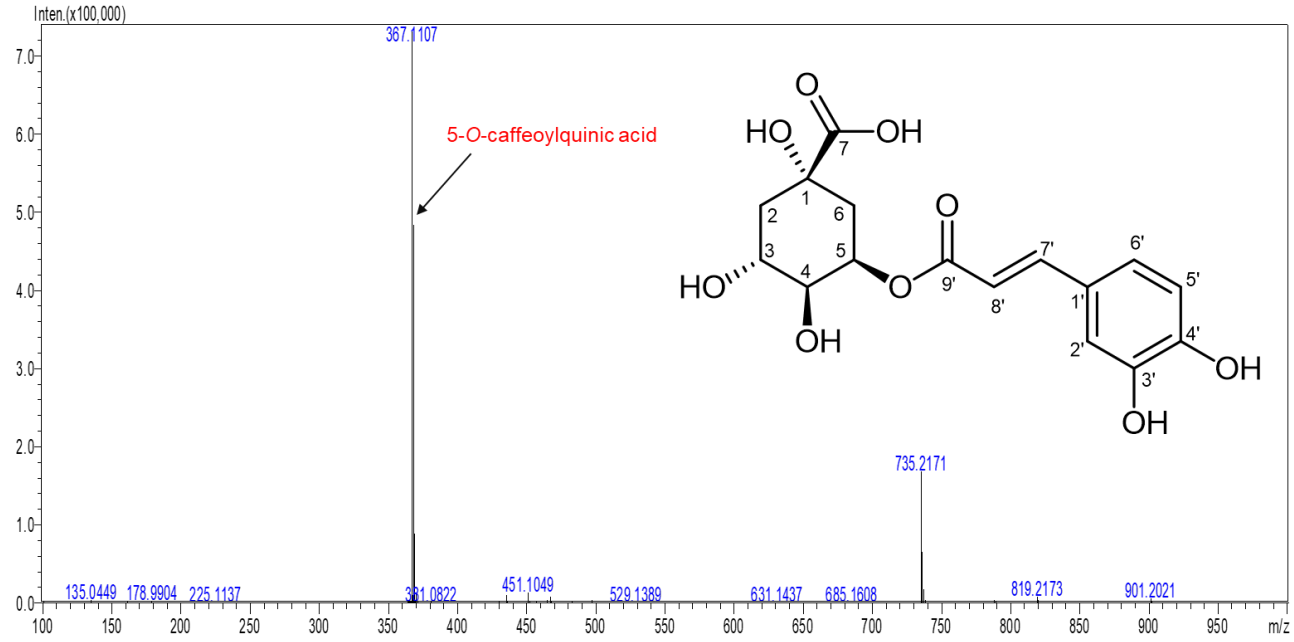

Appendix 24: MS of 5-*O*-caffeoylquinic acid (**5**).

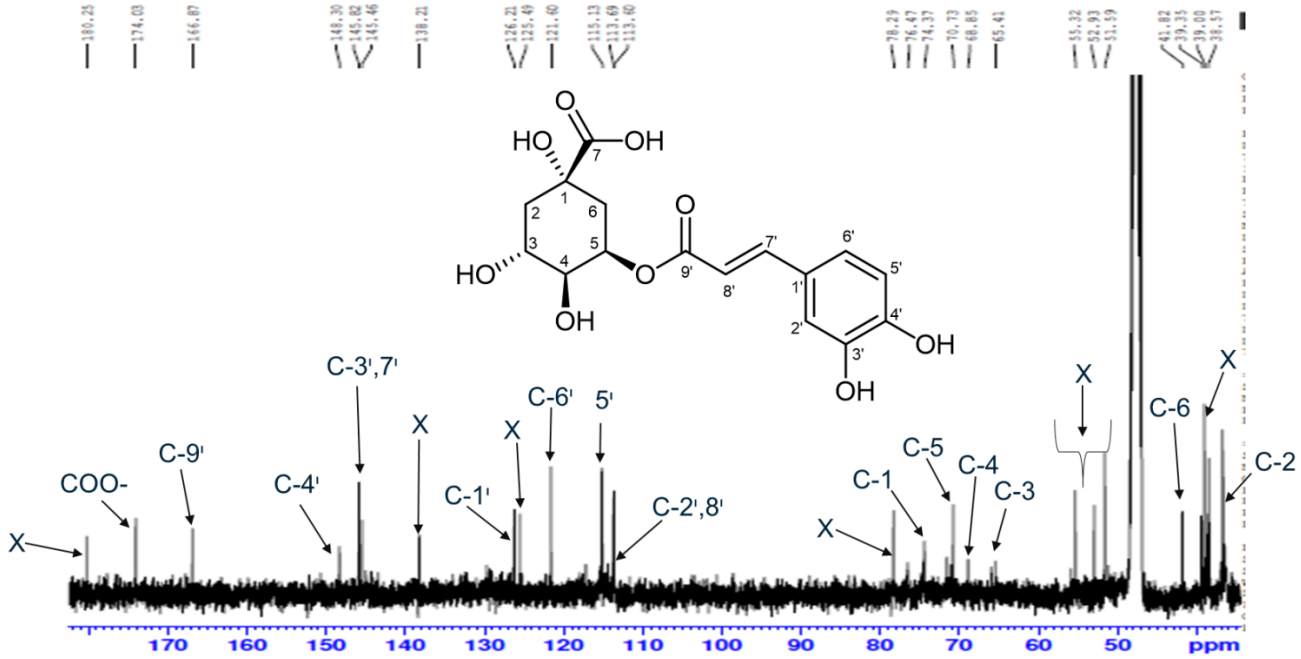

Appendix 25: ^{13}C-NMR spectrum of 5-*O*-caffeoylquinic acid (**5**).

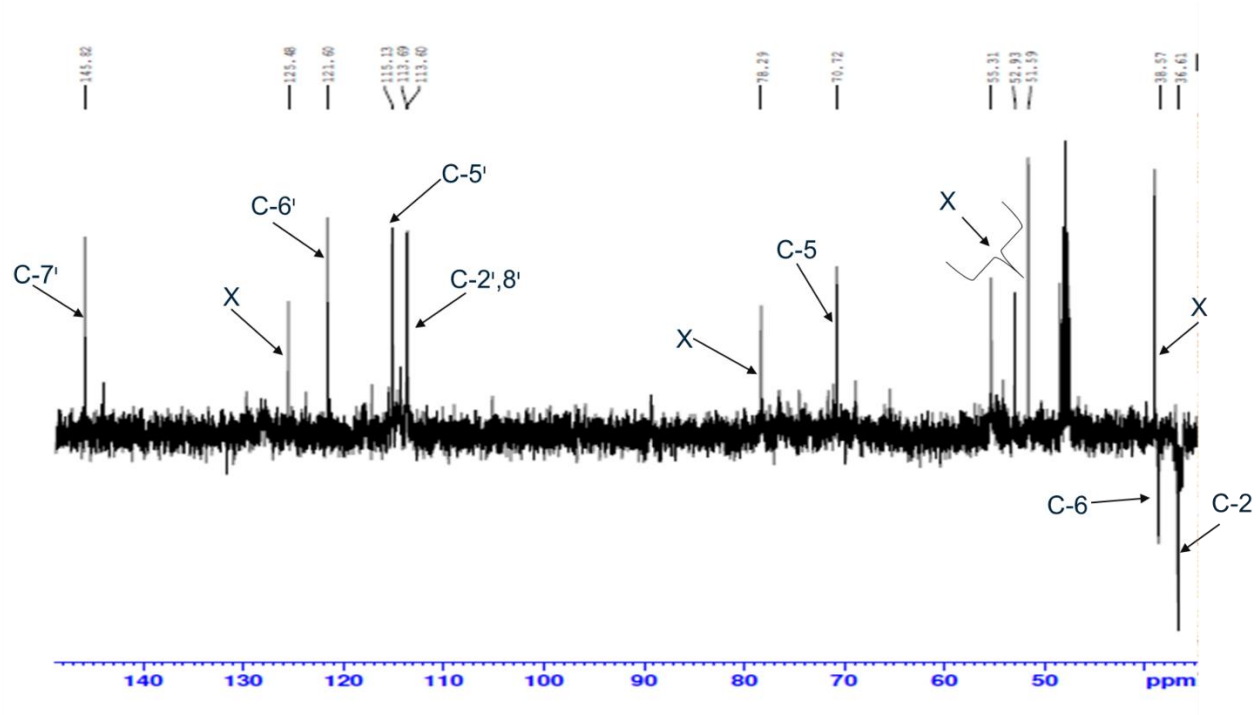

Appendix 26: DEPT 135 spectrum of 5-*O*-caffeoylquinic acid (**5**).

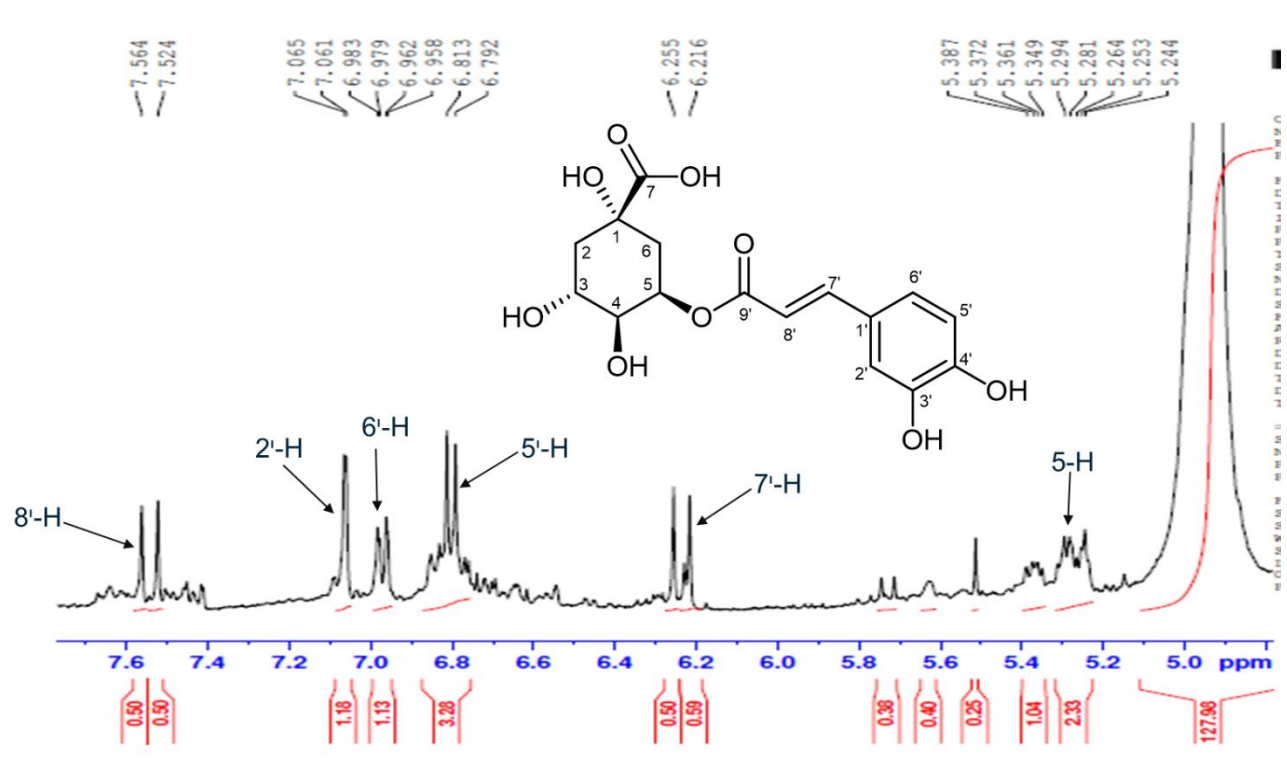

Appendix 27A: ^{1}H-NMR spectrum expansion of 5-*O*-caffeoylquinic acid (**5**).

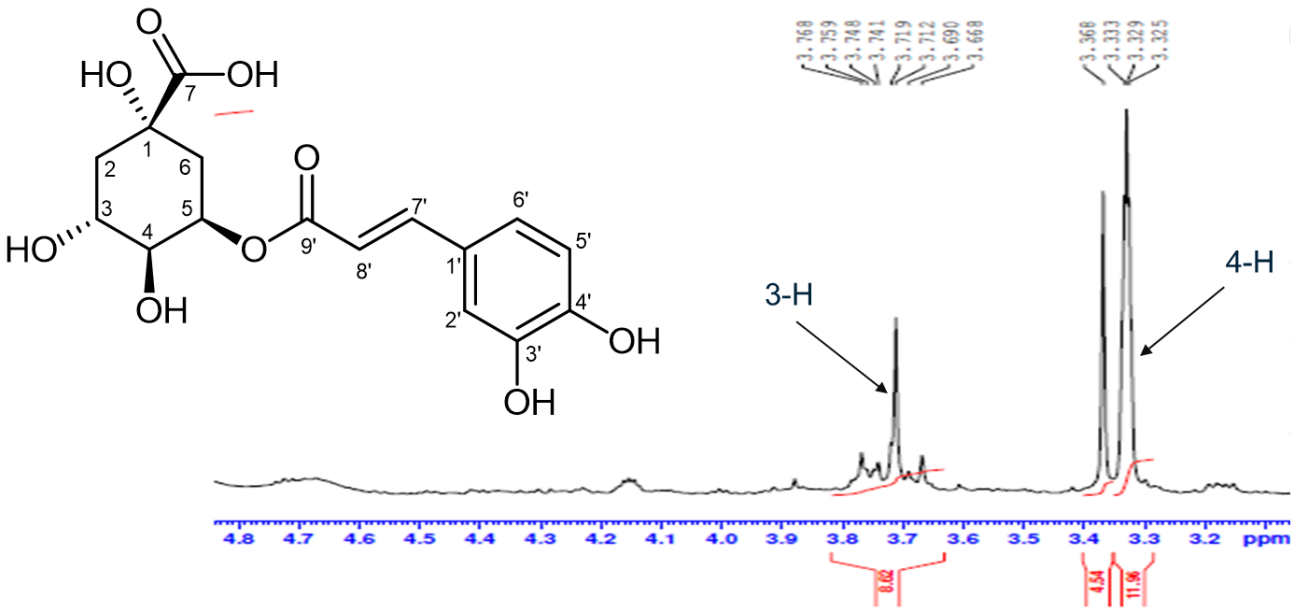

Appendix 27B: ^{1}H-NMR spectrum expansion of 5-*O*-caffeoylquinic acid (**5**).

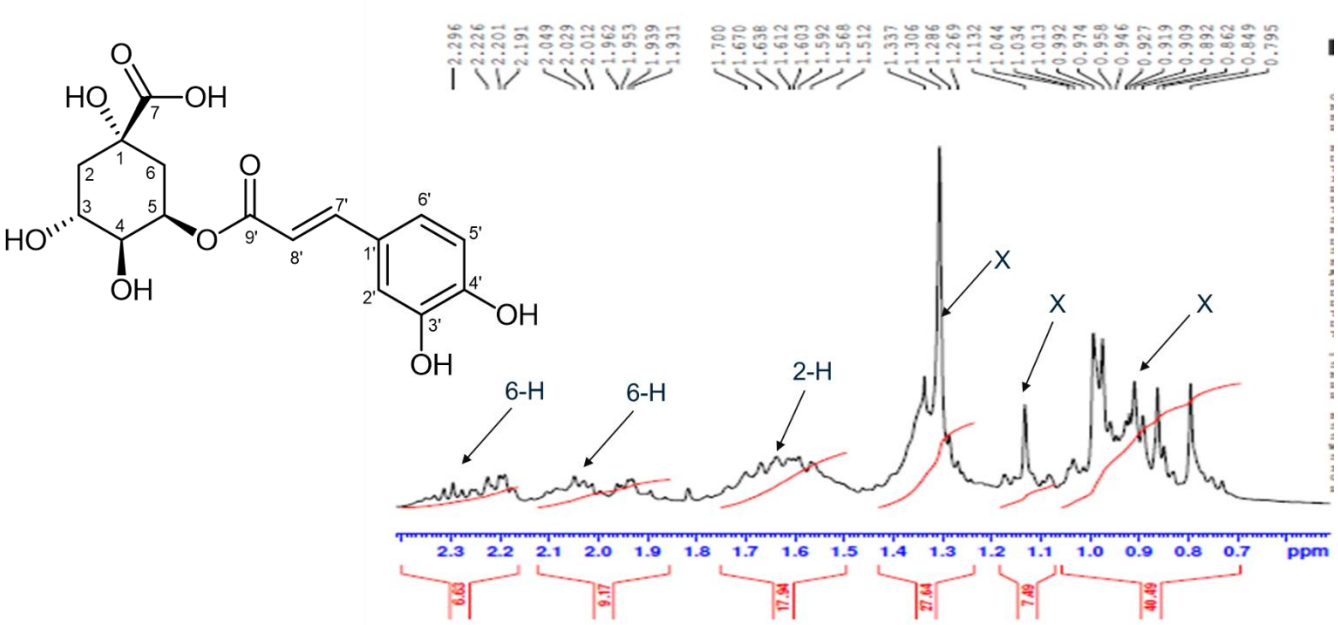

Appendix 27C: ^{1}H-NMR spectrum expansion of 5-*O*-caffeoylquinic acid (**5**).

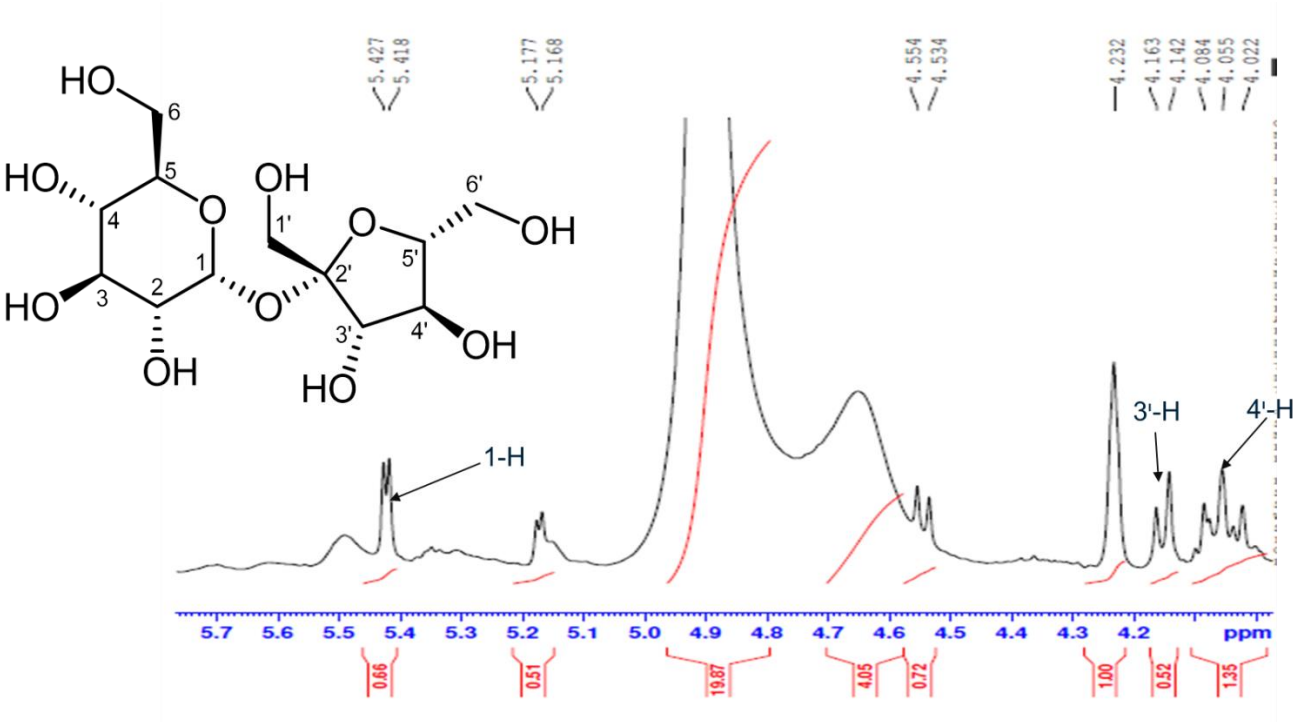

Appendix 28A: ^{1}H-NMR spectrum expansion of sucrose (**6**).

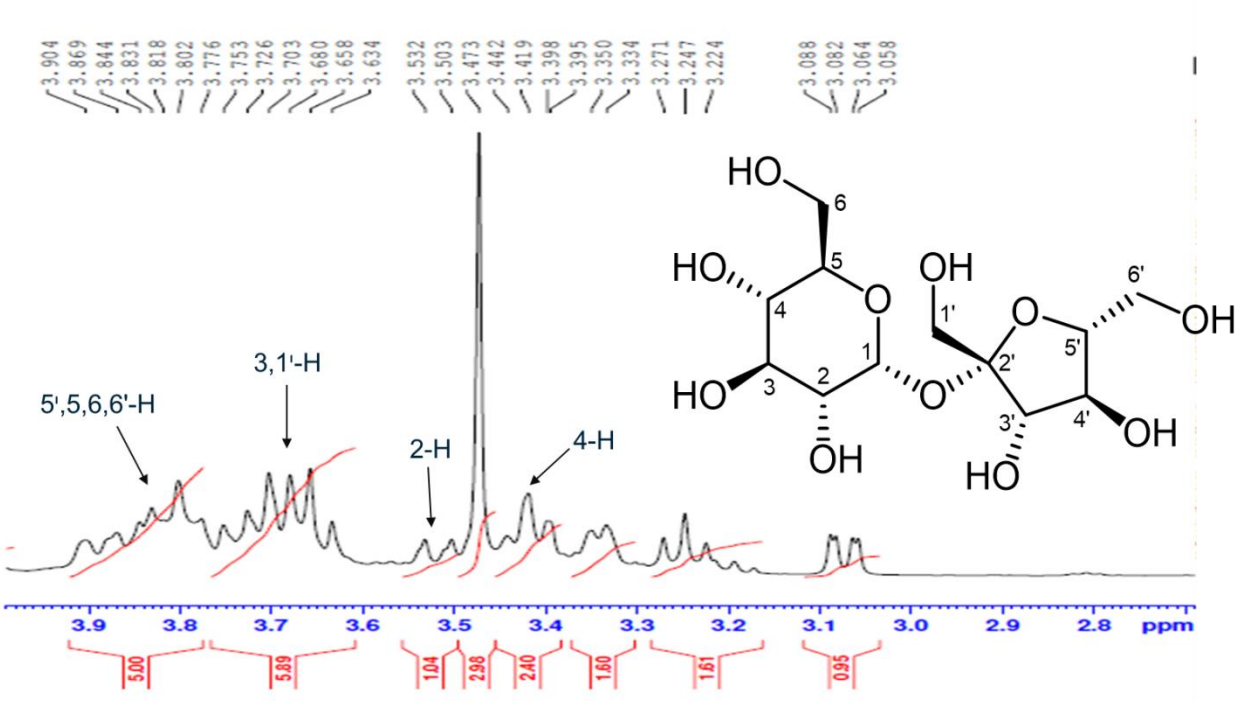

Appendix 28B: ^{1}H-NMR spectrum expansion of sucrose (**6**).

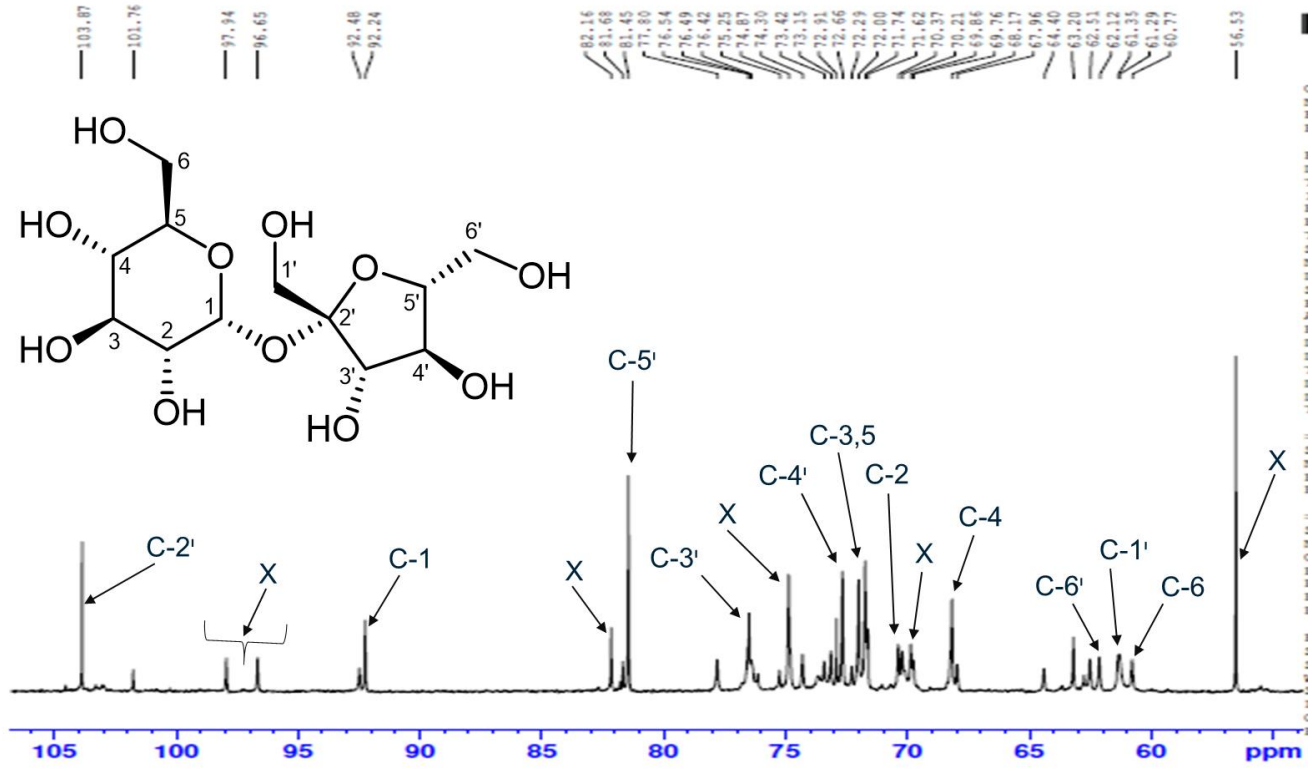

Appendix 29: ^{13}C-NMR spectrum of sucrose (**6**).

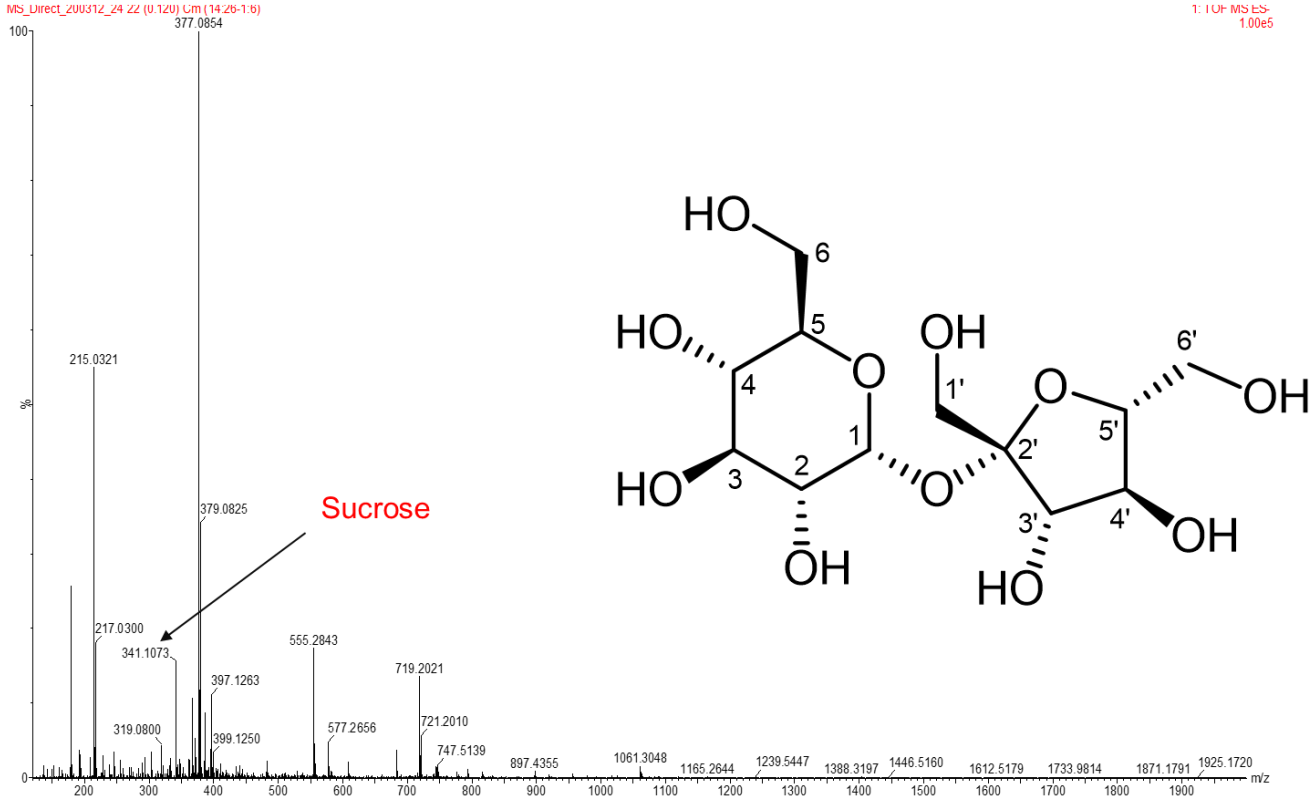

Appendix 30: MS of sucrose (**6**).

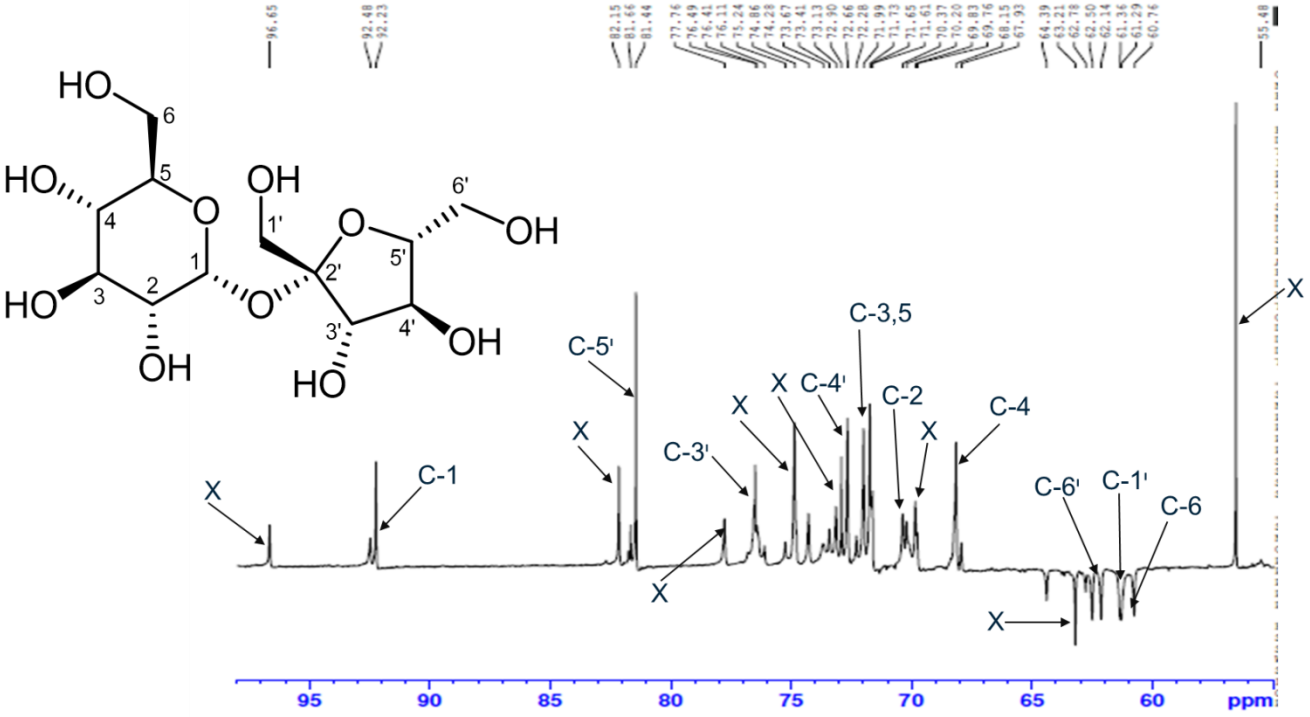

Appendix 31: DEPT 135 spectrum of sucrose (**6**).

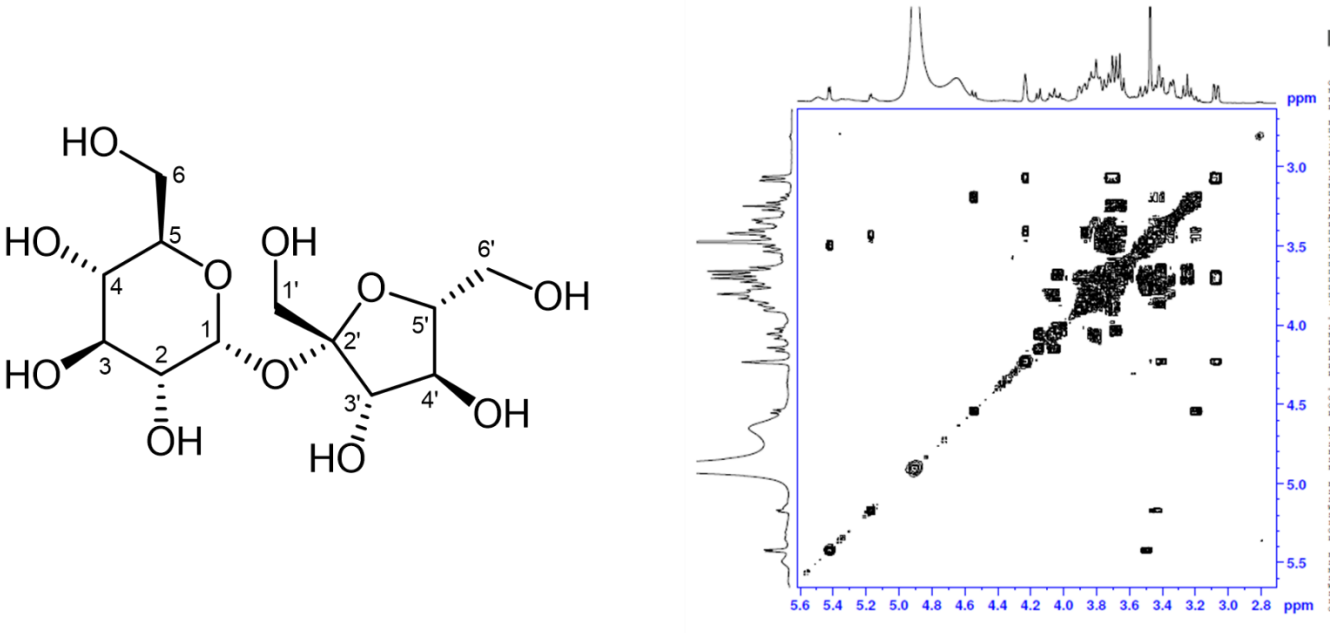

Appendix 32: ^{1}H-^{1}H COSY spectrum of sucrose (**6**).

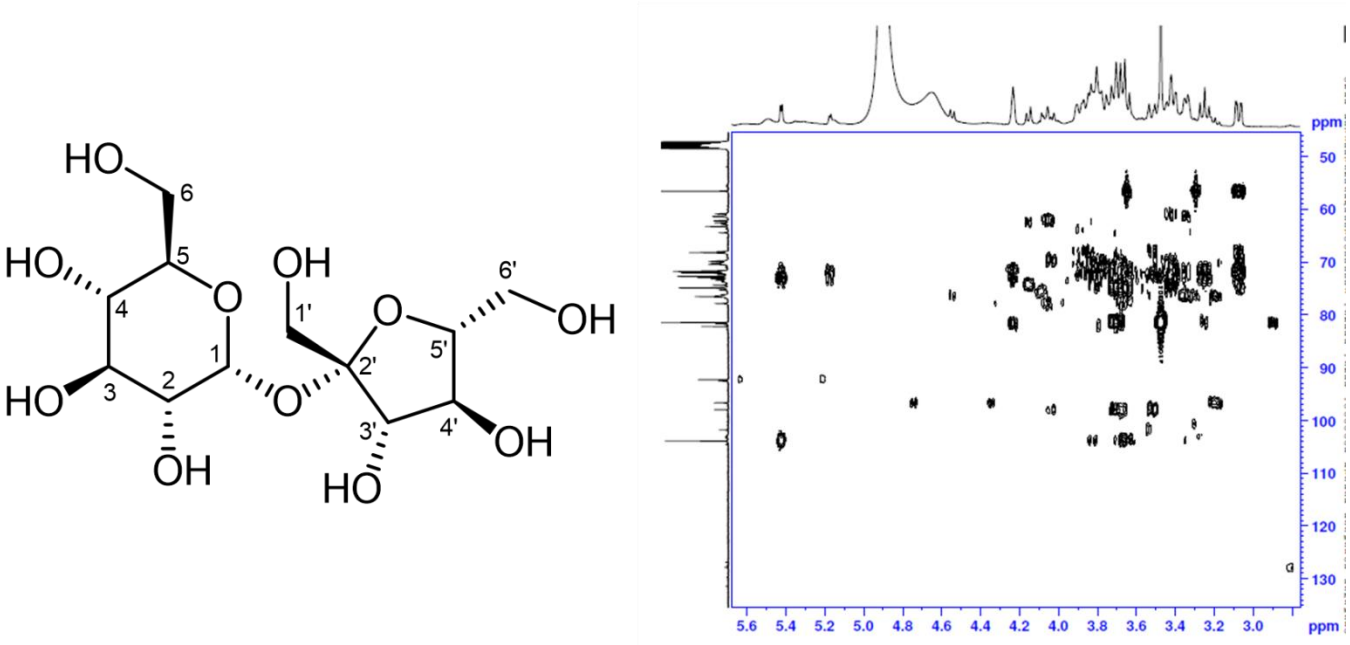

Appendix 33: HMBC spectrum of sucrose (**6**).

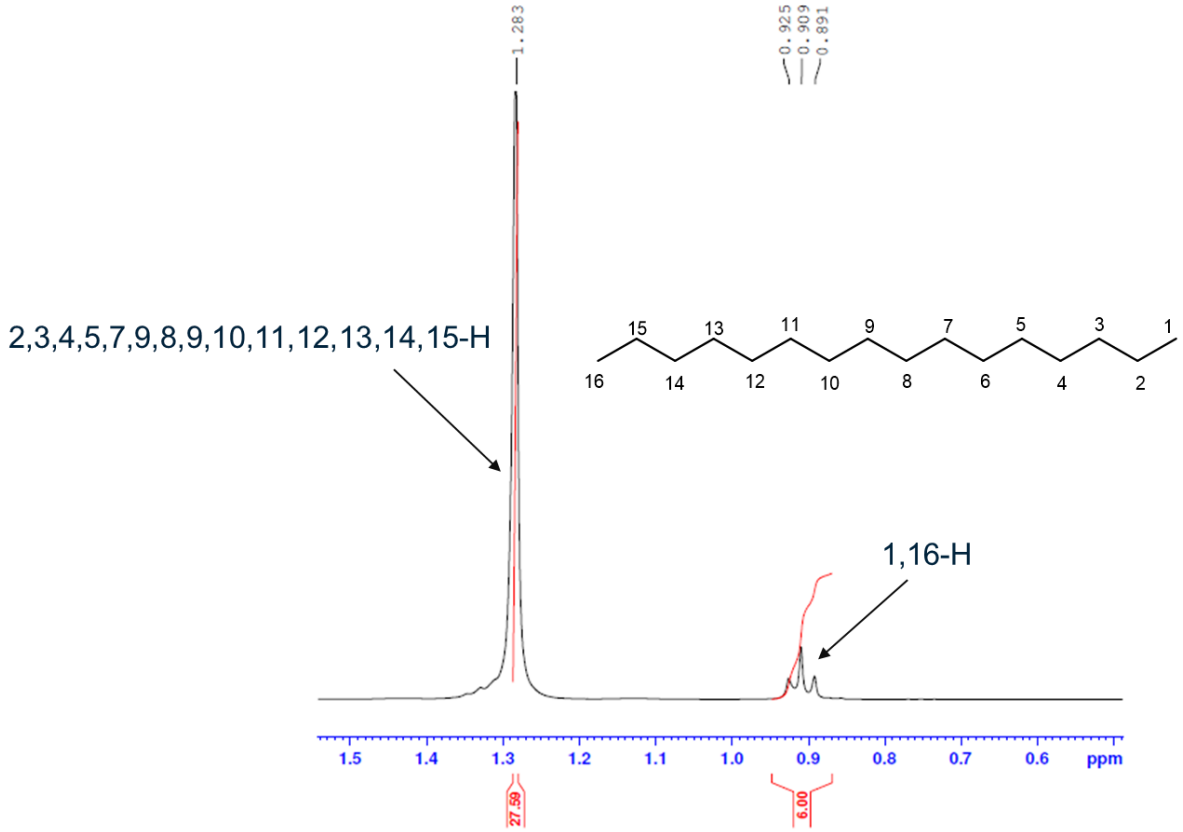

Appendix 34: ^{1}H-NMR spectrum expansion of hexadecane (**7**).

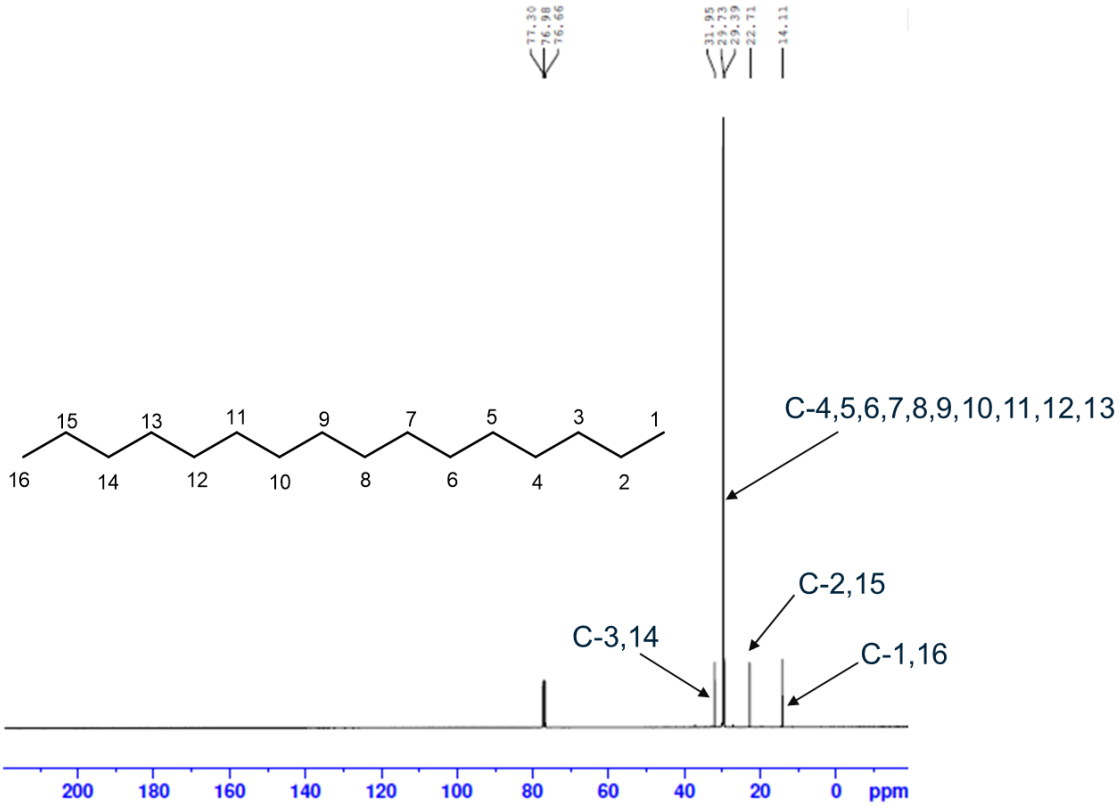

Appendix 35: ^{13}C-NMR spectrum of hexadecane (**7**).

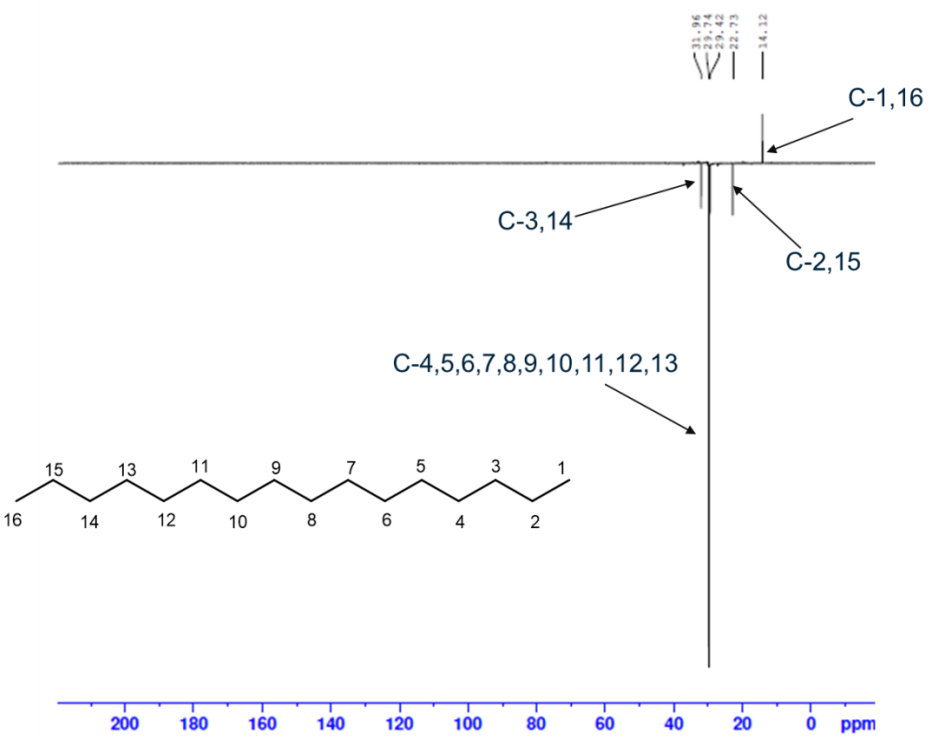

Appendix 36: DEPT 135 spectrum of hexadecane (**7**).

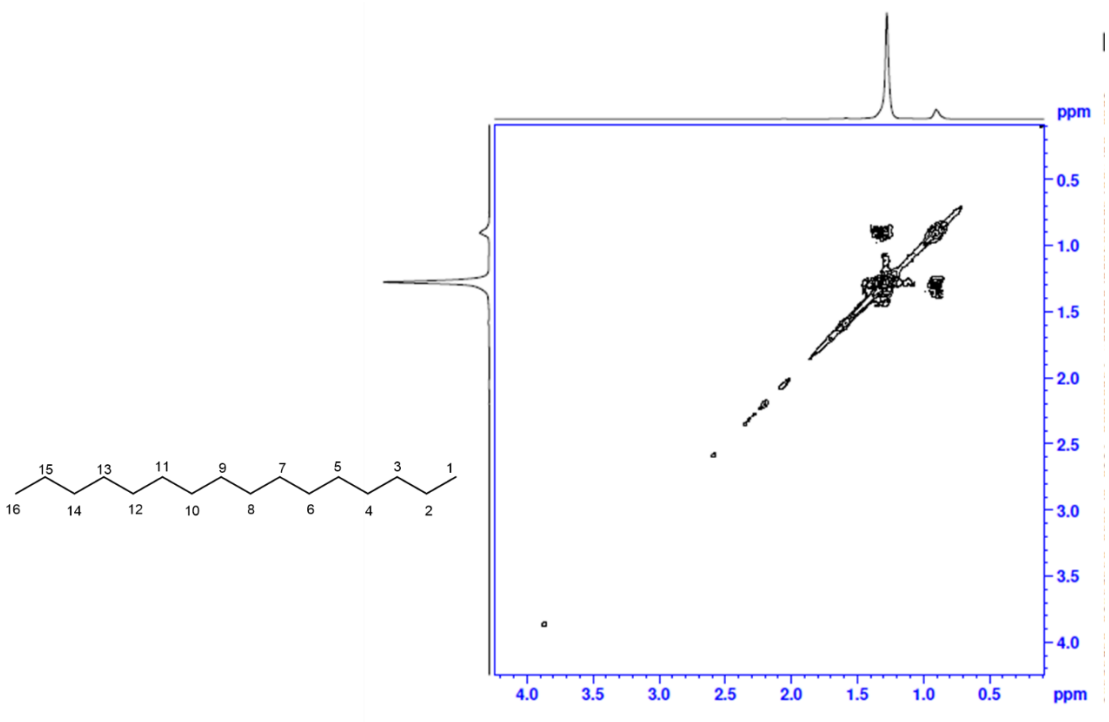

Appendix 37: ^{1}H-^{1}H COSY spectrum of hexadecane (**7**).

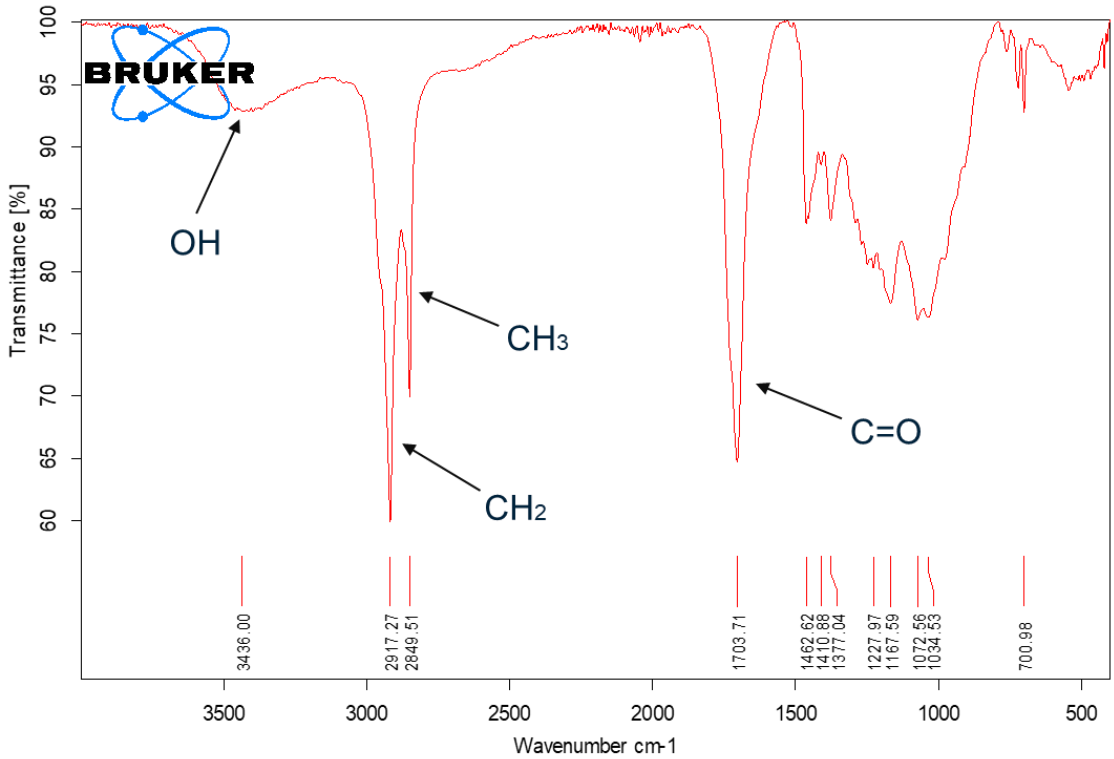

Appendix 38: **FT**IR spectrum of palmitic acid (**8**).

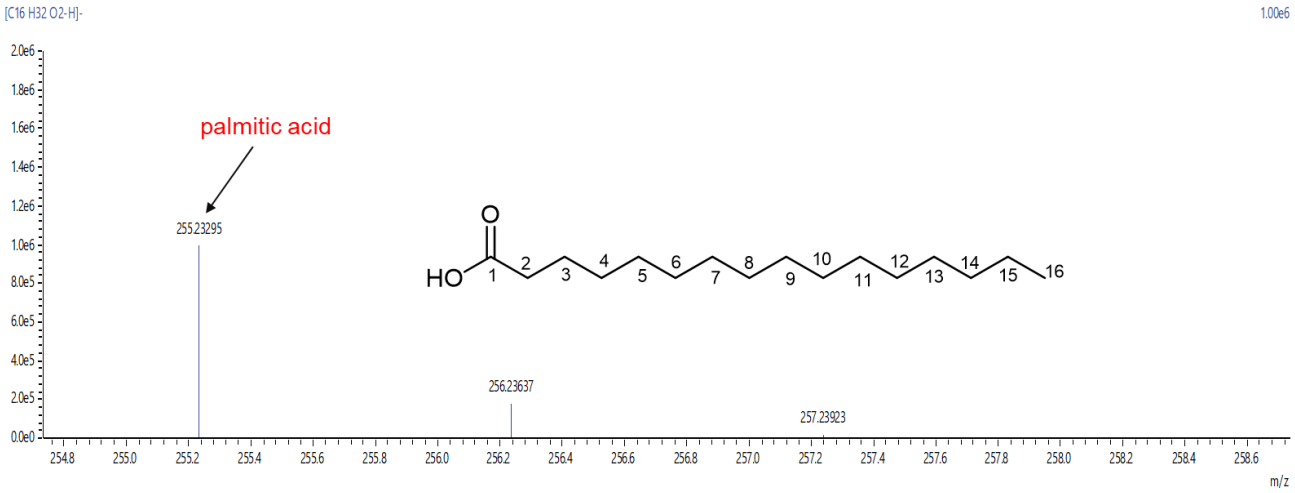

Appendix 39: MS of palmitic acid (**8**).

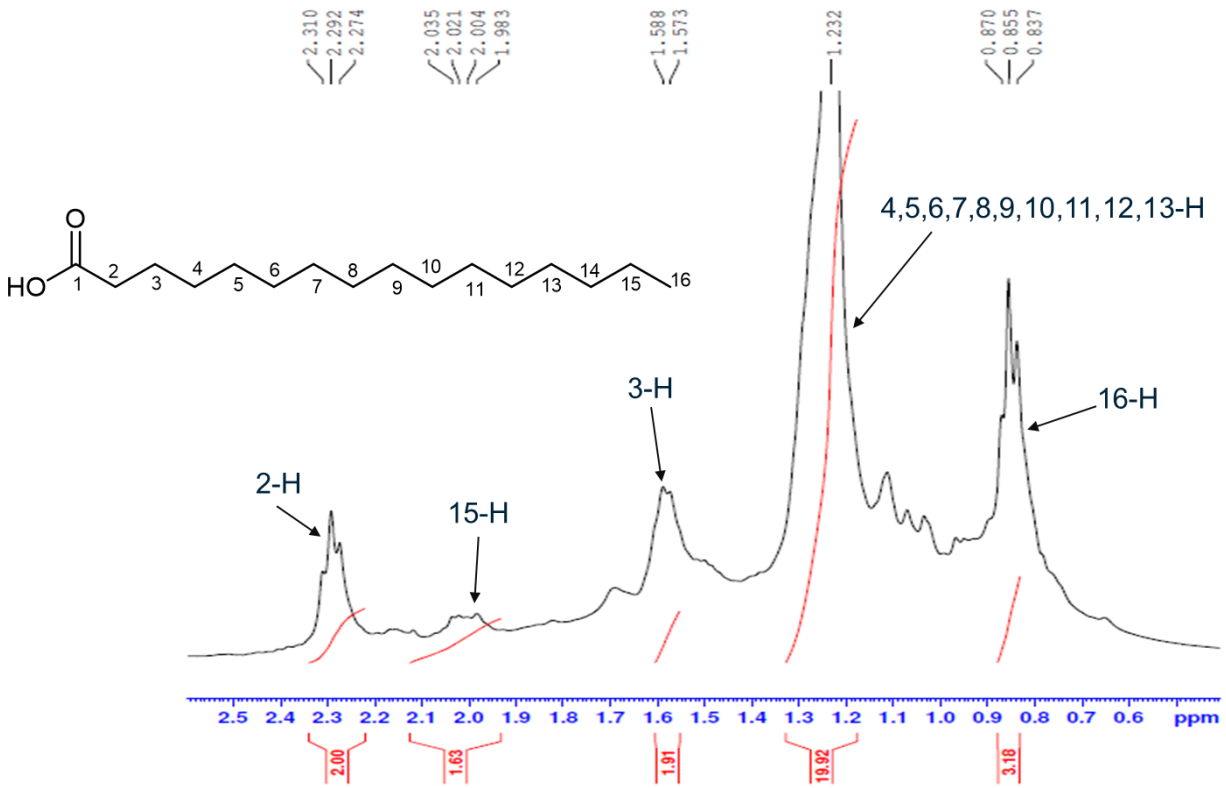

Appendix 40: ^{1}H-NMR spectrum expansion of palmitic acid (**8**).

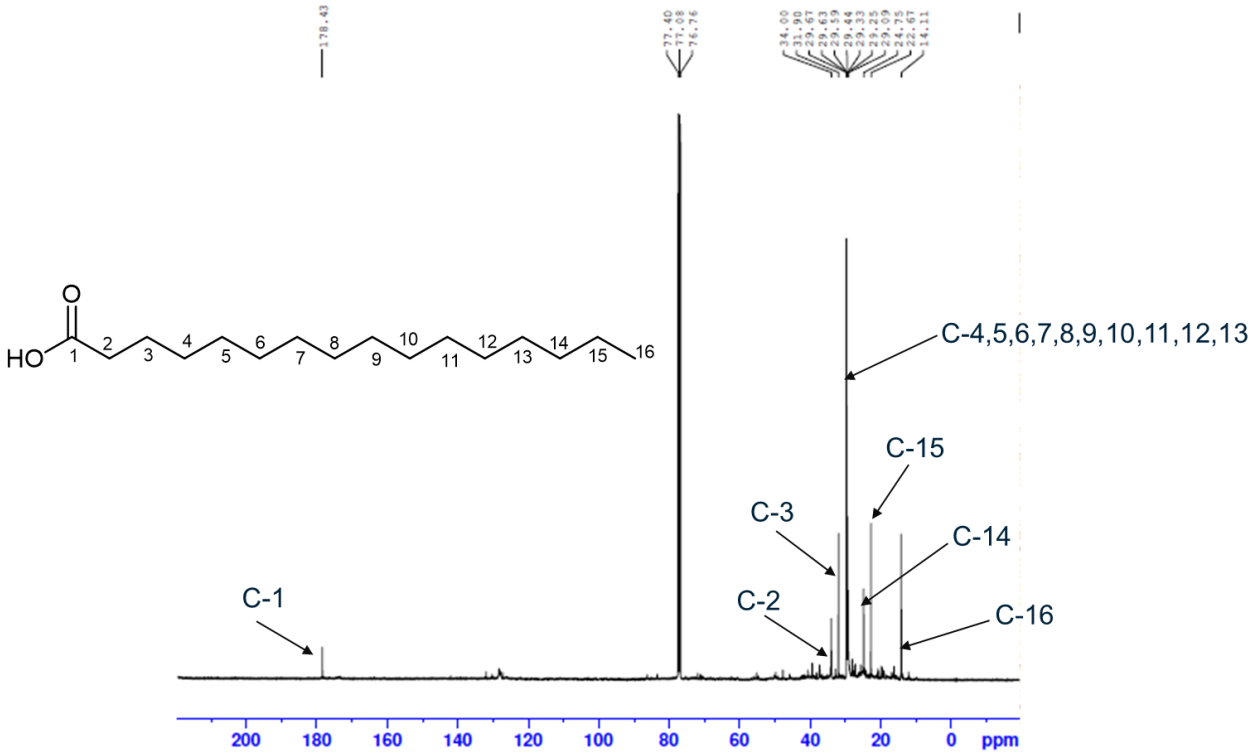

Appendix 41: ^{13}C-NMR spectrum of palmitic acid (**8**).

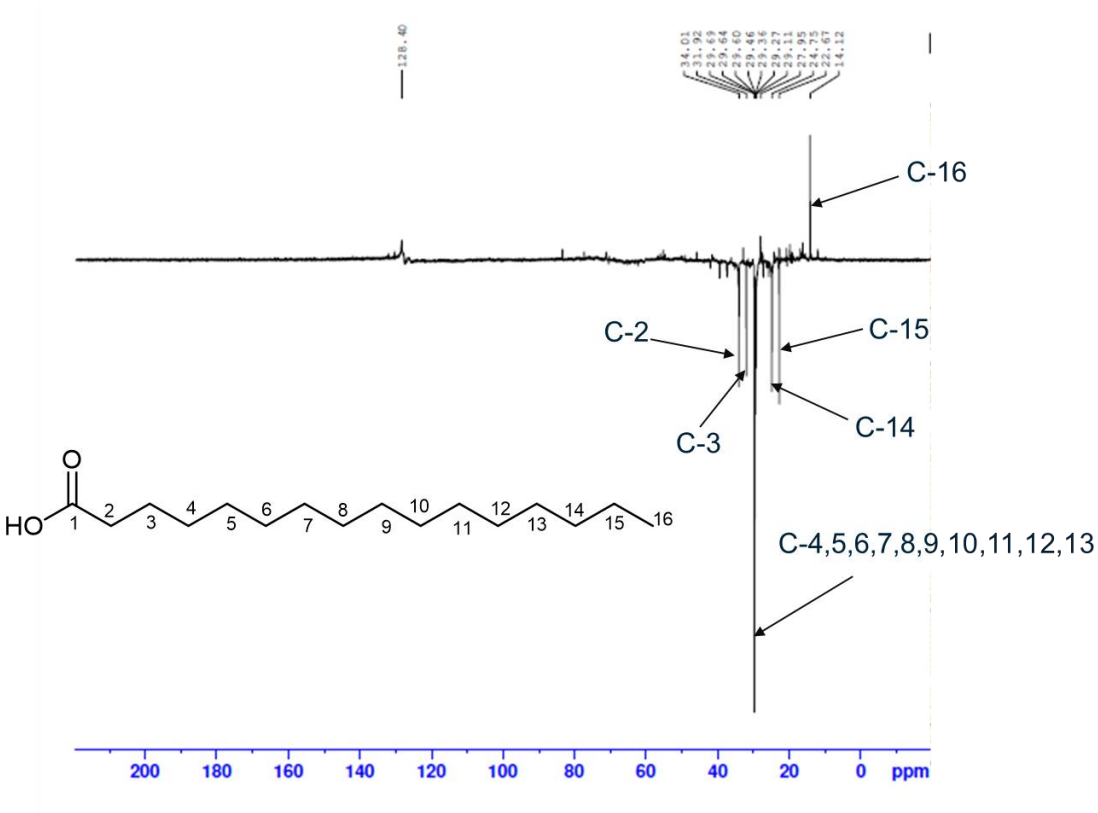

Appendix 42: DEPT 135 spectrum of palmitic acid (**8**).

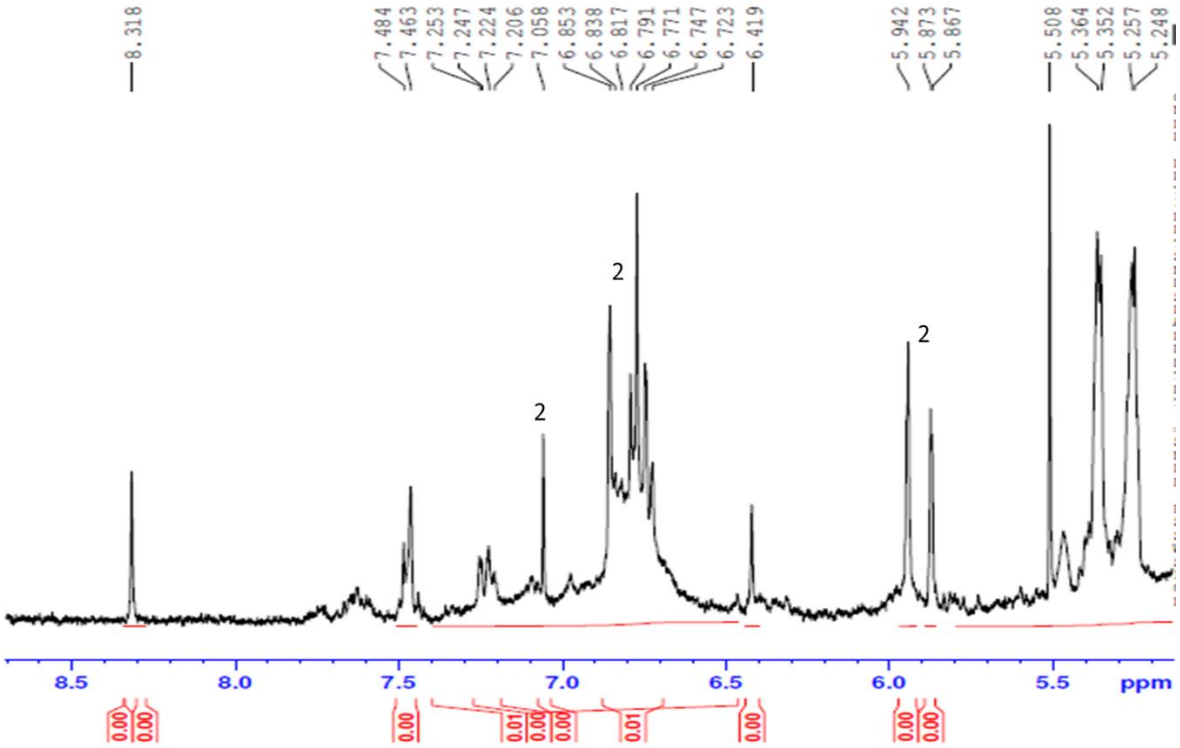

Appendix 43A. Representative ^{1}H-NMR spectrum of fraction S_1. 2, catechin.

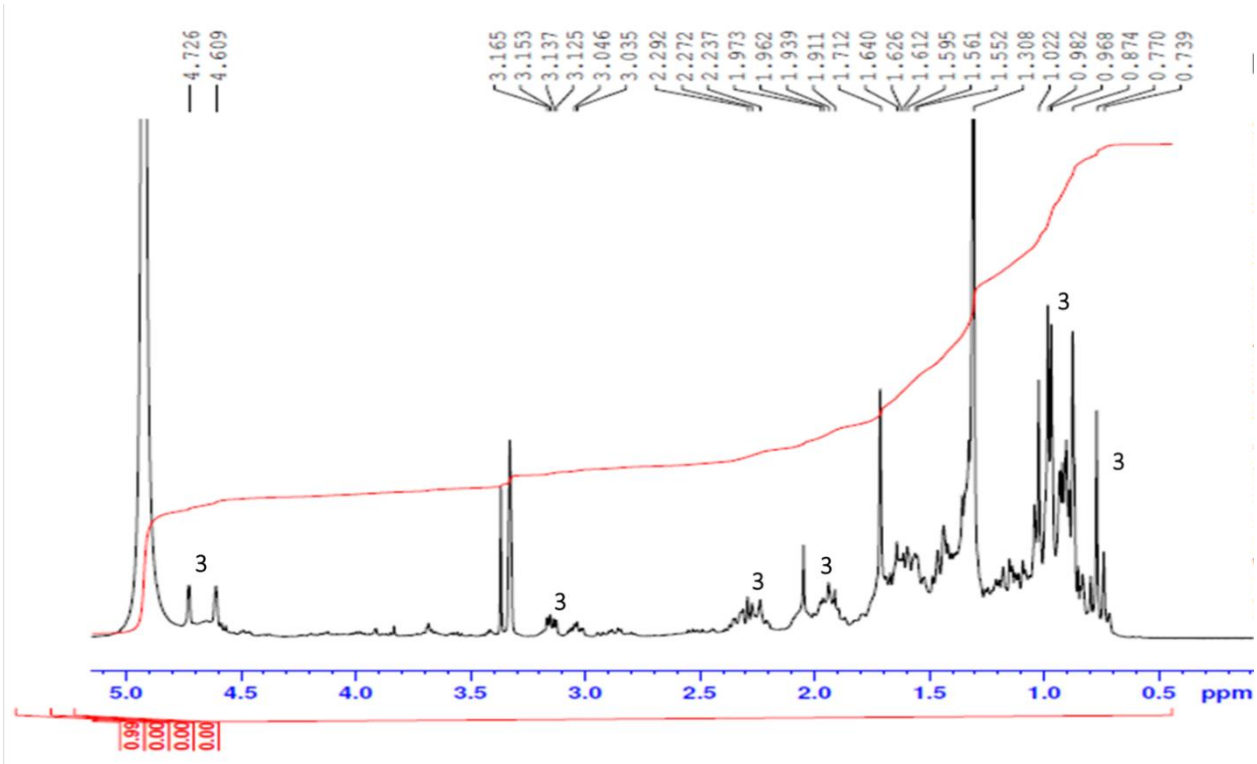

Appendix 43B. Representative ^{1}H-NMR spectrum of fraction S_1. 3, lupeol.

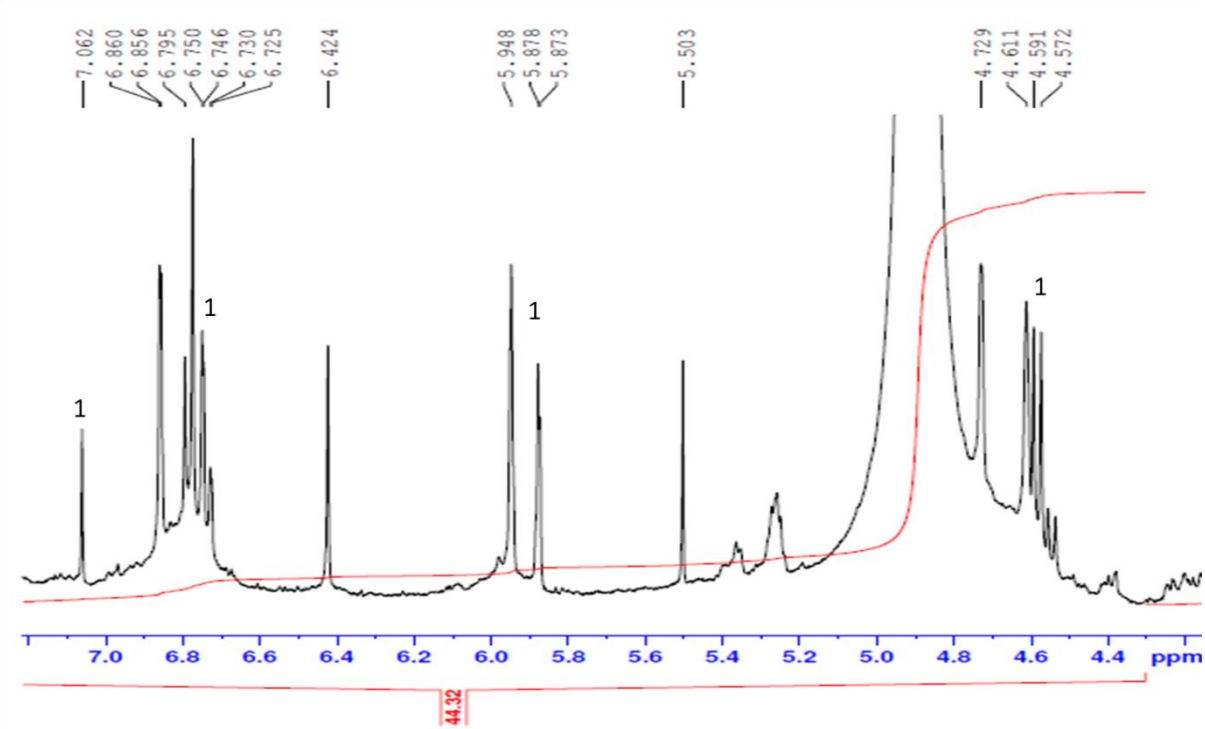

Appendix 44A. Representative ^{1}H-NMR spectrum of fraction S_2. 1, catechin.

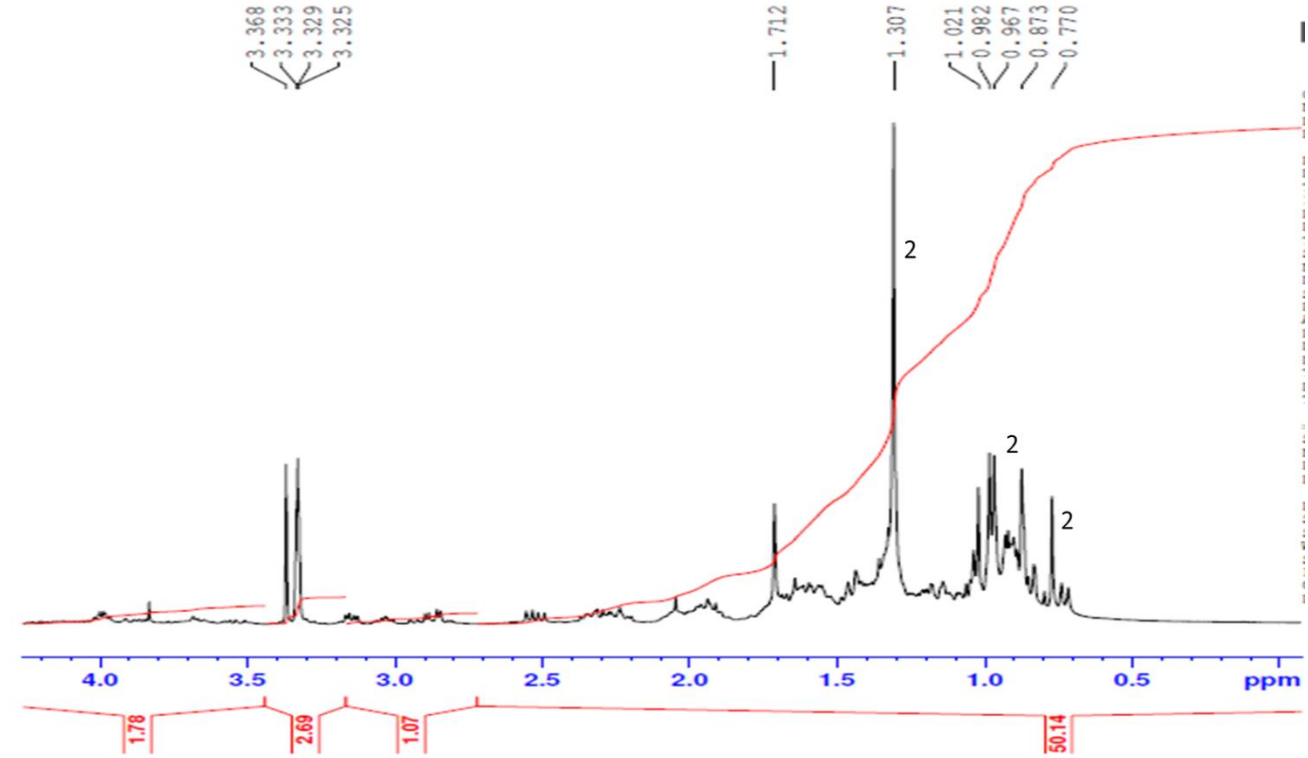

Appendix 44B. Representative ^{1}H-NMR spectrum of fraction S_2. 2, lupeol.

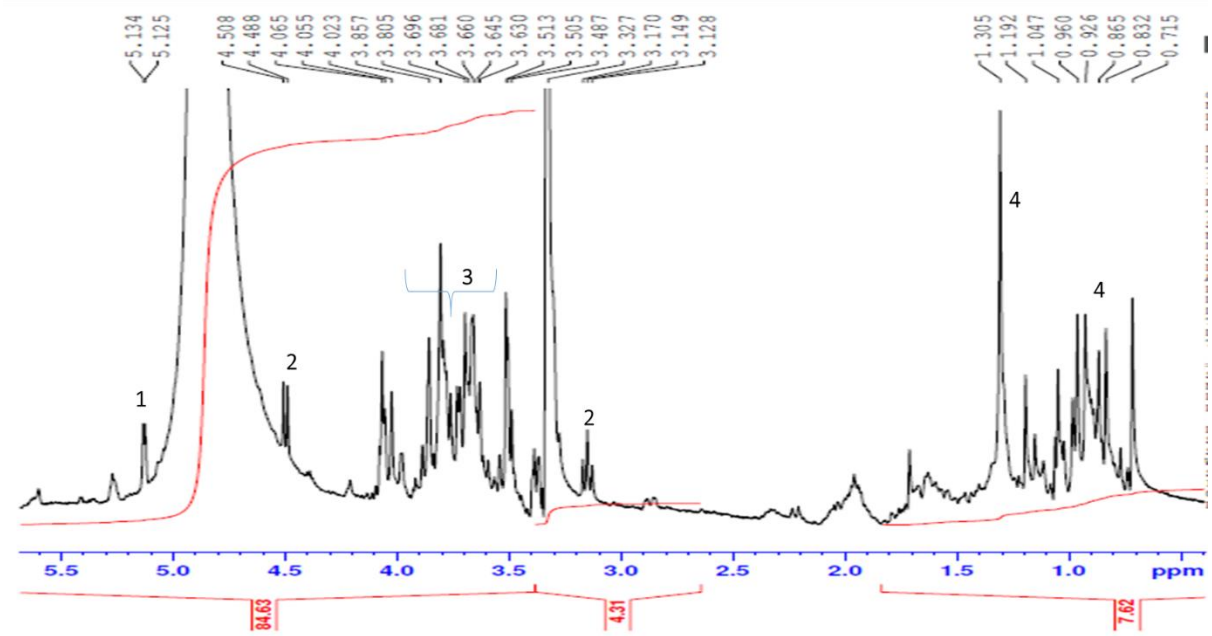

Appendix 45. Representative ^{1}H-NMR spectrum of R.crude. 1, α-glucose; 2, β-glucose; 3, glucose and fructose; 4, lupeol.

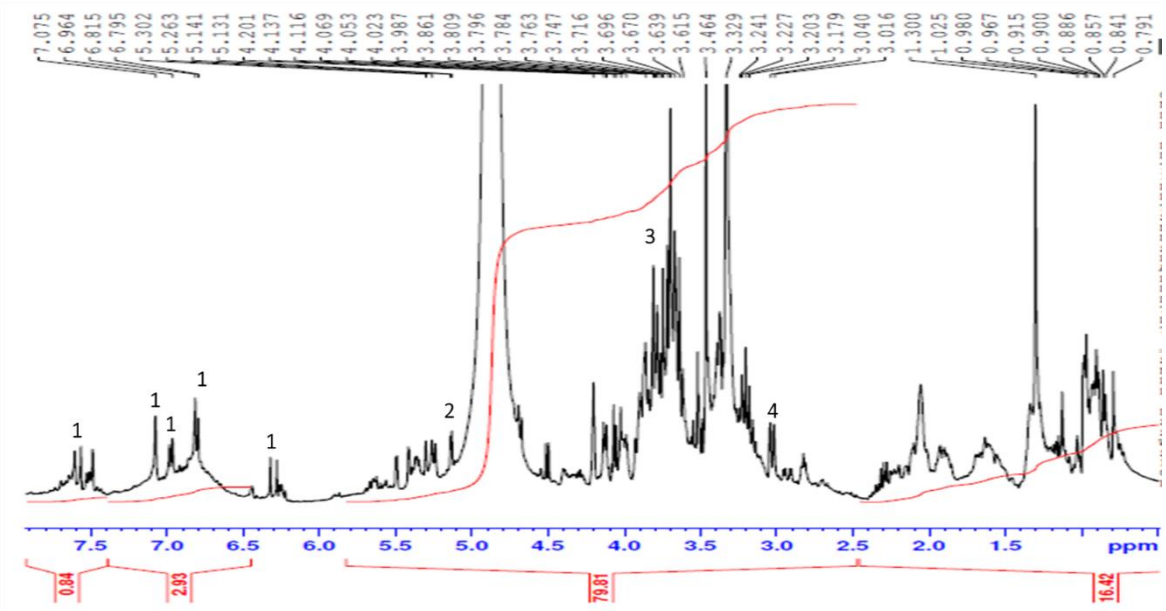

Appendix 46. Representative ^{1}H-NMR spectrum of LM.crude. 1, 5-*O*-caffeoylquinic acid; 2, α-glucose; 3, glucose and fructose; 4, β-glucose.

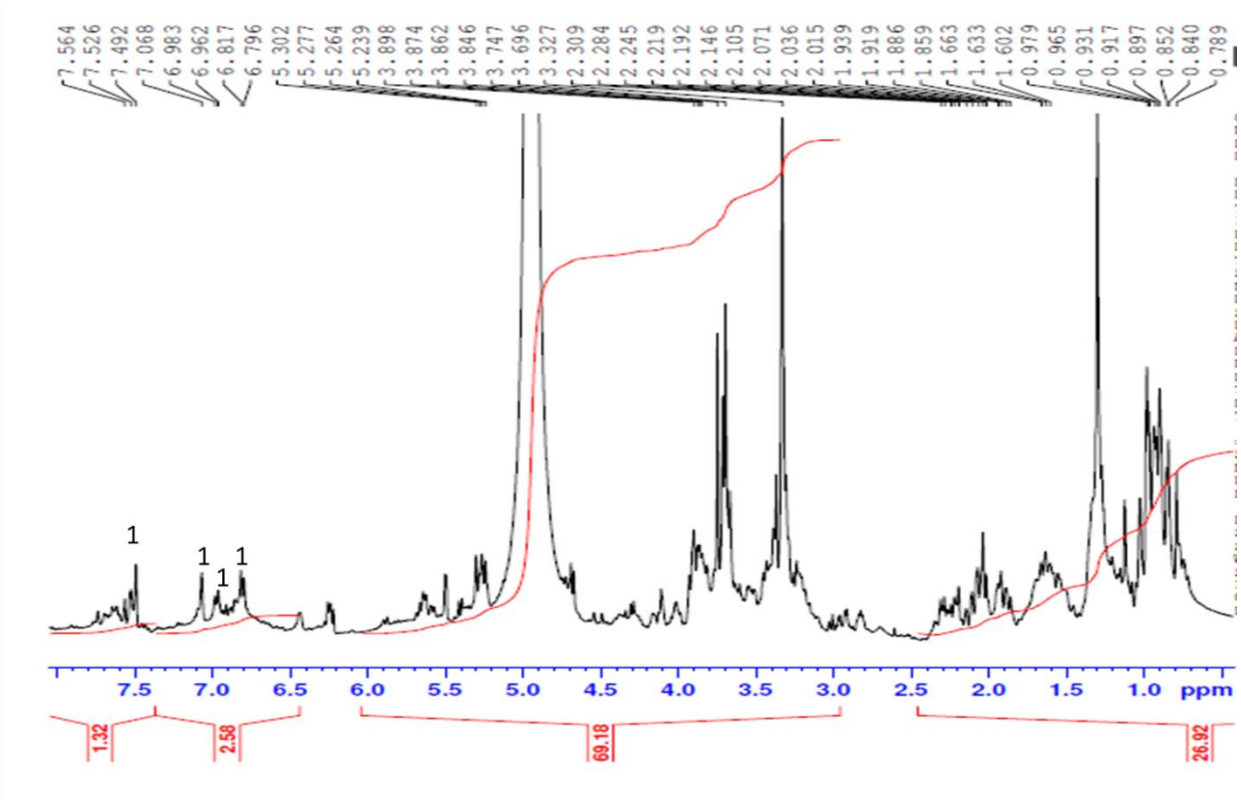

Appendix 47. Representative ^{1}H-NMR spectrum of fraction LM_2. 1, 5-*O*-caffeoylquinic acid.

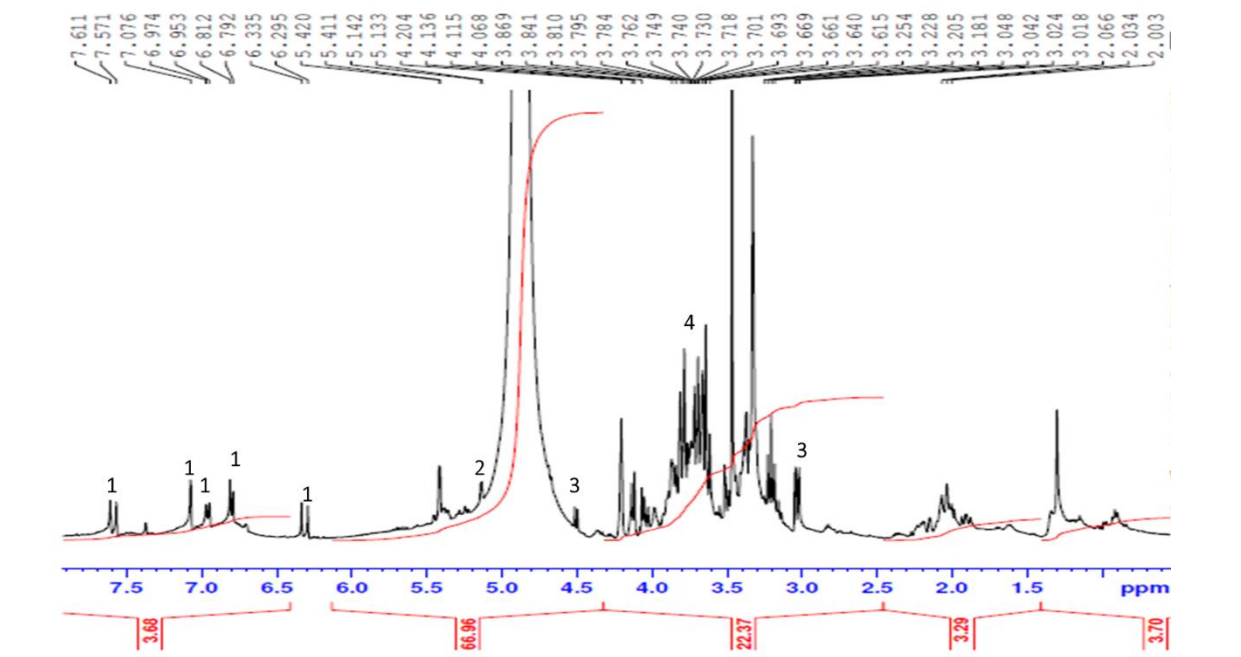

Appendix 48. Representative ^{1}H-NMR spectrum of fraction LM_3. 1, 5-*O*-caffeoylquinic acid; 2, α-glucose; 3, β-glucose; 4, glucose and fructose.

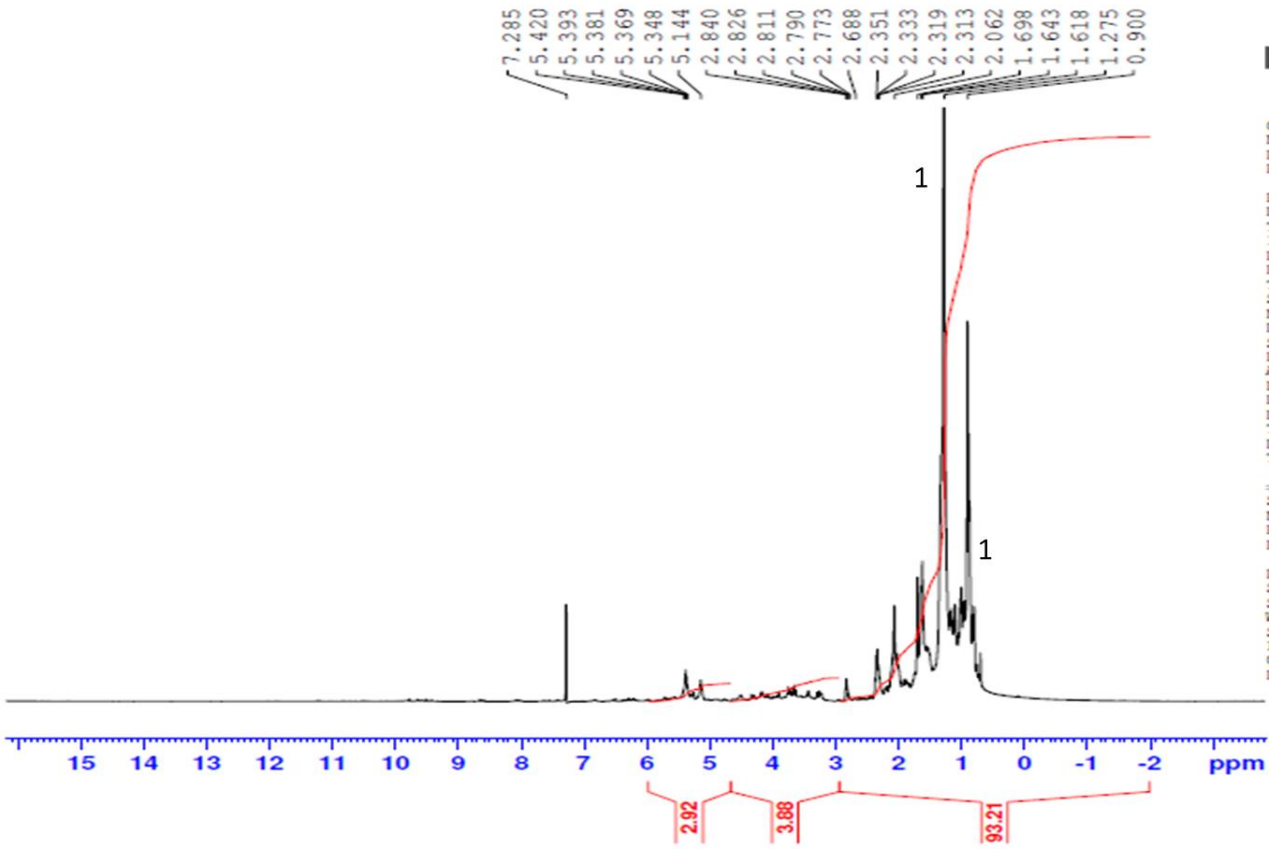

Appendix 49. Representative ^{1}H-NMR spectrum of LD.crude. 1, hexadecane.

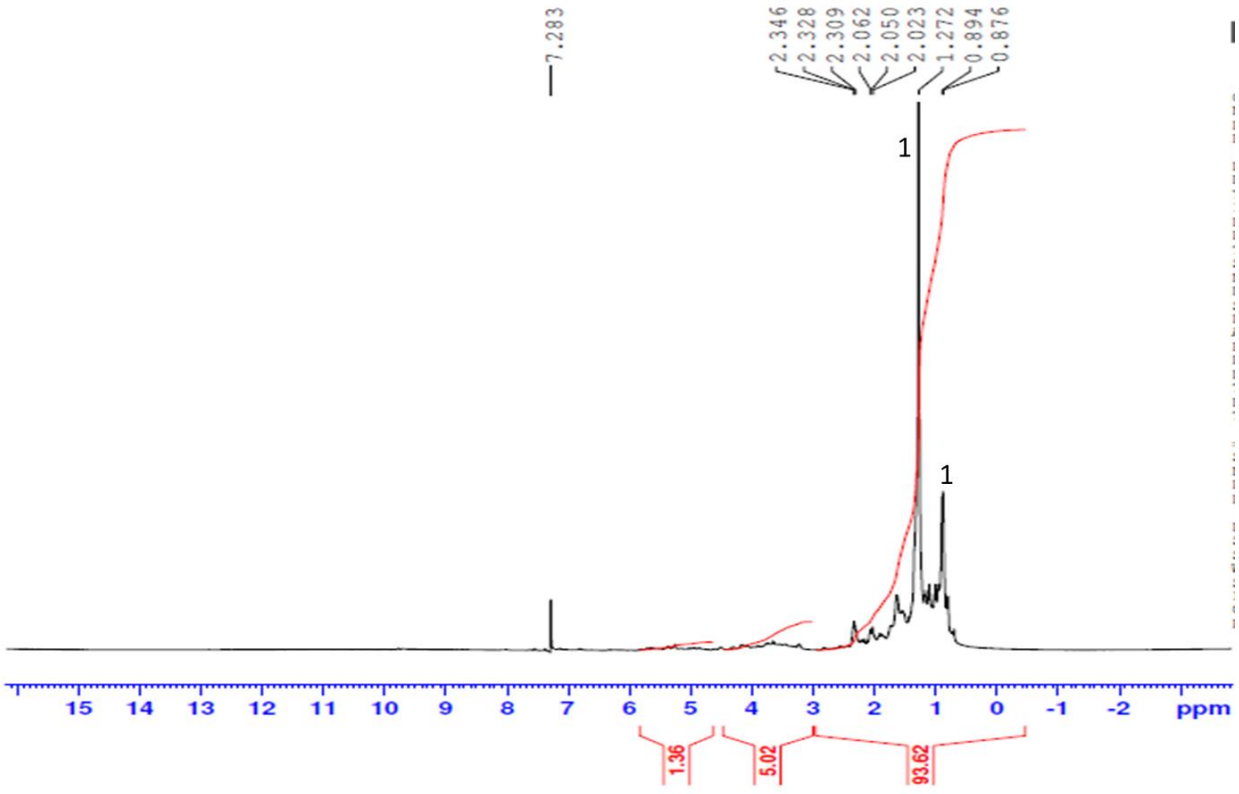

Appendix 50. Representative ^{1}H-NMR spectrum of fraction R_1. 1, hexadecane.

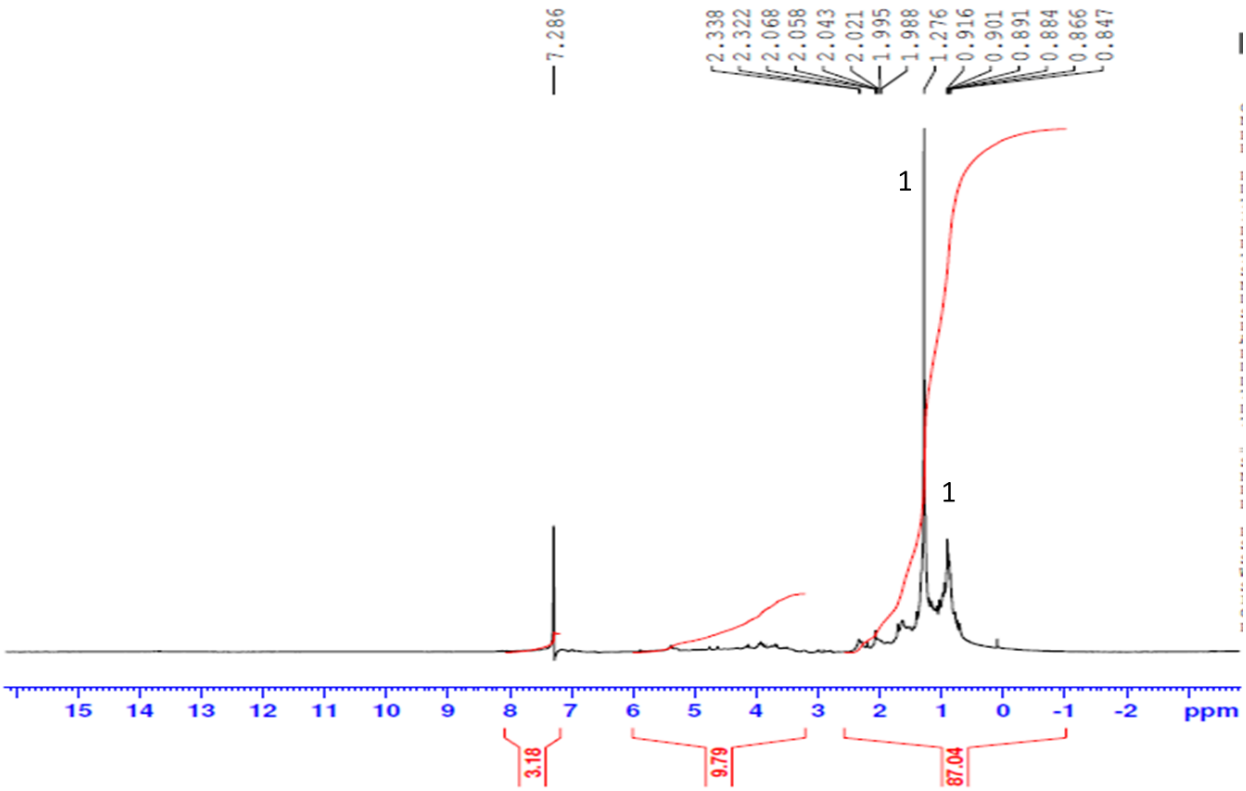

Appendix 51. Representative ^{1}H-NMR spectrum of fraction LD_3. 1, hexadecane.

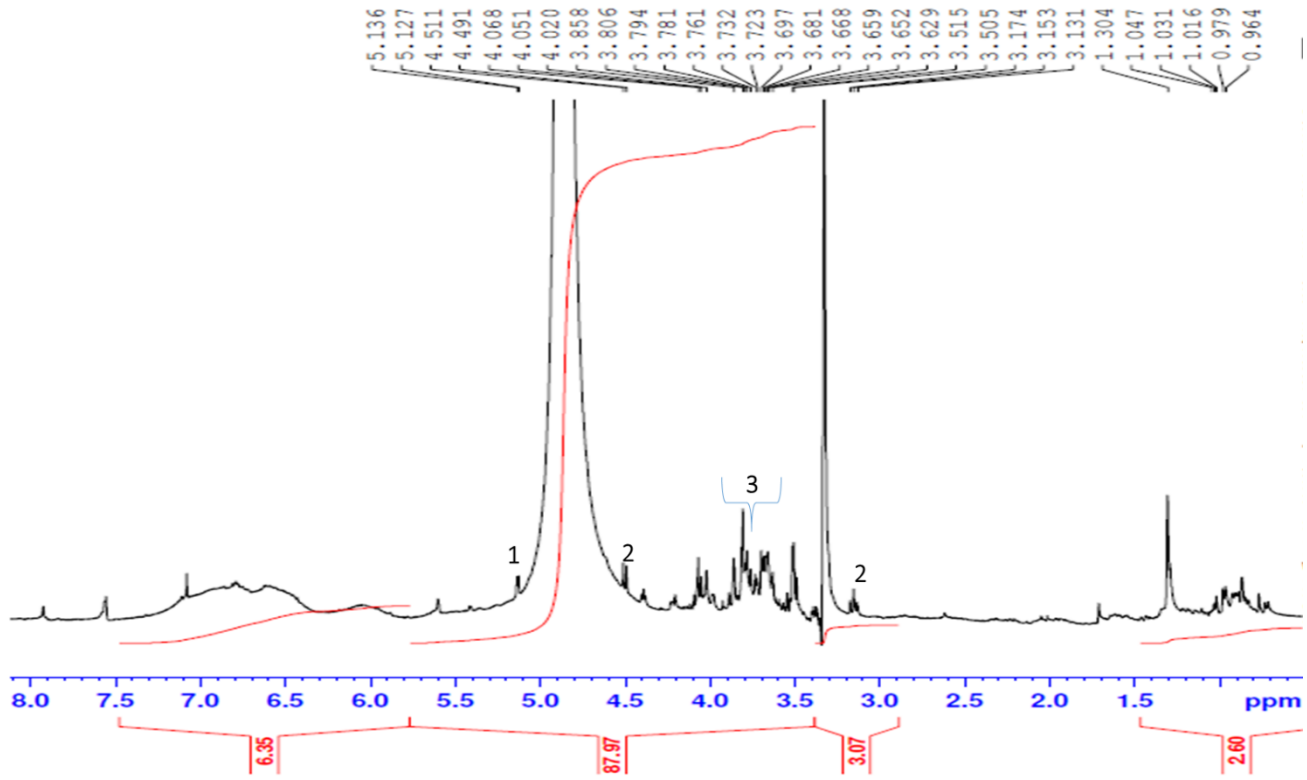

Appendix 52. Representative ^{1}H-NMR spectrum of S.crude. 1, α-glucose; 2, β-glucose; 3, fructose.

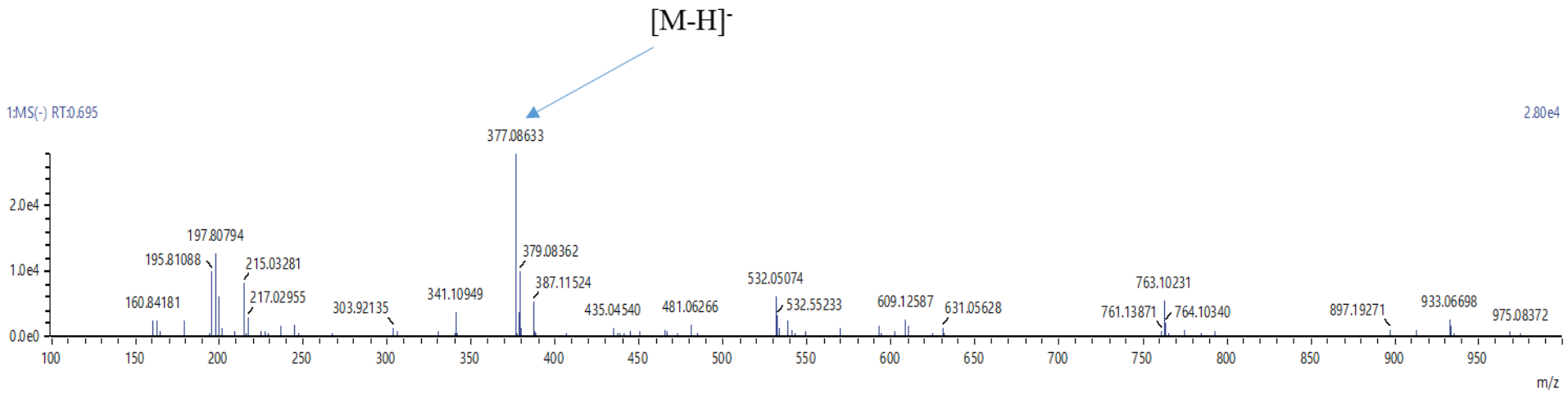

Appendix 53. MS of caffeic acid derivative.

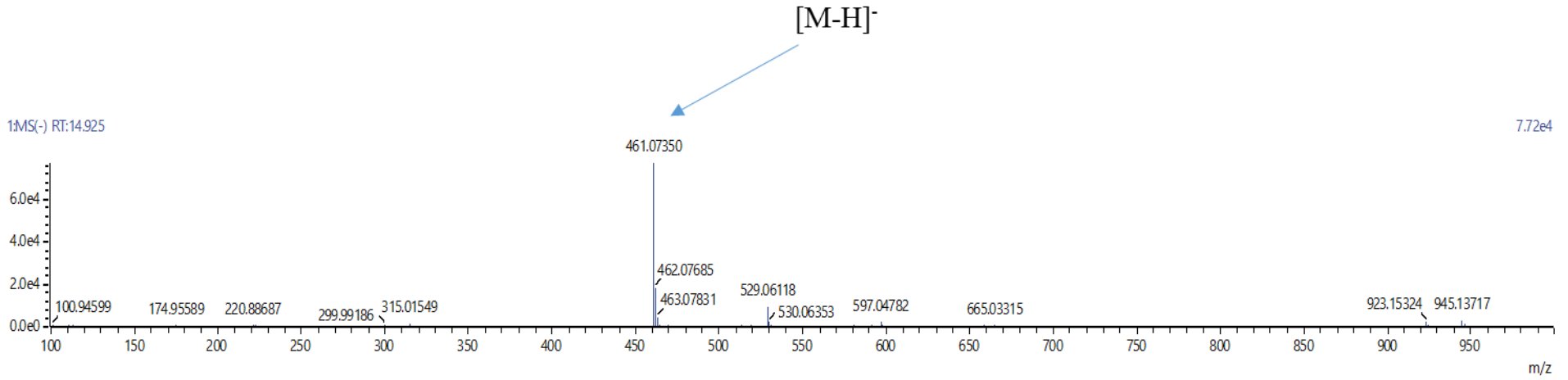

Appendix 54. MS of 4'-*O*-methylellagic acid-3-*O*-α-L-rhamnopyranoside.

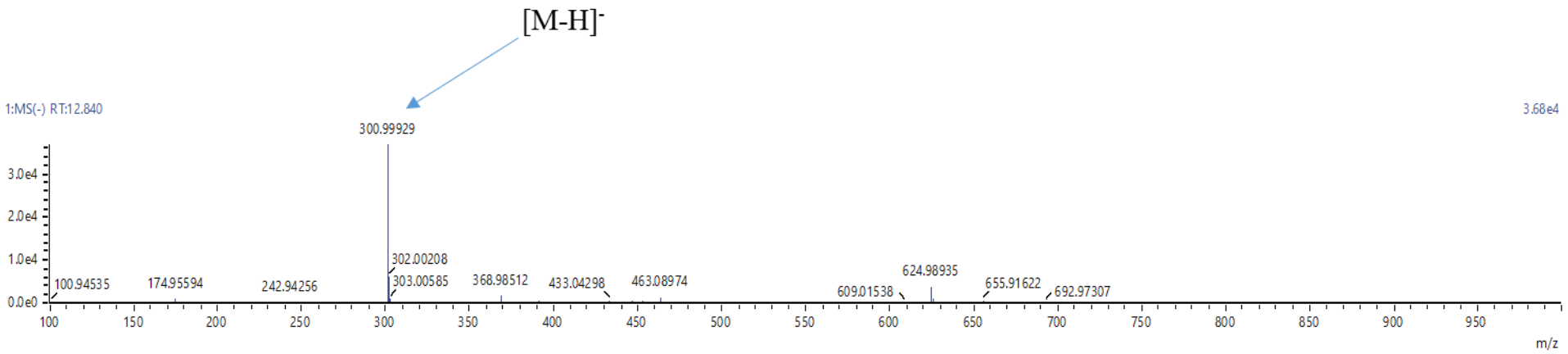

Appendix 55. MS of ellagic acid.

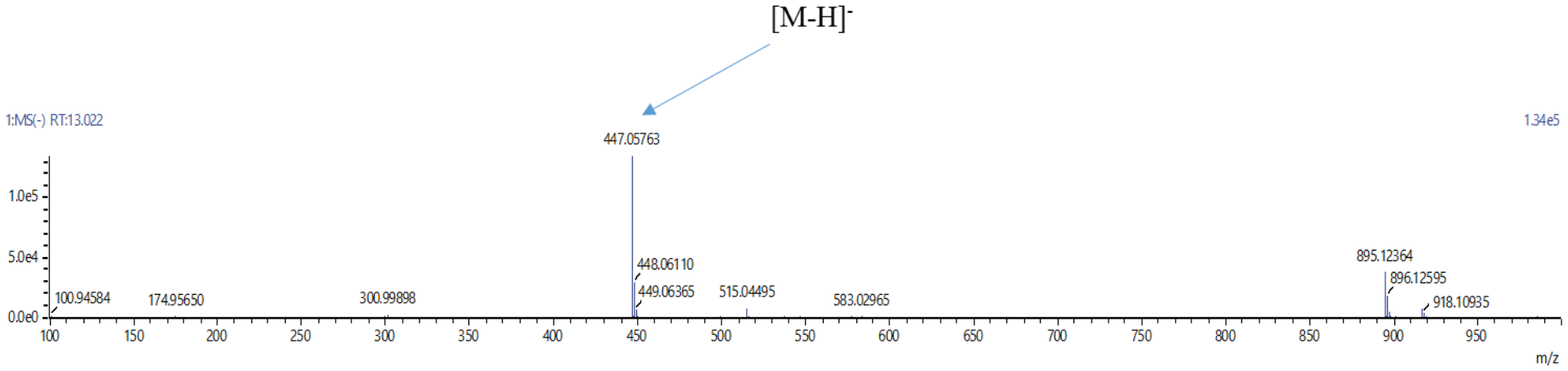

Appendix 56. MS of ellagic acid-rhamnopyranoside isomer I.

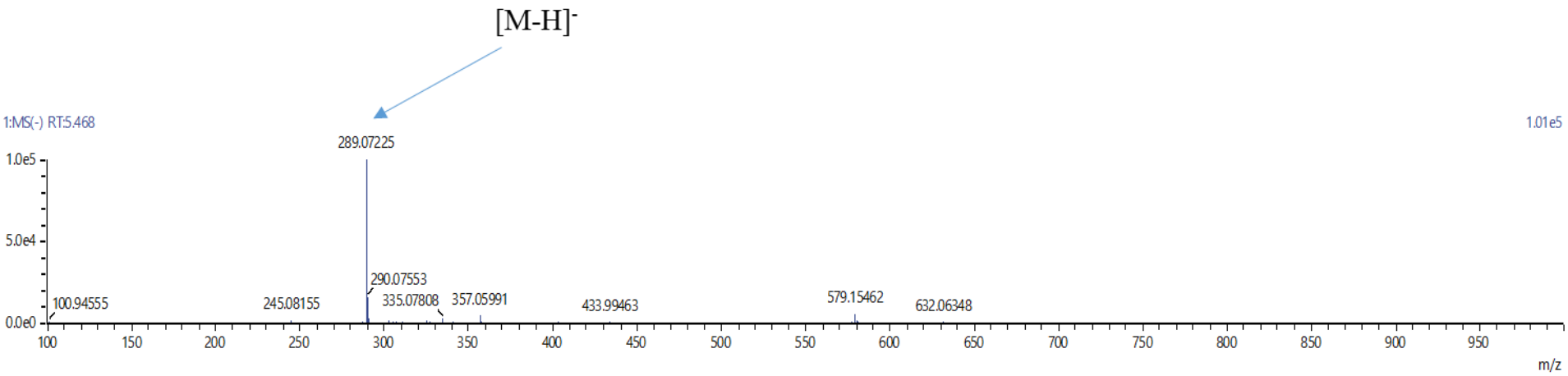

Appendix 57. MS of catechin.

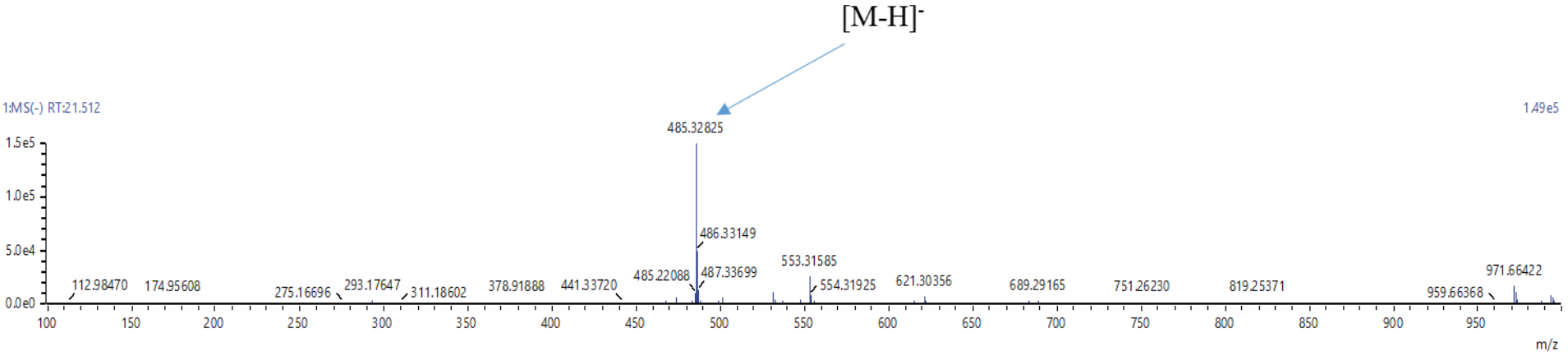

Appendix 58. MS of hydroxyglycyrrhetinic acid.

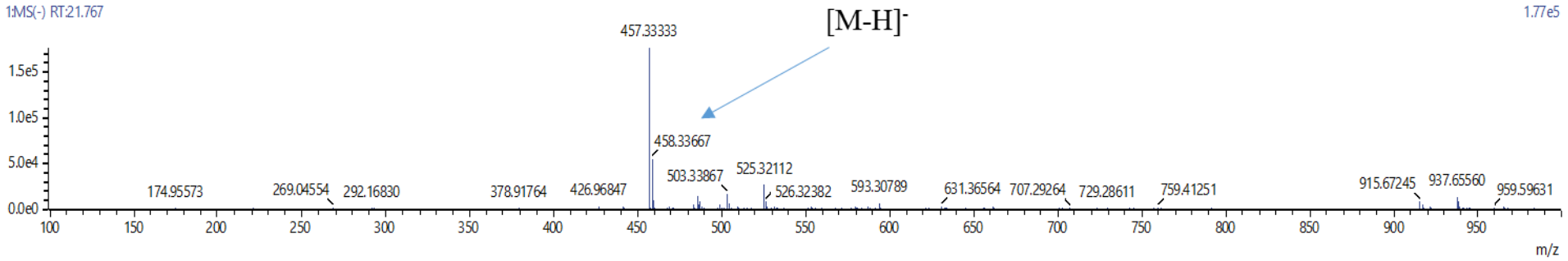

Appendix 59. MS of neotigogenin acetate.

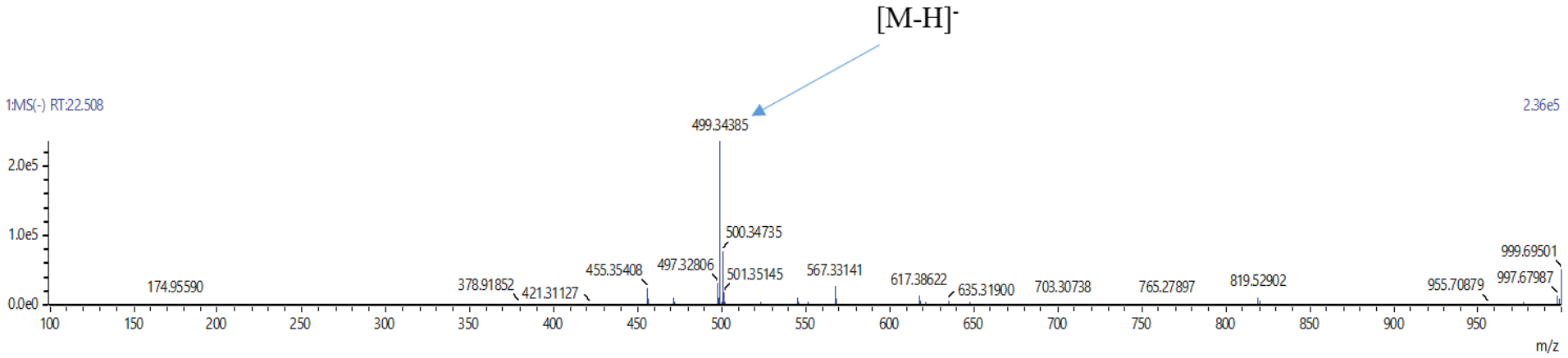

Appendix 60. MS of 25-hydroxy-3-epi-dehydrotumulosic acid.

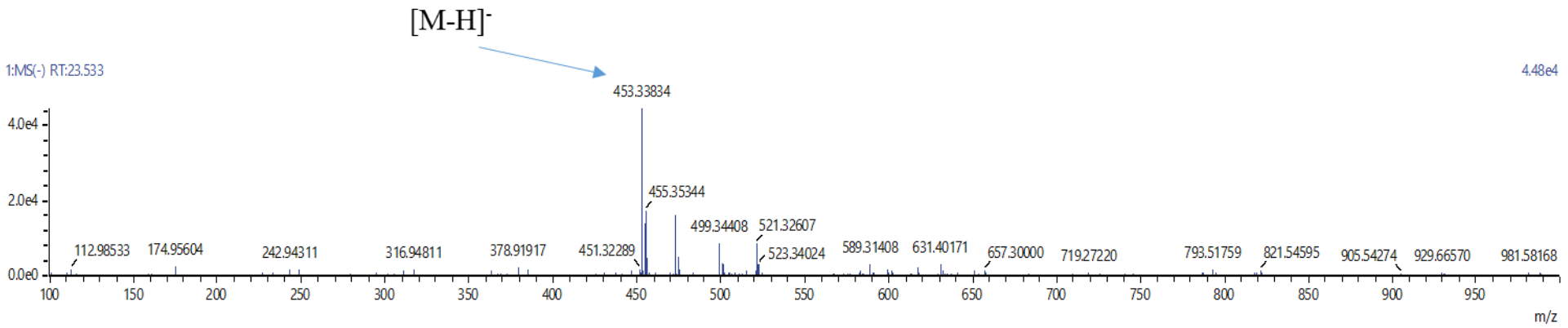

Appendix 61. MS of micromeric acid.

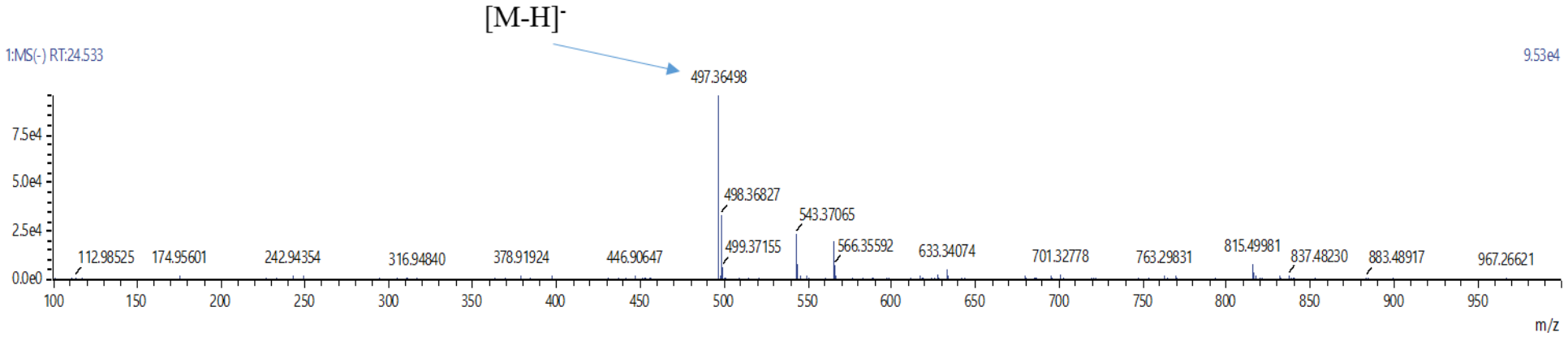

Appendix 62. MS of 3-acetylursolic acid.

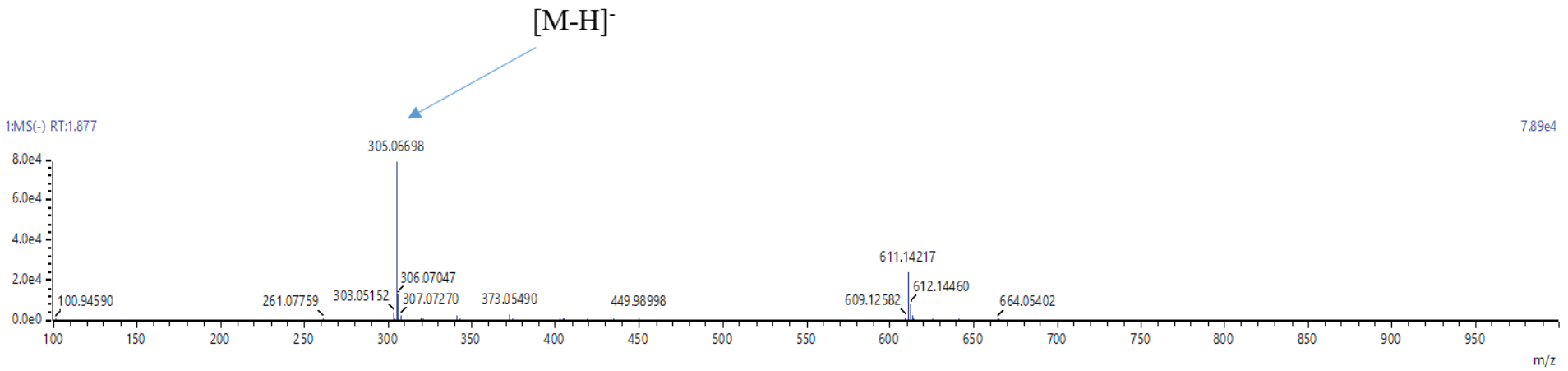

Appendix 63. MS of (epi)gallocatechin.

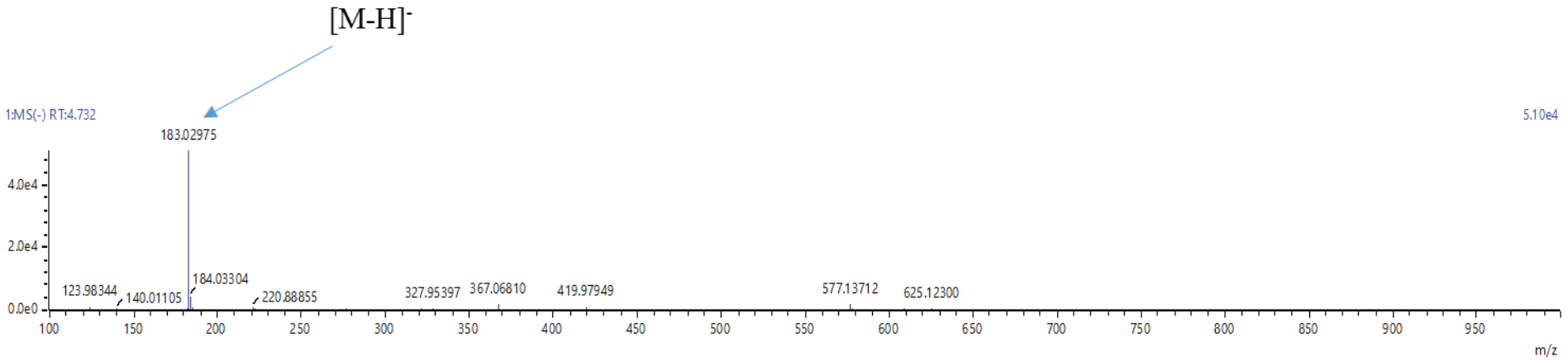

Appendix 64. MS of 4-*O*-methylgallic acid.

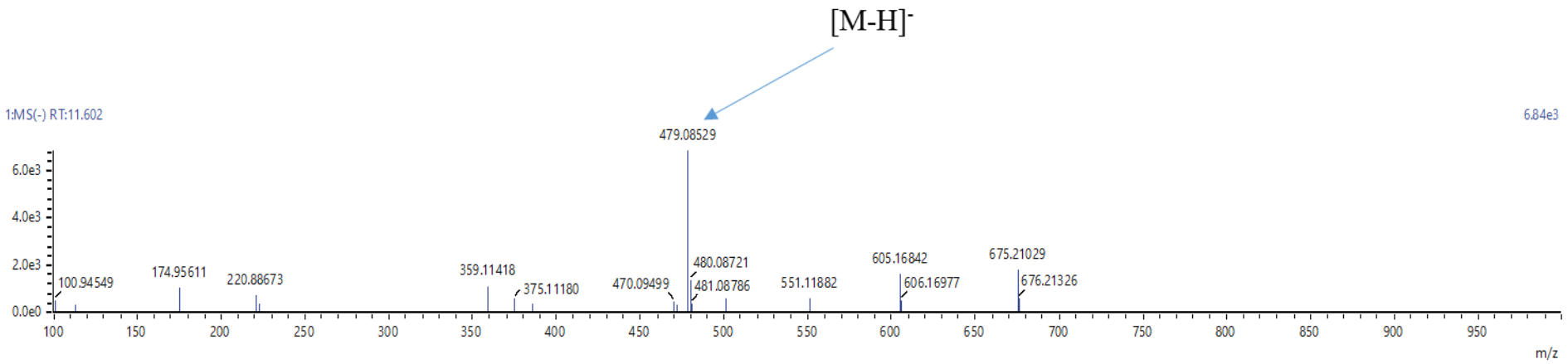

Appendix 65. MS of myricetin 3-*O*-glucoside.

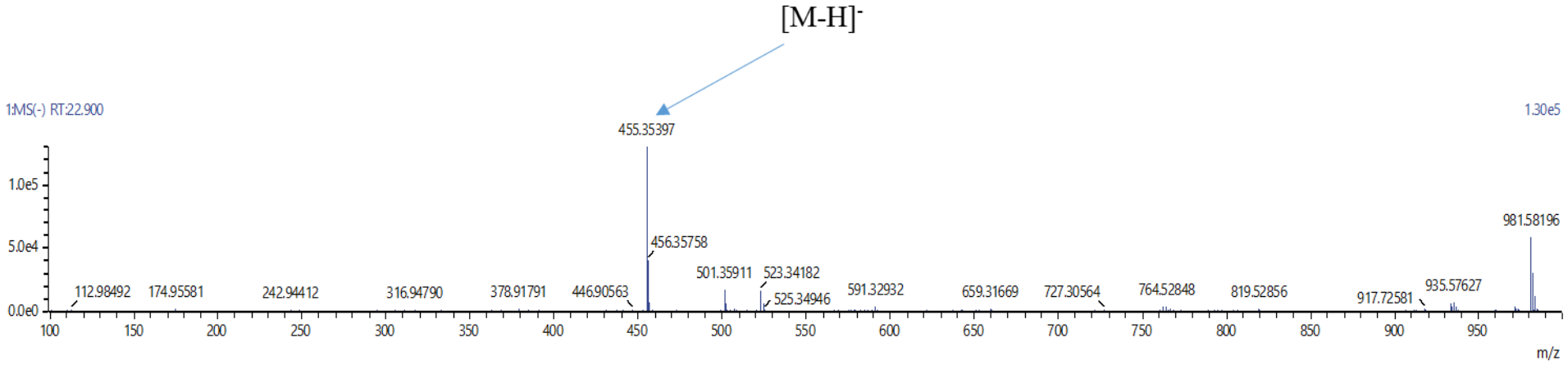

Appendix 66. MS of ursolic acid.

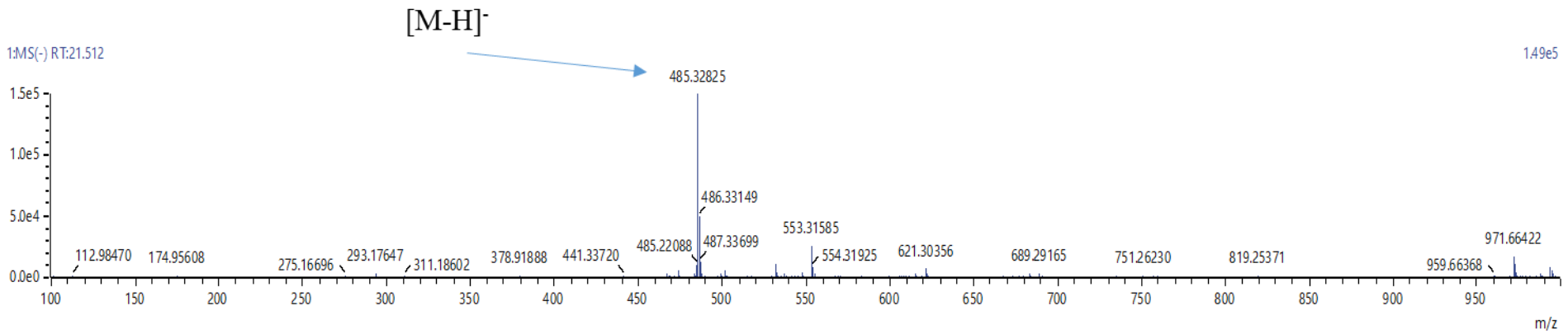

Appendix 67. MS of asiatic acid.

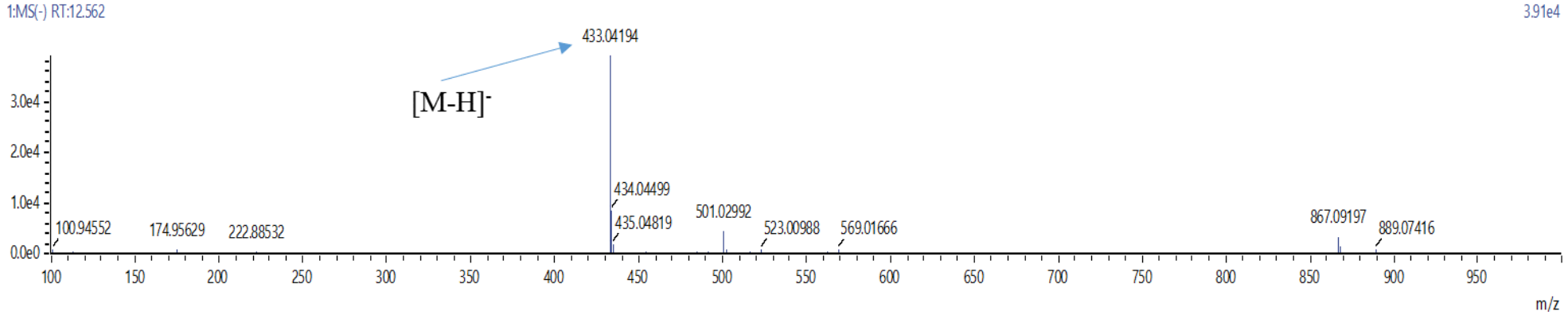

Appendix 68. MS of ellagic acid pentoside.

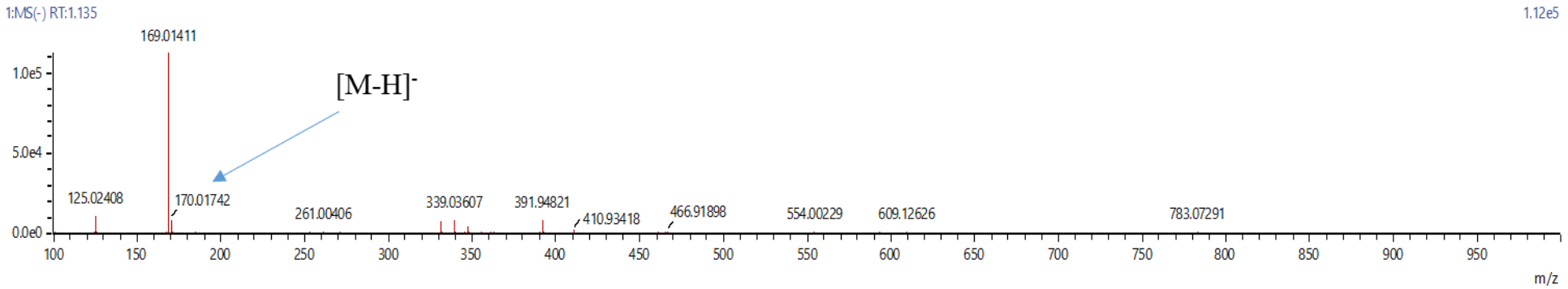

Appendix 69. MS of gallic acid.

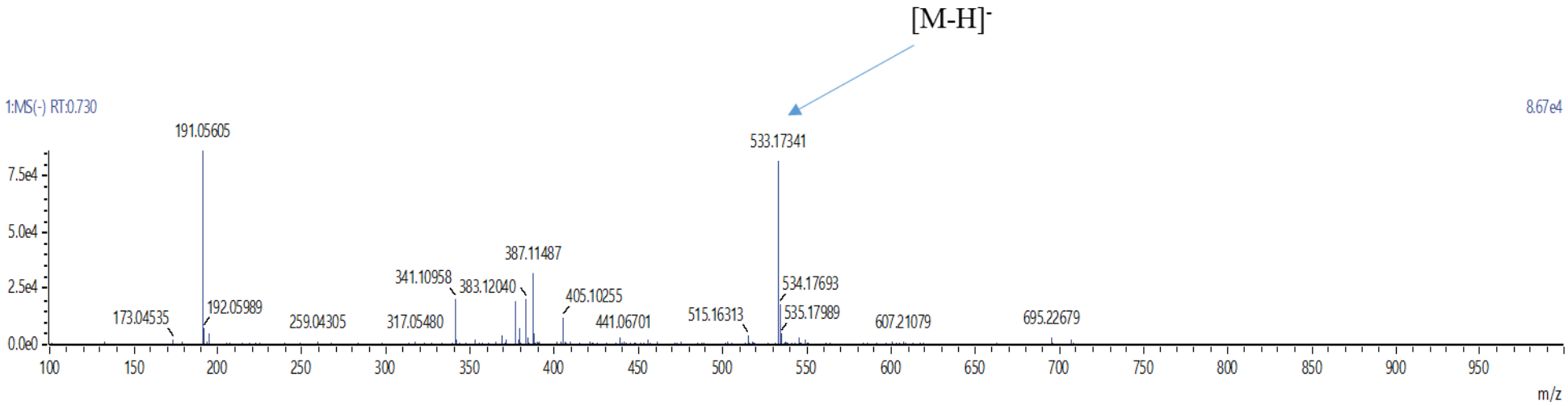

Appendix 70. MS of quinic acid + hexose$_2$.

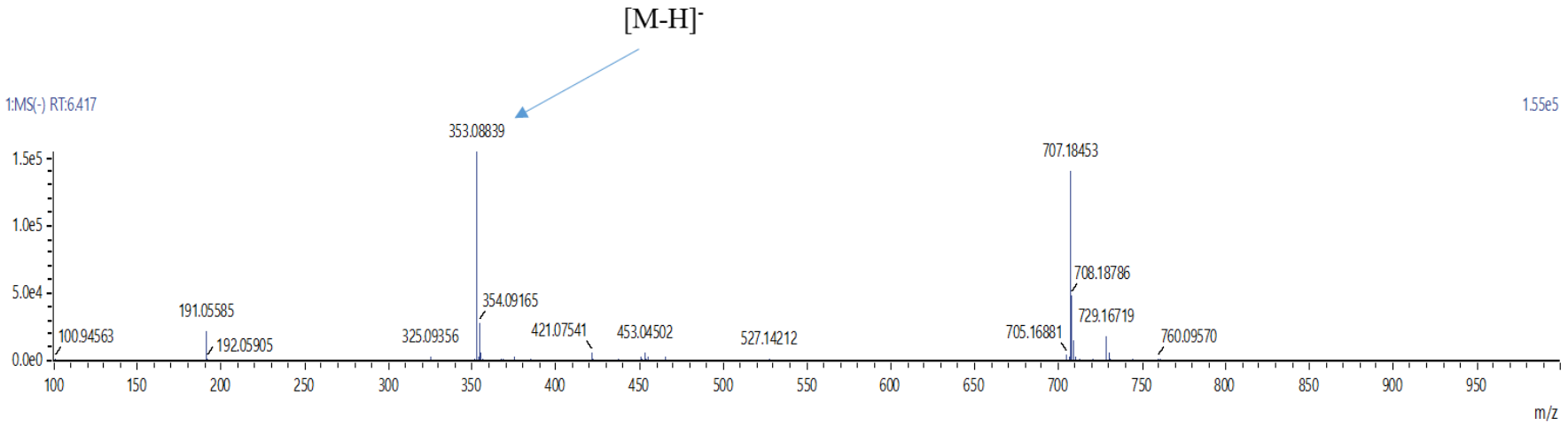

Appendix 71. MS of chlorogenic acid (3,4-dihydroxycinnamoylquinic acid; 5-caffeoylquinic acid).

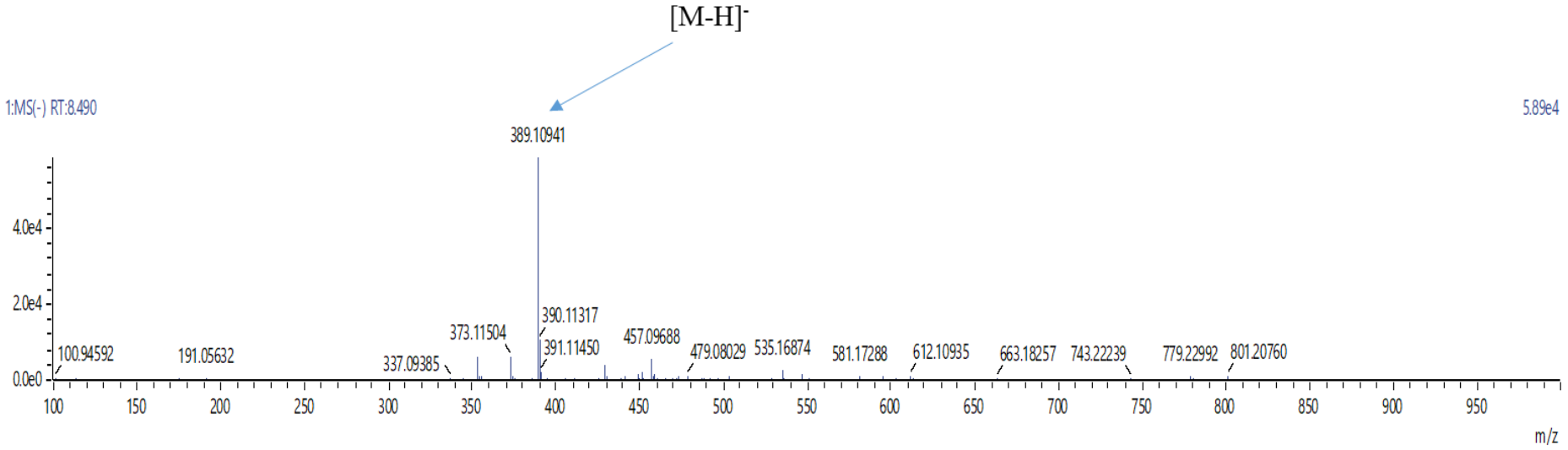

Appendix 72. MS of deacetyl asperuloside acid.

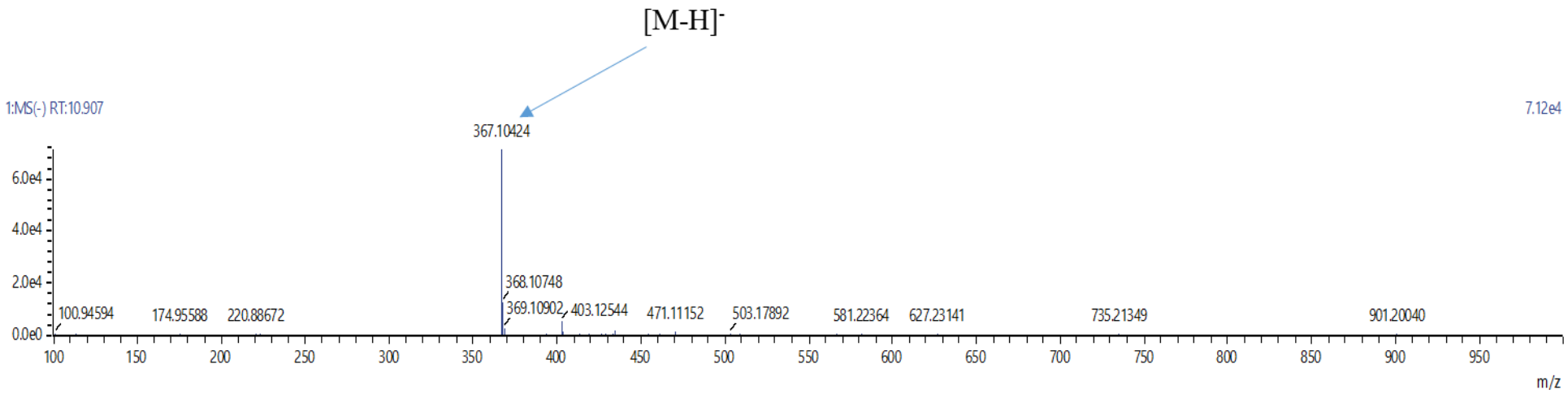

Appendix 73. MS of 5-methyl caffeoylquinic acid.

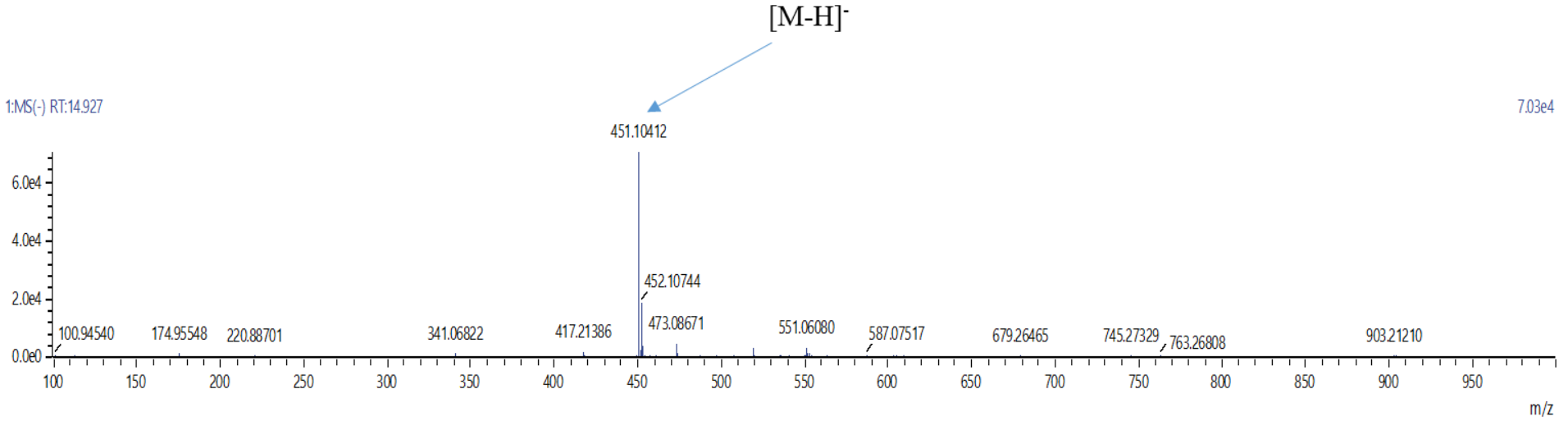

Appendix 74. MS of cinchonain I isomer.

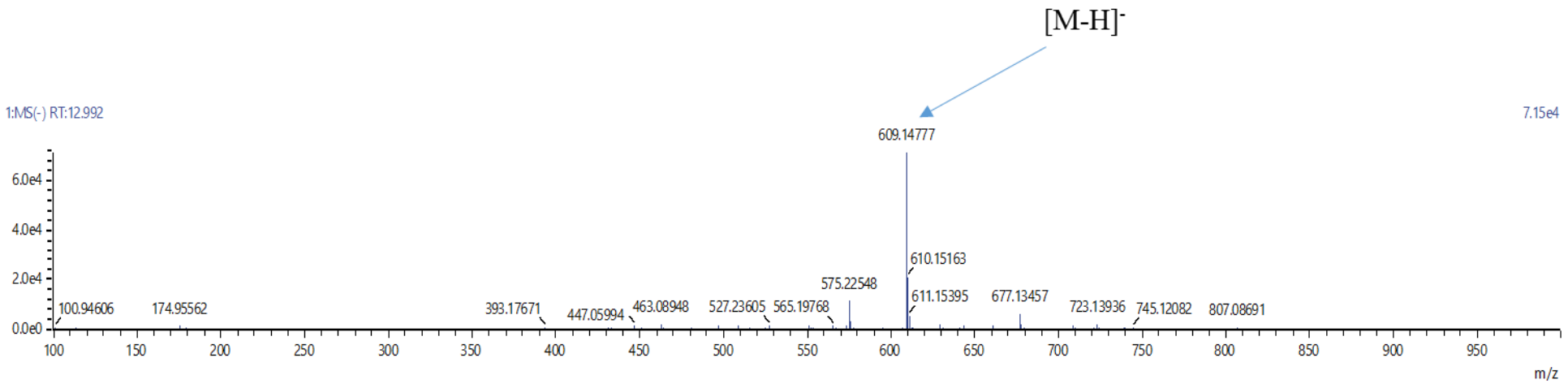

Appendix 75. MS of rutin.

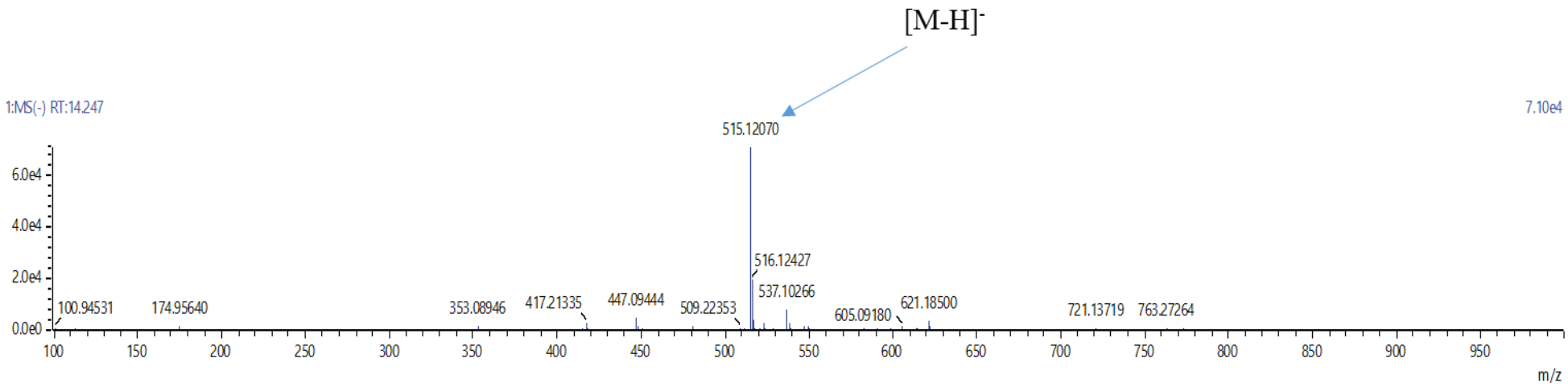

Appendix 76. MS of di-*O*-caffeoylquinic acid.

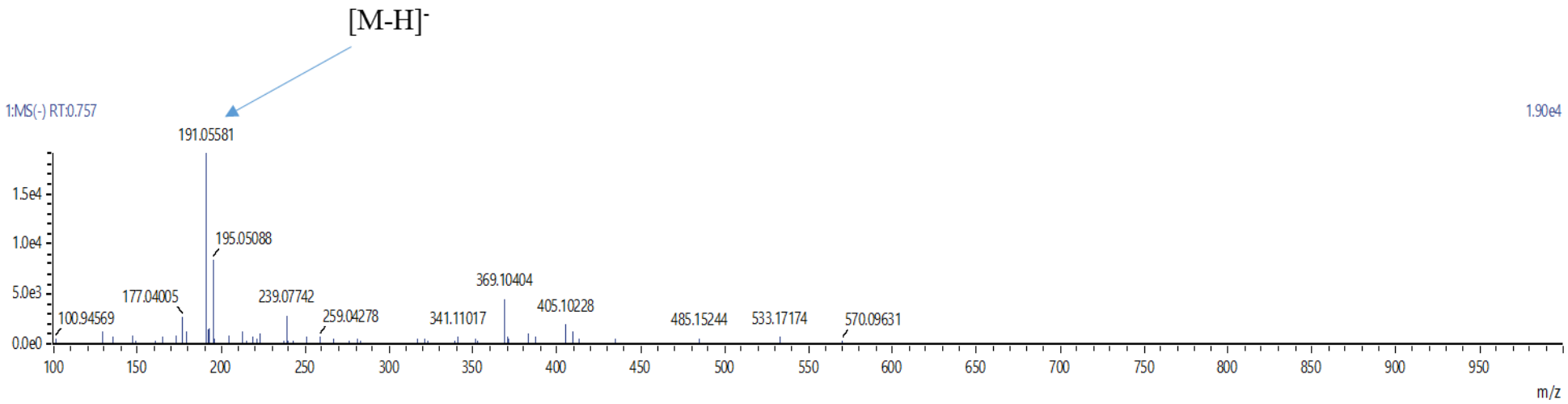

Appendix 77. MS of quinic acid.

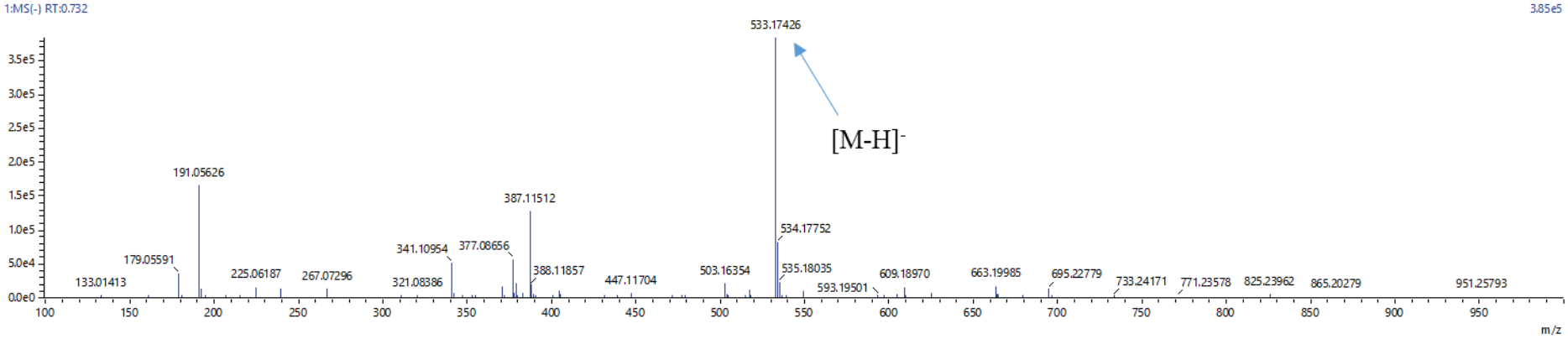

Appendix 78. MS of quinic acid + hexose$_2$.

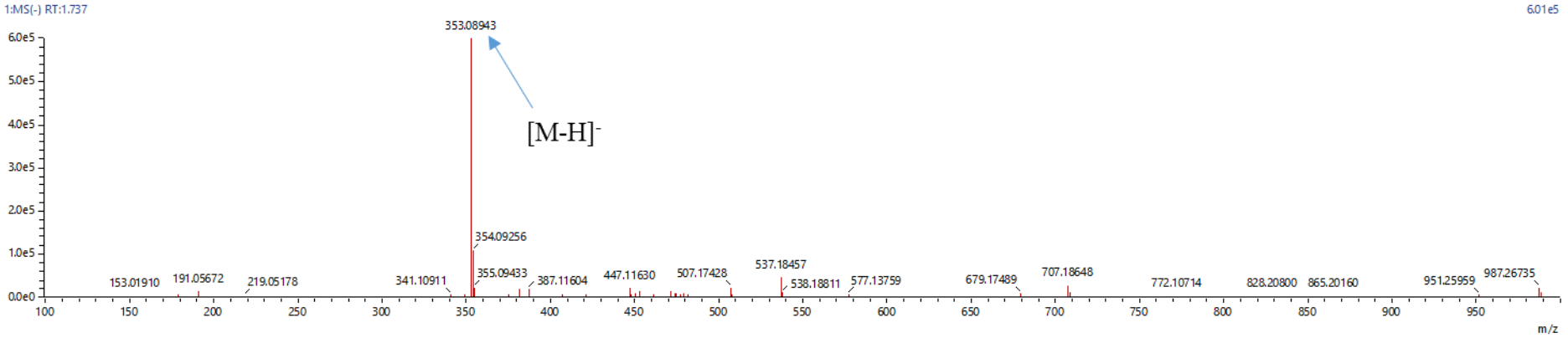

Appendix 79. MS of chlorogenic acid (3,4-dihydroxycinnamoylquinic acid; 5-caffeoylquinic acid).

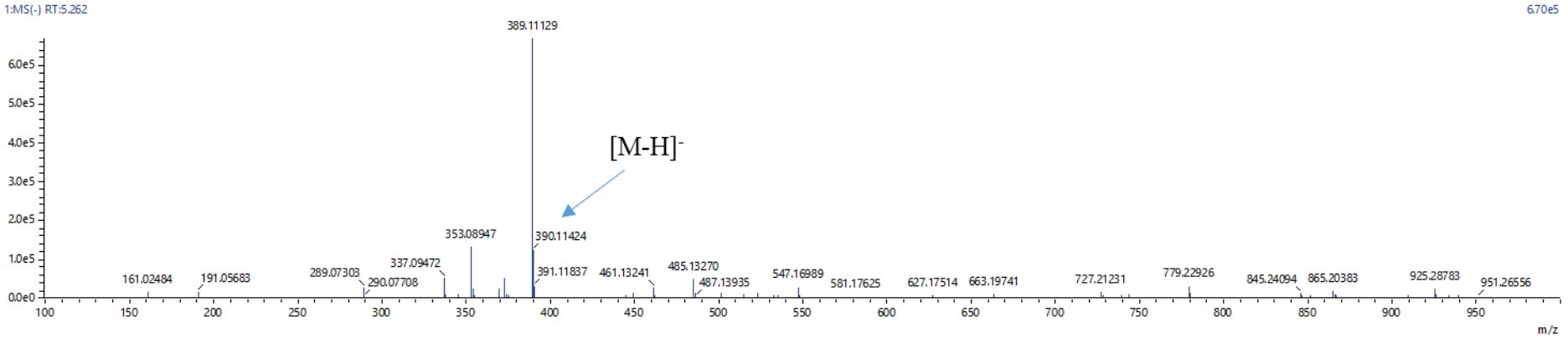

Appendix 80. MS of *trans*-resveratroloside.

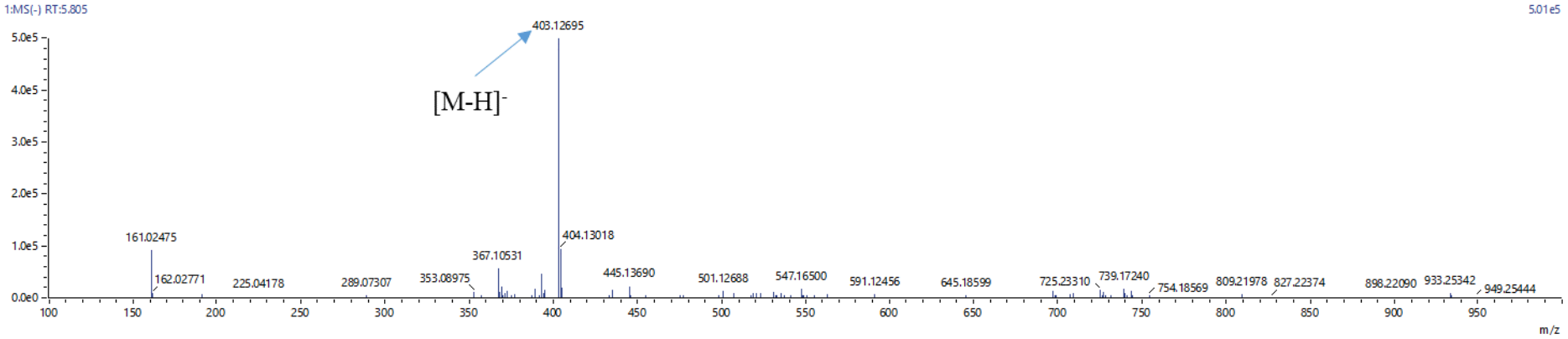

Appendix 81. MS of oleoside 11-methylester.

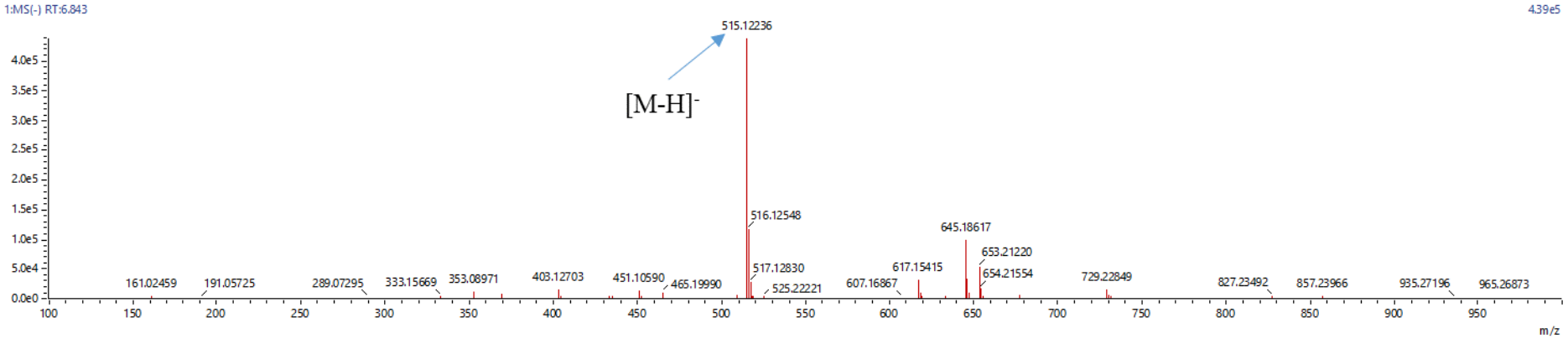

Appendix 82. MS of dicaffeoyl quinic acid isomer: 3,4−diCQA.

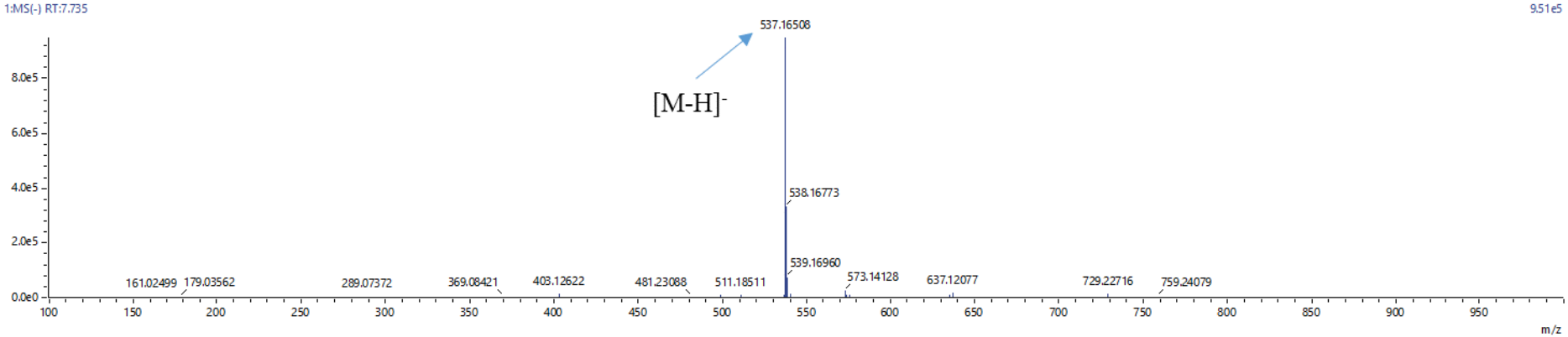

Appendix 83. MS of 4,8,4',8'-tetramethoxy-[1,1'-biphenanthrene]-2,7,2',7'-tetrol.

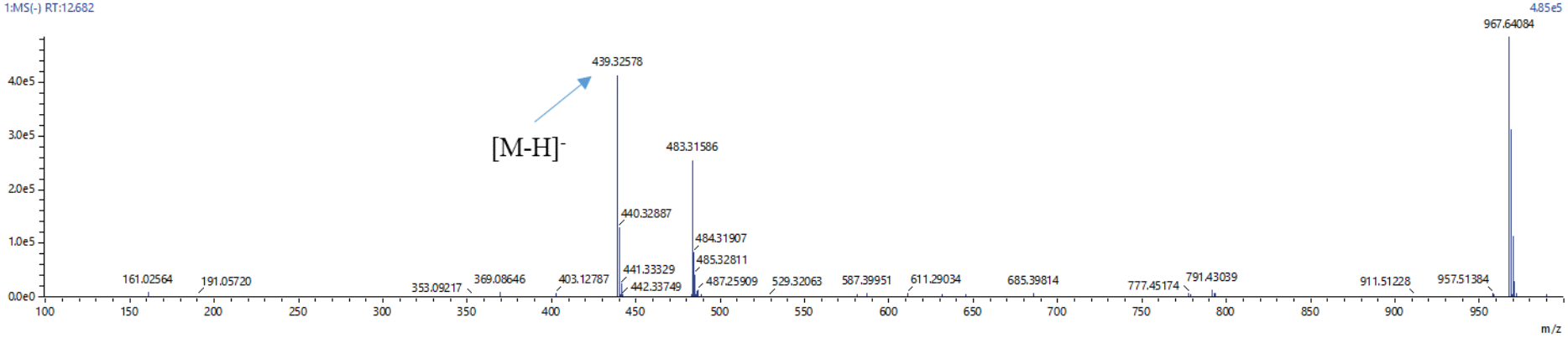

Appendix 84. MS of pfaffic acid.

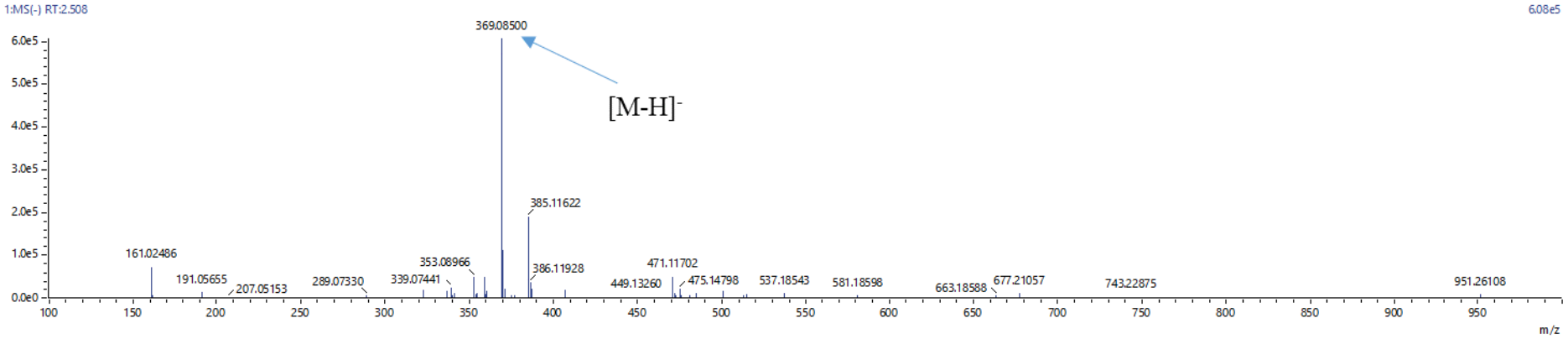

Appendix 85. MS of ferulic acid 4-*O*-glucuronide.

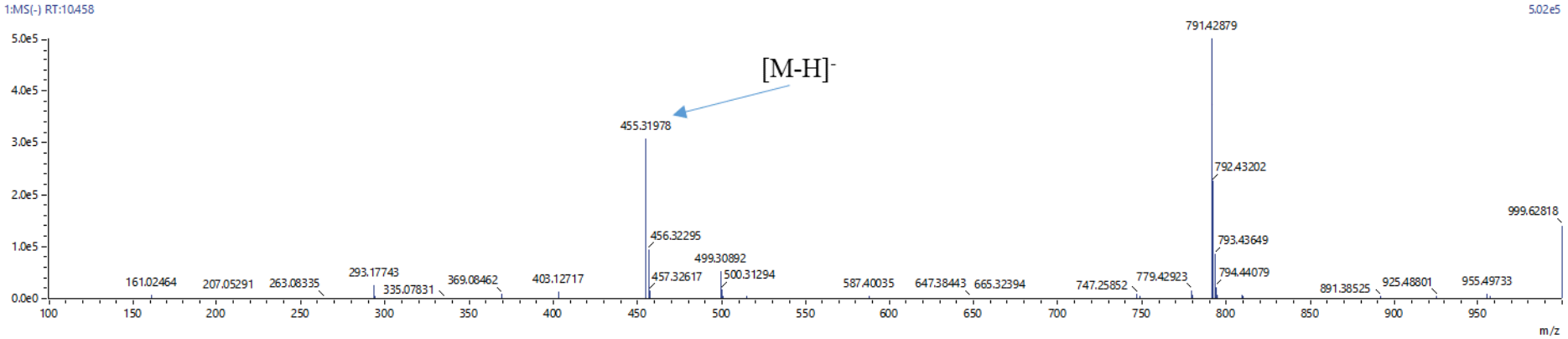

Appendix 86. MS of ursolic acid.

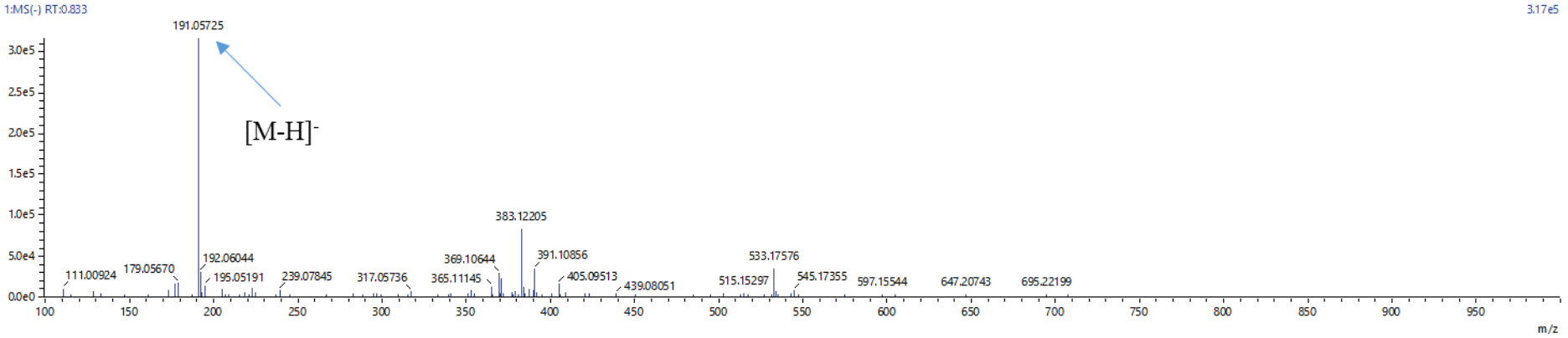

Appendix 87. MS of quinic acid.

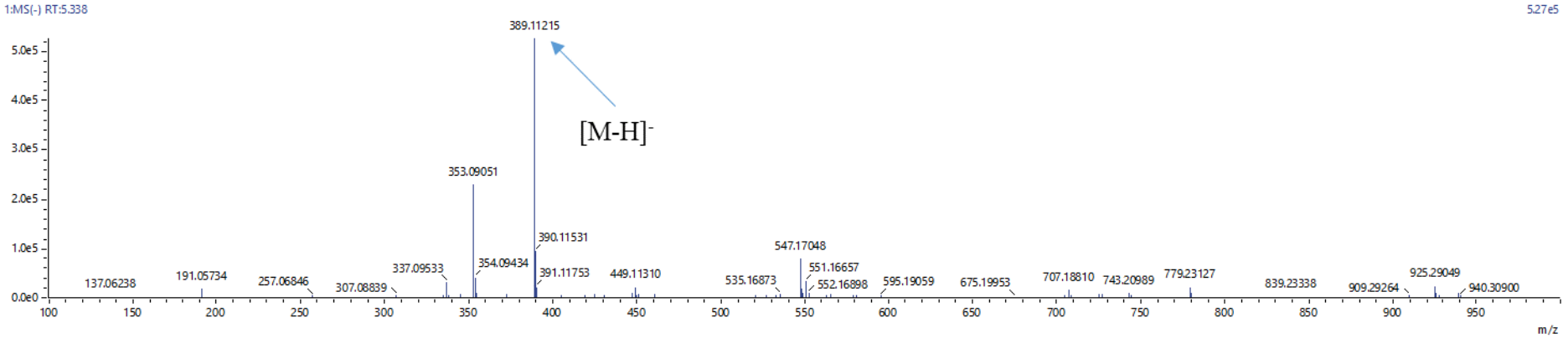

Appendix 88. MS of deacetyl asperuloside acid.

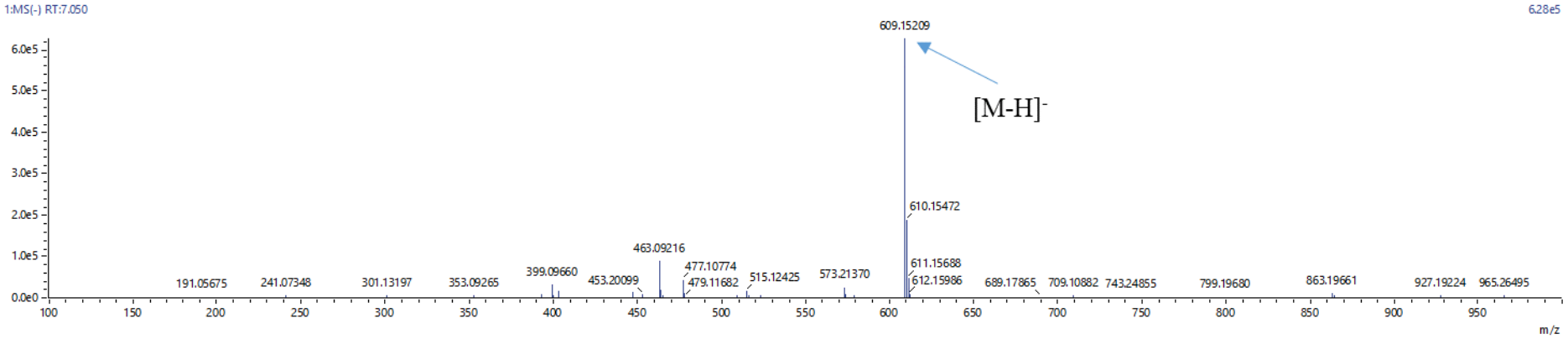

Appendix 89. MS of rutin.

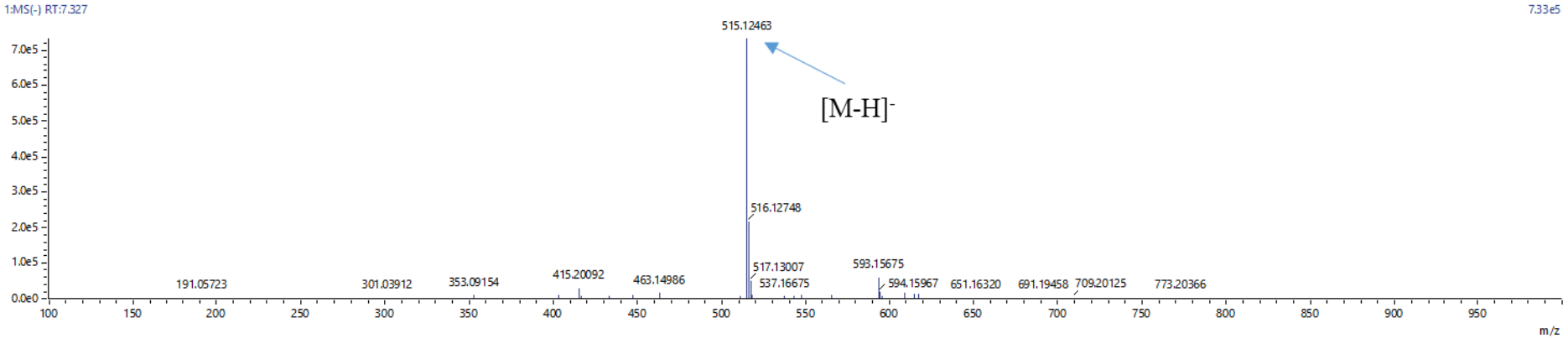

Appendix 90. MS of di-*O*-caffeoylquinic acid.

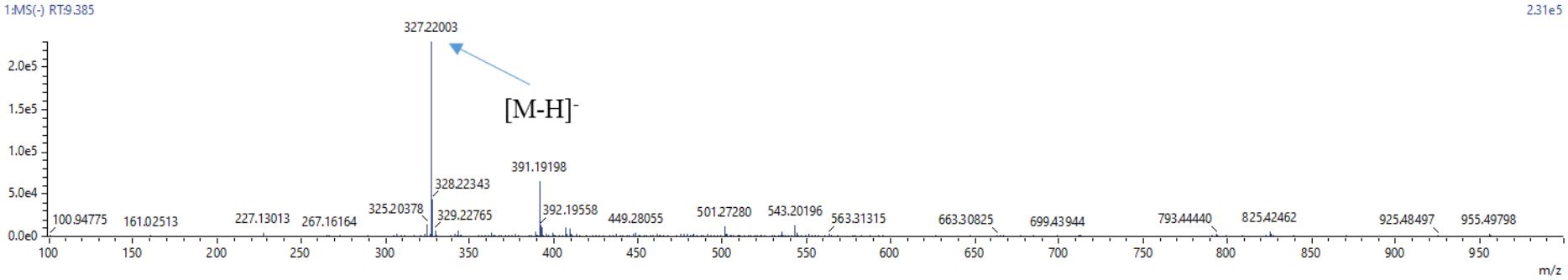

Appendix 91. MS of trihydroxy-octadecadienoic acid.

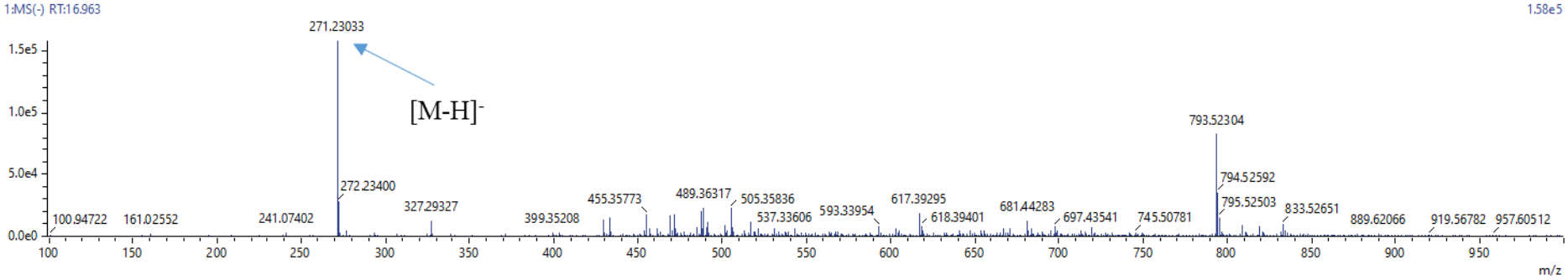

Appendix 92. MS of 15-hydroxyhexadecanoic acid.

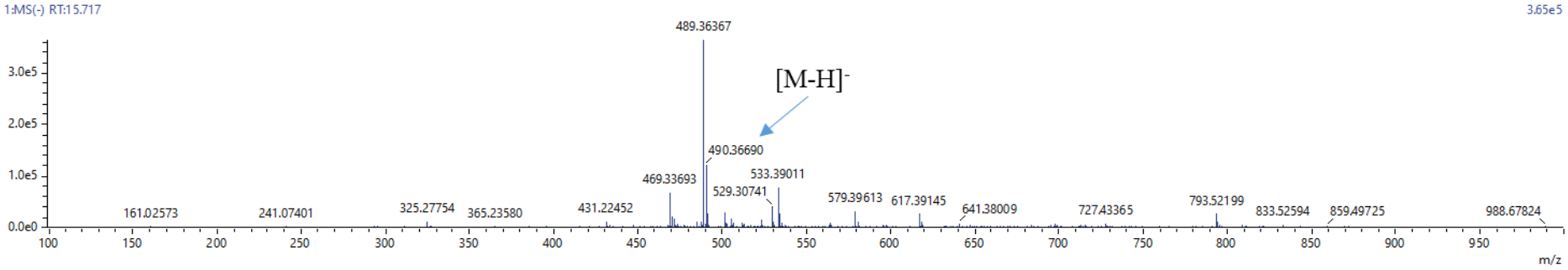

Appendix 93. MS of 3-α,24*R*,25-trihydroxytirucall-8-en-21-oic acid .

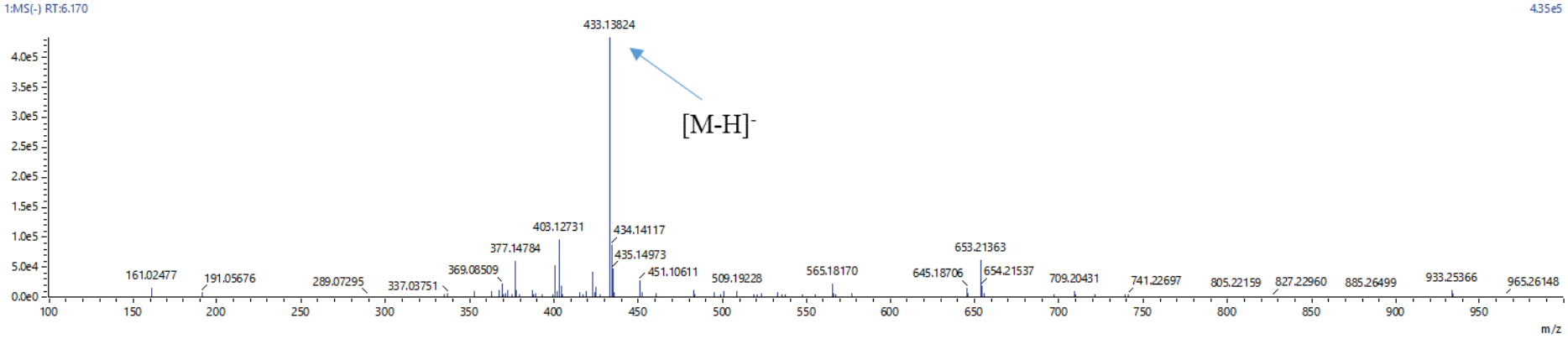

Appendix 94. MS of 6-α-hydroxyforsythide dimethyl ester.

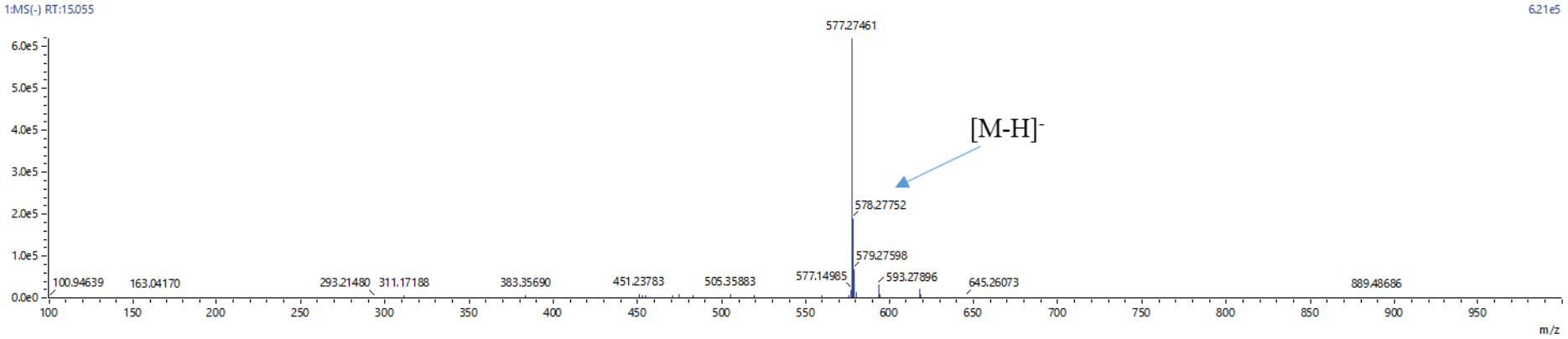

Appendix 95. MS of atractyloside G 2-*O*-β-D-glucopyranoside.

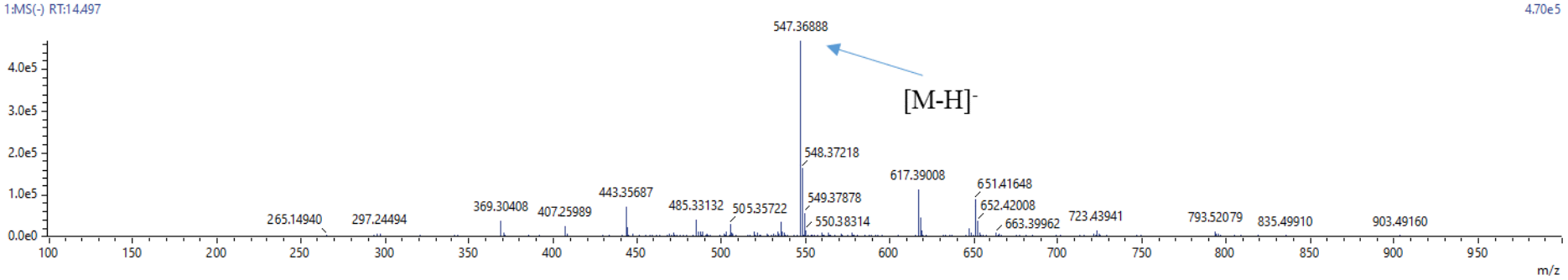

Appendix 96. MS of sibiricose A.

Appendix 97. Seasonal plant samples and voucher numbers of *B. salicina.*

Seasonal samples	Voucher Number	Dried samples (before extraction)	Dried extracts (after extraction)
Autumn			
Stem bark	BD 001	1.05 kg	83.31 g
Root	BD 002	0.78 kg	125.451 g
Leaf	BD 003	0.98 kg	-
DCM leaf	-	-	131.281 g
MeOH leaf	-	-	136.33 g
Winter			
Stem bark	BD 004	0.76 kg	140.75 g
Root	BD 005	0.29 kg	53.767 g
Leaf	BD 006	0.61 kg	-
DCM leaf	-	-	181.62 g
MeOH leaf	-	-	144.705 g
Spring			
Stem bark	BD 007	0.75 kg	129.5 g
Root	BD 008	0.33 kg	75.74 g
Leaf	BD 009	0.62 kg	-
DCM leaf	-	-	14.59 g
MeOH leaf	-	-	43.26 g
Summer			
Stem bark	BD 010	1.25 kg	156.022 g
Root	BD 011	0.88 kg	96.93 g
Leaf	BD 012	0.32 kg	-
DCM leaf	-	-	1.249 g
MeOH leaf	-	-	23.155 g